



THE UNIVERSITY *of* EDINBURGH

This thesis has been submitted in fulfilment of the requirements for a postgraduate degree (e.g. PhD, MPhil, DClinPsychol) at the University of Edinburgh. Please note the following terms and conditions of use:

- This work is protected by copyright and other intellectual property rights, which are retained by the thesis author, unless otherwise stated.
- A copy can be downloaded for personal non-commercial research or study, without prior permission or charge.
- This thesis cannot be reproduced or quoted extensively from without first obtaining permission in writing from the author.
- The content must not be changed in any way or sold commercially in any format or medium without the formal permission of the author.
- When referring to this work, full bibliographic details including the author, title, awarding institution and date of the thesis must be given.

**PROTEIN COMPLEXES IN
NEURODEGENERATIVE DISEASES**

Nicola P. Houston



Thesis Presented for the Degree of Doctor of Philosophy

The University of Edinburgh

2012

Abstract

The 14-3-3 family of proteins are important signalling proteins involved in a number of cellular processes. These include cell cycle regulation, apoptosis, signal transduction and cell signalling. There is also considerable evidence in the literature that 14-3-3 proteins play a vital role in the pathology of neurodegenerative diseases, including Alzheimer's, Parkinson's, Huntington's and Prion disease. The neurodegenerative disease of focus in this research is Spinocerebellar Ataxia Type 1 (SCA1). SCA1 is a polyglutamine-repeat disease and the interaction of the disease protein ataxin-1 with 14-3-3 proteins leads to the toxic accumulation and subsequent protein aggregation which is characteristic of this disease. This study focused on attempting to elucidate the structure of various domains of the disease protein and also in identifying potential inhibitors of this deleterious interaction. Unfortunately, structural studies were not successful due to a number of caveats encountered in the expression and purification of the ataxin-1 protein domains. By utilising computational methods and small molecule inhibitors, a number of potential lead compounds which possess the ability to at least partly disrupt the interaction of 14-3-3 ζ have been identified. As 14-3-3 proteins play roles in other neurodegenerative diseases, successful identification of potential drug lead treatments can have far reaching benefits in a number of neurodegenerative diseases including SCA1.

Lipid rafts are also involved in neurodegenerative disease pathology. Lipid rafts are cholesterol and sphingolipid rich domains which organise the plasma membrane into discrete microdomains and act as signalling platforms and processing centres which attach specific proteins and lipids. A number of disease proteins are processed at these membrane regions, including those involved in Alzheimer's, Parkinson's and Prion disease. This processing is a step which is critical in the pathology of disease and abnormal processing leads to the formation of toxic protein aggregates. Previous research in the lab identified the association of low levels of the five main brain isoforms of 14-3-3 proteins with rafts. This study expanded on this to positively identify the presence of the two phospho-forms of 14-

3-3, α and δ . The mechanism by which 14-3-3 proteins associate with rafts was also investigated, indicating that 14-3-3 associates with rafts via an unidentified raft-bound protein(s). In addition, the phosphorylation status and quaternary structure of 14-3-3 in the presence of sphingolipids has been explored.

Declaration

The work presented in this thesis is the original work of the author, unless referenced to other sources. This thesis has been composed by the author and has not been submitted in whole or part for any other degree.

Nicola Patricia Houston

Acknowledgements

First and foremost, I would like to thank my supervisor Professor Alastair Aitken for allowing me to conduct such an interesting research project in his lab and for his continued support and understanding throughout my studies. His scientific expertise is astounding and I am honoured to have been mentored by such an influential scientist.

I would like to thank current and previous members of the Aitken lab for their scientific insight and technical assistance throughout my PhD studies. In particular, I would like to thank Dr. Sebastian Beck for his scientific knowledge and patience at the start of my project. I would also like to extend my thanks to the collaborators who have contributed to this research.

An extra special thank you goes to Dr. Andrew Cronshaw for his invaluable help with mass spectrometry and 2-D electrophoresis as well as his friendship and support. I also thank Professor Lindsay Sawyer for his support as my second supervisor.

I would like to thank my wonderful family for their continued love, support and encouragement. And to all of my friends who have supported me, both professionally and personally over the course of my PhD, thank you; you know who you all are. An extra special thank you must go to Dr. Kelly Jobling for being an amazing friend and an absolute star.

The biggest thank you of all goes to my amazing husband Chris; without whom, this achievement would never have been possible. I am extremely thankful for his never ending love and support and will be eternally grateful that he helped me to achieve one of my dreams and make it a reality. For this, I dedicate this thesis to my husband, Chris.

Figures

Figure 1.1: Schematic Diagram of 14-3-3 and Phosphorylation Sites.....	4
Figure 1.2: Structure of 14-3-3.....	6
Figure 1.3: Alignment of Brain 14-3-3 Isoforms	10
Figure 1.4: Lipid Raft Model	31
Figure 1.5: Schematic Diagram of Ataxin-1	42
Figure 1.6: Model of Ataxin-1 Accumulation	49
Figure 2.1: Iodixanol Gradient Set-Up For Raft Isolation From Whole Rat Brain.....	76
Figure 2.2: Sucrose Gradient Set-Up for Raft Isolation from Whole Rat Brain	78
Figure 2.3: Diagram of IPG Strips Modified for Second-Dimension Separation.....	83
Figure 3.1: Cholesterol Assay of Rat Brain Fractions	95
Figure 3.2: BCA Assay of Rat Brain Fractions	96
Figure 3.3: SDS-PAGE of Raft Fractions Isolated from Rat Brain	97
Figure 3.4: Identification of Raft Fractions By Western Blotting for Flotillin-1	98
Figure 3.5: Identification of Rafts By Western Blotting for Prion Protein.....	99
Figure 3.6: SDS-PAGE After Chloroform: Methanol Extraction.....	101
Figure 3.7: 2D-PAGE Analysis of Lipid Raft Fractions	103
Figure 3.8: SDS-PAGE of Raft Fraction for Mass Spectrometry.....	104
Figure 3.9: Tryptic Digest Sequence of Phospho-14-3-3.....	107
Figure 3.10: Phospho-14-3-3 Peptide Following Endoproteinase Glu-C Digestion	107
Figure 3.11: MS/MS Control Data from Phosphorylated Peptide	109
Figure 3.12: MS/MS Control Data from Non-Phosphorylated Peptide	109
Figure 3.13: 14-3-3 Isoform Association with M β CD Treated Lipid Rafts.....	112
Figure 3.14: 14-3-3 Association with Lipid Rafts.....	113
Figure 3.15: SDS-PAGE of 14-3-3 ζ Fractions Collected from IMAC.....	115
Figure 3.16: SDS-PAGE of 14-3-3 ζ Cross-Linking.....	116
Figure 3.17: SDS-PAGE of Cross-Linked Kinase Assay Samples	118
Figure 3.18: Spectra of Kinase Assay Samples 1 and 2.....	120
Figure 3.19: Spectra of Kinase Assay Samples 1 and 4.....	121
Figure 3.20: Cross-Linking Analysis of 14-3-3 Proteins at Lipid Rafts.....	122
Figure 3.21: Akt Association with Lipid Rafts.....	125
Figure 4.1: Peptide Sequence in MCS	132
Figure 4.2: Simplified vector map of pTrcHisA'	132
Figure 4.3: SDS-PAGE of Fractions Collected from IMAC Purification	136
Figure 4.4: Ataxin-C Ion-Exchange	138
Figure 4.5: Ataxin-AC Ion-Exchange	139
Figure 4.6: Chromatogram of Ataxin-C Gel Filtration	140
Figure 4.7: Ataxin-1 Sequence and Domains.....	145
Figure 4.8: Simplified Vector Map for New Domains in pTrcHisA'	146
Figure 4.9: SDS-PAGE Following Induction of Ataxin 575-815 at A ₆₀₀ =0.4	151
Figure 5.1: Companies Contributing to EDULISS Database	157
Figure 5.2: Hydrogen Bond Donors and Acceptors	158
Figure 5.3: STP Image of PDB File 1QJB.....	159
Figure 5.4: SDS-PAGE of Purification Fraction for GST-ExoS	164
Figure 5.5: SDS-PAGE of Glutathione Test.....	165
Figure 5.6: Diagram of Proposed SPR Model	168
Figure 5.7: Output Trace from SPR Test.....	170
Figure 5.8: ELISA Assay	172

Figure 5.9: Comparison of Assay Buffers.....	174
Figure 5.10: Effect of Blocking Conditions on Assay.....	175
Figure 5.11: Graph of Absorbance Readings over Time	176
Figure 5.12: Normalised Assay Absorbance Values.....	177
Figure 5.13: Absorbance of Maltotetraose Concentrations Tested	179
Figure 5.14: Absorbance of DIPSO Concentrations Tested.....	180
Figure 5.15: Absorbance of 6-Phosphogluconic Acid Concentrations Tested	182
Figure 5.16: Absorbance of Adenosine 5'-Diphosphate Concentrations Tested.....	183

Tables

Table 1.1: Selected Isoform-Specific 14-3-3 Protein Interactions.....	15
Table 1.2: Ataxin-1 Interacting Proteins	45
Table 2.1: Molecular Biology Buffers	55
Table 2.2: Table of Primers	57
Table 2.3: Protein Expression Plasmids	62
Table 2.4: Strains of Competent Cells used in Protein Expression	62
Table 2.5: Ion-Exchange Conditions	68
Table 2.6: Buffers for SDS-PAGE.....	71
Table 2.7: Buffers for Immunoblotting	72
Table 2.8: Primary Antibodies for Immunoblotting	73
Table 2.9: Secondary Antibodies for Immunoblotting	73
Table 2.10: Buffers for Lipid Raft Isolation	74
Table 2.11: OptiPrep Gradients for Raft Isolation.....	75
Table 2.12: IsoElectric Focussing Procedure	82
Table 2.13: Equilibration Conditions	82
Table 2.14: Buffers for ELISA Assay	89
Table 3.1: MALDI-TOF Results	105
Table 3.2: LC-MS Results.....	106
Table 4.1: Ataxin-1 Domains.....	133
Table 4.2: Ataxin-AC MALDI-TOF Results	141
Table 4.3: Refined Crystallography Conditions for Ataxin-C.....	143
Table 4.4: New Ataxin-1 Domains	147
Table 4.5: Expression Trial Conditions for New Ataxin-1 Domains	148
Table 5.1: Compounds Tested for 14-3-3 ζ Binding Inhibition.....	161
Table 5.2: SPR Combinations Tested	167
Table 5.3: Assay Conditions Tested	176
Table 7.1: Full List of Compounds Identified from LIDAEUS.....	190

Abbreviations

A β	β -Amyloid
AC	AXH and C Terminus of Ataxin-1
AD	Alzheimer's disease
ADCA	Autosomal Dominant Cerebellar Ataxia
Akt/PKB	Protein Kinase B
APP	Amyloid Precursor Protein
ApoE4	Apolipoprotein E4
AXH	Ataxin-1/HBP1 region
BBB	Blood Brain Barrier
BCA	Bicinchoninic Acid Assay
BCR	Breakpoint Cluster Region
BSA	Bovine Serum Albumin
BSE	Bovine Spongiform Encephalopathy
CAG	Glutamine Codon
CAT	Histidine Codon
CHCA	α -Cyano-4-HydroxyCinnamic Acid
CJD	Creutzfeldt-Jakob disease
CKI α	Casein Kinase I α
CNS	Central Nervous System
CSF	Cerebrospinal Fluid
CV	Column Volume
DMP	Dimethyl Pimelimidate
DRPLA	Dentatorubral-Pallidoluysian Atrophy
ECL	Enhanced Chemiluminescence
EDULISS	EDinburgh University LIgand Selection System
ELISA	Enzyme-Linked Immunosorbent Assay
ExoS	Exo-Enzyme S
FPLC	Fast Protein Liquid Chromatography
GPI	Glycophosphatidylinositol
GST	Glutathione-S-Transferase
HBA	Hydrogen Bond Acceptor
HBD	Hydrogen Bond Donor
HBP1	HMG Box containing Protein-1
HD	Huntington's disease
HEK-293	Human Embryonic Kidney cells 293
HPLC	High Performance Liquid Chromatography
HRP	Horse Radish Peroxidase
IMAC	Immobilised Metal Affinity Chromatography
IPG	Immobilised pH Gradient
IPTG	Isopropyl-beta-D-thiogalactopyranoside
JNK	Jun N-terminal Kinase
LB	Luria Bertani
LDM	Low Density Membranes
LIDAEUS	Ligand Discovery At Edinburgh UniverSity
LRRK2	Leucine-Rich Repeat Kinase 2
MALDI-TOF	Matrix Assisted Laser Desorption Ionisation- Time Of Flight
M β CD	Methyl- β -Cyclodextrin

MW	Molecular Weight
MWCO	Molecular Weight Cut Off
NFT	Neurofibrillary Tangles
NLS	Nuclear Localisation Sequence
OD	Optical Density
PBS	Phosphate Buffered Saline
PCR	Polymerase Chain Reaction
PD	Parkinson's disease
PDB	Protein Data Bank
PI3K	Phosphoinositide 3-Kinase
PKA	Protein Kinase A
PKB/ Akt	Protein Kinase B
pAkt	Akt Phosphorylated on Ser473
PKC	Protein Kinase C
PrP ^C	Prion Protein
PrP ^{Sc}	Protease-Resistant form of Prion Protein
SBMA	Spinobulbar Muscular Atrophy
SCA	Spinocerebellar Ataxia
SCA1	Spinocerebellar Ataxia Type 1
SDS	Sodium-Dodecyl-Sulphate
SDS-PAGE	Sodium-Dodecyl-Sulphate Polyacrylamide Gel Electrophoresis
SDK1	Sphingosine Dependent Kinase 1
SN (pc)	Substantia Nigra (pars compacta)
SPR	Surface Plasmon Resonance
TB	Terrific Broth
TBS	Tris Buffered Saline
TBS-T	Tris Buffered Saline supplemented with Tween-20
UFSRAT	Ultra-Fast Shape Recognition with Atom Types
4-CN	4-Chloro-1-Naphthol

TABLE OF CONTENTS

ABSTRACT	I
DECLARATION.....	III
ACKNOWLEDGEMENTS	IV
FIGURES.....	V
TABLES.....	VI
ABBREVIATIONS	VII
TABLE OF CONTENTS.....	IX

14-3-3 PROTEINS, LIPID RAFTS AND NEURODEGENERATIVE DISEASES 1

1.1. 14-3-3 Proteins.....	2
1.1.1. Identification and Characterisation of 14-3-3 Proteins	2
1.1.2. The Crystal Structure of 14-3-3	5
1.1.3. 14-3-3 Isoforms	9
1.1.4. 14-3-3 and Neurodegenerative Diseases.....	18
1.2. Lipid Rafts.....	29
1.2.1. What are Lipid Rafts?	29
1.2.2. Lipid Raft Composition.....	30
1.2.3. Lipid Rafts and Neurodegenerative Diseases.....	34
1.3. Spinocerebellar Ataxia Type 1 (SCA1).....	39
1.3.1. Clinical Effects of SCA1.....	39
1.3.2. Disease Pathology	41
1.3.3. Ataxin-1 and 14-3-3.....	48
1.4. Aims of Project.....	53

MATERIALS AND METHODS 55

2.1. Molecular Biology.....	55
2.1.1. Agarose Gel Electrophoresis	56
2.1.2. Primer Design.....	56
2.1.3. Polymerase Chain Reaction (PCR) with Pfu Polymerase.....	57
2.1.4. Restriction Digest.....	58
2.1.5. Gel Extraction.....	59
2.1.6. Ligation of Insert DNA into Vector DNA.....	59
2.1.7. Preparation of Competent Bacteria	60
2.1.8. Transformation of Bacteria	60
2.1.9. Production of Glycerol Stocks.....	61
2.1.10. Purification of Plasmid DNA	61
2.1.11. Quantification of Plasmid DNA.....	61
2.2. Expression and Purification Techniques	62
2.2.1. Expression of Recombinant Proteins.....	63
2.2.2. Immobilised Metal Affinity Chromatography (IMAC) by Gravity Flow	64
2.2.3. Ion-Exchange Chromatography.....	68
2.2.4. Gel Filtration Chromatography	68
2.2.5. Concentration and Storage of Proteins	69

2.2.6. Protein Concentration Determination.....	70
2.3. Biochemical Techniques.....	71
2.3.1. SDS-PAGE.....	71
2.3.2. Immunoblotting	72
2.3.3. Lipid Raft Isolation from Whole Rat Brain.....	74
2.3.4. Cholesterol Assay	79
2.3.5. Cholesterol Depletion of Lipid Rafts.....	80
2.3.6. 2-Dimensional (2D) SDS-PAGE	81
2.3.7. In-Gel Digestion and Mass Spectrometry	84
2.3.8. Protein Crystallography.....	86
2.3.9. Cross-Linking.....	87
2.3.10. In-Vitro Kinase Assay.....	88
2.3.11. Enzyme-Linked Immunosorbent Assay - ELISA Assay	89
14-3-3 PROTEINS AND LIPID RAFTS	91
3.1. Introduction.....	91
3.2. Aims.....	93
3.3. Results	94
3.3.1. Lipid Raft Isolation from Rat Brain	94
3.3.2. Confirmation of Raft Isolation by Known Markers	97
3.3.3. Chloroform: Methanol Extraction for Lipid Raft Analysis	99
3.3.4. 2D Analysis Identifies Phospho-14-3-3 in Lipid Rafts	101
3.3.5. 14-3-3 in Rafts by Mass Spectrometry	104
3.3.6. 14-3-3 Association with Lipid Rafts.....	111
3.3.7. Purification of 14-3-3 ζ for Sphingosine-Dependent Phosphorylation and Effect on Dimerisation	115
3.3.8. <i>In Vitro</i> Kinase Assays to Investigate the Effects of Sphingosine	117
3.3.9. 14-3-3 is Predominantly Monomeric at Lipid Rafts	122
3.3.10. 14-3-3 in Rafts and Akt Phosphorylation.....	124
3.4. Discussion.....	126
SPINOCEREBELLAR ATAXIA TYPE 1 AND ATAXIN-1.....	129
4.1. Introduction.....	129
4.2. Aims.....	130
4.3. Results	131
4.3.1. Identification of Ataxin-1 'C' and 'AC' Domains	131
4.3.2. Expression of Ataxin-1 Domains	134
4.3.3. Purification of Ataxin-1 Domains.....	135
4.3.4. Confirmation of Protein Identity	141
4.3.5. Crystallography of Ataxin-C: Initial Trials.....	142
4.3.6. Identification of New Ataxin-1 Domains.....	144
4.3.7. Expression Trials of New Ataxin-1 Domains.....	148
4.4. Discussion.....	153

IDENTIFICATION OF COMPOUNDS FOR 14-3-3ζ INHIBITION	154
5.1. Introduction.....	154
5.2. Aims.....	155
5.3. Results	156
5.3.1. Identification of Compounds for 14-3-3 Inhibition	156
5.3.2. Purification of Proteins Required for Testing Potential Compounds.....	163
5.3.3. Methods for Testing Compound Inhibition	166
5.3.4. Testing Compounds to Block 14-3-3 ζ Interaction.....	178
5.4. Discussion.....	185
 GENERAL DISCUSSION.....	 186
 APPENDIX	 190
7.1. Compounds Identified for 14-3-3 ζ Inhibition	190
 REFERENCES	 202
 PUBLICATIONS	 228

CHAPTER 1

14-3-3 PROTEINS, LIPID RAFTS AND NEURODEGENERATIVE DISEASES

A number of proteins involved in a wide range of neurodegenerative diseases are known to interact with both 14-3-3 proteins and lipid rafts. Prior to undertaking this research, there was also a suggestion of a connection between lipid rafts and 14-3-3 proteins. The purpose of this research was to further explore these connections between all three factors and investigate possible means of preventing these interactions for the purposes of potential treatments in neurodegenerative diseases. This first chapter addresses the position which each of these factors holds in current literature and sets a basis for the background into the purposes of the research in this thesis. The main neurodegenerative disease studied is Spinocerebellar Ataxia Type 1, which is discussed in section 1.3.

1.1. 14-3-3 Proteins

The 14-3-3 family of proteins are generally classed as signalling adaptor proteins which primarily bind to phospho-serine and phospho-threonine motifs. A function for this protein family was first identified in the 1980s (Yamauchi et al. 1981; Ichimura et al. 1987) and since this, 14-3-3 protein research has expanded into a very broad field, encompassing eukaryotic organisms and intracellular signalling processes. A number of functions have been attributed to 14-3-3 and the number of identified interacting partners is continually increasing. To date, more than 400 14-3-3 target proteins have been identified, with a recent study of endogenous 14-3-3 ζ interacting proteins identifying 95 novel putative partners (Ge et al. 2010). This research has identified greater than 60 potential 14-3-3 ligands, which adds to the hundreds of ligands already identified through other studies (Jin et al. 2004; Pozuelo Rubio et al. 2004).

Here is a brief introduction to this ever increasing research field, with the most relevant areas highlighted with regards to the research presented.

1.1.1. Identification and Characterisation of 14-3-3 Proteins

The family of 14-3-3 proteins were first identified by Moore and Perez (1967). The proteins are named according to their migration positions on two-dimensional DEAE-cellulose chromatography ("14th" fraction) and starch gel electrophoresis ("3.3" inches). 14-3-3 proteins are small and acidic, with a molecular mass of 28-33 kDa (Toker et al. 1992). Despite being well known as an abundant brain protein, 14-3-3 proteins have now been found in almost all tissues, including heart and liver (Celis et al. 1990). The different isoforms display a range of isoform specificity, which is discussed in section 1.1.3.2. The location of 14-3-3 proteins is predominantly in the cytoplasmic compartment, however these proteins have also been detected in intracellular organelles including the Golgi apparatus and the nucleus as well as the plasma membrane (Celis et al. 1990). It is also well established that 14-3-3 protein expression is not confined to mammalian tissues, but have been

detected in all eukaryotic organisms and cells examined thus far (Aitken 2002; Fuller et al. 2006).

Studies by Jones and colleagues identified 14-3-3 proteins existing as dimers, fuelling theories that one function of 14-3-3 may be as an adaptor protein for signalling pathways (Jones et al. 1995a; Jones et al. 1995b). In addition, some 30 years ago, 14-3-3 was shown to activate tryptophan and tyrosine hydroxylases (Yamauchi et al. 1981; Ichimura et al. 1987). The first indication of 14-3-3 being a phosphorylation-dependent protein was discovered by Furukawa and colleagues when they observed that 14-3-3 activation of tyrosine hydroxylase required phosphorylation by a serine/threonine kinase (Furukawa et al. 1993). Subsequent studies into the phosphorylation-dependent nature of 14-3-3 led to the identification of the binding motif required for ligand binding with 14-3-3. A library of phosphorylated peptides was constructed by Muslin and colleagues based on Raf-1, indicating that 14-3-3 is a phosphoserine-binding protein (Muslin et al. 1996). This resulted in the binding motif being refined to RSXpSXP, whereby X is equal to any amino acid. This sequence motif is referred to as the mode I motif following the discovery of a second consensus motif (Yaffe et al. 1997). The second motif, known as mode II has been identified as RXXXpSXP. A third binding motif, mode III, which is also phospho-dependent has been identified as pS/T (X₁₋₂)-COOH (Ganguly et al. 2005).

Following the initial functional discovery for 14-3-3, a great many other attributes have been awarded to this promiscuous family of proteins. The discovery of the ability to activate tyrosine and tryptophan hydroxylases was shortly followed by the identification of 14-3-3 as a protein kinase C (PKC) inhibitor (Toker et al. 1992). 14-3-3 proteins were also found to interact with full-length c-Bcr and the BCR/Abl complex, indicating that 14-3-3 has a role in cell cycle control (Reuther et al. 1994) (see Figure 1.1). There are also a number of publications detailing the interaction between 14-3-3 and various kinases, including Raf-1, which support a role for 14-3-3 in signal transduction and as a 'protein scaffold' (Fantl et al. 1994; Freed et al. 1994; Fu et al. 1994; Liu et al. 1996; Honda et al. 1997; Fanger et al. 1998).

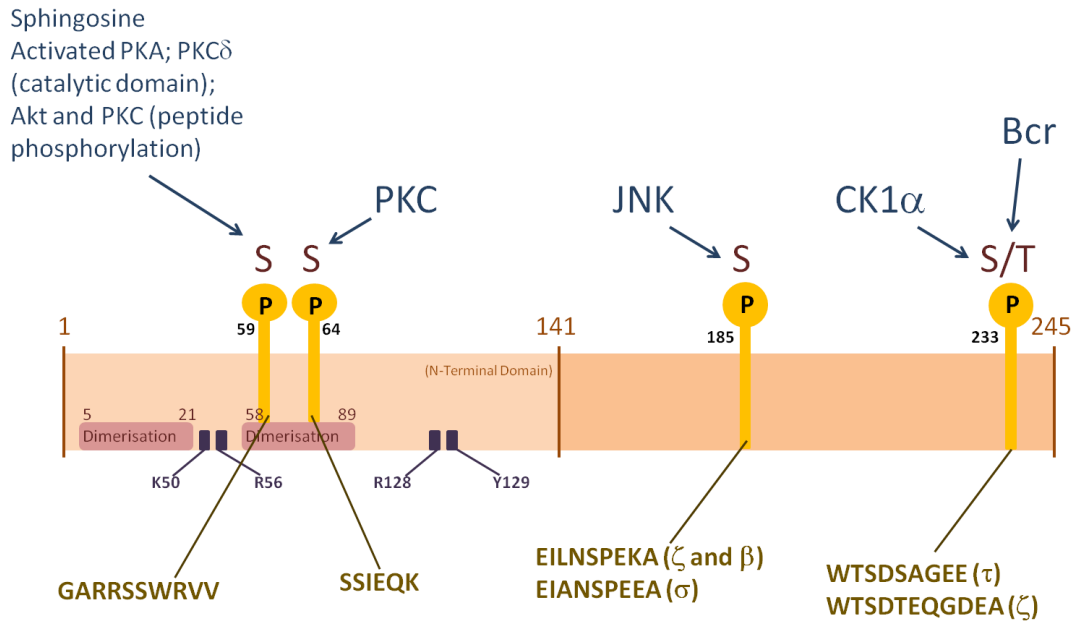


Figure 1.1: Schematic Diagram of 14-3-3 and Phosphorylation Sites

A number of kinases can phosphorylate 14-3-3. The phosphorylated residue (P) and the respective kinase(s) are highlighted. In addition, alternative sequences for different isoforms are detailed. The purple boxes represent residues which have been shown to be essential for phosphopeptide binding and the regions of the protein which are involved in dimerisation are also highlighted. This figure is updated from Aitken (2006).

The 1990s was an extremely prominent decade in 14-3-3 re-discovery. 14-3-3 proteins were found to interact in a phospho-independent manner (Fu et al. 1993; Petosa et al. 1998), regulate and interact with DNA (Hermeking et al. 1997; Todd et al. 1998; Chan et al. 1999), structural information was uncovered (Jones et al. 1995a; Liu et al. 1995; Xiao et al. 1995; Yaffe et al. 1997) and implications in neurodegenerative disease was discovered (Layfield et al. 1996; Ostrerova et al. 1999; Wiltfang et al. 1999). Since these developments, 14-3-3 research has further progressed, with greater establishment of a critical role in neurodegenerative disease (Waelter et al. 2001; Baxter et al. 2002; Chen et al. 2003; Mackie and Aitken 2005). The fact that 14-3-3 proteins display a range of functions including modulation of transcription, inhibition of apoptosis and regulation of the cell cycle and intracellular signalling pathways indicate that they are plausible therapeutic targets which should be approached with caution (Muslin and Xing 2000; Berg et al. 2003; Rosenquist 2003; Dougherty and Morrison 2004; Aitken 2006). The isoform

specificity of 14-3-3 proteins is detailed later which is an important factor to consider for therapeutic drug targeting.

1.1.2. The Crystal Structure of 14-3-3

The first crystal structures of 14-3-3 solved were those of 14-3-3 τ and 14-3-3 ζ (Liu et al. 1995; Xiao et al. 1995). Since then, the structures of all seven 14-3-3 isoforms have been solved in complex with bound ligands. These structures indicate that the proteins are dimeric and resemble a flattened horseshoe shape, containing a central channel, 35 Å long, 35 Å wide and 20 Å deep (see Figure 1.2). Each monomeric subunit is composed of nine anti-parallel α -helices with the four of the N-terminal forming the dimer interface and channel floor (Gardino et al. 2006). It is generally accepted that ligand binding occurs in the central channel which is also known as the amphipathic binding groove. The binding groove has a basic pocket which consists of two arginine and one lysine residues which are in contact with either a serine or threonine which is phosphorylated on the target. On one side of the groove, helices 3 and 5 comprise a cluster of charged and polar residues and on the other side of the groove, helices 7 and 9 comprise a patch of hydrophobic residues. It is important to note that the residues which form the groove are mainly conserved across the different 14-3-3 isoforms (Liu et al. 1995; Xiao et al. 1995; Yaffe et al. 1997; Petosa et al. 1998). Since many 14-3-3 ligands bind well to all isoforms, it was suggested that binding of 14-3-3 to target proteins was mediated through the conserved amphipathic groove and that the basic cluster of residues K49, R56 and R127 are required for interaction between 14-3-3 and the phospho-amino acid in the ligand (Liu et al. 1995). Mutational analysis (Zhang et al. 1997; Thorson et al. 1998; Wang et al. 1998) and co-crystallization studies (Yaffe et al. 1997; Petosa et al. 1998; Rittinger et al. 1999) have been employed to test this hypothesis. As residues on either side of the binding groove are required for 14-3-3 protein interactions, it has been proposed that dimeric 14-3-3 is essential for full functionality (Tzivion et al. 1998).

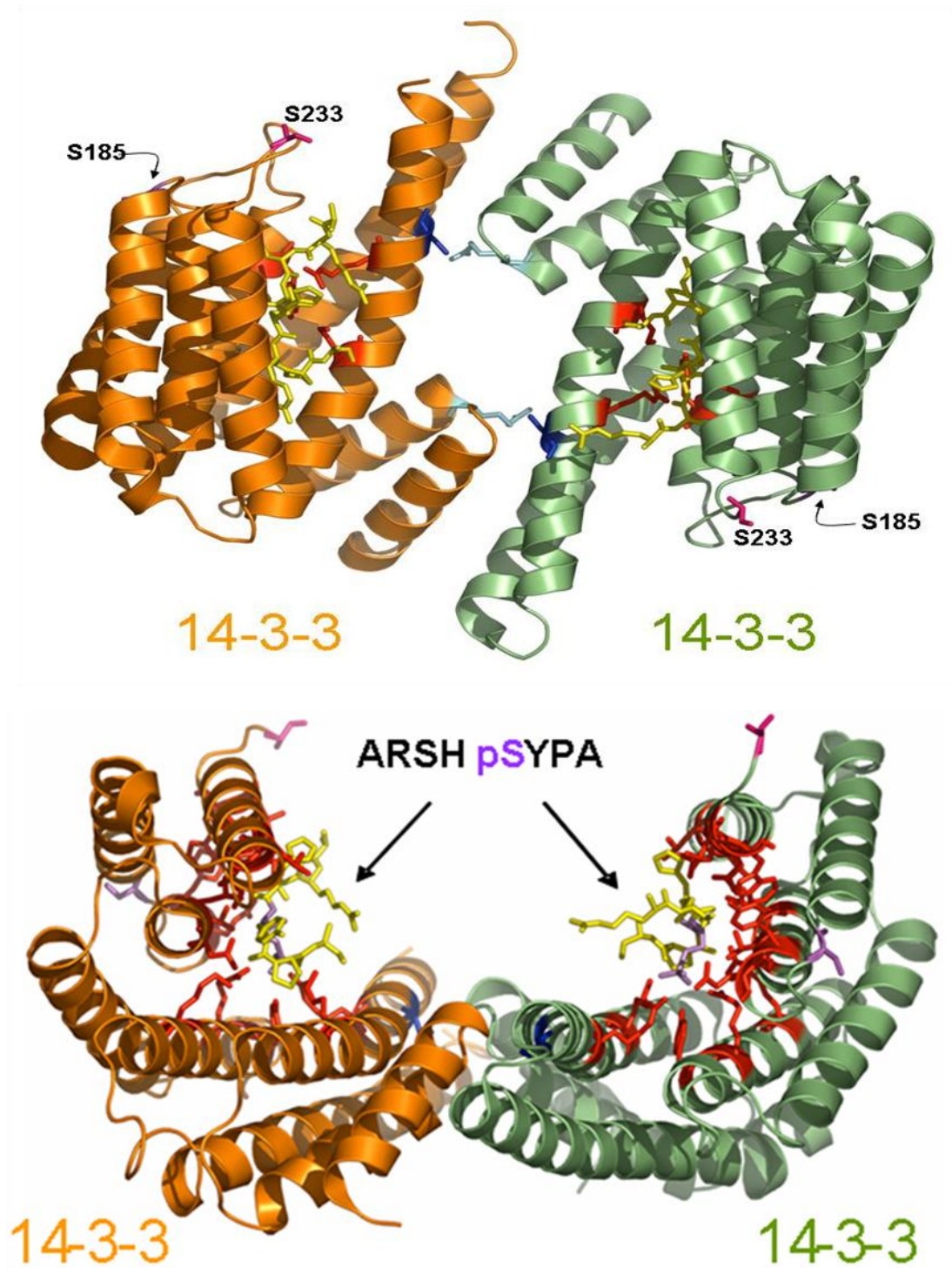


Figure 1.2: Structure of 14-3-3

Each of the 14-3-3 monomers in the above images is represented by a different colour. Each monomer has nine alpha helices and the basic pocket, which is in contact with a peptide, is represented by the red coloured residues. The peptide bound to the monomer is coloured yellow, with the phosphorylated serine purple. The mode of peptide binding presented is 'mode 1'. The top image is a 90° rotation of the lower image, which allows visibility of the dimer interface (Xiao et al. 1995; Yaffe et al. 1997; Rittinger et al. 1999).

Structural studies into 14-3-3 proteins have provided a wealth of knowledge into the mechanisms which allow 14-3-3s to interact with other proteins. Co-crystallization studies have shown that 14-3-3 binding peptides utilise the amphipathic binding groove, whether the peptide is phosphorylated or not. This is an extremely relevant piece of information with regard to research conducted in Chapter 5. One protein which can bind to 14-3-3 proteins in a phosphorylation independent manner is the ADP-ribosyltransferase Exoenzyme S (ExoS) from *Pseudomonas aeruginosa*. ExoS does require the presence of 14-3-3 for activation (Fu et al. 1993) and subsequent studies identified that 14-3-3 ζ binds to ExoS and that this interaction is required for ExoS activation (Masters et al. 1999). It has since been determined that the sequence DALDL in ExoS is essential for interaction with 14-3-3 (Henriksson et al. 2002). This sequence is also found in the unphosphorylated peptide R18 (with the sequence LDL) which is also a high affinity 14-3-3 binding peptide. This peptide was discovered by Fu and colleagues following the screening of a phage display library (Wang et al. 1999). Other proteins which bind to 14-3-3 in a phosphorylation independent manner include phospholipase A2, GP 1b alpha subunit of platelet membrane glycoprotein, Bax and p190RhoGEF (Aitken 2011). The interaction of 14-3-3 with these proteins does not utilise a phosphorylated serine or threonine residue to account for the interaction. The interaction sequences of these proteins share little similarity; however they have features of amphipathic helices consistent with 14-3-3 interaction.

Phosphorylation-independent interactions with 14-3-3 pose a problem with regard to the regulatory mechanism which phosphorylation provides. If a protein interacts with 14-3-3 in a phosphorylation-independent manner, what prompts the dissociation of the protein from 14-3-3? One possible suggestion was proposed by the group who identified the phospho-independent interaction of 14-3-3 with Bax (Nomura et al. 2003). They state that Bax phosphorylation was not identified to account for a phosphorylation-dependent interaction with 14-3-3. They suggest that Bax and 14-3-3 interact in healthy cells and following delivery of an apoptotic stimulus, interaction of a phosphorylated protein with 14-3-3 releases Bax protein.

The dimeric quaternary structure of 14-3-3 is mediated by the N-terminus of the protein and this has been demonstrated by crystallographic studies (Liu et al. 1995; Xiao et al. 1995). The dimer interface of 14-3-3 proteins is formed by the packing of helix 1 from one of the monomers against helices 3 and 4 from the other, producing a 6-8 Å hole in the centre. Buried in the dimer interface are a number of hydrophobic and polar residues (L12, A16, V62, I65 and Y82), which are highly conserved across mammalian 14-3-3 isoforms. This raises the suggestion of 14-3-3 proteins forming heterodimers, which is addressed in the following section (Jones et al. 1995a).

As 14-3-3 proteins are dimeric, this means they possess the ability to simultaneously bind two ligands. Utilising this function can have significant biological implications in a number of cellular processes. One possible purpose of this 14-3-3 function may be to modulate the activity of two different signalling proteins, by bringing them together. Alternatively, 14-3-3 dimerization may have an impact on subcellular localisation. One proposed theory is that one monomer of 14-3-3 functions as a targeting unit, binding an anchored ligand whilst the other monomer binds a 14-3-3 'cargo' protein. Examples of cargo proteins include Crm1, Cdc25 and the FOXOs, which are localised to the nucleus and cytoplasm respectively when bound to 14-3-3 (Rittinger et al. 1999). The interaction of these proteins with 14-3-3 alters the subcellular location of the 'cargo' for interaction with another protein in the same compartment. The site of the anchored ligand may aid in localising cargo proteins to specific intracellular compartments (Jones et al. 1995a; Huber et al. 2002; Yaffe 2002b).

1.1.3. 14-3-3 Isoforms

In mammals, there are seven isoforms of 14-3-3 (β , γ , ε , ζ , η , σ and τ); however, for the purposes of this research, the main focus will be on the five major brain isoforms of 14-3-3 (β , γ , ε , ζ , and η). In mammalian brain, two of these isoforms are phosphorylated on Ser185 (β and ζ) (Aitken et al. 1995b). The 14-3-3s are expressed in a number of tissues and account for 1% of total soluble brain protein (Boston et al. 1982). The different isoforms of 14-3-3 were named according to their reversed-phase HPLC positions (Ichimura et al. 1988).

The 14-3-3 family of proteins is highly conserved across a range of mammalian species and the isoforms are mainly identical, containing only a few diverse regions. The different isoforms and their alignment are shown in Figure 1.3.

1.1.3.1. Dimerisation and Phosphorylation

As previously stated, crystallisation of 14-3-3 proteins confirmed that they natively exist as dimers. As recombinant 14-3-3 proteins are always dimeric, this would suggest that the monomeric form is not thermodynamically favourable (Aitken et al. 2002). Yet, a recent study has found a novel splice variant of human 14-3-3 ε (named 14-3-3 epsilon sv) which, as a result of the splicing, has a deleted N-terminal α -helix (Han et al. 2010). As stated, this region is imperative for dimer formation (Jones et al. 1995b). GST pull-down and co-immunoprecipitation assays confirmed that the splice variant could not form a dimer with any of the other 14-3-3 isoforms. HEK293 cells were transfected with both the full length and the splice variant forms of 14-3-3 epsilon for 24 hours prior to UV irradiation. Flow cytometric analysis of the cells 24 hours post irradiation indicated that 14-3-3 epsilon sv could still prevent UV-induced apoptosis and therefore function as a monomer. This is at odds with other studies highlighting the importance of dimeric 14-3-3 for full functionality (Tzivion et al. 1998; Yaffe 2002a; Messaritou et al. 2010).

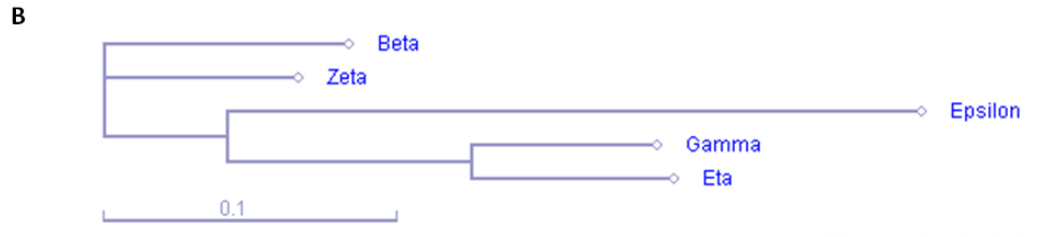
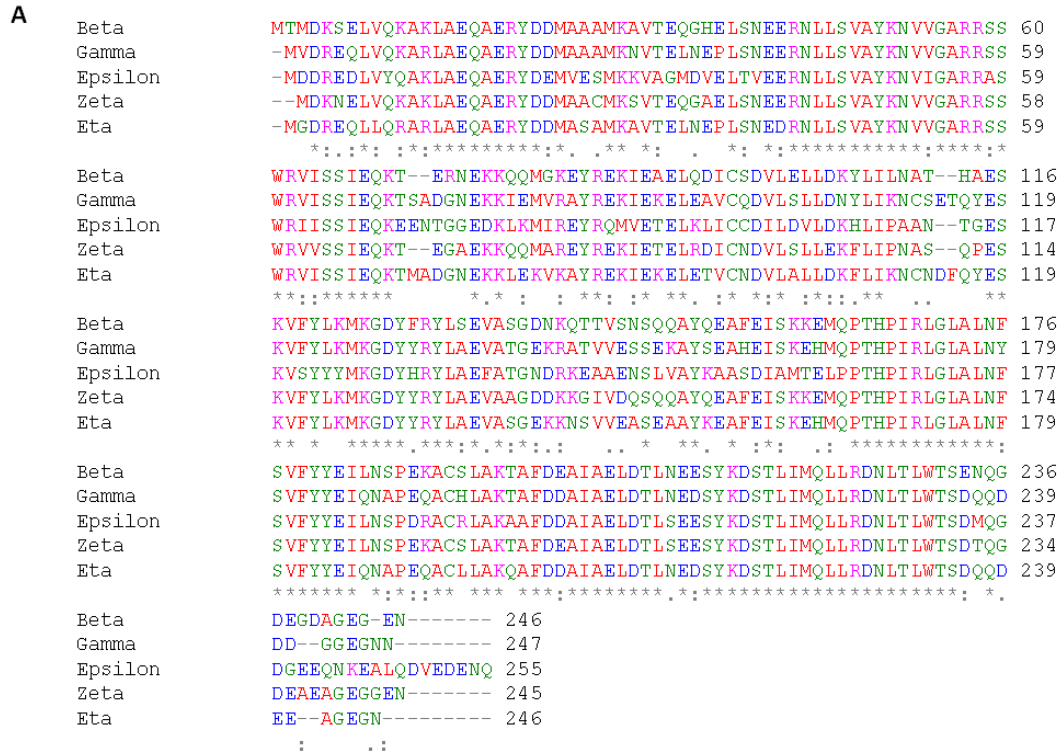


Figure 1.3: Alignment of Brain 14-3-3 Isoforms

A. Sequences of 14-3-3 brain isoforms aligned using the ClustalW server (<http://www.ebi.ac.uk/Tools/msa/clustalw2/>). Residues are coloured according to their physicochemical properties. AVFPMILW = Small (small + hydrophobic (incl. aromatic -Y)); DE = Acidic; RK = Basic; STYHCNGQ = Hydroxyl + Sulfhydryl + Amine + G. Characters on bottom row indicate the following:
 * = position of single, fully conserved residue;
 : = conservation between groups of strongly similar properties;
 . = conservation between groups of weakly similar properties.

B. Phylogenetic tree indicating the relationship between the different 14-3-3 isoforms generated using the facility at <http://pir.georgetown.edu/pirwww/index.shtml>. It is clear that beta and zeta isoforms are very similar, as are gamma and eta, with 14-3-3 epsilon being the most distinct brain isoform of 14-3-3.

14-3-3 proteins not only form homo-dimers, they also form hetero-dimers. This was discovered through cross-linking and co-immunoprecipitation studies which identified that 14-3-3 τ and 14-3-3 ζ can dimerise *in vitro* and 14-3-3 ϵ and 14-3-3 ζ dimerise *in vivo* (Jones et al. 1995a). Co-immunoprecipitation studies were conducted by transfecting myc-tagged 14-3-3 ϵ into COS cells to interact with endogenous 14-3-3 which had been overexpressed. As only little endogenous 14-3-3 co-immunoprecipitated with the tagged 14-3-3, it was concluded that 14-3-3 dimerisation is stable and not readily exchangeable.

More in-depth analysis of the heterodimers which 14-3-3 can form was conducted in PC12 cell lines which had been stably transfected with myc-tagged 14-3-3 ϵ and γ (Chaudhri et al. 2003). The results of these studies confirmed that 14-3-3 γ did dimerise with all endogenous 14-3-3 isoforms and also homodimerise. However, the strongest dimerization was detected between myc-tagged 14-3-3 γ and 14-3-3 ϵ . In stark contrast, the authors observed myc-tagged 14-3-3 ϵ dimerising with all endogenous 14-3-3 isoforms tested (β , η , γ and ζ) apart from endogenous 14-3-3 ϵ . There has been a suggestion as to why the ϵ isoform of 14-3-3 does not homodimerise well. Structural studies indicate that homodimerised 14-3-3 ζ is stabilized through three salt bridges in each half of the dimer interface. However, in 14-3-3 ϵ , only one of these salt bridges is present in the homodimer. This information led Gardino and colleagues to suggest that in order to increase the number of salt bridges and therefore stabilise the dimer interface, 14-3-3 ϵ preferentially dimerises with other 14-3-3 isoforms (Gardino et al. 2006).

The ability of 14-3-3 proteins to form heterodimers appears to be a conserved feature, as *Saccharomyces cerevisiae* 14-3-3 homologues BMH1 and BMH2 have also been found to exist mainly as heterodimers (Chaudhri et al. 2003). In keeping with the theory proposed on the ability of 14-3-3 to bind two ligands; one function which heterodimeric forms of 14-3-3 may have is to bring two distinct signalling proteins together which would bind specifically to different isoforms of 14-3-3 (Aitken et al. 2002). Functional relevance of homodimers may therefore be to alter the cellular localisation or activity of specific proteins.

One very important aspect of 14-3-3 heterodimerisation which should be addressed is the implications of heterodimers with the phosphorylated isoforms of 14-3-3; α and δ . The α and δ isoforms of 14-3-3 are the phosphorylated forms of β and ζ respectively. These proteins are phosphorylated by up to 50% in brain and this is the only tissue where these isoforms of 14-3-3 have been detected to date (Aitken et al. 1995b). One aspect which makes these isoforms all the more interesting is the fact that not all of the 14-3-3 isoforms contain this phosphorylation site, indicating that phosphorylation on Ser185 is an isoform-specific regulatory mechanism.

Following the identification of the phospho-forms, a function was soon attributed to them. Aitken and colleagues discovered that the phosphorylated isoforms improved the ability of 14-3-3 proteins to inhibit PKC two-fold (Aitken et al. 1995a). It has since been identified that Ser185 on 14-3-3 β , σ and ζ is phosphorylated by the stress activated Jun N-terminal kinase (JNK) (Tsuruta et al. 2004). Phosphorylation of these isoforms has serious consequences for apoptosis regulation by disrupting their interaction with pro-apoptotic proteins Bax, Bad, FOXO3a and c-Abl. This results in the release of these proteins into the cytoplasm to induce pro-apoptotic signalling (Tsuruta et al. 2004; Sunayama et al. 2005; Yoshida et al. 2005).

Other phosphorylation sites on 14-3-3 isoforms include Thr233 (14-3-3 ζ) and Ser233 (14-3-3 τ) which are mediated by casein kinase I α (CKI α) and the breakpoint cluster region (BCR) kinase, respectively (see Figure 1.1) (Dubois et al. 1997; Clokie et al. 2005). Phosphorylation of these sites appears to be isoform-specific. As only the non-phosphorylated form of 14-3-3 ζ had previously been shown to bind to Raf-1 in HEK cells (Rommel et al. 1996), the authors of the CKI α study concluded that 14-3-3 ζ phosphorylation on Thr233 is likely to negatively regulate interaction with Raf-1. There are also reports in the literature of 14-3-3 proteins having an additional phosphorylation site on Ser58 (Megidish et al. 1998). The phosphorylation of this site has been attributed to the activity of kinases including Sphingosine Dependent Kinase 1 (SDK1), PKB/Akt, caspase-cleaved PKC δ and PKA (Megidish et al. 1998; Powell et al. 2002; Hamaguchi et al. 2003; Woodcock et al. 2003; Ma et al. 2005). As this residue is buried deep within the dimer interface, it would not be expected to be

exposed given the stable formation of the 14-3-3 dimer. Woodcock and colleagues have investigated the implications which phosphorylation of this site has on dimer formation (Woodcock et al. 2003; Woodcock et al. 2010). This topic is of particular interest and is detailed and investigated further in Chapter 3.

1.1.3.2. Isoform-Specific Functions of 14-3-3 Isoforms

The majority of organisms investigated to date express more than one homologue of 14-3-3; *Saccharomyces cerevisiae* expresses only two isoforms of 14-3-3, whereas *Arabidopsis thaliana* expresses around thirteen 14-3-3 isoforms. The evolutionary conservation of multiple 14-3-3 isoforms has been explained and discussed by Rosenquist (et al. 2000). Here, the authors discuss common suggestions regarding 14-3-3 isoform specificity, including the possibility that all isoforms of 14-3-3 bind with relatively equal specificity to binding targets, and express very little isoform specificity. This theory has been supported through studies with *Arabidopsis thaliana* 14-3-3 isoforms, which were expressed in yeast and replaced all endogenous 14-3-3 (van Heusden et al. 1996). Despite these findings, the authors also discussed studies which disputed this theory. Another two *Arabidopsis thaliana* studies support the prospect of 14-3-3 isoform specificity. There were significant differences identified between five 14-3-3 isoforms to inhibit nitrate reductase (Bachmann et al. 1996) and nine isoforms displayed different affinities for a C-terminus peptide from the plant plasma membrane H⁺-adenosine triphosphatase (Rosenquist et al. 2000). Other possibilities to account for the conserved evolution of 14-3-3 isoforms include ensuring a high level of protein is available to conduct various cellular processes. Should a large amount of protein be required, by increasing the number of genes which encode that protein, this required quantity can be met. Another suggestion is that the different isoforms may be targeted to specific subcellular compartments, or are specifically expressed in different tissues. Finally, 14-3-3 isoforms may interact with a specific subset of binding partners, which would help to account for the diverse range of functions attributed to 14-3-3.

Table 1.1 lists a selection of mammalian proteins for which 14-3-3 isoforms display a range of isoform specificity. The majority of the studies involved yeast two hybrid screens or co-immunoprecipitation and 'pull-down' assays. However, as 14-3-3 proteins form heterodimers as well as homodimers (see section 1.1.3.1) this complicates determining isoform specific interactions. To overcome this issue, most of the studies involved over-expressing the 14-3-3 isoform of interest to produce homodimers. One potential issue with this method is that the physiological relevance of the interaction may be compromised, as natively, the 14-3-3 of interest may preferentially be heterodimeric. However, testing the functional specificity of heterodimers is a more challenging task. One main caveat of the studies listed in Table 1.1 is the poor range of isoform investigation; most have studied only a few isoforms and some do not report on isoform specificity. This is a factor which has been addressed in more recent studies and the results to date do provide an insight into mammalian 14-3-3 isoform specificity.

It is clear that particular interactions incur greater isoform specificity, although generally more than one isoform can bind a certain protein with varying affinities. The 14-3-3 isoforms found to interact with the proteins detailed in Table 1.1 are listed in order of isoform specificity.

An interesting observation highlighted by these studies is the way in which related 14-3-3 isoforms interact with other proteins. Figure 1.3B is a phylogenetic tree analysing the relationship between the different brain isoforms of 14-3-3. This shows that the β and ζ isoforms are very similar and γ and η are highly related, with ϵ sharing the least similarity between the other 14-3-3 isoforms. One would expect then that similarly related isoforms would behave and interact in a similar manner also. For a number of cases, this is true; A20, ADAM22, AKAP-lbc, CamKII, CDC25B, p27, PKC ζ and Raf-1. There appears to be greater consistency with β and ζ isoforms, however the same cannot be said of 14-3-3 γ and η . This is evident from 14-3-3 isoform interactions with A20 and ADAM22. Whilst both highly related β and ζ 14-3-3 interact with these proteins, 14-3-3 η also interacts with them; however

Table 1.1: Selected Isoform-Specific 14-3-3 Protein Interactions

Protein	14-3-3 Isoform(s)	Reference
A20	$\eta, \epsilon, \beta, \zeta$	(Vincenz and Dixit 1996)
ADAM22	$\zeta, \beta, \epsilon, \eta$	(Zhu et al. 2003; Zhu et al. 2005)
AKAP-lbc	β, ϵ, ζ	(Diviani et al. 2004)
Ataxin-1	ϵ, ζ	(Chen et al. 2003)
CamKII	$\eta, \gamma, \zeta, \text{slight } \tau$	(Davare et al. 2004)
Cbl	τ	(Liu et al. 1997)
CBP501	$\epsilon, \beta, \tau, \text{slight } \gamma, \zeta$	(Matsumoto et al. 2011)
Cdc2/cyclin B1	σ	(Chan et al. 1999)
CDC25B	$\eta, \beta, \zeta, \tau, \epsilon \text{ slight}$	(Mils et al. 2000; Manke et al. 2005)
CDC25C	γ, ϵ	(Chan et al. 1999; Dalal et al. 2004)
CDK11 ^{P110}	$\beta, \gamma, \epsilon, \tau, \text{slight } \zeta$	(Feng et al. 2005)
CLIC4	ζ, ϵ	(Suginta et al. 2001)
ER α	β	(Kim et al. 2011)
GR	η	(Wakui et al. 1997)
IGF-1	ϵ	(Craparo et al. 1997)
KSR1	$\gamma, \eta, \beta, \zeta, \tau$	(Jagemann et al. 2008)
MYPT1	β, ϵ, ζ	(Koga and Ikebe 2008)
NFAT	τ (5x greater), ζ	(Chow and Davis 2000)
PMCA4	ϵ	(Rimessi et al. 2005)
P27 ^{Kip1} (p27)	$\beta, \epsilon, \gamma, \tau, \zeta \text{ slight}$	(Sekimoto et al. 2004)
Par3 α/β	$\tau, \epsilon, \zeta, \beta \text{ slight}$	(Izaki et al. 2005)
Parkin	η	(Sato et al. 2006)
PKC ζ	$\tau, \gamma, \zeta, \epsilon, \beta, \eta$	(Van Der Hoeven et al. 2000)
p53	ϵ, γ, τ and σ	(Rajagopalan et al. 2010)
Raf-1	β and ζ	(Fantl et al. 1994; Freed et al. 1994)

The isoforms are listed in order of specificity. Where only one isoform is listed, generally that isoform was selected from a screen (e.g. yeast two hybrid) or proteomic study (identification by mass spectrometry). Not all 14-3-3 isoforms were necessarily tested per study. Abbreviations: A20 – zinc finger protein; ADAM22 – A disintegrin and metalloproteinase 22; AKAP-lbc – A-kinase anchoring protein-lbc; CamKII – Calcium and calmodulin-dependent kinase kinase; Cdc2 – cell division cycle 2 protein; CDC25C – cell division cycle 25C protein; CDK11 – cyclin dependent kinase 11; CLIC4 – chloride intracellular channel 4; ER α – estrogen receptor α ; GR – glucocorticoid receptor; IGF-1 – Insulin growth factor 1 receptor; MYPT1 – myosin-binding large subunit; NFAT – nuclear factor of activated T cells; PMCA4 – plasma membrane calcium pump.

there is no interaction with 14-3-3 γ . Instead, there is greater preference of interaction with 14-3-3 ϵ , which shares least similarity with the other isoforms. This does appear to be a running theme, with a number of interactions showing specificity for η and ϵ isoforms and not γ . What is also interesting is the number of interactions with 14-3-3 ϵ , indicating that this protein has a number of overlapping properties with other isoforms, despite displaying the lowest level of sequence similarity. It may be that we have yet to discover 14-3-3 ϵ specific functions.

There have also been studies into heterodimer-specific 14-3-3 interactions. Most importantly, these have been focussed on the implications on signalling complex formation as a result of preferential 14-3-3 heterodimer formation (Jagemann et al. 2008; Liang et al. 2008; Fischer et al. 2009; Kligys et al. 2009). The Jones group identified a preference of 14-3-3 ζ/τ dimers to interact with the SSH1 (Slingshot) phosphatase which is involved in keratinocyte migration (Kligys et al. 2009). Another group looked at the potential of both homo- and heterodimers of 14-3-3 to associate with Raf kinases (Fischer et al. 2009). The authors concluded that whilst Raf- A, B and C were studied, Raf-B had the strongest interaction with 14-3-3 isoforms and the presence of 14-3-3 ϵ suggested that 14-3-3 proteins studied were heterodimeric (Fischer et al. 2009). The location of the RAF proteins also impacts on their interaction with 14-3-3 proteins. The study found that Raf-A interacted least with 14-3-3 isoforms when analysing homodimers and this was also consistent in studies with heterodimers. Raf-B and Raf-C expressed in *Saccharomyces cerevisiae* associated with both homo- and heterodimeric forms of 14-3-3 (Fischer et al. 2009).

Salt and water homeostasis in epithelial sodium channels is also dependent on heterodimeric 14-3-3 (Liang et al. 2008). Knockdown studies of 14-3-3 isoforms revealed that a heterodimer of 14-3-3 β/ϵ is required for aldosterone regulation (Liang et al. 2008). Finally, one important 14-3-3 interaction is with the molecular scaffold kinase suppressor of Ras 1 (KSR1) and studies have shown that interaction is preferentially with 14-3-3 γ , both homodimeric and heterodimeric forms (Jagemann et al. 2008). The authors found that KSR1 binds to, and can be regulated

by, 14-3-3 γ heterodimers with 14-3-3 τ and ζ , however the role of different heterodimers in KSR1 regulation was not explored (Jagemann et al. 2008).

These studies indicate that the ability of different isoforms of 14-3-3 to heterodimerise has a profound impact on a variety of cellular processes and further investigation may yield more information on the isoform-specific importance of these proteins.

1.1.4. 14-3-3 and Neurodegenerative Diseases

14-3-3 proteins are predominantly found in the brain and the two phosphorylated isoforms of 14-3-3 are only detected in brain tissue. The high level of these proteins in brain suggests that they play an important role in a number of vital neuronal regulatory processes. This alone indicates that 14-3-3 proteins are likely to be crucial in neurodegenerative diseases and many research groups have identified a number of links with 14-3-3 proteins and neurodegeneration. A summary of the main neurodegenerative diseases and the role of 14-3-3 proteins follow.

1.1.4.1. Alzheimer's disease (AD)

The German psychiatrist and neuropathologist Alois Alzheimer (1864-1915) first described the disease which bears his name in 1907 following investigation of the patient Auguste D (Alzheimer 1907; Alzheimer et al. 1995). He reported that this 51-year-old female presented a "*strange disease of the cerebral cortex*" and reported that she presented symptoms of presenile dementia, displaying nerve cell loss, diffuse cortical atrophy and the characteristic plaques and tangles associated with the disease. It was his then colleague and director at the Munich psychiatric clinic, Emil Kraepelin, who named this condition as 'Alzheimer's disease'.

Nowadays, Alzheimer's disease is known as the most common form of progressive dementia, affecting millions of people worldwide. This neurodegenerative disease is characterized by the presence of β -amyloid plaques and neurofibrillary tangles which accumulate in the brains of patients (Glennner and Wong 1984; Goedert et al. 1988; Wischik et al. 1988). The majority of cases of AD are sporadic, however there are a small number of cases which occur through autosomal-dominant inheritance and the majority of these cases occur before the age of 65 (Terry and Davies 1980). Patients who develop AD before the age of 65 are classed as having 'presenile' or 'early-onset' dementia and patients developing the disease after the age of 65 are classed as having 'senile' or 'late-onset' dementia.

Four genes have been identified which can cause AD. The proteins which these genes encode are the presenilins (PSEN1 and PSEN2), amyloid precursor protein (APP) and Apolipoprotein E (ApoE). Mutations in the presenilins and APP lead to the production of amyloidogenic β -amyloid, which accumulates in neurons and forms the characteristic plaques. These three genes are typically associated with early-onset familial AD and are discussed in more detail later in this section. ApoE mutations are associated with late-onset familial AD. This protein has a role in cholesterol redistribution and is discussed in detail in section 1.2.3.1.

A link between AD and 14-3-3 has been identified. Layfield and colleagues identified 14-3-3 proteins in the neurofibrillary tangles (NFT) of AD brains (Layfield et al. 1996). In particular, 14-3-3 ϵ and γ have been identified through co-precipitation studies to bind to A β (β -amyloid) in rabbit brains (whose A β sequence is identical to human) and mass spectrometry analysis of rabbit and mouse brains identified 14-3-3 ϵ , ζ and η isoforms (Nelson and Alkon 2007).

14-3-3 ζ is also implicated in the tau phosphorylation complex (Agarwal-Mawal et al. 2003). Tau is a microtubule binding protein which, when hyperphosphorylated, forms neurofibrillary tangles. The interaction between glycogen synthase kinase 3 β (GSK3 β) and tau has been proposed to be mediated by 14-3-3, resulting in increased phosphorylation. However, 14-3-3 association with tau and GSK3 β has been identified in a 400-500 kDa protein complex; much larger than the combined sizes of these three proteins at ~167 kDa. This suggests that 14-3-3 alone is not likely to be the sole modulator of this interaction. In addition, both GSK3 β and tau are proteins of reasonable size; 47 and 60 kDa respectively. Given the size of these two proteins, it would rather difficult for both of these proteins to fit into the binding groove of 14-3-3 at the same time. The authors only investigated the role of 14-3-3 in the tau phosphorylation complex, so the roles of other proteins in this complex are unknown. The increased phosphorylation observed in this study may be due to the localisation function of 14-3-3, relocating one or both of these proteins independently to aid in the phosphorylation of tau by GSK3 β .

Additionally, 14-3-3 ζ binds to unphosphorylated tau protein at a binding site on the C-terminal microtubule binding domain (Hashiguchi et al. 2000). One group investigated the effects of tau phosphorylation on 14-3-3 ζ binding. Sadik and colleagues discovered that *in vitro* phosphorylation of tau with a range of kinases (PKA, PKB, GSK3 β , CDK2 and CK1) altered 14-3-3 ζ association (Sadik et al. 2009). They found that there was a ~2.5-fold increase in 14-3-3 ζ association with tau protein phosphorylated with PKA or PKB compared to unphosphorylated protein. Phosphorylation with the other kinases did not result in any significant change in 14-3-3 ζ association compared to unphosphorylated protein. The authors concluded that 14-3-3 has a higher affinity for phosphorylated tau protein and that phosphorylation by PKA or PKB generates a phosphorylation-dependent binding site at the N-terminal projection domain for 14-3-3 interaction. They also investigated the other brain 14-3-3 isoforms for association with phosphorylated tau and found that in addition to 14-3-3 ζ , both the β and η isoforms of 14-3-3 are involved in phosphorylation dependent and independent association with tau. In addition, tau phosphorylation creates an additional 14-3-3 binding site. This binding site only becomes available at the N-terminus of the protein following phosphorylation by PKA or PKB (Sadik et al. 2009). This comprehensive study identified this additional phosphorylation site on tau as Ser214 which is present in rat brain and co-immunoprecipitates with 14-3-3 *in vivo*. 14-3-3 interaction at this site reduces tau aggregation, prompting the authors to suggest that the interaction may change the conformation of tau to maintain it in a non-aggregated state (Sadik et al. 2009).

The presenilins (PSEN 1 and 2) and APP are the three proteins which have pathogenic mutations which contribute to familial forms of AD (Hardy 1997). PSEN1 is involved in the regulation of APP, which affects the size of β -amyloid (A β) fragments produced. A β_{1-40} is non-amyloidogenic, but A β_{1-42} is amyloidogenic. PSEN1 interacts with δ -catenin (also known as NPRAR (neural plakophilin-related arm-repeat protein) or neurojungin) (Tanahashi and Tabira 1999) as does 14-3-3 ζ in a phospho-dependent manner (Mackie and Aitken 2005). Mutation of Ser1072 on δ -

catenin abolishes binding of 14-3-3 in both transfected cells and *in vitro*. Despite this connection having no pathophysiological role in AD, it does support another link between 14-3-3 and neurodegenerative diseases.

1.1.4.2. Parkinson's disease (PD)

The condition known as 'Parkinson's disease' was first described by the physician James Parkinson in 1817 as a form of 'shaking palsy'. However, the first European reference of the disease was actually in the late 16th century by William Shakespeare, who referred to the disease as 'palsy' of old age in several of his plays (Stien 2005). PD is mainly classed as a sporadic disease, yet extremely few environmental factors or triggers have been identified to date (Tanner 2003; Taylor et al. 2005; Dick et al. 2007). Most cases of PD present at 60 years of age and typically last about 15 years before the patient dies from the disease, most commonly from pneumonia (reviewed in Lees et al. 2009). PD is characterised by bradikinesia, which is a reduction in speed of initial voluntary movements which progressively reduce in speed, amplitude or repetition; resting tremor, muscle rigidity and postural instability. Pathophysiologically, PD is characterised by depletion of dopaminergic neurons of the substantia nigra pars compacta (SNpc) and the presence of intracellular inclusions, including Lewy bodies, in various areas of the brain, including the SN, hypothalamus, brain stem, hippocampus and the cortex (Nussbaum and Polymeropoulos 1997).

The first connection between Parkinson's disease and 14-3-3 was shown by Ostrerova and colleagues (et al. 1999) when they suggested that 14-3-3 and the PD-disease protein α -synuclein share 40% sequence homology over a limited part of their sequence. They also discovered that α -synuclein interacts with 14-3-3 and ligands of 14-3-3, leading to over-expression and toxicity. Further investigation into the shared interactions of 14-3-3 and α -synuclein revealed that dopamine homeostasis is disrupted due to reduced α -synuclein levels as a result of aggregation (Perez et al. 2002). The levels of 14-3-3/ α -synuclein complexes are

increased in dopaminergic neurons in the SN, indicating that 14-3-3 contributes to dopamine dependent neurotoxicity through selective vulnerability of dopaminergic neurons (Xu et al. 2002). 14-3-3 is also sequestered into Lewy bodies by α -synuclein, possibly preventing the anti-apoptotic role of 14-3-3 (Kawamoto et al. 2002).

A recent study has found a neuroprotective quality of 14-3-3 in PD (Yacoubian et al. 2010). In an α -synuclein transgenic mouse model, mRNA expression for a number of 14-3-3 isoforms (ϵ , γ and θ) was down-regulated; leading to the conclusion that reduced expression is a key factor in PD progression. This was supported by the fact that over-expression of these same isoforms resulted in a neuroprotective effect; by reducing the formation of α -synuclein inclusions and protecting against chemical inducers of PD in various dopaminergic cell lines (Yacoubian et al. 2010). These results support the theory that 14-3-3 sequestration into Lewy bodies can have a significant impact on α -synuclein toxicity.

Another aspect which links 14-3-3 with PD is through 14-3-3 η interaction with the disease protein parkin (Sato et al. 2006). The linker region of parkin ubiquitin ligase contains a 14-3-3 binding sequence, allowing interaction with 14-3-3 η . Binding of 14-3-3 to the linker region suppressed ubiquitin ligase activity. The authors also noted that α -synuclein relieved this negative regulation of parkin through sequestration of 14-3-3 η . This led the authors to conclude that 14-3-3 η is a regulating protein which links α -synuclein with parkin in PD pathogenesis (Sato et al. 2006).

Finally, 14-3-3 has been shown to interact with the leucine-rich repeat protein kinase 2 (LRRK2), whereby genetic mutations predispose patients to develop PD (Nichols et al. 2010). When this enzyme is phosphorylated on Ser910 and Ser935, interaction with 14-3-3 occurs, preventing aggregation of LRRK2. Recent studies have shown that a number of PD mutations alter this phosphorylation state, disrupting the interaction of LRRK2 with 14-3-3 (Li et al. 2011b). *In vivo* analysis has shown that disrupting 14-3-3 interaction with LRRK2 alters the cytoplasmic localization of LRRK2, leading to the formation of inclusion bodies (Nichols et al. 2010). These studies indicate that 14-3-3 interaction with LRRK2 is vital in preventing neurotoxic accumulation of LRRK2 aggregates.

Collectively, the studies presented here suggest that whether by direct or in-direct methods, 14-3-3 proteins play a major role in the pathogenesis of PD.

1.1.4.3. Huntington's disease (HD)

The condition referred to as 'Huntington's disease' first gained attention following the reports by Osler (1893). He was referring to the original transcripts of George Huntington (Huntington 1872) after whom the disease is named. Huntington's observations on the disease were those of a hereditary form of chorea which he found to exist "*almost exclusively on the east end of Long Island*". It was not until 20 years later that Osler gave the disease the attention it deserves. In 1932, Vessie (1932) investigated the ancestry of the families whom Huntington studied and identified that 1,000 cases across 12 generations descended from 2 brothers in Suffolk, England.

HD is an autosomal-dominant, progressive neurodegenerative disease, characterised by a distinct phenotype of chorea, dystonia, cognitive decline, poor coordination and behavioural difficulties. The disease typically presents around middle-age, however due to the genetic nature of the disease, age of onset can be at any time (reviewed in Walker 2007). HD is one of the polyglutamine-repeat diseases, resulting from an expanded polyglutamine tract in the protein huntingtin (htt). The length of this tract is inversely correlated with age of onset of disease. This expanded protein can form intranuclear and intracytoplasmic inclusions, which are comprised of a number of proteins, including α -synuclein and 14-3-3 (Waelter et al. 2001).

In HD, GABA (gamma aminobutyric acid) receptor expression is increased (Cepeda et al. 2004). It is the GABAergic neurons of the basal ganglia which are most vulnerable in HD and dysfunction results in the choreal symptoms witnessed in patients. There is no evidence to suggest that levels of 14-3-3 are altered in HD disease models, however reduced 14-3-3 ζ binding to GABA_BR1 receptor subunits has been discovered (Couve et al. 2001). The interaction of 14-3-3 with the GABA_BR1

subunit prevents dimerization of GABA_BR1 and GABA_BR2; a step vital for eliciting agonist response (Bowery and Enna 2000; Filippov et al. 2000). This suggests that functional expression of GABA receptors is involved in HD pathogenesis, leading to neurodegeneration. In addition, 14-3-3 interacts with huntingtin-associated protein 1 (HAP1) (Rong et al. 2007), which regulates the trafficking of GABA receptors to the membrane from the endoplasmic reticulum; another factor which is disrupted in HD (Twelvetrees et al. 2010).

Waelter and colleagues (et al. 2001) studied aggresome-like inclusions in human 293 Tet-Off cells and found that they contained ubiquitinated mutant huntingtin and 14-3-3 proteins. They concluded that the inclusions were neurotoxic, causing ultrastructural changes and were formed as a result of failure in proteasomal degradation (Waelter et al. 2001). Since then, it has been shown that 14-3-3 interaction with the N-terminal domain of huntingtin is critical for aggresome formation and targeting (Wang et al. 2009).

There is further information regarding the role of 14-3-3 and the formation of huntingtin aggregates from transfection studies. A study in N2A cells identified interaction between 14-3-3 β , γ , η and ζ with the N-terminus of polyglutamine expanded huntingtin (Omi et al. 2008). This investigation found that suppression of siRNA for 14-3-3 ζ prevented aggregate formation; however the same could not be shown for the other 14-3-3 isoforms. The authors concluded that 14-3-3 ζ participates in the aggregation of non-native, aggregation-prone proteins under non-native conditions (Omi et al. 2008).

Finally, 14-3-3 proteins play a role in the transcriptional status of the huntingtin protein in HD. It has been shown that Huntington's disease binding protein 2 (HDBP2) interacts with 14-3-3 β , a factor which influences the subcellular localization of HDBP2 (Sichtig et al. 2007). This has implications on the expression of huntingtin, as it has been previously shown that HDBP2 regulates gene expression of huntingtin in neuronal cells (Tanaka et al. 2004).

1.1.4.4. Creutzfeldt-Jakob Disease (CJD)

CJD, along with Gertsmann-Straussler disease, fatal familial insomnia and kuru are forms of human prion disease. Approximately 15% of prion disease cases are inherited through mutations in the PRNP gene and the other cases of disease are either acquired or sporadic. The worldwide incidence of CJD is 0.5-1 case per million population (Alperovitch et al. 1994). The majority of human prion disease cases are sporadic however variant CJD (vCJD) can be acquired in humans from cattle infected with bovine spongiform encephalopathy (BSE), the variation of the disease in cattle (Ironsides et al. 1996; Will et al. 1996). The disease is known as scrapie in sheep.

CJD is a transmissible spongiform encephalopathy (TSE). It is a rapidly progressing fatal central nervous system disorder which is characterised by rapidly progressing dementia and in more than 90% of cases, patients die within a year of displaying disease symptoms (Brown et al. 1994). The transmissible agent of the disease has been termed as a proteinaceous infectious agent; also known as prion (Prusiner 1982) and the normal mammalian cellular gene coding for the prion protein (PrP) has been identified (Oesch et al. 1985).

The first indications of a link between 14-3-3 and CJD were uncovered from a screen for protein markers in cerebrospinal fluid (CSF) for pre-mortem diagnosis (Harrington et al. 1986; Hsich et al. 1996). The original assumption for the presence of 14-3-3 in the CSF was assumed to be due to a leakage of brain proteins from a massive neuronal disruption (Hsich et al. 1996). The authors also concluded that the rate of neuronal destruction should be proportional to the quantity of 14-3-3 present. Since then, much more has been learnt about the significance of 14-3-3 proteins in the CSF of CJD patients. Kenney and colleagues discovered that the concentration of 14-3-3 in the CSF of CJD patients is actually considerably higher than in patients suffering from other neurodegenerative diseases (Kenney et al. 2000). Now, a CSF assay for 14-3-3 proteins is a standard procedure for diagnosing CJD and remains the highest diagnostic tool in CJD (WHO 1998). Comprehensive studies have also been conducted to identify that the 14-3-3 isoforms which appear

in the CSF are β , γ , ϵ and η (Wiltfang et al. 1999). This provides some degree of differentiation between which isoforms of 14-3-3 are specific to CJD from other neurodegenerative diseases.

Further to their identification in the CSF, the distribution of 14-3-3 proteins is also significantly altered in scrapie-infected murine brain (Baxter et al. 2002). This study, conducted in an established rodent scrapie model, immunolabelled different 14-3-3 isoforms to identify their localisation in normal and scrapie-affected brain. One difference observed from immunoblot analysis of brain extracts from both normal and affected brain was the reduction in levels of 14-3-3 τ . In normal brain, the level of this isoform is significantly lower than the other detected isoforms (except for 14-3-3 σ), and in the scrapie brain, the level of this protein drops below the limit of detection by immunoblotting (Baxter et al. 2002). The authors proposed that the reduction in 14-3-3 τ may be due to its presence only in the hippocampus in normal brain, a region which is severely damaged in neurodegeneration. The levels of the other 14-3-3 isoforms (γ , η , β and ζ) are expressed at similar levels in both infected and normal brain. In normal brain, these isoforms are widely distributed; however in disease brain the labelling patterns in the thalamus and hippocampus identified the absence of these isoforms. The authors attributed the region-specific reduction in 14-3-3 detection to be a result of disease pathology. The areas which are most severely affected by the disease are those which displayed the greatest differences in 14-3-3 isoform distribution when compared to normal brain (Baxter et al. 2002).

1.1.4.5. Amyotrophic Lateral Sclerosis (ALS)

Amyotrophic lateral sclerosis (ALS) is a neurodegenerative disorder characterised by the depletion of large motor neurons in the brain, brainstem and spinal cord. The disease presents in adults and is clinically recognized by progressive fatal paralysis resulting in death by respiratory failure over the space of three to five years (reviewed in Siddique and Ajroud-Driss 2011). ALS is a predominantly sporadic disease of unknown etiology. Almost a decade and a half after the first descriptions of a progressive muscular atrophy, the first gene attributed to cause a familial form of the disease was identified in *SOD1* (copper/ zinc superoxide dismutase) (Rosen 1993). Since then, a further 10 genes have been found linked to the disease (Siddique and Ajroud-Driss 2011).

At present, there are number of studies which support involvement of 14-3-3 proteins in ALS. ALS patients, both sporadic and familial cases, display hyaline inclusions and proteinaceous cytoplasmic aggregates, similar to Lewy bodies (Bruijn et al. 1997; Watanabe et al. 2001; Corcoran et al. 2004; Kawamoto et al. 2004). Kawamoto and colleagues found that these inclusions contained abundant 14-3-3 protein, leading the authors to suggest that 14-3-3 may play an integral role in inclusion formation (Kawamoto et al. 2004).

Bcl2-associated athanogene 3 (BAG3) has been shown to be important in targeting Hsp70 substrates involved in the binding to dynein to aggresomes (Gamerdinger et al. 2011). It was previously known from a QUICK (Quantitative Immunoprecipitation Combined with Knockdown) study that 14-3-3 ζ binds to BAG3 (Ge et al. 2010). This useful method for identifying protein-protein interactions employs stable isotope labelling with amino acids (SILAC), RNAi induced knockdown, co-immunoprecipitation and quantitative mass spectrometry. Briefly, cells are metabolically labelled by SILAC before knocking out the protein of interest by RNAi and incubating cell lysates with an immobilized antibody for the protein of interest. Finally, precipitated proteins are analysed by mass spectrometry and compared to untreated controls.

Histone deacetylase 6 (HDAC6) has been found to have a 14-3-3 binding site (Johnson et al. 2010). HDAC6 is known to regulate aggresome formation and possibly play a role in microtubule stability (reviewed in Li et al. 2011a). All these factors contribute to the suggestion that 14-3-3 proteins play a role in inclusion formation in ALS.

14-3-3 proteins also have an additional role in aggregate formation, through binding to the 3' untranslated region (3' UTR) of the low molecular weight neurofilament (NF-L) mRNA (Ge et al. 2007). In ALS patients, the mRNA levels of NF-L in the spinal cord are increased and it has been proposed that changes in NF-L stoichiometry can lead to aggregate formation. Binding of 14-3-3 to the 3' UTR of NF-L mRNA also involves other proteins which comprise the aggregates found in both familial and sporadic ALS (Volkening et al. 2009). This is an additional point which supports a role for 14-3-3 in ALS pathophysiology.

1.1.4.6. Spinocerebellar Ataxia Type 1 (SCA1)

For the purposes of this research, the most important role of 14-3-3 in neurodegenerative disease is that in which it plays in spinocerebellar ataxia type 1 (SCA1). As this disease is an integral part of the research presented, it is fully discussed, along with the involvement of 14-3-3 in section 1.3.

1.2. Lipid Rafts

The fluid mosaic model of cell membranes, described by Singer and Nicholson (1972), proposes that membrane proteins are suspended in a fluid lipid bilayer, in which proteins and lipids are free to diffuse laterally, without constraints. The lipid raft hypothesis expands on this model, suggesting that small, moving platforms, which attach specific lipids and proteins are present in the bilayer (Simons and Ikonen 1997). Due to the ever-changing heterogeneous composition of lipids and proteins, the structure of lipid rafts is dynamic, contributing to the wide range of signal transduction roles in which rafts are involved. In addition, the association of specific proteins with lipid rafts has an impact on pathology of a number of neurodegenerative diseases. Here, the role of these processing microdomains and their involvement in neurodegeneration is explored.

1.2.1. What are Lipid Rafts?

Lipid rafts are plasma membrane microdomains which are enriched in cholesterol and sphingolipids and attach specific proteins (Simons and Ikonen 1997). These raft entities have been described as relay stations in intracellular signalling and platforms for the transportation of selected membranes (Simons and Ikonen 1997). Located predominantly in the plasma membrane, rafts have been found formed in internal compartments, including the Golgi apparatus (Gkantiragas et al. 2001). There are two types of lipid raft studied in detail; caveolae, also known as little caves; and planar lipid rafts, which are non-caveolar or glycolipid rafts. Both raft types have been estimated to be approximately 25-100 nm in diameter (Allen et al. 2007).

Often referred to as detergent resistant membranes (DRMs), from the procedure by which they are extracted (Brown and Rose 1992), this term is widely accepted as a cluster of lipid rafts. The study by Brown and Rose (1992) was the first to address the detergent-resistant nature of lipid rafts; however previous studies had identified the link between specific proteins and a lipid-rich region of the plasma membrane

(reviewed by Thompson and Tillack 1985). Prior to this point, research into raft domains of the plasma membrane was rather sporadic; however since the discovery of lipid rafts, a flurry of studies have been conducted, identifying a wide range of cellular processes implicated by rafts. Some of the biological processes proposed to be influenced by raft domains include apoptosis, signal transduction, synaptic transmission, protein sorting and disease signalling (Brown and London 1998; Simons and Toomre 2000; Harris and Siu 2002; Simons and Ehehalt 2002; Tsui-Pierchala et al. 2002).

Over the years, a number of questions have arisen over the validity of lipid rafts and whether they are mere artefacts of the procedure employed for their extraction (Heerklotz 2002; Edidin 2003; Munro 2003; Pike 2003; Simons and Vaz 2004). These doubts were not aided by the planar nature of rafts rendering them indistinguishable in the plasma membrane. Fortunately, advances in technology, predominantly microscopy, have resulted in the observation of rafts in synthetic vesicles (Garner et al. 2008; Owen et al. 2009). This convincing data demonstrates the existence of small, dynamic and selective cholesterol-rich heterogeneous regions, or lipid rafts, in the plasma membranes of living cells (Zheng and Foster 2009b; Lingwood and Simons 2010).

1.2.2. Lipid Raft Composition

At present, lipid rafts are viewed as dynamic, nanoscale domains which are enriched in cholesterol, sphingolipids and GPI-anchored proteins (Hancock 2006). The sphingolipids in rafts associate laterally with each other, with the sphingolipid head group occupying a larger area of the exoplasmic leaflet than their hydrocarbon chains. Any gaps in between sphingolipids are filled by cholesterol molecules. These clusters of cholesterol and sphingolipids act as assemblies in the exoplasmic leaflet which are also rich in saturated phosphatidylcholine. The exoplasmic leaflet is also enriched in glycosphingolipids and sphingomyelin, whilst the cytoplasmic leaflet is enriched in phosphatidylethanolamine and phosphatidylserine. Proteins

associate with rafts on the exoplasmic leaflet, either through GPI-anchors or with transmembrane domains (Brown and Rose 1992; Simons and Ikonen 1997). Figure 1.4 is a diagram of a lipid raft in the plasma membrane.

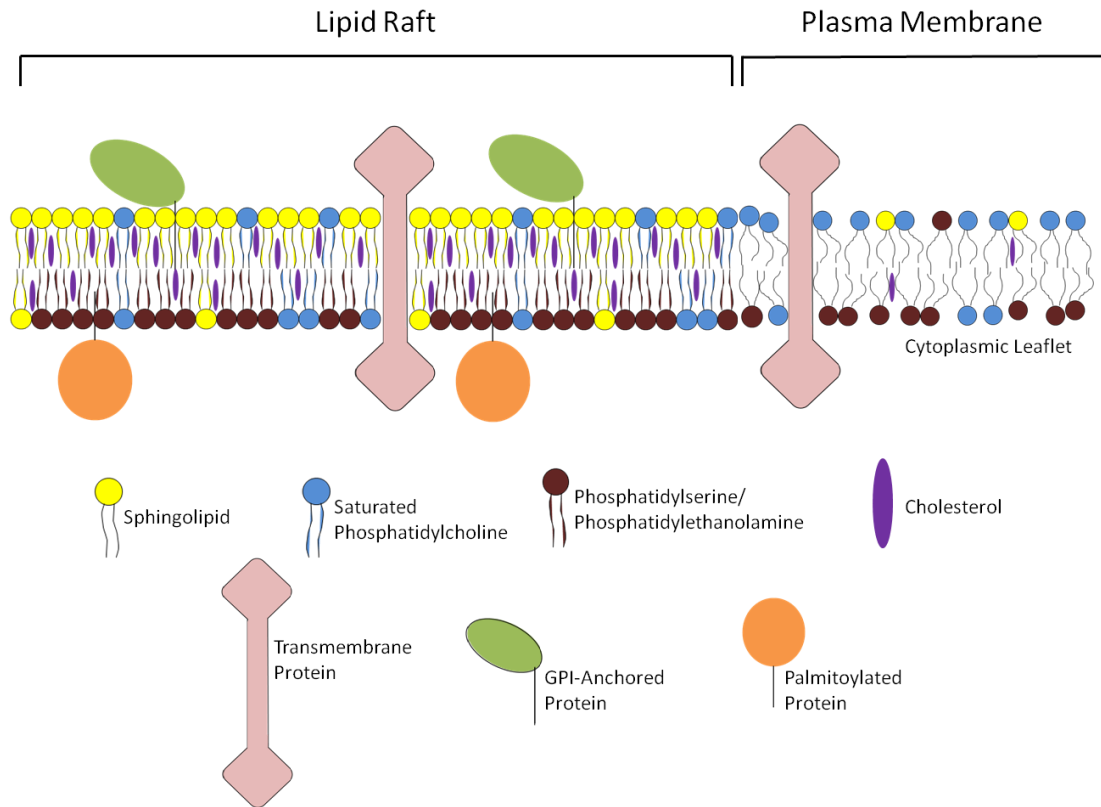


Figure 1.4: Lipid Raft Model

Schematic diagram of a lipid raft domain in relation to the plasma membrane. Lipid rafts are proposed to be in the liquid ordered domain and are rich in sphingolipids, saturated phosphatidylcholine and cholesterol. Proteins which preferentially partition into rafts include GPI-anchored, palmitoylated and particular transmembrane proteins. The bulk plasma membrane is proposed to be in the liquid disordered phase. The inner leaflet, cytoplasmic face, is depleted in cholesterol with comparison to the outer leaflet and is enriched in phosphatidylserine and phosphatidylethanolamine.

A number of proteins have also been found to associate with lipid rafts, by naturally partitioning into the liquid-ordered phase which rafts create. Proteomic studies into rafts are aplenty, however not without issue (Pike 2009; Zheng and Foster 2009a). One problem with raft proteomic studies is the low abundance of membrane proteins for analysis and conventional mass spectrometry techniques have experienced difficulty in analysing transmembrane domain proteins. Another factor

which affects raft protein identification is the heterogeneous nature of lipid rafts. In spite of these issues, a number of proteins have been identified as being raft associated.

Initial studies into lipid rafts identified that GPI-anchored proteins are insoluble in Triton X-100 (Hoessli and Rungger-Brandle 1985; Low 1989; Brown and Rose 1992; Cinek and Horejsi 1992; Fiedler et al. 1993; Chatterjee and Mayor 2001) and the GPI-anchor is attached to rafts (Rodgers et al. 1994). In addition, a number of tyrosine kinases were also found to be concentrated at rafts (Draberova and Draber 1993; Rodgers et al. 1994; Shenoy-Scaria et al. 1994; Field et al. 1995; Robbins et al. 1995; Field et al. 1997; Wu et al. 1997; Davy et al. 2000) and these studies identified that palmitoylated proteins may preferentially partition into rafts as a result of the saturated acyl chain (Melkonian et al. 1999). The proteins identified from these studies cemented the role of lipid rafts as signalling platforms and their implications in cell signalling (Simons and Ikonen 1997; Zajchowski and Robbins 2002). This led to the suggestion that lipid rafts enhance cell signalling by concentrating pathway components or excluding interfering proteins at a localised region of the plasma membrane.

There have been at least 250 proteins quantified and validated as authentic raft proteins (Patra 2008), which have a range of cellular functions, including roles in signalling, structure, differentiation, metabolism, growth, migration and death (Patra 2008; Zhang et al. 2010). Proteomic analysis of rafts has been conducted in a number of cell types which include hippocampal neurons (Ledesma et al. 2003), human umbilical vein endothelial cells (Sprenger et al. 2004), Jurkat T cells (Haller et al. 2001), internal organelles (Poston et al. 2011) amongst many others (Nebl et al. 2002; Foster et al. 2003; Blonder et al. 2004; Osterhues et al. 2006; Zhai et al. 2009). These studies identified raft marker proteins, including GPI-anchored proteins, the palmitoylated protein flotillin-1 and caveolin, confirming that the analysis was of raft membrane domains. These studies largely identified similar classes of proteins, although the exact composition does vary from study to study. This may be due to the heterogeneous nature of these domains, with different rafts being composed of

different lipid and protein populations (Pike 2004). Cytoskeletal proteins are one sub-group that are readily detected (Ledesma et al. 2003). It has been suggested that the association of cytoskeletal proteins may not be raft-specific, due to the high abundance of these proteins in the cell as a whole (Ledesma et al. 2003; Zhang et al. 2010).

The localisation of certain proteins to a specific region of the plasma membrane supports the hypothesis that these membrane regions are involved in the pathology of a range of human diseases. Some lipid-raft related diseases include a number of cancers, diabetes, cardiomyopathy and hypertension to name but a few (reviewed in Zhang et al. 2010). The main interest in regards to the presented research is the role of lipid rafts in neurodegenerative diseases, which is addressed in the following section.

In addition to the links with neurodegeneration, rafts are also of interest due to their connection with 14-3-3 proteins. The first indications of a link between 14-3-3 proteins and lipid rafts was in a study by Assossou (et al. 2003). This study, conducted in the protozoan *Toxoplasma gondii*, an intracellular parasite known to cause severe infection in animals and humans, found 14-3-3 proteins localised mainly in the cytoplasmic compartment however a small proportion of the protein was also detected in lipid raft membrane fractions (Assossou et al. 2003). The authors suggested that 14-3-3 proteins associating with lipid raft domains may have implications in signal transduction.

Since then, greater links between 14-3-3 proteins and lipid rafts have been established. Dr. Carolyn Brechin conducted extensive research into the association of 14-3-3 proteins with rafts during her Ph.D. (Brechin 2006). She discovered that a number of 14-3-3 isoforms associate with lipid rafts and that the association can be disrupted by a small dimeric fourteen-three-three peptide inhibitor (difohein). This research provides the basis for further investigations into 14-3-3 association with lipid rafts.

1.2.3. Lipid Rafts and Neurodegenerative Diseases

Lipid rafts have been found implicated in a number of human diseases and neurodegenerative diseases are not exempt. Cholesterol does not possess the ability to cross the blood brain barrier (BBB), rendering the brain solely responsible for the synthesis and transport of cholesterol between cell types. As the brain consists of ~2% cholesterol which is synthesised *de novo*, any variety of factors can significantly impact functions in the CNS (Zipp et al. 2007; Schengrund 2010). The importance of cholesterol is echoed in the hypothesis that gradual changes in lipid raft composition, which occur with age, can eventually surpass a threshold where they present themselves as symptoms of disease (Schengrund 2010). This section addresses the role of lipid rafts in neurodegenerative disease pathology.

1.2.3.1. Alzheimer's disease

As detailed in section 1.1.4.1, the characteristics of AD are well defined; however the pathological changes which result in AD are not so clear. Changes affecting the disease proteins tau and A β (Hardy et al. 1998) are widely accepted as initiating factors of the disease. In addition, a genetic risk factor for AD in the form of apolipoprotein E4 (apoE4) was identified in 1993 (Strittmatter et al. 1993). ApoE is a constituent of liver-synthesized very low density lipoproteins which are involved in the redistribution of cholesterol and lipids among cells (Mahley 1988). Mouse studies into the impact of ApoE proteins have identified some very interesting points. Comparative studies into the distribution of cholesterol in the plasma membrane between mice expressing different forms of ApoE found that ApoE4 mice had more cholesterol in the exofacial leaflet than ApoE3 mice, yet the total amount of cholesterol was the same (Hayashi et al. 2002). In addition, another study found that mice expressing ApoE4 displayed protein and lipid compositional changes at rafts in comparison with ApoE3 mice (Igbavboa et al. 2005). The compositional changes combined with the risk factor element of ApoE4 support a theory for lipid rafts being implicated in AD pathology (Schengrund 2010).

This is further supported by the abnormal processing of AD proteins at rafts. The amyloid pre-cursor protein (APP) was identified as being raft associated (Parkin et al. 1999) leading to the proposal that abnormal processing of this protein at rafts may be a key stage in disease pathology. Proteolytic processing of APP produces the A β peptides which are the major constituents of the plaques found in AD brains. There are two pathways for processing of APP; the non-amyloidogenic pathway, where APP is cleaved by α -secretase within the A β sequence, precluding peptide formation, and releasing a soluble N-terminal fragment sAPP α . The amyloidogenic pathway sees APP cleaved by β -secretase, producing a soluble N-terminal fragment sAPP β , and a short C-terminal fragment which is membrane-bound and subsequently cleaved by γ -secretase, releasing the A β peptide. It is now clear that proteolytic cleavage of APP is dependent on lipid rafts (Simons et al. 2001; Ehehalt et al. 2003).

Further analysis into the role of rafts and proteolytic processing identified that cholesterol depletion of N2a cells reduced β -cleavage, and a reduction of cholesterol levels by 20-30% produced a 50-60% reduction in the secretion of A β (Ehehalt et al. 2003). In contrast, the levels of α -cleavage were increased, further supporting a regulatory role for rafts in disease pathology (Ehehalt et al. 2003). This appears to be supported by patients who receive cholesterol lowering drugs displaying a lower prevalence of the disease (Jick et al. 2000; Wolozin et al. 2000).

These studies all support the hypothesis that compositional changes of rafts have an impact on signal transduction, resulting in intracellular alterations which contribute to the development of AD.

1.2.3.2. Parkinson's disease

There are also links between lipid rafts and PD, with at least 3 disease proteins found associating with raft domains (Fallon et al. 2002; Fortin et al. 2004; Hatano et al. 2007). For clinical symptoms of PD, see section 1.1.4.2.

One of the disease proteins identified as associating with lipid rafts is α -synuclein (Fortin et al. 2004). Raft association of α -synuclein was coupled with the discovery that the synaptic localisation of this protein is also raft-mediated (Fortin et al. 2004). In addition, investigations with the PD-associated mutation, A30P, disrupted raft association and abolished normal synaptic localization of α -synuclein. These results suggest that in PD, the A30P mutation contributes to pathogenesis through disrupting raft association and any changes to lipid rafts may contribute to disease pathology through the disruption of specific association of proteins. Further investigation by this group identified that α -synuclein association with rafts is mediated by lipids and not through protein interactions (Kubo et al. 2005). A recent study has also identified a connection between a raft-marker protein, caveolin-1, and α -synuclein (Madeira et al. 2011). Cell culture analysis in N2a cells identified that up-regulation of α -synuclein increased the expression of caveolin-1. Over-expression of α -synuclein resulted in N2a cell death, as expected with neuronal cell death reported in PD pathology. However knock-down of caveolin-1 expression rescues the cell death which is induced by α -synuclein. This indicates that α -synuclein toxicity is mediated by a raft-bound protein (Madeira et al. 2011).

The ubiquitin-ligase protein parkin has also been found to associate with lipid rafts (Fallon et al. 2002). Despite this discovery, at present there is no connection between parkin association at rafts and disease pathology. The authors do suggest that parkin mutations may affect signal transduction, membrane plasticity and synaptic transmission (Fallon et al. 2002) however further investigation is required to identify a causative link between raft association and disease pathology.

Missense mutations in LRRK2 contribute to PD and this protein has also been identified in lipid rafts (Hatano et al. 2007) extracted from cell culture and also mouse brain. The association of LRRK2 with cellular membrane structures, could

indicate a role for this protein in membrane trafficking (Hatano et al. 2007). Like parkin, a causative link between LRRK2 raft association and pathogenesis has not been identified, however the authors of this study hypothesise that association of a number of PD proteins with rafts may be a factor for inducing neuronal degeneration.

Finally, a recent study comparing the composition of lipid rafts isolated from the frontal cortex of human brain identified significant alterations in the lipid composition of rafts in PD brain (Fabelo et al. 2011). The lipid alterations suggest that rafts in PD brain exist in a viscous liquid-ordered state, which can have a significant impact on signal transduction, raft thermodynamics and spatial organization. At present, it is not clear whether the altered lipid composition of rafts is a consequence of the disease, or whether this is a contributing factor to disease progression; however the authors do comment that their data likely points to a causative mechanism in PD (Fabelo et al. 2011).

1.2.3.3. Creutzfeldt-Jakob disease

The proteinaceous agent of CJD, PrP (see section 1.1.4.4) is attached to lipid rafts by its GPI-anchor (Naslavsky et al. 1997). The cellular form of the protein, PrP^C, and the protease-resistant form, PrP^{Sc}, are both found in lipid rafts. Following their identification at these domains, it further transpired that alterations in lipid raft composition promotes the formation of the PrP^{Sc} form of the protein, confirming that association of PrP^C with lipid rafts is required for conversion to the proteinaceous form (Naslavsky et al. 1999). Conversion is dependent on the GPI-anchor of the protein and is reduced when rafts are depleted of cholesterol (Simons and Ehehalt 2002). For conversion to occur, the raft domain must be infected by the proteinaceous form, PrP^{Sc} (Baron et al. 2002), inducing the posttranslational modification which alters the protein structure from an α -helix to a β -sheet conformation (Pan et al. 1993; Prusiner 1998). This structural change promotes protein aggregation and fibrillization (Kazlauskaite et al. 2003), of which accumulation in neuronal cells leads to disrupted function and cell death (Johnson and Gibbs 1998).

Further support for lipid raft involvement in CJD pathology is evident from the neuronal cell line study which identified that disruption of raft formation confers protection against prion neurotoxicity (Bate et al. 2004). Dose-dependent administration of a cholesterol synthesis blocker, squalastatin, reduced the accumulation of PrP^{Sc} in N2a cells and SH-SY5Y cells pre-treated with squalastatin display resistance to PrP^{Sc} toxicity (Bate et al. 2004).

This brief overview confirms that lipid rafts play an integral role in neurodegenerative disease pathology and that further investigations can uncover more information with regards to a potential treatment and also a greater understanding of disease pathology.

1.3. Spinocerebellar Ataxia Type 1 (SCA1)

There is a group of at least 20 autosomal dominant cerebellar ataxias (ADCAs) which are generally referred to as spinocerebellar ataxias (SCAs). The term 'spinocerebellar' is a hybrid derived from the clinical signs and neuroanatomical regions associated with the diseases (Margolis 2003). There are three ADCAs which were classified clinically by Harding (1982) and ADCA I encompasses SCA1, SCA2 and SCA3. SCAs 1, 2, 3, 6, 7 and 17 are all members of the polyglutamine-repeat family of diseases. The other SCAs arise from a variety of different genetic mutations.

There are a total of nine known polyglutamine-repeat diseases, which include the SCAs along with Huntington's disease (HD), dentatorubral pallidoluysian atrophy (DRPLA) and spinobulbar muscular atrophy (SBMA) (Zoghbi and Orr 2000). All of these diseases are genetically inherited, neurodegenerative diseases which have similar pathogenesis and symptoms.

Spinocerebellar Ataxia Type 1 (SCA1) was the first of the spinocerebellar ataxias to be described and affects 1-2 people in every 100,000. The rarity of this disease should not detract from its severity and the urgent need for current treatments into such a debilitating condition. Here the clinical symptoms and pathogenesis of the disease are discussed.

1.3.1. Clinical Effects of SCA1

SCA1 is a late onset autosomal dominant neurodegenerative disorder which is characterised by cerebellar ataxia in conjunction with pyramidal and extrapyramidal symptoms, peripheral neuropathy, oculomotor abnormalities and cognitive impairment, which have varying degrees of severity (Matilla-Duenas et al. 2008). Symptoms may begin at any age between 4 and 74, but in the majority of cases, symptoms begin to appear in the third and fourth decade. From the age of onset, the disease usually lasts between 10 and 20 years. At disease onset, the majority of patients display multi-systemic symptoms which are present for 1-2

years. The clinical symptoms at disease onset include pyramidal signs, which can present themselves before ataxia, cerebellar ataxia syndrome, and in the majority of patients, ophthalmoplegia, which is a weakness or paralysis of the muscles which control eye movement. Disease progression leads to the presence of a number of other symptoms which occur in variable degrees of severity. These symptoms include dysphonia (vocal disorder), dysarthria (poor speech articulation), dysphagia (difficulty swallowing), tongue atrophy, deep sensory loss, peripheral sensory-motor axonal neuropathy, pes-cavus (claw-foot) and amyotrophy (wasting of muscle tissue). The most common extrapyramidal symptom is dystonia or fasciculations (muscular twitches or spasms). Generally, the latter symptoms which are detailed present themselves as the disease progresses. In addition, with disease progression, the severity of ophthalmoplegia increases and gaze-evoked nystagmus occurs (the inability to hold gaze in an eccentric position). These uncontrolled eye movements are absent in the later stages of disease and the number of saccades (involuntary rapid eye movements) increase but slow down in velocity as the disease progresses to the later stages (Sasaki et al. 1996).

The clinical symptoms of SCA1 are very similar to those of the other SCAs; however there are means of distinguishing SCA1 from the other SCA subtypes. Schols and colleagues (2008) conducted studies with patients suffering from a variety of ADCAs and discovered that, following magnetic stimulation of the motor cortex, it was possible to completely differentiate SCA1 patients from SCA patients. By studying the motor evoked potentials (MEPs) produced from nerve stimulation, it was clear that SCA1 patients have a prolonged central motor conduction time and nerve conduction studies indicate that SCA1 patients have a slower conduction velocity in comparison to other SCA patients (Schols et al. 2008).

At present, there is no treatment for SCA1 or its symptoms. The main aim of current treatments is to provide palliative care for patients.

1.3.2. Disease Pathology

There are a number of mechanisms which can contribute to SCA1 pathology. There have been propositions that the polyglutamine repeat itself, along with polyglutamine toxicity and subsequent protein interactions, can all play a role in the initiation of the disease. Here provides a brief overview of the potential initiating factors in this debilitating disease.

1.3.2.1. The Polyglutamine Tract

The ATXN1 gene (previously denoted SCA1) was first identified in 1993 (Orr et al. 1993) indicating that the mutation is a result of an expansion of a translated glutamine (CAG) repeat located within exon 8 of the gene. The ATXN1 gene encodes a novel 792-830 residue protein, named ataxin-1 (Banfi et al. 1994). This protein contains the coding region for a polyglutamine tract which is formed by the CAG repeats. As the number of repeats in the tract can vary between normal and disease states, the full length of the protein is affected, i.e. the exact length of the protein is dependent on the length of the glutamine tract. In normal alleles, the tract contains between 6 and 44 repeats. When the number of repeats is greater than 20, CAT (histidine) nucleotide interruptions are present, to maintain the stability of the tract (Chung et al. 1993). In disease alleles, the number of repeats is larger; between 39 and 82. A key point in disease alleles is that the CAT interruptions are absent (Jodice et al. 1994). This absence of CAT nucleotides indicates that a substitution of histidine (CAT) to glutamine (CAG) may be the initial de-stabilising event in the progression of the disease (Goldfarb et al. 1996). Studies have identified an inverse correlation between the increased number of CAG repeats in the tract and the age of onset of the disease (Jodice et al. 1994). As the number of repeats in the polyglutamine tract increases, onset of disease is at an earlier age and with a more rapid progression and subsequent younger death, suggesting that polyglutamine tract expansion results in a toxic gain-of-function. Additionally, studies suggest that parental transmission can affect the length of the polyglutamine tract (Chung et al.

1993). Paternal transmission in 63% of cases studied increased the repeat number, whereas maternal transmission in 69% of cases either decreased or did not alter the number of repeats.

1.3.2.2. Ataxin-1 Aggregation

Ataxin-1 is a novel protein, which is predominantly located in the nucleus of neuronal cells and in the cytoplasm of non-neuronal cells (Servadio et al. 1995). Figure 1.5 shows a schematic diagram of the protein. Expression in neuronal cells is 2-4 times greater than in peripheral tissues (which include skeletal muscle, heart, liver and lymphoblasts). It is the Purkinje cells of the cerebellum which are affected in SCA1 (Zoghbi 1995) and intriguingly, ataxin-1 is found in both the nucleus and cytoplasm here (Servadio et al. 1995). This is the same for both affected and unaffected individuals, suggesting that the location of the mutant protein does not have an influence on disease pathology.

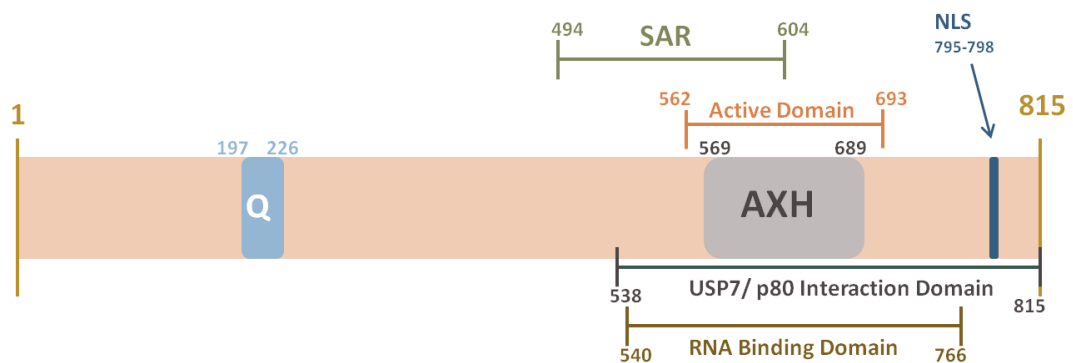


Figure 1.5: Schematic Diagram of Ataxin-1

The ataxin-1 protein contains a glutamine tract (Q), an ataxin-1/HBP1 (AXH) domain and a Self-Association Region (SAR). Other domains involved in ataxin-1 interaction and regulation are also highlighted. NLS; Nuclear Localisation Sequence.

The main characteristic of SCA1 is the formation of insoluble protein aggregates as a result of misfolded ataxin-1 (Perutz et al. 1994; Skinner et al. 1997; Cummings et al. 1998). However, it is important to note, transgenic mice studies have identified that

ataxin-1 aggregation is not required for SCA1 pathogenesis, yet localisation of the ataxin-1 protein to the nucleus is (Klement et al. 1998). The function of ataxin-1 remains unknown; however studies indicate that the protein may play a role in synaptic plasticity and neuronal functions (Matilla et al. 1998). ATXN1 null mice display reduced motor and learning capabilities, yet do not display any symptoms of SCA1, suggesting that lack of protein function does not lead to disease. In fact, ataxin-1 aggregation is accredited with a gain-of-function; through the ability to form aggregates. This has also been supported through human genetic analysis, which discovered that humans with a large deletion in the ATXN1 gene do not suffer from SCA1, but do suffer from seizures and mental retardation (Davies et al. 1999).

Ataxin-1 aggregates also contain ubiquitin, the 20S proteasome and a molecular chaperone HDJ-2/ HSDJ (DnaJ Hsp40) (Cummings et al. 1998). This suggests that changes in the protein conformation due to the expanded polyglutamine tract render the protein resistant to proteasomal degradation (Cummings et al. 1998). Interestingly, at sufficiently high levels, the unexpanded form of the protein can also lead to disease pathology, suggesting the wild-type form may adopt more than one stable conformation, which in abundance, may be toxic (Fernandez-Funez et al. 2000). There is also evidence that the cerebellar leucine-rich acidic nuclear protein (LANP), a predominantly Purkinje cell expressed protein, interacts with ataxin-1 in a glutamine-repeat related manner and is also present in aggregates (Matilla et al. 1997). LANP is a nucleoplasmic shuttling protein involved in a range of cellular processes. LANP interacts with the transcriptional repressor p120E4F and it has been shown that LANP interaction with ataxin-1 relieves this repression (Cvetanovic et al. 2007). The authors concluded that this discovery is in-keeping with previous findings that the earliest pathological change in SCA1 mice is transcriptional misregulation (Lin et al. 2000; Serra et al. 2004).

1.3.2.3. Ataxin-1 Interactions

Another factor which contributes to disease pathology is the interactions involving ataxin-1. A number of studies, mainly employing cell culture and yeast two-hybrid systems, have been conducted to identify interacting proteins. Table 1.2 lists ataxin-1 interacting proteins identified to date. One of the first ataxin-1 interactions identified was with the ubiquitin-like nuclear protein, A1Up (Davidson et al. 2000). Identified from a yeast-two hybrid screen, this interaction provided the first indications that ataxin-1 may be somewhat involved in the ubiquitin/ proteasome system and play a role in the formation and regulation of nuclear multimeric protein complexes (Davidson et al. 2000). The next breakthrough in ataxin-1 interactions was the discovery that the protein binds RNA in a tract length-dependent manner (Yue et al. 2001). The authors of the study found that as the length of the polyglutamine tract increases, the ability to bind RNA decreases; leading the authors to suggest that ataxin-1 has a role in RNA metabolism, a function which can be altered with increasing tract length.

A number of ataxin-1 interactions are also influenced by the length of the polyglutamine tract, including LANP, the polyglutamine-binding protein-1 (PQBP1), the zinc-finger transcription factor Sp1, the transcriptional repressor Capicua (CIC) and the RNA-binding motif protein 17 (RBM17) (Matilla et al. 1997; Okazawa et al. 2002; Lam et al. 2006; Goold et al. 2007; Lim et al. 2008). Interactions which are dependent on the length of the polyglutamine tract suggest that alterations in the protein conformation could give rise to a number of aberrant protein interactions. Most interestingly is the fact that the majority of protein interactions occur through the C-terminal of ataxin-1; a region containing a number of interaction motifs (see Figure 1.5) but not the glutamine tract itself.

The interacting proteins listed in Table 1.2 are mainly involved in transcription, RNA processing, post-translational modifications and signal transduction.

Table 1.2: Ataxin-1 Interacting Proteins

Cellular Process	Interacting Proteins	Region of Interaction	PolyQ Modulation?	Reference
Transcription	Boat	SAR	Yes	(Mizutani et al. 2005)
	Capicua (CIC)	AXH	No	(Lam et al. 2006; Lim et al. 2006)
	CCNK	Unknown	Unknown	(Lim et al. 2006)
	DAZAP2	Unknown	Unknown	(Lim et al. 2006)
	DERP6	Unknown	Unknown	(Lim et al. 2006)
	DNAJA3	Unknown	Unknown	(Lim et al. 2006)
	GFI-1/senseless	AXH	No	(Tsuda et al. 2005)
	HDAC3	Unknown	Yes	(Tsai et al. 2004)
	HIVEP1	Unknown	Unknown	(Lim et al. 2006)
	LANP	C-terminus and polyQ	Yes	(Matilla et al. 1997; Cvetanovic et al. 2007)
	NCOR2/SMRT	C-terminus (most likely AXH)	No	(Tsai et al. 2004)
	PQBP1	Unknown	Yes	(Okazawa et al. 2002)
	SIX5	Unknown	Unknown	(Lim et al. 2006)
	Sp1	AXH	Yes	(Goold et al. 2007)
	SPEN	Unknown	Unknown	(Lim et al. 2006)
	Tip60	Region encompassing the SAR	Yes	(Serra et al. 2006)
	UbcH6	C-terminus	No	(Lee et al. 2008)
	YY1AP1	Unknown	Unknown	(Lim et al. 2006)
ZXH1	Unknown	Unknown	(Lim et al. 2006)	
RNA Processing	A1Up	SAR	No	(Davidson et al. 2000; Lim et al. 2006)
	A2BP1	Unknown	Unknown	(Lim et al. 2006)
	p80 coilin	C-terminus	No	(Hong et al. 2003; Lim et al. 2006)
	PQBP1	Unknown	Unknown	(Okazawa et al. 2002)
	PUM1	Unknown	Unknown	(Lim et al. 2006)
	RBM9	Unknown	Unknown	(Lim et al. 2006)
	RBM17	C-terminus	Yes	(Lim et al. 2008)
	TAP/NXF-1	Unknown	Unknown	(Irwin et al. 2005)

Cellular Process	Interacting Proteins	Region of Interaction	PolyQ Modulation?	Reference
Ubiquitination	CHIP	Unknown	No	(Al-Ramahi et al. 2006)
	SP1	AXH	Yes	(Goold et al. 2007)
	UbcH6	C-terminus	No	(Lee et al. 2008)
	Ubiquitin	Unknown	Yes	(Duyckaerts et al. 1999)
Phosphorylation	LANP	PolyQ	Yes	(Matilla et al. 1997)
Sumoylation	Sumo-1	Multiple Domains	Yes	(Riley et al. 2005)
Stabilization	USP7	C-terminus	Yes	(Hong et al. 2002)
	14-3-3	C-terminus	Yes	(Chen et al. 2003)
Signal Transduction	CRK			(Lim et al. 2006)
	Drd2-Signalling			(Goold et al. 2007)
	Glutamate Signalling			(Serra et al. 2004)
	IGF			(Gatchel et al. 2008)
	Notch Pathway			(Tong et al. 2011)
	RA/thyroid hormone-signalling			(Goold et al. 2007)
	Wnt-signalling			(Goold et al. 2007)
	14-3-3			(Chen et al. 2003)

One of the most important interacting proteins with regards to disease pathology is that with 14-3-3 (Chen et al. 2003). As this interaction is integral to this research, it is detailed fully in section 1.3.3.

One interaction which merits further explanation is that with the co-chaperone/ubiquitin ligase CHIP (C terminus of Hsp70-interacting protein). There appears to be a conflict between different research groups as to the effect CHIP has on disease pathology (Al-Ramahi et al. 2006; Choi et al. 2007). One group proposes that CHIP is neuroprotective, targeting expanded ataxin-1 for degradation and suppressing toxicity of the expanded protein (Al-Ramahi et al. 2006). The other group reports that ubiquitinated expanded ataxin-1 becomes insoluble and increases the formation of protein aggregates (Choi et al. 2007). Both studies investigated the potential of CHIP to interact with ataxin-1, both normal and expanded forms and the ability of CHIP to ubiquitinate these proteins. Both groups also identified the CHIP domain which is required for interaction with ataxin-1 however this is where the similarities end. The study by Choi and colleagues was conducted in a cell culture system (Choi

et al. 2007), whereas the study by Al-Ramahi and colleagues was carried out in *Drosophila*, however the solubility of ataxin-1 following ubiquitination was not investigated (Al-Ramahi et al. 2006). Despite the conflicting suggestions by these two groups, there have been no further insights into the role of CHIP in SCA1 pathology published to date. It may be that CHIP does confer neuroprotective properties, which may include sequestration of toxic proteins into insoluble aggregates. What is clear is that while cell culture and *Drosophila* models are highly informative, they do not inform us as to the exact mechanisms which occur in human brain and caution must be exercised when investigating potential therapeutic agents.

Another ataxin-1 interacting protein of great interest is Brother of ataxin-1, also known as Boat (Mizutani et al. 2005). The human protein shares 33% sequence homology with human ataxin-1. Interest in Boat stemmed from its AXH domain, also a feature of ataxin-1. The AXH domains of both human proteins share 66% sequence homology and a number of ataxin-1 interactions in this region with transcriptional regulators are also shared with Boat. The most significant structural difference between these two proteins is the lack of a glutamine tract in Boat (Mizutani et al. 2005). Both proteins are expressed in Purkinje cells and mouse models of SCA1 show a reduction in Boat expression at as early as three weeks, suggesting that Boat expression may be a marker for disease. Boat interacts directly with ataxin-1 via the self-association region (SAR) of ataxin-1. The interaction of Boat with ataxin-1 suppresses glutamine-repeat-expanded cytotoxicity and the reduction in Boat levels in SCA1 models could account for the increase in self-associated mutant ataxin-1, leading to the increased toxicity of the protein (Mizutani et al. 2005). Further studies into the role of Boat has found that the homologous protein displaces ataxin-1 from interactions with the transcriptional repressor Capicua leading to suppressed neurodegeneration in animal studies (Bowman et al. 2007). Overall, current research indicates that this protein, while similar to ataxin-1 is neuroprotective in SCA1 models through a number of different interactions, despite the obvious structural similarities with the disease protein.

1.3.3. Ataxin-1 and 14-3-3

The most important interaction of ataxin-1 with regards to this research is the one with 14-3-3. The beginnings of a connection with 14-3-3 and ataxin-1 arose from the finding that ataxin-1 has a phosphorylation site on Ser776 (Emamian et al. 2003). One very important factor of phosphorylation at this site in disease pathology is that the protein is only phosphorylated in the nucleus and not the cytoplasm of Purkinje cells. Phosphorylation of the expanded form of the protein resulted in transgenic mice displaying abnormal Purkinje cell morphology and nuclear inclusions, indicating that the phosphorylation of this residue of the expanded protein is critical for degeneration of Purkinje cells in SCA1 (Emamian et al. 2003).

Subsequently, Chen and colleagues were investigating the role of Ser776 phosphorylation in SCA1 pathology (Chen et al. 2003). They found that ataxin-1, phosphorylated by the kinase Akt/ PKB on Ser776, interacts with 14-3-3 ζ and ϵ and the strongest interaction is with expanded ataxin-1 (Chen et al. 2003). The study, conducted in a number of cell lines and transgenic *Drosophila* flies, identified that the interaction of phosphorylated ataxin-1 with 14-3-3 not only stimulates the formation of aggregates, but stabilizes ataxin-1 and prevents its degradation. It was also discovered that ataxin-1 phosphorylation on Ser776 is as a result of the kinase Akt, which creates the 14-3-3 binding site; therefore interaction of ataxin-1 with 14-3-3 is phosphorylation-dependent. These findings led the authors to suggest that potential therapeutic agents for SCA1 may be targeted towards reducing Akt kinase activity (Chen et al. 2003). An image of the interaction is shown in Figure 1.6. The disease model proposed by the authors suggests that stabilization of expanded ataxin-1 by interaction with 14-3-3 leads to a toxic accumulation of this protein complex, particularly in the nucleus. This accumulation in Purkinje cells eventually leads to cell death and subsequent neurodegeneration (Chen et al. 2003).

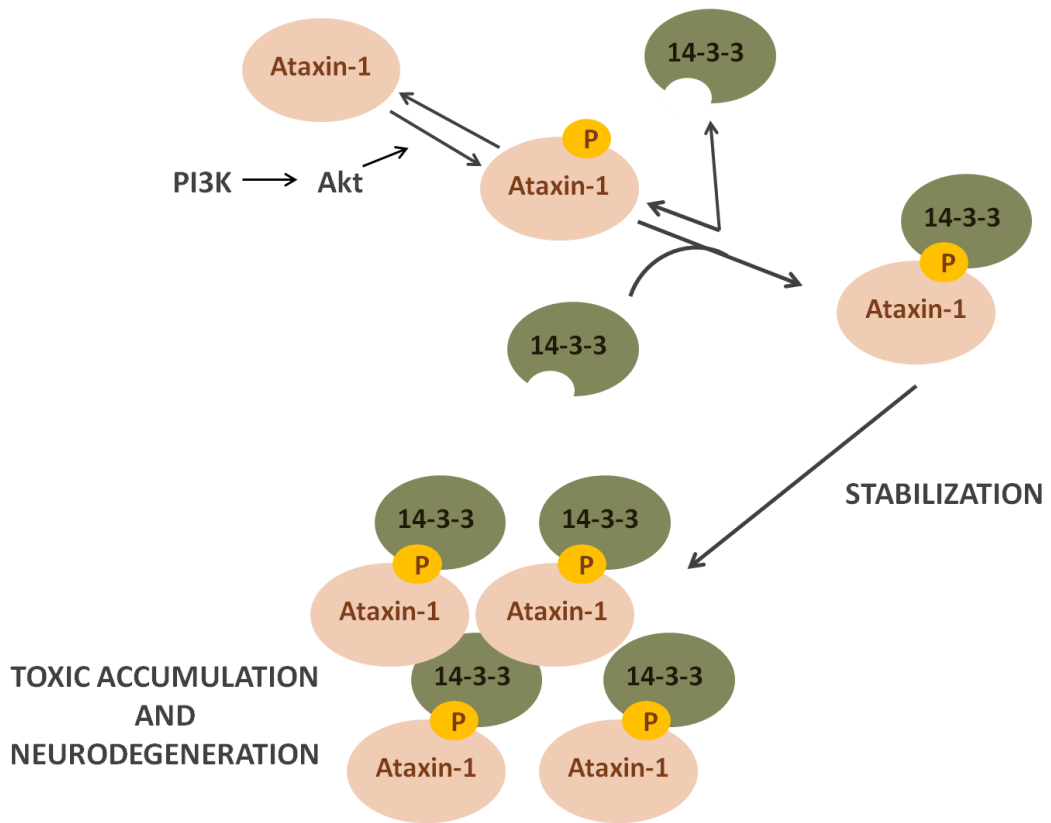


Figure 1.6: Model of Ataxin-1 Accumulation

Following phosphorylation of ataxin-1 on Ser776, 14-3-3 ζ and ϵ can interact with the disease protein. 14-3-3 binds more strongly with expanded ataxin-1, resulting in a gradual accumulation of the toxic protein complex. This toxic accumulation eventually results in neuronal cell death and subsequent neurodegeneration. This model is adapted from that presented by Chen (et al. 2003).

Since this extremely important discovery in SCA1 pathology, questions have arisen as to the exact mechanism by which phosphorylation occurs. A more recent study has found that inhibition of Akt activity had no effect on ataxin-1 phosphorylation, yet inhibition of the cyclic AMP-dependent protein kinase (PKA) did result in a reduction in ataxin-1 phosphorylation at Ser776 (Jorgensen et al. 2009). One major difference between the two studies is the experimental techniques employed to identify the kinase. Chen and colleagues first identified that Akt can phosphorylate ataxin-1 by an *in vitro* kinase assay, after ataxin-1 sequence analysis identified a consensus motif for Akt at Ser776 (Chen et al. 2003). Following confirmation of phosphorylation by *in vitro* kinase assays, *in vivo* analysis was carried out in HeLa cells, which confirmed the groups' initial findings. In contrast, Jorgensen and

colleagues conducted their studies in transgenic mice models (Jorgensen et al. 2009). They conclude that a mammalian model of the human disease presents additional factors, which can affect the activity of endogenous kinases. They concur that Akt would be expected to phosphorylate Ser776 on ataxin-1 due to the recognition motif, however it appears that a higher level regulatory mechanism in the cerebellum prevents Akt from phosphorylating this residue (Jorgensen et al. 2009). However, it is still unclear which kinase in human cerebellum is responsible for ataxin-1 phosphorylation at Ser776 (Umahara and Uchihara 2010).

In order to try and better understand the disease mechanisms in humans, Umahara and colleagues investigated the localisation of 14-3-3 proteins in human brains of patients with SCA1 (Umahara et al. 2007). The results of this study found that in SCA1 brain, 14-3-3 was found in the cytoplasm and nucleus of a number of neuronal cells, including Purkinje cells, pontine neurons, dentate nucleus neurons and anterior horn cells of the spinal cord. Isoform-specific analysis of 14-3-3 localisation found that pontine neurons were extremely positive for 14-3-3 β ; Purkinje cells contained 14-3-3 τ and the dentate nucleus neurons contained both isoforms (Umahara et al. 2007). In addition, 14-3-3 ζ was found concentrated in neuronal nuclei of all brain regions affected by SCA1, indicating that 14-3-3 ζ is the most widely distributed isoform in SCA1 brains.

Other studies into the interaction between 14-3-3 and ataxin-1 have found that the formation of complexes in the cerebellum and brainstem differ significantly (Jafar-Nejad et al. 2011). Mouse studies, with mice lacking a 14-3-3 ϵ allele, identified that this haploinsufficiency rescues a number of SCA1 phenotypes, most notably, motor related phenotypes and cerebellar pathology (Jafar-Nejad et al. 2011). The study also found that mice heterozygous for 14-3-3 ϵ displayed lower levels of ataxin-1, both mutant and wild type, and the number of protein complexes present in the cerebellum was reduced. Unfortunately, despite these very promising findings, a number of other phenotypic symptoms which are not related to the cerebellum were not rescued, and the authors discovered that the mice died from respiratory dysfunction. This led to the suggestion that the mechanism by which 14-3-3 ϵ plays a

role in disease pathology is limited to the cerebellum. To test this, comparisons were made between the cerebellum and the brainstem; both regions which are severely affected by SCA1. By immunoblotting, it was determined that the levels of 14-3-3 ϵ in the brainstem and the cerebellum were the same and that ataxin-1 co-immunoprecipitated with 14-3-3 from both regions. Analysis of the size of the protein complexes formed by ataxin-1 found that there were a greater number of large complexes in the cerebellum compared to the brainstem. This led to the conclusion that ataxin-1 has different interaction partners in different brain regions, which adds to the complexity of the disease pathology (Jafar-Nejad et al. 2011).

There is also evidence to suggest 14-3-3 and phosphorylation of Ser776 are involved in ataxin-1 interactions with splicing factors (de Chiara et al. 2009; Lai et al. 2011). The ataxin-1 protein sequence contains a conserved region which allows the protein to interact with splicing factors (de Chiara et al. 2009). This region overlaps the 14-3-3 binding site and the NLS. The region of the splicing factors which ataxin-1 has a recognition motif for is known as the UHM (U2AF Homology Motif) and it has been previously suggested that serine phosphorylation regulates UHM association (Selenko et al. 2003). de Chiara and colleagues investigated whether phosphorylation of Ser776 by Akt had any effect on association of ataxin-1 with the UHM region of the splicing factor U2AF65 and found that phosphorylation reduced association three fold (de Chiara et al. 2009). In light of more recent data, that the kinase PKA may be responsible for phosphorylation *in vivo*, it would be interesting to see if phosphorylation by PKA had any effect on U2AF65 association, as the authors also identified that ataxin-1 association of U2AF65 does have a positive effect on splicing (de Chiara et al. 2009). The study also found that interaction of 14-3-3 with ataxin-1 prevents interaction with U2AF65, however ataxin-1 with a S776A mutation did not interact with 14-3-3 and interaction with the splicing factor was not affected. This suggests that preferential association of ataxin-1 with splicing factors compared with 14-3-3 prevents ataxin-1 self association and subsequent aggregation (de Chiara et al. 2009).

Following identification of ataxin-1 association with splicing factors, Lai and colleagues further investigated the phosphorylation status of ataxin-1 at Ser776 (Lai et al. 2011). They found that by comparing cytoplasmic and nuclear pS776-ataxin-1 levels from mouse cerebellum that, over a 2 hour incubation period, the levels of phosphorylated protein in the nucleus decreased; indicating that ataxin-1 is subject to phosphatase activity in the nucleus (Lai et al. 2011). A comparison of 14-3-3 levels with phosphatase activity discovered that the level of 14-3-3 was inversely correlated with phosphatase activity, i.e. 14-3-3 levels were lower in the nucleus of cerebellar extracts, suggesting that 14-3-3 prevents dephosphorylation of ataxin-1 in the cytoplasm (Lai et al. 2011). The effect of phosphorylation on protein stabilisation was also investigated and showed that a S776D mutation, to a phospho-mimicking residue, was sufficient to stabilise ataxin-1, yet this mutated protein was unable to interact with 14-3-3. By addition of a competitive 14-3-3 peptide inhibitor, R18, interaction with S776-ataxin-1 was disrupted and the ataxin-1 protein dephosphorylated (Lai et al. 2011). The group then went on to identify the phosphatase responsible as Protein Phosphatase 2A (PP2A). One final point that this study uncovered is the fact that the association of 14-3-3 with ataxin-1 must be disrupted in order for ataxin-1 to be transported into the nucleus (Lai et al. 2011). However, there was no investigation into how this mechanism occurs in Purkinje cells. As nuclear localisation of ataxin-1 is key to disease pathology, this is one instance which suggests that 14-3-3 may be neuroprotective, yet this is at odds with the evidence that 14-3-3 contributes to the formation of the toxic aggregates in SCA1. This highlights the complexity of the pathology of this disease and the role that 14-3-3 plays.

1.4. Aims of Project

14-3-3 proteins are implicated in a wide range of cellular processes, including the pathology of neurodegenerative diseases. In addition, lipid raft domains of the plasma membrane have also been identified as the processing centres for a number of disease proteins in neurodegeneration. Previous research conducted in this laboratory had identified the association of 14-3-3 proteins with lipid rafts; leading to the hypothesis that the presence of 14-3-3 proteins and neurodegenerative disease proteins at lipid rafts may be connected to disease pathology.

Previous research had identified the five main brain isoforms of 14-3-3 associating with rafts. Therefore, one of the main aims of this project was to determine whether the two phospho-forms of 14-3-3, α and δ , also associated with lipid rafts. As these two phospho-forms are only present in brain tissue, this may bear some significance in relation to neuronal processes. To investigate this, immunoblotting with antibodies specific for the phosphorylated epitope of these isoforms was conducted, following raft protein separation by 2D SDS-PAGE.

In addition to the links between 14-3-3 proteins, lipid rafts and neurodegenerative diseases, is the functional implications which sphingolipids present in lipid rafts can elicit on 14-3-3 proteins. 14-3-3 has been shown to be phosphorylated on a residue buried within the dimer interface in the presence of sphingosine. 14-3-3 natively exists as a dimer; a conformation which is essential for full protein function. Alterations to the protein structure can have implications on the cellular processes which 14-3-3s are involved in, which may include neurodegenerative diseases. As sphingosine is present in lipid rafts, I hypothesise that the quaternary structure of 14-3-3 may be altered at lipid rafts, altering the functional capacity of the protein. This theory was investigated by *in vitro* kinase assays and cross-linking analysis in lipid rafts.

Finally, one neurodegenerative disease of particular interest in this research was Spinocerebellar Ataxia Type 1 (SCA1). Interaction of the disease protein, ataxin-1, with 14-3-3 has been shown to contribute to the formation of aggregates which is a key characteristic of this disease. This knowledge prompted the investigation into

identifying small molecule inhibitors which can prevent this toxic interaction. To identify potential inhibitors, a collaborative study was conducted with the Computational Biology Group based at Edinburgh University. This study identified a number of potential inhibiting compounds, which were tested following the development of an ELISA assay method. In addition, the production of ataxin-1 protein constructs was also investigated for future inhibitor analysis.

CHAPTER 2

MATERIALS AND METHODS

All reagents were purchased from Sigma-Aldrich (Dorset, UK) at analytical grade unless otherwise stated.

2.1. Molecular Biology

Table 2.1: Molecular Biology Buffers

Buffer	Components	Concentration
Luria Bertani (LB) media	Peptone/Tryptone Yeast Extract Sodium Chloride	10 g/L 5 g/L 10 g/L
LB agar	Bacto-Agar in LB media	15 g/L
SOC media pH 7.0	Bacto-tryptone Bacto-yeast extract Sodium chloride Potassium chloride Magnesium chloride (hydrated) Magnesium sulphate (hydrated) Glucose	20 g/L 5 g/L 10 mM 2.5 mM 10 mM 10 mM 20 mM
Terrific Broth (TB) media	Tryptone Yeast Extract Dipotassium Phosphate Monopotassium Phosphate	12 g/L 24 g/L 12.5 g/L 2.3 g/L
TAE Buffer	Tris-HCl Acetic acid EDTA pH 8.0	40 mM 20 mM 1 mM
6 x DNA gel loading buffer	Bromophenol blue Xylene Cyanol FF Glycerol EDTA	12.6% (w/v) 12.6% (w/v) 30% 120 mM
Phosphate Buffered Saline (PBS) pH 7.4	Sodium phosphate Potassium phosphate Potassium chloride Sodium chloride	10 mM 1.8 mM 2.7 mM 137 mM

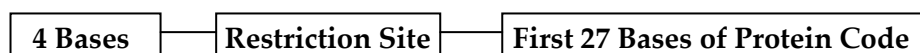
2.1.1. Agarose Gel Electrophoresis

1% agarose gels were routinely prepared by heating 1 g molecular biology grade agarose in 100 ml of TAE buffer (40 mM Tris-HCl, pH 8.0, 20 mM acetic acid, 1 mM EDTA) until dissolved. The agarose was allowed to cool before adding 5 µl of CYBRsafe (Invitrogen, Paisley, UK) which allows DNA to be visualised under UV light. The gel was submerged in TAE buffer and DNA samples were prepared using 6 x loading dye (Promega, Southampton, UK) to a final concentration of 1 x before loading into the wells. DNA fragments were separated at 170 V and visualised under UV light.

2.1.2. Primer Design

Sense primers were designed using the following approach:

Start with four bases which do not form part of the primer to protect the restriction site as restriction enzymes bind to this prior to digestion. Regularly used bases were CCCA. The restriction site is added before adding at least the first 27 bases of the protein to be cloned. If possible, the end of the protein sequence code should contain guanine or cytosine bases. These bases form three hydrogen bonds with each other, making primer binding more stable. When required, frame bases were added after the restriction site to ensure that the protein sequence was in frame.



Antisense primers were designed using the following approach:

Again begin with four bases which do not form part of the primer to protect the restriction site. For this primer, the bases GTGC were routinely used. Next, the restriction site was added before inserting a stop codon, such as TTA. The stop codon is required to ensure proper translation of the protein. Finally, the protein sequence is added. For the anti-sense primer, it is the reverse-complement of the last 27 bases which is added.



Table 2.2: Table of Primers

Protein Expression Plasmid	Direction	Species	Primer Sequence	Restriction Site
Ataxin-1 575-815	Sense	Human	CCCACTCGAGATGAAAGGC TCCATCATCCAGTTGGCC	XhoI
Ataxin-1 718-815	Sense	Human	CCCACTCGAGATGGGCAGC AGACACAGGTATGCCGAGC AG	XhoI
Ataxin-1 740-815	Sense	Human	CCCACTCGAGATGAATGGC GAACTGAAGTTTCCAGAGA AA	XhoI
Ataxin-1 575-815, 740-815, 718-815	Antisense	Human	GTGCAAGCTTTTACTTGCCT ACATTAGACCGGCCTTCAAT	HindIII
14-3-3 ζ Full-length	Sense	Human	CCCAGGATCCATGGATAAAA AATGAGCTGGTTCAG	BamHI
14-3-3 ζ Full-length	Antisense	Human	GTGCGAATTCTTAATTTTCCC CTCCTTCTCCTGCTTCAGC	EcoRI

2.1.3. Polymerase Chain Reaction (PCR) with Pfu Polymerase

PCR was performed on a PCR Sprint Thermal Cycler PCR machine (Thermo Fisher Scientific, Waltham, MA). For accurate DNA amplification, Pfu polymerase was used. A typical PCR reaction was set up as follows¹:

10 x Pfu polymerase buffer	-	5 μl
Pfu polymerase (2.5 U)	-	1 μl
Sense primer (1 μM)	-	1 μl
Antisense primer (1 μM)	-	1 μl
dNTPs (10 mM)	-	4 μl
DNA template	-	1 μl
dH ₂ O	-	<u>37 μl</u>
Total volume	-	<u>50 μl</u>

¹ The final concentration for each reagent is given in parenthesis. Various concentrations of the DNA template were used depending on the DNA sample being cloned.

The following PCR programme was used:

1 x	-	95°C melt	-	60 sec.	
35 x	-	}	95°C melt	-	30 sec.
			55°C anneal	-	45 sec.
			68°C <i>t extend</i> ²	-	
1 x	-	72°C hold	-	10 min.	

2.1.4. Restriction Digest

Restriction digests were performed to cut PCR products to produce sticky ends for DNA ligation. This method is known as a PCR product digest. Restriction digests were also performed analytically to check that insert DNA had ligated into plasmid DNA. This method is known as an analytical digest.

2.1.4.1. PCR Product Digest

Restriction digests were set up with PCR products and vector DNA as follows³:

10 x Buffer	-	6 µl
BSA (1 mg/ ml)	-	6 µl
Enzyme 1 (10 U)	-	3 µl
Enzyme 2 (10 U)	-	3 µl
DNA template (50 ng)	-	30 µl
dH ₂ O	-	<u>12 µl</u>
Total Volume	-	<u>60 µl</u>

Digests were incubated at 37°C for 2 h.

² The extension time (*t extend*) is 2 min/ kb of protein.

³ The final concentration for each reagent is given in parenthesis.

2.1.4.2. Analytical Digest

Analytical restriction digests were set up as follows⁴:

10 x Buffer	-	3 μ l
BSA (1 mg/ ml)	-	3 μ l
Enzyme 1 (10 U)	-	1 μ l
Enzyme 2 (10 U)	-	1 μ l
DNA template (200 ng)	-	20 μ l
dH ₂ O	-	<u>2 μl</u>
Total Volume	-	<u>30 μl</u>

Digests were incubated at 37°C for 2 h.

2.1.5. Gel Extraction

Gel extraction was performed using either the QIAquick gel extraction kit (Qiagen, Crawley, UK) or the Gel Purification Kit (Promega, Southampton, UK). In both cases, the procedure was carried out according to the manufacturer's instructions.

2.1.6. Ligation of Insert DNA into Vector DNA

A ratio of 1:3 of vector: insert was calculated using the following equation:

$$\frac{\text{vector (ng)} \times \text{insert size (kb)}}{\text{vector size (kb)}} \times \text{molar ratio of } \frac{\text{insert}}{\text{vector}} = \text{insert (ng)}$$

The concentration of the vector and insert was estimated by comparing the DNA fragments separated on agarose gel electrophoresis with known concentrations of DNA molecular weight markers. The ligation reaction mixture was prepared to a total volume of 10 μ l with the relevant concentrations of vector and insert DNA. 1 μ l of T4 DNA ligase (NEB, Ipswich, MA) and 1 μ l 10 x ligase buffer were added and the reaction was made up to a total volume of 10 μ l with nuclease-free water.

⁴ The final concentration for each reagent is given in parenthesis.

Reactions were incubated either at room temperature for 3 h, or overnight at 4°C. After incubation, the whole 10 µl of ligated DNA was transformed into Top10 *Escherichia coli* cells.

2.1.7. Preparation of Competent Bacteria

Escherichia coli strains used included Top10 for DNA production and BL21 (DE3) (both Invitrogen, Paisley, UK), *Rosetta 2* and *Rosetta-gami 2* (DE3)pLysS (Novagen, Merck, Darmstadt, Germany) for protein production. Production of competent bacteria was based on a modified version of the Hanahan (1983) method. A single colony of the cell line was inoculated in 5-10 ml of LB broth supplemented with appropriate antibiotic and incubated overnight at 37°C, with shaking at 200 rpm. This overnight inoculation was added to 200 ml of pre-warmed LB supplemented with antibiotic and grown to an O.D. at 600 nm of between 0.4 and 0.7. The total volume was divided into 50 ml fractions and incubated on ice for 20 min prior to centrifugation at 4500 rpm at 2°C for 10 min. After supernatant removal, cells were resuspended in 10 ml ice-cold 100 mM CaCl₂ on ice. The mixtures were combined, set in ice and incubated at 4°C for 2 h. Cells were harvested by centrifugation at 4500 rpm at 2°C for 10 min and resuspended in 2 ml ice-cold 100 mM CaCl₂ with 20% (v/v) glycerol. 100 µl aliquots were stored at -80°C until further use.

2.1.8. Transformation of Bacteria

Bacterial cells were transformed with DNA using the heat shock method. For transformation, ~1 µg of DNA was added to 50 µl of competent cells and incubated on ice for 20 min, to allow the DNA to bind to the cells. The mixture was then heat-shocked at 42°C for 90 seconds before returning to ice for 2 min. After incubation, 500 µl of SOC media was added to the mixture and incubated at 37°C, shaking at 200 rpm for at least 90 min. The cell suspension was spread onto agar plates supplemented with appropriate antibiotic and incubated at 37°C overnight. Negative controls were set up minus DNA.

2.1.9. Production of Glycerol Stocks

Glycerol stocks were produced to allow seeding of bacterial cultures without previous transformation. 500 μ l of bacterial culture with an O.D. of greater than 0.6 at 600 nm was added to 500 μ l 100% glycerol to make a glycerol stock. This was thoroughly mixed before storing at -80°C until further use.

2.1.10. Purification of Plasmid DNA

2.1.10.1. Small Scale Purification

A bacterial colony was picked into 10 ml LB media supplemented with appropriate antibiotic and incubated overnight at 37°C, with shaking at 200 rpm. The culture was centrifuged at 13,000 rpm in a bench top centrifuge for 5 min to pellet the bacteria. Qiagen's QIAquick mini-prep kit was used to purify the plasmid DNA, according to the manufacturer's instructions. The DNA was eluted into 50 μ l of protease-free water.

2.1.10.2. Large Scale Purification

A bacterial colony was picked into 100 ml LB media supplemented with appropriate antibiotic and incubated overnight at 37°C, shaking at 200 rpm. Plasmid DNA was isolated using Qiagen's maxi-prep kit, according to the manufacturer's instructions. The DNA was eluted into 500 μ l of protease-free water.

2.1.11. Quantification of Plasmid DNA

The concentration of plasmid DNA was measured using a Nanodrop® Spectrophotometer ND-1000. Absorbance was measured at 260 nm and nuclease-free water was used as a blank before measuring the concentration of 1 μ l of the DNA sample. Concentration was measured in ng/ μ l.

2.2. Expression and Purification Techniques

Proteins which were routinely expressed and purified for the purposes of this research are detailed in Table 2.3.

Table 2.3: Protein Expression Plasmids

Construct Name	Source	Growth Temp.	A ₆₀₀ induction	IPTG Conc.	Time for Induction
His-Ataxin-1 'C'	IMAGE clone (S. Beck)	37°C	0.7-0.8	0.5 mM	16 h
His-Ataxin-1 'AC'	IMAGE clone (S. Beck)	37°C	0.7-0.8	0.5 mM	16 h
His-14-3-3ζ	N. Houston	16°C	0.6	0.5 mM	16 h
GST-ExoS 88-453	Bengt Hallberg	37°C	0.6	0.5 mM	4 h

The p-Trc-His-A' expression vector, employed for cloning His-fusion proteins, contains an ampicillin resistance gene. The pGEX-2TK expression vector, employed for GST-fusion proteins cloning, also carries an ampicillin resistance gene. For procedures requiring antibiotic selection, a final concentration of 100 µg/ml of ampicillin was used in addition to any other antibiotics required for selection. Employed *E. coli* strains and the required antibiotics are detailed in Table 2.4.

Table 2.4: Strains of Competent Cells used in Protein Expression

<i>E. coli</i> Strain	Antibiotic	Final Concentration
BL21(DE3)	n/a	n/a
Rosetta 2	Chloramphenicol	34 µg/ml
Rosetta-Gami 2	Streptomycin	50 µg/ml
	Tetracycline	12.5 µg/ml
	Chloramphenicol	34 µg/ml

2.2.1. Expression of Recombinant Proteins

Recombinant proteins (see Table 2.3) were transformed into the *E. coli* strains of competent cells, as detailed in Table 2.4 and selected on agarose plates supplemented with appropriate antibiotic. A 100 ml culture was grown overnight from a single colony in LB media supplemented with appropriate antibiotic (see Table 2.4). A 1/10 dilution of the starter culture was made into the same medium and grown at 37°C, 200 rpm until the relevant O.D. at 600 nm was reached (see Table 2.3). Protein expression was induced by addition of isopropyl-beta-D-thiogalactopyranoside (IPTG) at the concentration indicated in Table 2.3. Cultures were then transferred to the temperature for optimum growth (Table 2.3) in a shaking incubator at 200 rpm for either 4 h, or overnight (16 h). Cultures were harvested by centrifugation at 6500 rpm until the total volume had been clarified. Pellets were resuspended in 20 ml of 1xPBS and transferred to Falcon tubes. The mixture was centrifuged at 4500 rpm for 30 min. The supernatant was removed and pellets were stored at -80°C until further use.

For expression trials, 500 µl samples were collected at various time points and centrifuged at 13,000 rpm for 5 min to pellet the cells. Cell pellets were resuspended in 250 µl of 3 x SDS Loading Buffer and boiled at 100°C for 5 min before either storing at -20°C until further use or running on SDS-PAGE.

2.2.2. Immobilised Metal Affinity Chromatography (IMAC) by Gravity Flow

2.2.2.1. Ataxin-1 'C' and 'AC'

Ataxin-1 'C' and 'AC' domains were predominantly purified using gravity flow columns charged with 100 mM cobalt chloride (CoCl₂). Columns were prepared with a column volume (CV) of 5 ml. This consisted of Sepharose beads charged with Co²⁺. The process of charging and regenerating the column after each purification procedure was carried out according to the protocol detailed in *The QIAexpressionist Handbook* (Qiagen, Crawley, UK, 2001).

All procedures for protein purification were carried out at 4°C unless otherwise stated. For purification by gravity flow IMAC, a -80°C pellet was resuspended in ice-cold lysis buffer (1 x PBS, 1 mM EDTA, 1 mM DTT, 0.1% Triton X-100, pH 7.5). A protease inhibitor tablet (Roche Diagnostics Ltd, U.K.) was added prior to lysis. Once completely resuspended and smooth, the cell suspension was sonicated at 10 microns for 8 periods of 30 seconds, with a 30 second break between each sonication. The sonicated cell lysate was incubated on ice for 30 min and clarified through centrifugation at 15,000 rpm (27,100 x g), 4°C for 25 min in a Sorvall SS-34 rotor. The supernatant of the clarified lysate was filtered through a 0.45 µm filter.

The filtered lysate was applied to the gravity flow column and sealed inside. The column was then tumbled for 1 h at 4°C to allow the lysate to fully interact with the Co²⁺ ions on the Sepharose beads. After tumbling, the column was opened and the flow-through from the beads collected in a Falcon tube. Collection was stopped before the remaining volume was less than that of the column volume, so as not to allow the Sepharose beads to dry out. Following this is a lengthy wash-step with 10 CV of wash buffer (20 mM imidazole, 20 mM Tris, 0.3 M NaCl, pH 7.4). This wash step is important to remove any non-specific binding proteins which would contaminate the protein of interest. The eluate of the wash step is also collected, in the event that the protein of interest may be eluted at extremely low imidazole concentrations.

To elute the ataxin-1 proteins, the optimum concentration of imidazole had been determined by Dr. Sebastian Beck to be 200 mM. Therefore, the proteins were eluted with a minimum of 7 CV of elution buffer (200 mM imidazole, 20 mM Tris, 50 mM NaCl, pH 7.4). The elution fractions were collected in 1 CV increments. Each elution fraction collected was also treated with 200 µl of protease inhibitors (25 mM DTT, 98 mM EDTA plus one protease inhibitor tablet per 50 ml) and stored at 4°C.

2.2.2.2. 14-3-3ζ

14-3-3ζ was purified using 1 ml gravity-flow IMAC columns containing NTA beads charged with 100 mM nickel chloride (NiCl₂). Beads were prepared by washing 2 ml of bead slurry with 50 ml of dH₂O by centrifugation at 4,500 rpm in a benchtop centrifuge. Once the supernatant was removed, beads were transferred to a column where the remaining liquid was drained prior to charging the beads with 2 ml of 100 mM NiCl₂. Excess liquid was left to drain before washing with 10 ml of dH₂O followed by 10 ml of Equilibration Buffer (20 mM sodium phosphate, 500 mM sodium chloride, 50 mM imidazole, pH 8). Charged beads were stored at 4°C until required.

A bacterial pellet stored at -80°C was resuspended in 40 ml of Lysis Buffer (20m M sodium phosphate, 500 mM sodium chloride, 20 mM imidazole, pH 8.0) plus a protease inhibitor tablet (Roche Diagnostics Ltd, UK) while on ice. Once no clumps were visible, the lysate was vortexed, to ensure complete re-suspension. Once completely resuspended and smooth, the cell suspension was sonicated at 10 microns for 8 periods of 30 seconds, with a 30 second break between each sonication. The lysate was centrifuged at 27,000 × g (15,000 rpm) in an SS-34 rotor for 1 h at 4°C. After centrifugation, the supernatant was filtered through a 0.2 µm filter and the filtrate applied to the charged NTA beads for incubation at 4°C for 1 h with rotation. Typically, the filtrate and charged beads were incubated in a 50 ml Falcon tube. The protein/bead mixture was then centrifuged at 1,000 rpm for 5 min and the supernatant collected. This was termed the 'flow-through'. Beads were

resuspended in 40 ml of Equilibration Buffer and rotated at 4°C for 30 min. Again, the mixture was centrifuged at 1,000 rpm for 5 min and the supernatant collected. This was termed the 'wash'. Beads were transferred to a gravity-flow column and the protein was eluted with a total volume of 20 ml Elution Buffer (20 mM sodium phosphate, 500 mM sodium chloride, 250 mM imidazole, pH 8). Eluate was collected in either 1 or 2 ml fractions. To ensure that all protein which had bound to the column was removed, a final wash with 10 ml of Wash Buffer (20 mM sodium phosphate, 500 mM sodium chloride, 500 mM imidazole, pH 8) was carried out. This also allows the charged NTA beads to be used more than once for subsequent protein purification.

Fractions were analysed by SDS-PAGE (see section 2.3.1) and those which contained the protein of interest were pooled for further concentration. As the protein is eluted from the column with a high imidazole concentration, the protein buffer was changed to either 25 mM HEPES (pH 7) or PBS in a vivaspin (see section 2.2.4).

All procedures were carried out at 4°C unless otherwise stated.

2.2.2.3. ExoS

GST-tagged proteins were purified with Glutathione-Sepharose beads. Beads were prepared by washing 1.5 ml of bead slurry in 20 ml of PBS by centrifuging at 1,500 rpm for 5 min in a benchtop centrifuge. The supernatant was removed and beads washed in 20 ml PBS with 0.1% Triton X-100 and centrifuged at 1,500 rpm for 5 min. The supernatant was removed and the beads washed once again in 20 ml PBS and centrifuged at 1,500 rpm for 5 min. Beads were stored at 4°C until required.

A bacterial pellet stored at -80°C was resuspended in 40 ml of ice-cold PBS containing one protease inhibitor tablet. Lysozyme was added to give a final concentration of 1 mg/ml before incubating the mixture on ice for 30 min. Following incubation, 0.2 ml of 1 M DTT and 4.5 ml of 10% Triton X-100 was added to the mixture, before sonicating at 10 microns for 6 periods of 30 seconds, with a 30 second break between each sonication. The lysate was then centrifuged at 12,000

rpm (17,000 × g) for 1 h in an SS-34 rotor. Following centrifugation, the supernatant was filtered through a 0.22 µm filter and the filtrate added to the prepared Glutathione-Sepharose beads for incubation at 4°C for 2 h with rotation. The protein/bead mixture was centrifuged at 1,500 rpm for 5 min and the supernatant removed. The beads were washed four times with PBS by resuspending and centrifuging at 1,500 rpm and removing the supernatant. The beads were then washed once, in the same manner, with 1.2 M NaCl before finally washing twice with PBS. When the final supernatant was removed, the beads were left as 50% slurry.

For glutathione elution, the bead slurry was aliquoted into 1 ml fractions and the PBS was removed by centrifuging at 3,000 rpm in a benchtop centrifuge. To each fraction, 500 µl of Glutathione Elution Buffer (10 mM reduced glutathione, 50 mM Tris-HCl pH 8) was added and incubated at room temperature for 30 min with tumbling. After incubation, fractions were centrifuged at 3,000 rpm for 20 seconds and the supernatants pooled. This was termed as fraction 1. The elution step with Glutathione Elution Buffer was repeated until 4 fractions were collected and these fractions were separated on 12% SDS-PAGE. Fractions containing the protein of interest were pooled together and the glutathione removed from the protein by dialysing with PBS.

All procedures were carried out at 4°C unless otherwise stated.

2.2.3. Ion-Exchange Chromatography

This step was employed when protein fractions from IMAC purification were not of sufficient purity. This purification step was carried out on a BioCAD 700E Perfusion Chromatography Workstation. Cation exchange was employed and details are given in Table 2.5.

Table 2.5: Ion-Exchange Conditions

Protein	Ion-Exchange Column	Buffer A	Buffer B
Ataxin-1 'C'	Cation (MonoS)	10 mM MES (pH 6)	10 mM MES, 2 M NaCl (pH 6)
Ataxin-1 'AC'	Cation (MonoS)	10 mM MES (pH 6)	10 mM MES, 2 M NaCl (pH 6)

The ion-exchange column was equilibrated with Buffer A for 90 min before the protein was loaded onto the column. The chromatography procedure began with a 10 min step of 100% Buffer A before a gradient step of 0-100% Buffer B for 45 min. The run ended with a final 10 min step of 100% Buffer B.

Fractions were collected with an Advantec SF-2120 fraction collector and those containing protein were analysed on SDS-PAGE and pooled for further analysis.

2.2.4. Gel Filtration Chromatography

In order to separate proteins according to their size and shape, gel filtration chromatography was employed. This method is unlike other chromatography methods, whereby proteins being separated bind to the solid phase. Instead, proteins are 'retained' in the column for varying amounts of time, depending on the size of the protein and matrix employed in the column, i.e. not adsorptive.

For Ataxin-C purification, a Superose 12 10/30 chromatography column of 24 ml with a molecular weight range of 1-300 kDa was used. Superose comprises of a cross-linked, agarose-based medium with a bead size of approximately 8-12 μm . The method was carried out on a BioCAD Perfusion Chromatography Workstation with

an Advantec SF-2120 fraction collector connected to collect individual fractions for further analysis. Samples were prepared to 100 μ l and run over 80 min with a buffer of 20 mM Tris, 150 mM NaCl pH 7.4 at a flow rate of 0.5 ml/min.

2.2.5. Concentration and Storage of Proteins

Purified recombinant proteins must be concentrated for further analysis, particularly crystallography. Proteins were concentrated into buffers which were suitable for the protein, e.g. 14-3-3 ζ is stable in HEPES buffer. Occasionally, proteins would be required to be in a particular buffer for certain assays or crystallography conditions. In order to change buffers and concentrate proteins, the following methods were employed:

1. A Vivaspin concentrator (Sartorius Stedim Biotech, Germany).

Depending on the size of protein to be concentrated, a concentrator with a suitable MWCO (molecular weight cut-off) was used. One caveat of this method is the loss of protein yield due to the protein sticking to the filtration membrane. This can be overcome through keeping the Vivaspin on ice after centrifugation and gently resuspending the sample before using a fine-tip pipette or needle and syringe to remove the protein sample.

2. A Slide-a-Lyzer Dialysis Cassette (Thermo Fisher Scientific, Waltham, MA).

For dialysis of GST-tagged proteins, a cassette with a MWCO of 3.5 kDa was used. The cassette was prepared according to the manufacturer's instructions prior to injecting the protein sample. The cassette was placed in a large beaker containing ~800 ml of PBS and incubated at 4°C with mixing. After a few hours, the buffer was changed and dialysis continued overnight. The buffer was changed periodically over the following 24 h to ensure sufficient dialysis.

2.2.6. Protein Concentration Determination

2.2.6.1. Bradford Assay

Protein concentration was determined according to the Bradford (1976) method. Samples were made up to 50 μl in dH_2O and 200 μl of Bradford dye reagent (Bio-Rad, Hertfordshire, UK) was added to each sample to give a 1:4 ratio of sample to reagent. Samples were incubated at room temperature for 5 min and the absorbance measured at 595 nm. Samples were analysed in triplicate and compared with a standard curve constructed using serial dilutions of bovine serum albumin (BSA).

2.2.6.2. Bicinchoninic acid (BCA) Assay

For determination of protein concentration of raft fractions, whereby lipids interfere with the Bradford assay reagent, a BCA assay kit from Pierce (Rockford, IL) was used according to the manufacturer's instructions. Samples were made up to 50 μl in dH_2O and incubated with 1 ml working reagent (1:20 ratio) for 30 min at 60°C. The working reagent is produced by mixing 50 parts of reagent A (BCA containing solution) with 1 part of reagent B (4% cupric sulphate). Following incubation, samples were cooled to room temperature and the absorbance measured at 562 nm. Absorbance values were compared with a BSA standard curve to calculate protein concentration.

2.3. Biochemical Techniques

2.3.1. SDS-PAGE

Proteins were routinely separated by size under denaturing conditions by SDS-PAGE based on the method of King and Laemmli (1971). Tris-glycine gels of varying percent acrylamide were used according to the size of proteins to be analysed.

Table 2.6: Buffers for SDS-PAGE

Buffer	Components	Concentration
Stacking Gel	Acrylamide Tris-HCl pH 6.8 SDS Ammonium persulphate TEMED	5% (w/v) 0.125 M 0.1% (w/v) 0.1% (w/v) 0.04% (v/v)
Resolving Gel	Acrylamide Tris-HCl pH 8.8 SDS APS TEMED	10-15% (w/v) 0.375 M 0.1% (w/v) 0.1% (w/v) 0.1% (w/v)
Tris-Glycine running buffer	Glycine Tris SDS	0.192 M 0.025 M 0.1% (w/v)
Laemmli Buffer (3 x SDS Loading buffer)	Tris-HCl pH 6.8 Glycerol SDS β -mercaptoethanol Bromophenol Blue	0.15 M 30% (v/v) 6% (w/v) 15% (v/v) 0.1% (w/v)
Coomassie Blue Stain	Acetic acid Methanol Coomassie brilliant blue (G250/ R250)	10% (v/v) 45% (v/v) 0.2% (w/v)
Destain	Acetic acid Methanol	10% (v/v) 30% (v/v)

Mini-PROTEAN Tetra Cell apparatus from Bio-Rad (Hertfordshire, UK) was employed for running small gels. Vertical slab gels were produced using 5 ml of resolving gel (components listed in Table 2.6) and overlaid with 2 ml of stacking gel (see also Table 2.6). Gels were fitted into the Mini-PROTEAN Tetra Cell apparatus and the tank reservoirs were filled with Tris-glycine running buffer (Table 2.6).

Samples were mixed with the appropriate volume of 3 x SDS loading buffer (Laemmli's buffer, Table 2.6) and boiled for 5 min at 100°C before loading onto the stacking gel for separation. Molecular weight markers from Bio-Rad (Precision Plus Protein Standards, both Unstained and Pre-stained) or NEB (ColorPlus Prestained Protein Marker) were loaded alongside the samples, with a molecular weight range from 10-250 kDa. Gels were run by application of 200 V for approximately 1 h, or until the dye front had just run off the bottom of the resolving gel. Gels were either Coomassie blue stained (see Table 2.6 for stain and destain buffers) or transferred to nitrocellulose membrane for immunoblotting (as described in section 2.3.2 below).

2.3.2. Immunoblotting

Following SDS-PAGE separation, proteins were transferred from the gel to nitrocellulose membrane at a constant current of 0.2 A for 90 min using the Trans-blot SD semi-dry transfer apparatus (Bio-Rad, Hertfordshire, UK) in the presence of transfer buffer (see Table 2.7).

Table 2.7: Buffers for Immunoblotting

Buffer	Components	Concentration
Transfer Buffer	Glycine Tris Methanol	0.192 M 0.025 M 20% (v/v)
Ponceau S stain	Ponceau S Trichloroacetic acid	0.1% (w/v) 3% (w/v)
TBS-Tween (TBS-T)	Tris-HCl pH 7.5 NaCl Tween-20	0.02 M 0.137 M 0.1% (v/v)
Blocking Buffer	Non-fat dried milk (Marvel)	5% (w/v) in TBS-T
Blocking Buffer (for phospho-specific reactions)	BSA	1% (w/v) in TBS-T
Stripping Buffer	Glycine-HCl pH 2.0 SDS	0.025 M 1% (w/v)
Phosphate Buffered Saline (PBS) pH 7.4	Sodium phosphate Potassium phosphate Potassium chloride Sodium chloride	10 mM 1.8 mM 2.7 mM 137 mM

After transfer, the membrane was stained with Ponceau S to check protein transfer efficiency. The membrane was destained with dH₂O and TBS-T prior to incubation with blocking buffer for 1 h on a belly-dancer shaker. The membrane was washed 3 times with TBS-T for 5 min per wash. Primary antibodies (see Table 2.8) were diluted to the appropriate concentration in blocking buffer for membrane incubation at 4°C overnight. Membranes were washed again in TBS-T (3 × 5 min) and incubated in the corresponding secondary antibody conjugated to horse radish peroxidase for 1 h at room temperature. Secondary antibodies were also diluted to the appropriate concentration in blocking buffer. The secondary antibodies employed and their respective concentrations are found in Table 2.9. Following secondary antibody incubation, membranes were again washed in TBS-T (3 × 5 min) followed by a 10 min wash in dH₂O. The membrane was finally incubated with the enhanced chemiluminescence (ECL) system (Millipore, Bedford, MA) and exposed to autoradiographic film (Kodak, Herts, UK) for varying periods of time.

Table 2.8: Primary Antibodies for Immunoblotting

Antibody	Dilution	Host	Supplier/Origin
14-3-3 PAN	1:2000	Rabbit	Alastair Aitken and co-workers, Edinburgh
14-3-3 pSPEKA	1:250	Sheep	Alastair Aitken and co-workers
14-3-3 β	1:2000	Rabbit	Alastair Aitken and co-workers
14-3-3 ε N-terminal	1:2000	Rabbit	Alastair Aitken and co-workers
14-3-3 ε C-terminal	1:2000	Rabbit	Alastair Aitken and co-workers
14-3-3 γ	1:3000	Rabbit	Alastair Aitken and co-workers
14-3-3 η	1:2000	Rabbit	Alastair Aitken and co-workers
14-3-3 ζ	1:2000	Rabbit	Alastair Aitken and co-workers
Flotillin-1 C-20	1:500	Goat	Santa Cruz Biotechnology, Santa Cruz, CA
Prion Protein, 6H4	1:3000	Mouse	Prionics AG, Zurich
Phospho-Akt (Ser473) (D9E)	1:2000	Rabbit	Cell Signalling Technology, Danvers, MA

Table 2.9: Secondary Antibodies for Immunoblotting

Species	Dilution	Supplier/Origin
Goat/Sheep	1:2000	Sigma-Aldrich, Dorset, UK
Rabbit	1:20,000	Abcam, Cambridge, UK
Mouse	1:5000	Sigma-Aldrich, Dorset, UK

Membranes were routinely incubated in stripping buffer (see Table 2.7) for 30 min at room temperature to disrupt the interaction between the antigen and the antibody. The membrane was then washed 4 times with PBS for 10 min per wash to neutralise the pH. Membranes were incubated in blocking buffer and the immunoblotting procedure repeated. Generally, nitrocellulose membranes were not stripped more than once.

2.3.3. Lipid Raft Isolation from Whole Rat Brain

All procedures were carried out at 4°C unless otherwise stated.

Table 2.10: Buffers for Lipid Raft Isolation

Buffer	Components	Concentration
MES Buffered Saline (MBS) ⁵	MES pH 6.5	0.025 M
	NaCl	0.150 M
	Triton X-100	1% (v/v)
	CaCl ₂	0.001 M
	MgCl ₂	0.001 M
Low Density Membrane (LDM) Buffer	Sucrose	0.25 M
	Tricine pH 7.8	0.02 M
	EDTA	0.001 M

2.3.3.1. Raft Isolation Employing OptiPrep Iodixanol Gradients

Lipid rafts were prepared based on the method of Chamberlain and co-workers (Chamberlain et al. 2001; Chamberlain and Gould 2002). Other studies have employed similar methods (Parkin et al. 1999; Martens et al. 2000; Miura et al. 2001; Taverna et al. 2004; Gil et al. 2005).

A whole rat brain was weighed prior to homogenisation on ice in MBS containing 1% (v/v) TX-100 (see Table 2.10) with 20 strokes of a Dounce homogeniser. The homogenate was passed through a wide-barrel needle at least 5 times before incubation on ice for 15 min. The homogenate was centrifuged at 3,000 rpm (1100 x g) for 15 min in a Sorvall SS-34 rotor to sediment tissue debris. Once again, the

⁵ Immediately prior to homogenisation, protease and phosphatase inhibitors were added.

supernatant was passed through a wide-barrel needle 5-10 times and incubated on ice for another 15 min. OptiPrep Solution (Axis-Shield, Dundee, UK) is an aqueous solution comprising 60% (w/v) iodixanol in water. A combination of OptiPrep Solution and LDM buffer (see Table 2.10) were added to the homogenate to adjust the density to 25% (v/v) iodixanol.

OptiPrep gradients were prepared and are detailed in Table 2.11.

Table 2.11: OptiPrep Gradients for Raft Isolation

Volume OptiPrep	Volume LDM Buffer	Iodixanol Gradient
1.25 ml	13.75 ml	5% (v/v)
2.5 ml	12.5 ml	10% (v/v)
5 ml	10 ml	20% (v/v)

Discontinuous iodixanol gradients were constructed in thin walled polycarbonate tubes. For each raft isolation procedure, 6 tubes were set up, loading 3.3 ml of iodixanol/homogenate into the bottom of each tube. This was overlaid with 2 ml of 20% (v/v) iodixanol, followed by 2 ml of 10% (v/v) iodixanol. This was overlaid with 2 ml of 5% (v/v) iodixanol and finally the tubes were balanced by adding LDM buffer. A diagram of the tubes once set up is shown in Figure 2.1. Gradients were centrifuged at 33,000 rpm (121,000 x g) in a Sorvall TH641 swinging bucket rotor for 2 h.

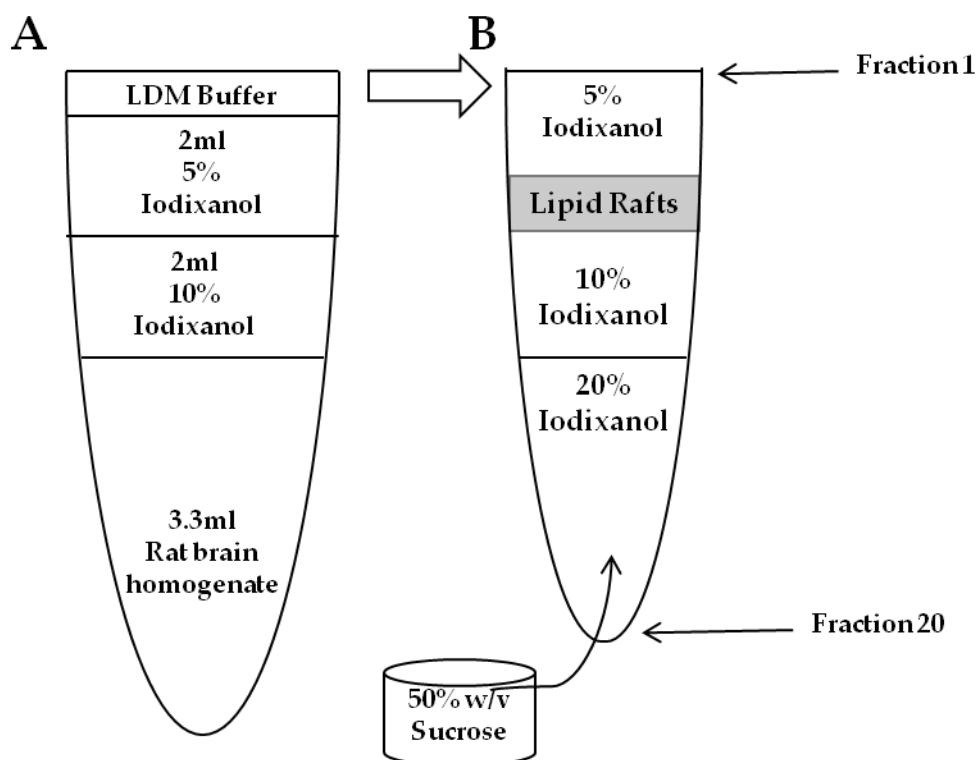


Figure 2.1: Iodixanol Gradient Set-Up For Raft Isolation From Whole Rat Brain

Lipid rafts were isolated from rat brain by TX-100 extraction, followed by flotation on an iodixanol density gradient.

- A. Representation of iodixanol gradients set up prior to centrifugation. The final concentration of iodixanol expressed as a percentage is labelled in each layer.
- B. Representation of the gradients after centrifugation. The area where the lipid rafts are found is indicated by the grey region. The gradient was collected as 20 fractions, 0.5 ml each. Fractions were collected by sucrose displacement, as shown in the diagram. Fractions were collected from the top of the tube by a fraction collector. In most cases, fraction 10 contained the lipid rafts.

After centrifugation, an opaque band was visible between the 5% and 10% iodixanol gradients which contain the lipid rafts (Figure 2.1). Twenty 0.5 ml fractions were collected by sucrose displacement and the use of a fraction collector. Fractions were stored at -20°C .

2.3.3.2. Raft Isolation Employing Sucrose Density Gradients

An alternative method of lipid raft isolation was also employed. The OptiPrep method is useful as the procedure is shorter than using sucrose gradients; however previous studies have shown the sucrose gradient method to produce more concentrated raft fractions.

Again, a whole rat brain was weighed prior to homogenisation on ice in MBS containing 1% (v/v) TX-100 (see Table 2.10) with 30 strokes of a Dounce homogeniser. The homogenate was centrifuged at 1,100 x g for 10 min in a Sorvall SS-34 rotor to sediment tissue debris. To determine the protein concentration of the cleared homogenate, a BCA assay (detailed in section 2.2.6.2) was carried out. It is important to determine protein concentration through a BCA assay and not a Bradford assay, as the lipids present in the homogenised rat brain interfere with the Bradford reagent and do not provide clear results.

As the density of TX-100 is 1.07 g/ml, a 1% (v/v) solution has a detergent concentration of 10.7 mg/ml. The protein concentration was adjusted to 2 mg/ml by addition of homogenisation buffer to give a detergent to protein ratio of 5:1 (w/w). An equal volume of 80% (w/v) sucrose in MBS was added to the cleared homogenate and passed through a wide barrel needle at least 5 times to ensure complete mixture of the two components.

Discontinuous sucrose density gradients were constructed in thin walled polycarbonate tubes. For each raft isolation procedure, 6 tubes were set up. To begin, 5 ml of 40% sucrose/brain homogenate mix was added to the bottom of each tube. This was then overlaid with 5 ml of 30% sucrose in MBS; ~2 ml of 5% sucrose in MBS and finally 5% sucrose in MBS was added to the top of each tube to ensure equal weight for balancing. The set up of the tubes prior to centrifugation is shown in Figure 2.2. Gradients were centrifuged at 38,000 rpm (160, 165 x g) in a Sorvall TH641 swinging bucket rotor for 17 h overnight.

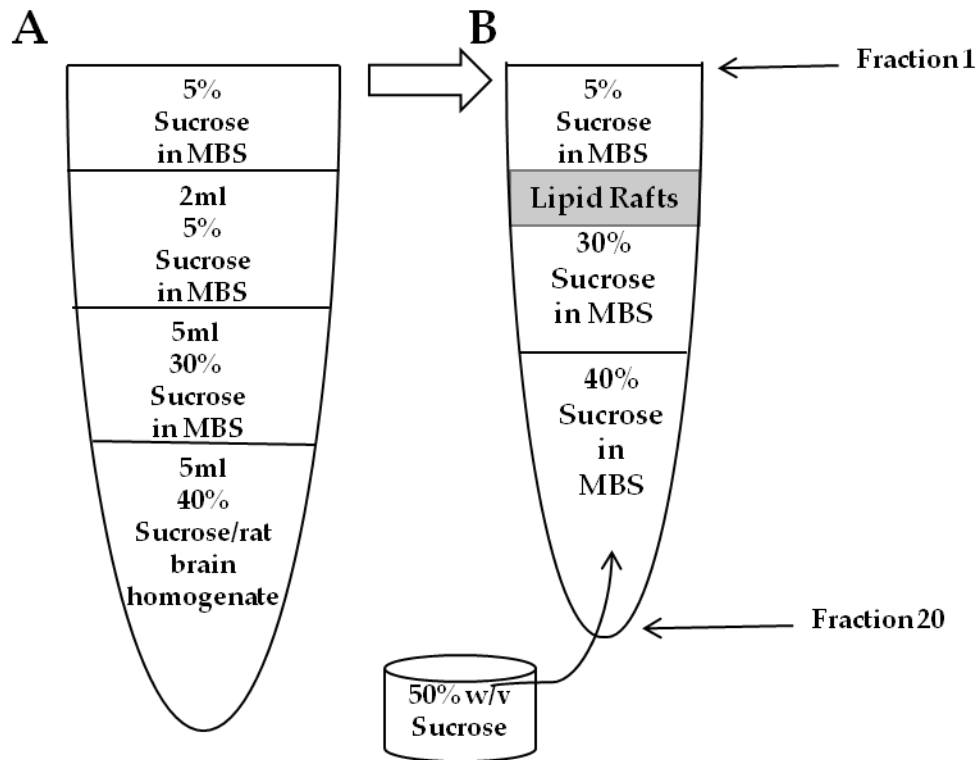


Figure 2.2: Sucrose Gradient Set-Up for Raft Isolation from Whole Rat Brain

Lipid rafts were isolated from rat brain by TX-100 extraction, followed by flotation on sucrose density gradients.

- A. Representation of sucrose density gradients set up with rat brain homogenate prior to centrifugation.
- B. Representation of the gradients after centrifugation. The grey region indicates the lipid rafts. The gradient was collected as 20 fractions of 0.5 ml. As is shown in the diagram, fractions were collected from the top of the tube by sucrose displacement. In most cases, fraction 8 contained the rafts.

After centrifugation, a white interface was visible between the 5% sucrose and the 30% sucrose gradients (Figure 2.2). This white interface contains the lipid rafts. Once again, twenty fractions at 0.5 ml were collected by sucrose displacement. The fractions were collected using a fraction collector. After collection, the fractions were stored at -20°C .

2.3.4. Cholesterol Assay

Cholesterol assays were routinely carried out on fractions isolated from rat brain to identify lipid rafts. Infinity Reagent was purchased from Thermo Electron (Waltham, MA) and the procedure carried out according to the manufacturer's instructions. Briefly, 10 μ l of sample was mixed with 1ml of Infinity Reagent and incubated at 37°C for 5 min.

The assay consists of two sequential enzyme reactions. Cholesterol oxidase converts cholesterol to cholest-4-en-3-one. This reaction creates a by-product of hydrogen peroxide, which combines with hydroxybenzoic acid and 4-aminoantipyrine to form quinoneimine dye. This reaction is driven by peroxidase and the quinoneimine dye absorbs at 500-550 nm.

Following incubation, absorbance (Abs) was measured at 500 nm and compared with a 2 mg/ml cholesterol standard prepared in the same way.

$$\text{Sample cholesterol concentration} = \frac{\text{Abs}_{500\text{nm}} \text{ sample}}{\text{Abs}_{500\text{nm}} \text{ standard}} \times 2 \text{ mg/ml}$$

2.3.5. Cholesterol Depletion of Lipid Rafts

2.3.5.1. Chloroform: Methanol Extraction

Lipid raft fractions were treated with chloroform: methanol extraction, a procedure which effectively removed lipids while concentrating the protein in the sample. Two peak raft fractions were extracted for each raft experiment. Each 500 μ l fraction was split into two 250 μ l fractions and 1 ml of chloroform: methanol (2:1 ratio) was added to each 250 μ l fraction. Tubes were inverted approximately 20 times to ensure the reagents were thoroughly mixed and briefly vortexed before centrifuging for 20 sec. After centrifugation, two layers were separated by a white interface. The lower layer, the solvent layer, was removed using a fine-tip pipette. The procedure was repeated a further two times to ensure sufficient extraction. Finally, the upper, aqueous layer was also removed, leaving the white interface remaining. The white interfaces were resuspended in 5 μ l of dH₂O and combined for further analysis.

2.3.5.2. Methyl- β -CycloDextrin (M β CD)

Fresh lipid rafts were treated with methyl- β -cyclodextrin to deplete cholesterol levels for protein analysis. The peak fractions from a fresh raft preparation were diluted in an equal volume of MBS buffer and centrifuged in a Beckman TL-100 centrifuge at 60,000 rpm (250,000 \times g) for 20 min to pellet the rafts. The supernatant was removed and the rafts were resuspended in 200 μ l of 20 mM M β CD per raft fraction and incubated at 37°C for 2 h to deplete the cholesterol. Following incubation, the mixture was centrifuged as before and the supernatant containing the proteins was used for further analysis.

2.3.6. 2-Dimensional (2D) SDS-PAGE

2D SDS-PAGE was carried out in order to identify different isoforms of 14-3-3 by iso-electric point (pI) and molecular weight.

2.3.6.1. Sample Rehydration to IPG Strips

Protein samples were prepared and resuspended in Rehydration Buffer (Genomic Solutions, Cambridgeshire, UK). The concentration of the protein and the volume of rehydration buffer required depended on the IPG strips used. In most cases, Immobiline DryStrip pH 4-7, 11 cm IPG strips (GE Healthcare, Buckinghamshire, UK) were used. Protein samples were prepared to between 50 and 300 µg concentrations and a total volume of 280 µl in Rehydration Buffer. Samples were pipetted into a rehydration tray and an IPG strip was gently overlaid. The strip was moved slowly over the solution to ensure that the whole strip was in contact with the solution and there were no air bubbles. Finally, 1 ml of mineral oil was coated on top of each strip to prevent the strips drying out during rehydration. The rehydration tray was covered and the strips were left to rehydrate at room temperature overnight.

2.3.6.2. IsoElectric Focussing

IPG strips which had been rehydrated were focussed using an Ettan IPGphor II IsoElectric Focusing System (Amersham Biosciences, Bucks, UK).

The mineral oil was carefully removed by gentle pipetting and the strips were transferred to IPG strip holders which are used for the focussing step. Moistened wicks were added to each end of the strips to ensure good contact with the electrodes. Again, 1 ml of mineral oil was used to coat the strips to prevent drying out during the focussing step.

The focussing procedure used is shown in Table 2.12.

Table 2.12: IsoElectric Focussing Procedure

Step	Voltage Mode	Voltage (V)	Time (h:min)
1	Step and Hold	500	4:00
2	Gradient	1000	1:00
3	Gradient	6000	2:30
4	Step and Hold	6000	20:00

2.3.6.3. IPG Strip Equilibration

Focussed IPG strips were equilibrated in an SDS buffer system to prepare the strips for second-dimension separation. Equilibration buffer⁶ (6 M Urea, 4% SDS, 30% glycerol, 50 mM Tris-HCl, pH 6.8) was freshly prepared for each equilibration. The equilibration buffer was supplemented with either DTT or IAM and incubated at 37°C with gentle agitation as shown in Table 2.13.

Table 2.13: Equilibration Conditions

Buffer Supplement	Incubation Time (mins)
50 mM DTT	45
50 mM DTT (fresh)	30
150 mM IAM	15

2.3.6.4. Second-Dimension Separation

Equilibrated IPG strips were separated by SDS-PAGE on the second dimension. However, as the samples were focussed on 11 cm IPG strips and the second dimension supports 7 cm strips, the IPG strips were cut to size for second-dimension separation. IPG strips with a pH range of 4-7 were used as the pI of 14-3-3 is approximately 4.5 (Aitken et al. 1995b). This meant that the focussed IPG strip could be shortened at the pH 7 end. A diagram of this is shown in Figure 2.3.

⁶ Bromophenol blue was also added to provide a dye-front for second-dimension separation.

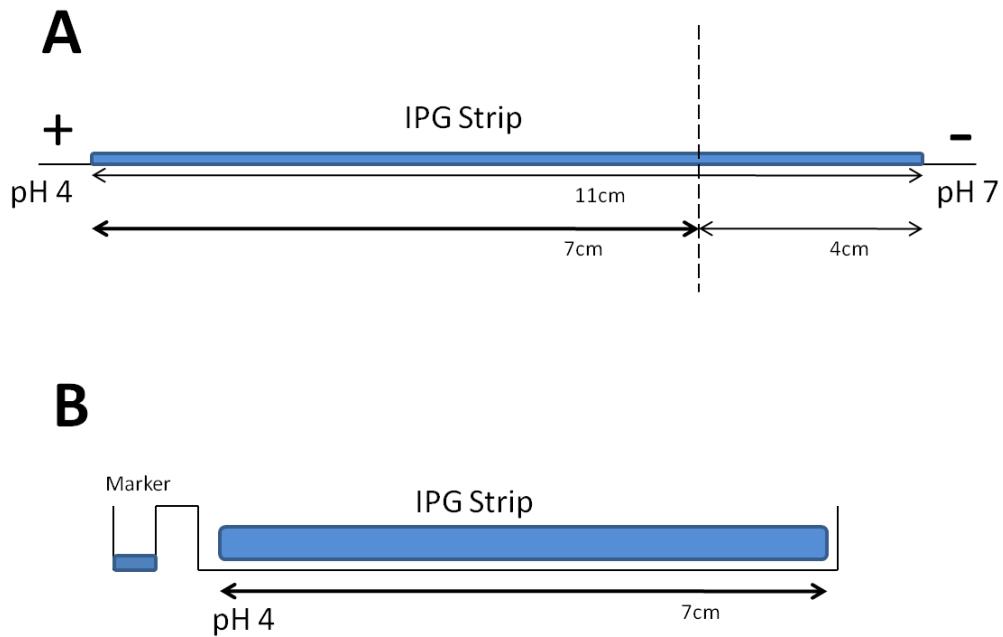


Figure 2.3: Diagram of IPG Strips Modified for Second-Dimension Separation

Protein samples were rehydrated onto IPG strips and separated according to pI by iso-electric focussing. IPG strips used for iso-electric focussing are 11 cm long, however only strips 7 cm long can be separated on second-dimension.

- A.** Diagram showing the modification of an IPG strip for second-dimension separation.
- B.** Diagram showing how the modified IPG strip is loaded into the second-dimension gel.

The second-dimension separation was carried out on NuPAGE 4-12% Bis-Tris Zoom Gel 1.0 mm X IPG Well gels in the presence of MOPS buffer (both Invitrogen, Paisley, UK). An XCell *SureLock* Mini Cell (Invitrogen, Paisley, UK) was employed for second-dimension separation. IPG strips were loaded with the pH 4 end of the strip adjacent to the molecular weight marker lane. Gels were run by application of 100-200 V. Second-dimension separation SDS-PAGE was usually ran at a lower voltage than tris-glycine SDS-PAGE to prevent smearing of protein samples. Separation was continued until the dye-front had run off the resolving gel.

After 2D separation was completed, gels were either stained with Coomassie Blue dye or transferred to nitrocellulose membrane for immunoblotting (see section 2.3.2).

2.3.7. In-Gel Digestion and Mass Spectrometry

2.3.7.1. In-Gel Digestion of Protein Bands

Following SDS-PAGE, protein bands were revealed through staining with Coomassie Blue (R250) or Colloidal Coomassie stain (Thermo Fisher Scientific, Waltham, MA). Individual bands were excised according to Aitken and Learmonth (2002). Briefly, gel pieces were incubated with 300 μ l of 200 mM NH_4HCO_3 / 50% acetonitrile for 30 min. This step is repeated a further 2 times to ensure removal of SDS. Proteins were reduced by incubation with 20 mM DTT/ 200 mM NH_4HCO_3 / 50% acetonitrile for 1 h at room temperature. Bands were washed three times in 200 mM NH_4HCO_3 / 50% acetonitrile to remove the DTT prior to alkylating cysteine residues by incubation in 50 mM iodoacetamide/ 200 mM NH_4HCO_3 / 50% acetonitrile for 20 min at room temperature in the dark. Bands were washed three times in 20 mM NH_4HCO_3 / 50% acetonitrile and centrifuged at 13,000 rpm in a benchtop centrifuge for 2 min. The gel pieces were covered in 100% acetonitrile, to shrink them and turn them white. After 5 min, or once the pieces had turned white, the acetonitrile was removed and the gel pieces left to dry. The gel pieces were rehydrated with trypsin solution (Promega, Southampton, UK) and 50 mM NH_4HCO_3 on ice. Once the gel pieces had swelled, they were incubated at 32°C overnight.

The peptides were collected in the supernatant and further extraction was achieved through sonication for 10 min. Peptides were stored at -20°C until analysis by mass spectrometry. For long term storage, peptides were kept at -80°C.

Occasionally, peptides would be sub-digested with the Endoproteinase Glu-C enzyme (Boehringer Mannheim, Mannheim, Germany) by addition of the enzyme to the tryptic digests after at least 90 min of incubation with trypsin alone. Where enzymatic sub-digestion has been applied, details are provided in the text.

2.3.7.2. Concentration of Peptides for Mass Spectrometry

Occasionally, dilute peptides would be concentrated for mass spectrometry. This involves a simple clean-up procedure by solid-phase extraction through the use of a ZipTip (Millipore, Bedford, MA). A ZipTip is a miniature reverse-phase column which is packed into a 10 μl pipette tip. A C_{18} ZipTip contains a 0.5 μl bed volume of C_{18} silica (15 μm , 200 \AA). Briefly, the tip is pre-wet by washing three times with 100% acetonitrile and equilibrated three times with 0.1% trifluoroacetic acid (TFA) in high-purity water. Peptides are bound to the ZipTip by aspirating and dispensing the sample 10-15 times. The ZipTip is then washed with 0.1% TFA as before. Peptides are eluted from the ZipTip with 0.1% TFA in 50% acetonitrile. Eluted samples were applied directly to a MALDI-TOF target plate for analysis.

2.3.7.3. Matrix-Assisted Laser-Desorption Ionization-Time-of-Flight (MALDI-TOF) Mass Spectrometry

Peptides were analysed on a Voyager DE-STR MALDI-TOF mass spectrometer (Applied Biosystems, Paisley, UK). A 0.5 μl aliquot of peptides was mixed with 0.5 μl of α -cyano-4-hydroxycinnamic acid (CHCA) matrix and loaded onto a MALDI-TOF target plate. The plate is placed into the mass spectrometer where a laser pulse ionises the peptides allowing them to enter the flight tube. The peptides are separated according to their mass to charge ratio. As they reach the mass detector at different times, a distinct signal is produced for each peptide.

The computer program Data Explorer was used to calibrate the spectra using the internal calibration peaks provided by the trypsin. Once the peaks had been processed, they were database searched using in-house licensed MASCOT software. The results from the database search provide probability scores for any identification based on either a statistical score or a molecular weight search (MOWSE) score. The known mass of matched peptides is compared with experimental calculated masses and the higher the probability or score, the greater the confidence level that the correct protein has been identified (Henkin et al. 2004).

2.3.7.4. Liquid Chromatography-Mass Spectrometry (LC-MS)

Peptides were analysed on an LTQ LC-MS system consisting of an Agilent 1200 Series HPLC (Agilent Technologies, Berkshire, UK) with a Kasil sealed fused silica pre-column (Next Advance, Averill Park, NY) packed to a length of approximately 3 cm with Pursuit C₁₈, 5 µm particle size (Varian, Agilent Technologies, Berkshire, UK) reverse phase column and PicoTip Emitter analytical column PF 360-75-15-N-5 (New Objective, Woburn, MA) packed to a length of approximately 20 cm with Pursuit C₁₈, 5 µm particle size (Varian, Agilent Technologies, Berkshire, UK). The column was equilibrated with solvent A (0.1% formic acid in 2.5% acetonitrile) and eluted with a linear gradient from 0 to 10% over 6 to 8 min; from 8 to 60% over 8 to 35 min; from 60 to 100% over 35 to 40 min; solvent B (0.1% formic acid, 0.025% TFA in 90% acetonitrile) over 45 min at a flow rate of 5 µl/min.

The LTQ mass spectrometer (Thermo Fisher Scientific, Waltham, MA) was fitted with a nanoLC ESI source. Data dependent acquisition was controlled by Xcalibur software and database searching was achieved using in-house licensed MASCOT software.

2.3.8. Protein Crystallography

2.3.8.1. Sitting Drop Vapour Diffusion

A multi-channel pipette was used to transfer 50 µl of the crystal screen (Hampton screen 1+2, Hampton Research, Aliso Viejo, CA) from the 96-well plate into a 96-well Crystal Clear Duo Plate for robotic crystallography trials. Once the plate was prepared, it was inserted into the crystal robot (Oryx-8, Douglas Instruments, Berkshire, UK) and set up following the manufacturer's instructions. The Crystal Clear Duo Plate allows two ratios of protein: reservoir to be tested. Drops were 50% protein: 50% reservoir and 30% protein: 70% reservoir. Plates were sealed with crystal tape (Crystal Clear, Manco Inc., Ohio) and stored at 17°C to promote crystal formation.

2.3.8.2. Hanging Drop Vapour Diffusion

For the hanging drop method, a Linbro 24 well plate was greased with petroleum jelly. Each well contained 0.5 ml of the reservoir solution. A volume of 2 μ l of the protein sample was pipetted into the centre of a 22 mm siliconised circular cover slip, immediately followed by an equal volume of the reservoir solution pipetted into the protein drop. The drop was not mixed and the coverslip was inverted immediately over the corresponding well of reservoir solution. The coverslips were twisted 45° to ensure a good seal before incubating the tray at 17°C.

2.3.9. Cross-Linking

In order to test the quaternary structure of 14-3-3 proteins, cross-linking experiments were employed. Cross-linking is a technique where two or more molecules are chemically joined together by a covalent bond. The cross-linking agent has the ability to chemically attach to specific functional groups on the protein or molecule and attachment between two groups stabilizes the tertiary or quaternary protein structure. There are a number of cross-linking agents which have different properties to accommodate the ability to cross-link a variety of proteins and molecules. Variable properties of cross-linkers include chemical specificity, water-solubility and spacer arm length, including the ability to reverse the cross-linking process.

Previous research conducted in the lab had identified the cross-linker dimethyl pimelimidate (DMP) to be the optimal cross-linker for 14-3-3 ζ . Cross-linking experiments were employed to identify the conformational status of 14-3-3 ζ under various assay conditions. Typical cross-linking experiments were set up as follows:

20 μ g 14-3-3 ζ Protein + 6 μ l DMP (35 mM) + 15 μ l PBS

Samples were incubated at room temperature for 16 h. The reaction was stopped due to the addition of 3 x Sample Buffer prior to analysis on SDS-PAGE.

2.3.10. In-Vitro Kinase Assay

To test 14-3-3 ζ phosphorylation, kinase assays were carried out. Assays were set up with a number of variables however the basic components of each reaction were as follows:

PKA Reaction Buffer ⁷ (10 x)	-	10 μ l
10mM ATP	-	10 μ l
PKA (1000 U)	-	10 μ l
14-3-3 ζ (100 μ g)	-	40 μ l
dH ₂ O ⁸	-	<u>---- μl</u>
		<u>100 μl</u>

To test that phosphorylation was due to kinase activity, control assays were set up in the absence of kinase. Sphingosine was added to the reaction mixture to give a final concentration of 50 μ M. Once all the reagents had been added to the mixture, the volume was adjusted to 100 μ l with dH₂O and incubated at 30°C. After incubating for 2 h, the reaction was stopped by the addition of 3 x sample buffer or freezing at -20°C. Samples were then cross-linked (as described in section 2.3.9) to test the conformation of 14-3-3.

⁷ 1 x PKA Reaction Buffer (NEB) comprises 50 mM Tris-HCl, 10 mM MgCl₂, pH 7.5 at 25°C.

⁸ The volume of dH₂O added varied according to any additional reagents (e.g. sphingosine or control lipids) that were being tested to give a final volume of 100 μ l.

2.3.11. Enzyme-Linked Immunosorbent Assay - ELISA Assay

The enzyme-linked immunosorbent assay (ELISA) was employed for investigating the inhibition potential of 14-3-3 ζ by selected compounds.

Table 2.14: Buffers for ELISA Assay

Buffer	Components	Concentration
TBS	Tris-HCl pH 7.5 NaCl	0.02 M 0.137 M
Wash Buffer	Tween 20	0.05% (v/v) in TBS
1 x Blocking Buffer	Non-fat dried milk (Marvel)	3% (w/v) in Wash Buffer
2 x Blocking Buffer	Non-fat dried milk (Marvel)	6% (w/v) in Wash Buffer

A 96-well microplate coated with anti-GST antibody (GE Healthcare, Buckinghamshire, UK) was used for binding assays. GST-Exo-enzyme S (GST-ExoS) was immobilized to the wells by incubating 500 ng of protein in 100 μ l of 2 x blocking buffer for 1 h at room temperature. Following incubation, wells were washed with 200 μ l of wash buffer five times. Wells were then blocked for 1 hour with 1 x blocking buffer to prevent non-specific binding of protein. For compound testing; concentrations tested were determined according to the solubility of the compound. The range of concentrations analysed are provided in the text. Compounds were prepared in 2 x blocking buffer (minus Tween 20) and incubated with 500 ng of 14-3-3 ζ for 20 min at room temperature. Following incubation, the protein: compound mixtures were added to the appropriate wells and incubated for 1 h at room temperature. Wells were washed prior to the addition of a 14-3-3-specific antibody (Pan 14-3-3). The antibody was prepared in 1 x blocking buffer and 100 μ l of this added to each well and incubated for 1 h at room temperature. Wells were washed again before addition of the corresponding secondary antibody (100 μ l in 1 x blocking buffer) and incubated for another hour at room temperature. Wells were washed a final three times.

To detect the antibody, the HRP substrate 4-chloro-1-naphthol (4-CN) was used. This reagent produces an insoluble end product which, when it reacts with HRP, produces a blue visible colour. The optimal absorbance for this reagent is 495 nm. The plate reader used for detecting the assay results, a Wallac Victor² 1420

Multilabel Counter, had an absorbance filter at 485 nm. This wavelength is still within the absorbance range of the substrate and is therefore suitable for detection of the reagent. The 4-CN was prepared according to the manufacturer's instructions (Sigma-Aldrich, Dorset, UK) and 100 μ l was added to each well. The absorbance was measured around 5 min after addition of the 4-CN reagent.

To aid interpreting the assay results, a control well where no compounds were tested and a well with only the 4-CN reagent were prepared to give absorbance values at both extremes for the particular assay being carried out. Wells which produced a high absorbance were deemed as a negative result, indicating that the compound being tested had failed to inhibit the interaction between 14-3-3 ζ and ExoS. Wells which produced a low absorbance were deemed as a positive result, indicating that the compound being tested had successfully inhibited the interaction between 14-3-3 ζ and ExoS.

CHAPTER 3

14-3-3 PROTEINS AND LIPID RAFTS

3.1. Introduction

A number of studies have shown that lipid rafts play an integral role in neurodegenerative disease progression (see section 1.2.3). Many proteins which are processed at lipid rafts also interact with the 14-3-3 family of proteins. These protein interactions have also been shown to be a critical stage in disease progression. The fact that many disease proteins interact with 14-3-3 and are processed at lipid rafts leads to the suggestion that there may be a connection between lipid rafts and 14-3-3 proteins.

In order to test this hypothesis, studies were carried out to identify whether 14-3-3 proteins are associated with lipid raft domains. A previous student (Dr. Brechin) identified the five main brain 14-3-3 isoforms as associating with lipid rafts. Dr. Brechin also investigated how 14-3-3s associate with rafts. Her results indicate that 14-3-3s do not associate directly, but possibly through interaction with a membrane-bound protein.

Dr. Brechin was unable to demonstrate the association of phosphorylated 14-3-3 isoforms with lipid rafts. The β and ζ isoforms of 14-3-3 are the only two identified to date which are endogenously heavily phosphorylated on Ser185 (Aitken et al. 1995b). These isoforms are known as α and δ , respectively, and are only found present in brain tissue. Approximately 50% of the β and ζ isoforms are phosphorylated in brain. The presence of these isoforms heavily phosphorylated only in brain suggests an important function, possibly in neurodegenerative disease. In addition, phosphorylation of 14-3-3 can significantly alter protein function by negative regulation of protein interactions (Toker et al. 1992; Dubois et al. 1997; Aitken et al. 2002; Aitken 2011).

Identifying phospho-14-3-3s associating with lipid raft domains may be a critical step in understanding neurodegenerative disease pathology and may provide significant drug targets for the treatment of disease. Here, research has been undertaken in order to establish an association between phospho-14-3-3 isoforms and lipid rafts and to determine whether phosphorylation has an effect on protein interaction partners at lipid raft domains.

In addition, sphingosine, a sphingolipid present in lipid rafts, has also been found to have links with 14-3-3 phosphorylation. The β , η and ζ isoforms of 14-3-3 have been shown to be phosphorylated by a “sphingosine-dependent kinase”, which has now been identified as the kinase domain of PKC δ following caspase-3 cleavage (Hamaguchi et al. 2003). The site of phosphorylation, Ser58, is a residue buried within the dimer interface (Megidish et al. 1998) and it appears that in the presence of sphingosine, this residue is exposed, allowing phosphorylation by a kinase.

Woodcock and colleagues (Woodcock et al. 2003; Ma et al. 2005; Woodcock et al. 2010) have identified that 14-3-3 ζ can be phosphorylated by PKA on Ser58 but only in the presence of sphingosine; an effect which results in the conversion of 14-3-3 into a monomer. One thing that is unclear from their research is whether 14-3-3 monomerises due to the presence of sphingosine or through phosphorylation on Ser58.

Due to the abundance of sphingosine in rafts, further investigating the role of sphingosine on 14-3-3 phosphorylation is also an area of interest. In addition, the effect of sphingosine on 14-3-3 at lipid rafts is an area which has not been explored and there is potential for the structural formation of 14-3-3 present at lipid rafts to have a number of implications on neurodegenerative diseases.

3.2. Aims

Phospho-forms of 14-3-3 in Lipid Rafts

As neurodegenerative disease proteins not only interact with 14-3-3, but are also processed at lipid rafts, identification of the phospho-forms of 14-3-3 at rafts may have implications on disease pathology.

How 14-3-3 Isoforms Associate with Lipid Rafts

Previous studies with difopein have shown that 14-3-3 association with lipid rafts is not membrane-bound (see Introduction section 1.2.2). This indicates that 14-3-3 must be associating with rafts through interaction with another membrane-bound protein. Identifying the protein(s) which 14-3-3 interacts with may highlight neurodegenerative disease proteins providing more detail on neurodegenerative disease pathology. In addition, different isoforms or phospho-forms may associate through interactions with different proteins.

Does Sphingosine Affect 14-3-3 Phosphorylation And/ Or Quaternary Structure?

Does the presence of sphingosine have an effect on 14-3-3? Sphingosine is a sphingolipid present in lipid rafts. If sphingosine can affect the phosphorylation status of 14-3-3 or the quaternary structure of the protein, this may have a significant impact on protein function.

Akt Phosphorylation in Lipid Rafts

The kinase Akt also associates with lipid rafts. This endogenous kinase may contribute to the structural changes initiated by sphingosine, altering the function of 14-3-3 proteins.

3.3. Results

3.3.1. Lipid Raft Isolation from Rat Brain

Several methods have been detailed in the literature with regard to isolating lipid rafts. Here, two methods were routinely used. These employed Optiprep gradients (see section 2.3.3.1 in Materials and Methods) and sucrose density gradients (see section 2.3.3.2 in Materials and Methods).

The main raft isolation method employed for this research was the Optiprep method. Compared with other studies, this method appears to produce slightly more diffuse raft fractions, however one positive is that lipid rafts can be isolated from whole rat brain in a less time-consuming way compared with the sucrose gradient method. However, during this research, when the sucrose gradient method was employed, the resulting raft fractions appeared to be 'clumpy' and more difficult to work with. Due to this, both methods were employed, but the Optiprep gradient method was found to be the best and therefore the preferred method for this research.

Isolation of lipid rafts from whole rat brain with the Optiprep gradient method produces 2-3 peak fractions of lipid rafts. As the overall amount of rafts which can be isolated from rat brain is spread out over a number of fractions, to ensure using a sufficient amount for experimental analysis, these fractions were pooled together, to produce more physiologically relevant and accurate results.

In order to identify the lipid raft fractions, a cholesterol assay was routinely employed. Full details are provided in the Materials and Methods section 2.3.4. Once the cholesterol concentration of each fraction was calculated, the results were plotted and are shown in Figure 3.1.

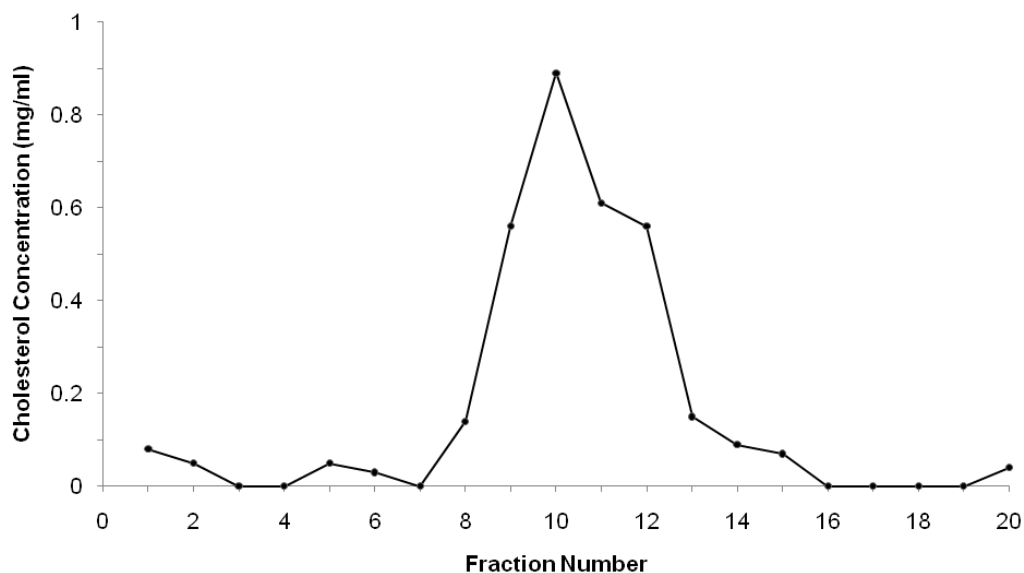


Figure 3.1: Cholesterol Assay of Rat Brain Fractions

Lipid rafts were isolated from whole rat brain by TX-100 isolation followed by flotation on Optiprep gradients. From the isolation procedure, 20 fractions were collected and subjected to a cholesterol assay. Experimental details are provided in Chapter 2. The peak raft fraction is fraction 10. Adjacent fractions also contain high levels of cholesterol indicating that they also contain lipid rafts. For lipid raft analysis, the two main peak fractions from each tube were combined.

Figure 3.1 shows the results from the Optiprep gradient isolation method. It clearly shows the peak raft fractions, however they are dispersed over a number of fractions. For raft analysis, the two peak fractions would be combined together to increase the overall amount of rafts analysed. Peak raft fractions can also be identified by protein concentration. The protein concentration of the rafts is greater than that of the adjacent fractions. To determine the protein concentration, a Bradford Assay (section 2.2.6.1 in Materials and Methods) was originally used. However, the high concentration of lipids in these samples interacts with the Bradford reagent, affecting the outcome of the assay. A more suitable means of determining protein concentration is to use a Bicinchoninic Acid (BCA) assay (section 2.2.6.2 in Materials and Methods). The results from the BCA assay of the Optiprep fractions are shown in Figure 3.2.

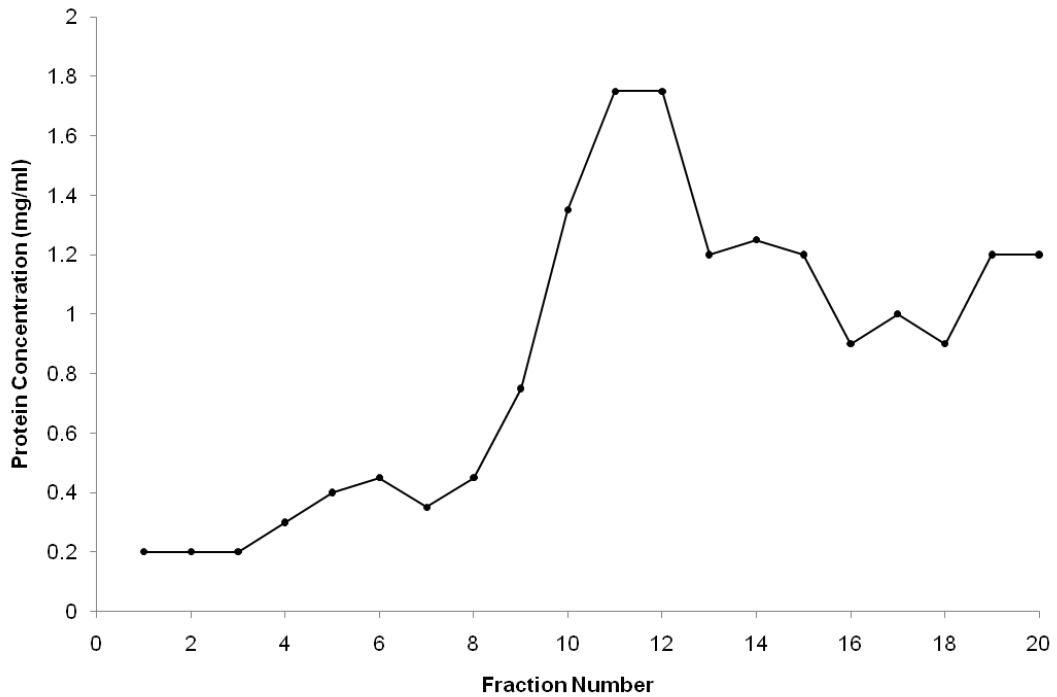


Figure 3.2: BCA Assay of Rat Brain Fractions

Lipid rafts were isolated from whole rat brain by TX-100 isolation followed by flotation on Optiprep gradients. Each of the 20 fractions collected were subjected to BCA assay to determine protein concentration. All experimental details are provided in Chapter 2. As the image shows, protein concentration increases to the peak raft fractions, which are identified from the cholesterol assay. The protein concentration of the fractions slightly decreases before increasing to indicate the cytosolic protein fractions, which are rich in protein.

The results of the BCA assay are consistent with those from the cholesterol assay. Fractions which are high in cholesterol are also high in protein, a characteristic of lipid rafts. The last few fractions are also high in protein as these are the cytosolic protein fractions. The results from the BCA assay can be tested by Coomassie staining the fractions collected from the rat brain homogenate. These results are shown in Figure 3.3.

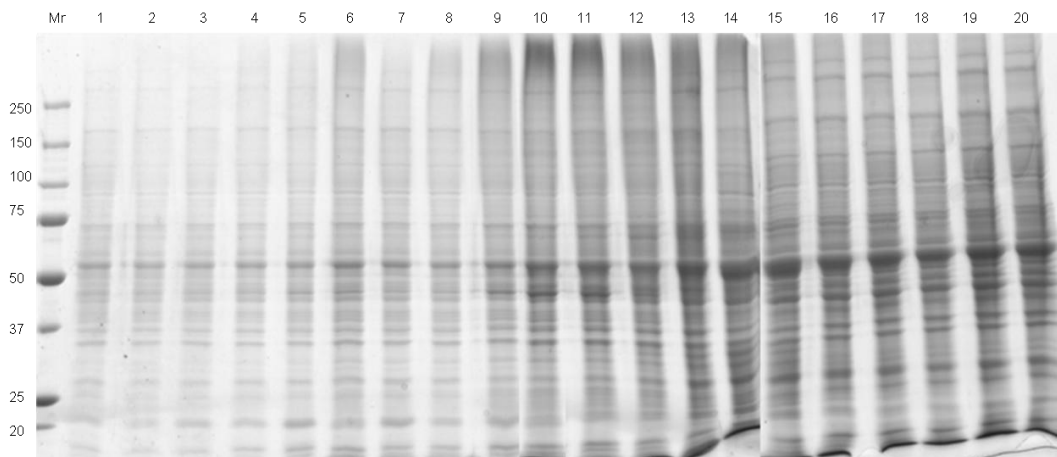


Figure 3.3: SDS-PAGE of Raft Fractions Isolated from Rat Brain

Fractions collected from the Optiprep raft isolation method were mixed with an appropriate volume of 3 × Sample Buffer and separated on 12% SDS-PAGE. Following protein separation, gels were stained with Coomassie Blue dye followed by incubation with de-stain solution until protein bands could be visualised. The gel indicates that fractions 1-9 are low in protein. Fractions 10-13 are much higher in protein and these fractions contain the lipid rafts. There is a slight drop in intensity from fraction 14, increasing in intensity correlated with protein concentration up to fraction 20. Fractions 16-20 are the cytosolic protein fractions.

It is clear that the Optiprep gradient isolation method is successful at isolating lipid rafts from whole rat brain. Similar results were obtained when using both fresh and frozen rat brain, which is beneficial, as it is more convenient to obtain rat brains and store them at -80°C until required. It is not surprising that using frozen rat brain should not affect lipid rafts as they are also termed detergent resistant membranes. The very name suggests that they are resistant to detergents and therefore should be resistant to freezing and thawing. These tests were also carried out on the sucrose density gradient fractions and produced similar results (data not shown).

3.3.2. Confirmation of Raft Isolation by Known Markers

After isolating lipid rafts from rat brain homogenate, it is important to clarify that the cholesterol-rich fractions are in fact, lipid rafts. The various methods of confirming that the cholesterol-rich fractions are rafts were employed.

3.3.2.1. Flotillin-1/ Reggie-2

The flotillin/ reggie proteins were identified and named by two independent research groups in 1997. One group identified two proteins of 47 kDa while screening for proteins upregulated in retinal ganglion cells during axon regeneration after optical nerve lesion in goldfish (Schulte et al. 1997; Lang et al. 1998). The group named the proteins 'reggie'; deriving the term from 'regeneration' due to the proteins functions. Simultaneously, a group investigating associating caveolae proteins identified 'flotillin' (Bickel et al. 1997; Galbiati et al. 1998). This group also identified flotillin as a marker for "*the buoyant, Triton-insoluble membrane fraction in brain*" which we refer to as lipid rafts. The group named the protein due to the fact they "*float like a flotilla of ships*" in the lipid raft fraction (Bickel et al. 1997). To add to the confusion, flotillin-1 = reggie-2 and flotillin-2 = reggie-1. For the purpose of this research, combined with the associated discovery to lipid rafts, the proteins will be referred to as flotillins.

In order to identify the lipid rafts, all of the fractions collected from the rat brain gradient were separated on SDS-PAGE and immunoblotted with a flotillin-1 antibody. The fractions which contain the flotillin-1 protein were identified as the raft fractions. The immunoblot with flotillin-1 from the Optiprep method is shown in Figure 3.4.



Figure 3.4: Identification of Raft Fractions By Western Blotting for Flotillin-1

Raft fractions isolated by flotation on Optiprep gradients were separated by SDS-PAGE on 12% acrylamide gels. Proteins were transferred to nitrocellulose membrane and probed with flotillin-1 primary antibody. All experimental details are given in Chapter 2. The western blot indicates the presence of the flotillin-1 protein in fractions 9-12. This is concurrent with previous data indicating that these fractions contain lipid rafts.

3.3.2.2. Prion Protein (PrP)

An alternative identification procedure is to test the rafts for the presence of the prion protein (PrP). Prion protein is a GPI-anchored protein (Stahl et al. 1987) which associates with lipid rafts (Vey et al. 1996; Naslavsky et al. 1997). Once again, rat brain gradient fractions were separated on SDS-PAGE and were immunoblotted with prion protein antibody (see Table 2.8 in Materials and Methods). Fractions which contained the protein were identified as lipid rafts. The immunoblot from the Optiprep isolation method is shown in Figure 3.5.

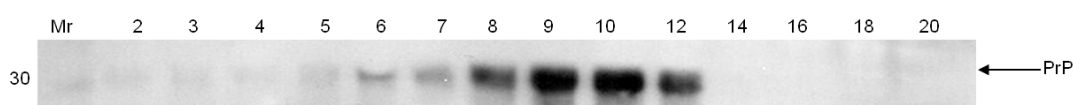


Figure 3.5: Identification of Rafts By Western Blotting for Prion Protein

Raft fractions were transferred to nitrocellulose membrane and probed with the prion protein primary antibody. Experimental details are provided in the Methods. The fractions containing the prion protein (fractions 8-12) correspond to those identified by other methods as lipid rafts.

3.3.3. Chloroform: Methanol Extraction for Lipid Raft Analysis

Analysing lipid raft proteins can be very difficult due to the high cholesterol content. When running lipid raft fractions on SDS-PAGE, the samples can smear quite badly, resulting in poor quality results and occasionally difficulty in interpreting data.

In order to overcome these issues, a method of cholesterol depletion employing chloroform: methanol extraction was developed. The exact details of the procedure used are detailed in section 2.3.5 of Materials and Methods. It should be noted that this procedure is extremely effective when the analysis does not require any proteins to still be active, i.e. this method was employed for procedures such as SDS-PAGE in which proteins are denatured nevertheless.

The method consists of subjecting raft containing fractions to the solvents in a ratio of 2:1 (chloroform: methanol). This combination of solvent and alcohol produces a

general extraction solvent, which allows the lipids to dissolve. The chloroform dissolves neutral lipids while the methanol disrupts hydrogen bonds of polar lipids which are membrane bound. This ensures that all of the lipids can be removed from the fraction, leaving only protein to be analysed.

When carrying out the procedure, the fraction splits into three components; an upper aqueous layer, a white interface and a lower solvent layer. The lower solvent layer is removed prior to the addition of more solvent mixture. Fresh solvent mixture is added to ensure sufficient extraction of the lipids. Once the extraction is complete, the upper aqueous layer can be removed, leaving the protein-rich interface remaining. An additional bonus of this procedure, other than removing lipids, is that the protein in the sample is concentrated. Once the samples had been treated by the extraction procedure, they could be used without requiring any further concentration steps. For all lipid raft experiments, the two peak raft fractions would be extracted and combined for further analysis.

The result of employing the chloroform: methanol extraction was extremely effective. In order to clarify that the method was suitable for raft studies, all of the component layers from the extraction were separated on SDS-PAGE and stained with Coomassie blue. This was to ensure that no protein was lost through the procedure, which could have seriously affected experimental results. Figure 3.6 shows that the protein is concentrated to the interface and no protein is lost to either the aqueous or solvent layers of the extraction.

This clearly shows that the chloroform: methanol extraction is an effective method for removing the lipids which had made analysis difficult, without losing any of the proteins associated with lipid rafts.

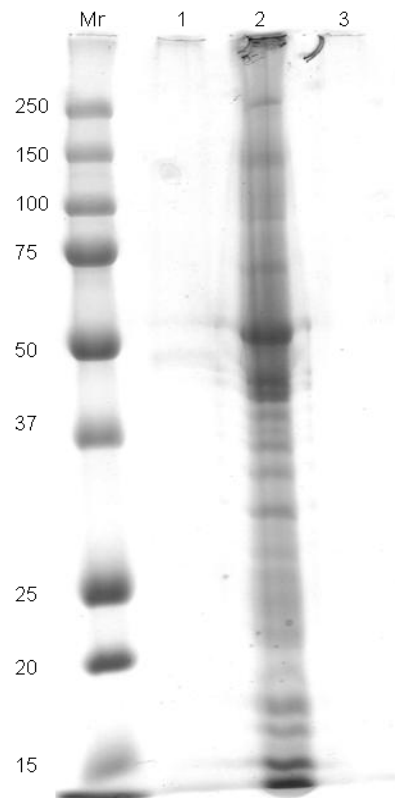


Figure 3.6: SDS-PAGE After Chloroform: Methanol Extraction

Each of the fractions from chloroform: methanol extraction of lipid rafts were analysed on a 12% SDS-PAGE gel. The samples loaded onto the gel are as follows: Mr = Molecular weight marker (Bio-Rad); Lane 1 = Upper aqueous layer; Lane 2 = White interface; Lane 3 = Lower solvent layer. It is clear from the gel that the protein in the lipid raft fraction is concentrated to the interface, which is retained for further analysis of raft proteins.

3.3.4. 2D Analysis Identifies Phospho-14-3-3 in Lipid Rafts

A previous student in the lab, Dr. Brechin, identified the five main brain isoforms of 14-3-3 as associating with lipid rafts (Brechin 2006) although association of the phosphorylated forms was not confirmed. Immunoblotting with an antibody which recognises all 14-3-3 isoforms confirmed that 14-3-3 was detected in raft fractions subjected to chloroform: methanol extraction (data not shown). However, identifying the phospho-forms was not so simple. The previous difficulty in detection led to the hypothesis that, if present, the phospho-forms would be in much lower abundance than the other isoforms. This would make detection by 1D

analysis very difficult. The decision was therefore taken to analyse the proteins by 2D SDS-PAGE. As the two phospho-forms of 14-3-3 are very similar in molecular weight and iso-electric point (pI), an additional benefit would allow identifying whether both or just one of the phosphorylated isoforms are present at lipid rafts.

For phospho-14-3-3 identification, peak raft fractions were identified and subjected to chloroform: methanol extraction. These experiments employed raft fractions isolated with Optiprep gradients, so the two peak raft fractions were treated and combined. The proteins were resuspended in a volume of Rehydration Buffer required for the IPG strip used. Full details of the 2D procedure are provided in section 2.3.6 of Chapter 2.

Once the 2D procedure was completed, separated proteins were transferred to nitrocellulose membrane for immunoblotting. Full experimental details and antibodies used are given in section 2.3.2 of Chapter 2. In order to identify the phospho-forms of 14-3-3, the membrane was probed with primary antibodies specific for the N-terminal region of the β and ζ isoforms of 14-3-3 (Figure 3.7A). The blot shows two distinct elongated spots and slightly different pI values. This indicates the presence of both phospho- and non-phospho-forms of the 14-3-3 proteins. The black arrow highlights the phosphorylated isoforms, which are slightly more acidic than the un-phosphorylated forms, shown by the white arrow.

To identify phospho-forms of 14-3-3 the same blot was stripped and blocked before re-probing with the phospho-specific antibody, pSPEKA. This antibody, which was characterised by former student, Dr. Samuel Clokie (Clokie 2005), is named as such due to the epitope which the antibody recognises on the 14-3-3 protein, when phosphorylated. The result from this blot is shown in Figure 3.7B. The blot in Figure 3.7B has been cropped to represent the hatched area in Figure 3.7A. It is clear that the spots detected with the phospho-specific antibody match those detected by the antibodies which detect the N-terminus of the protein, regardless of phosphorylation state.

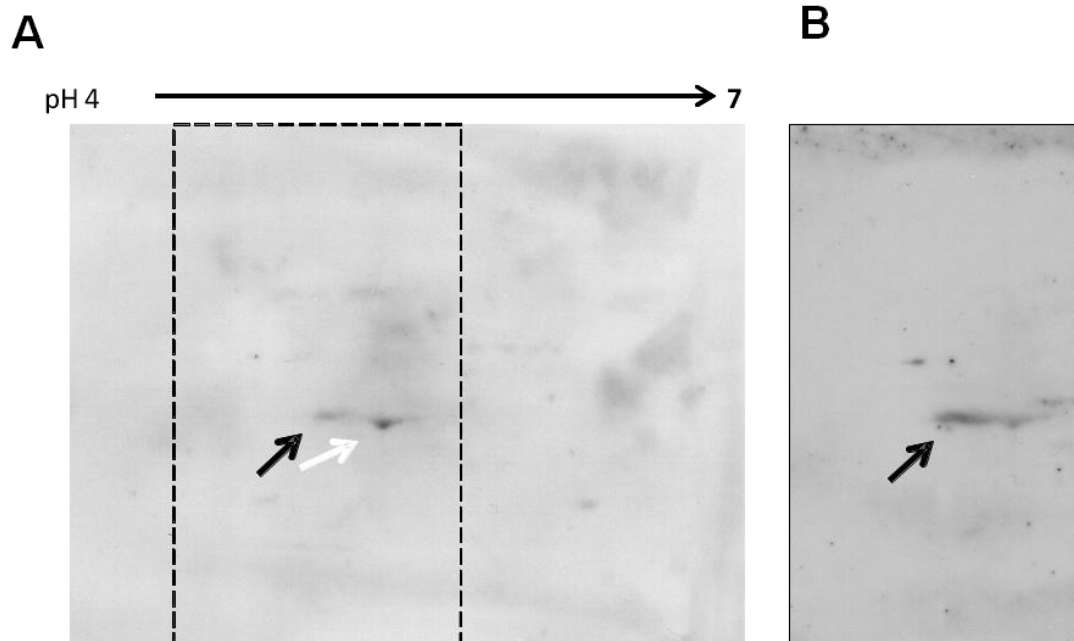


Figure 3.7: 2D-PAGE Analysis of Lipid Raft Fractions

Lipid raft fractions were subjected to chloroform: methanol extraction and separated by 2D SDS-PAGE before immunoblotting with 14-3-3 specific antibodies.

- A. Immunoblotting with antibodies specific for the N-terminus of the β and ζ isoforms of 14-3-3. These antibodies recognise both the phosphorylated and un-phosphorylated forms of 14-3-3 (Martin et al. 1993). The black arrow indicates the phosphorylated isoforms of 14-3-3 (α and δ) and the white arrow indicates the un-phosphorylated 14-3-3 isoforms (β and ζ).
- B. Immunoblotting with 14-3-3 phospho-specific antibody. This antibody is specific for isoforms of 14-3-3 (α and δ) which are phosphorylated at Ser185. The arrow indicates the phosphorylated 14-3-3 isoforms present in lipid rafts. The corresponding part of the 2D gel shown is indicated by the hatched box in A.

The results shown here conclusively identify the presence of the phosphorylated isoforms of 14-3-3 (α and δ) at lipid rafts. The presence of the isoforms is at a lower level than the non-phosphorylated isoforms of 14-3-3; however their presence may prove to be significant. The fact that the phospho-forms have only been identified in brain tissue indicates that the presence of these proteins may be an important factor in many neuronal regulatory processes which occur, including those which may be involved in neurodegenerative disease.

3.3.5. 14-3-3 in Rafts by Mass Spectrometry

The identification of the α and δ isoforms of 14-3-3 at lipid rafts has a number of potential implications in neurodegenerative diseases. One thing that is uncertain is how abundant these proteins are at lipid rafts. It is well established that the 14-3-3 proteins comprise 1% of total brain protein (Boston et al. 1982) suggesting that they are present in great abundance; however the distribution of the proteins at lipid rafts is not known.

To gauge an estimate of the proportions of phosphorylated 14-3-3 to un-phosphorylated 14-3-3 at lipid rafts, mass spectrometry was employed. A lipid raft fraction was depleted of cholesterol using the chloroform: methanol extraction procedure and run on a 4-12% Bis-Tris Gel (Invitrogen, Paisley, UK). A 14-3-3 ζ control was run alongside the raft fraction. This is shown in Figure 3.8.

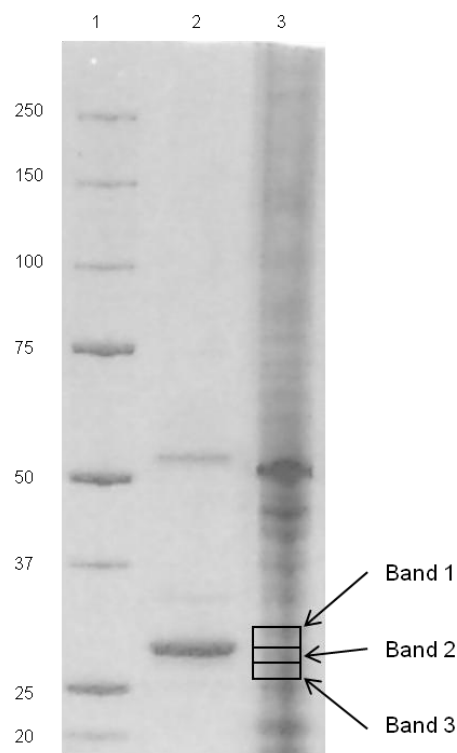


Figure 3.8: SDS-PAGE of Raft Fraction for Mass Spectrometry

4-12% Bis-Tris gel (Invitrogen) showing; Lane 1 – Molecular weight marker (Bio-Rad); Lane 2 – 14-3-3 control sample; Lane 3 – Lipid raft fraction treated with chloroform: methanol extraction. The boxed area indicates the bands excised for digestion and subsequent mass spectrometry.

In the raft lane, there are no definitive bands around the 30 kDa region, so three bands were tightly cut in that area, corresponding to the 14-3-3 ζ control which was run in the adjacent lane. These three bands were digested with trypsin (full details in section 2.3.7) and analysed by mass spectrometry on MALDI-TOF. The results are displayed in Table 3.1 below.

Table 3.1: MALDI-TOF Results

Mass spectrometry results from raft proteins digested with trypsin.

Band	Hit Number	Isoform Detected	MOWSE Score
1	7	Epsilon	39
2	3	Zeta/Delta	47
	7	Gamma	36
	16	Beta/Alpha	29

The results from the MALDI-TOF mass spectrometry identified the epsilon, gamma, beta/zeta and alpha/delta isoforms of 14-3-3, however, none of these proteins produced very good MOWSE scores. This result is promising, as it proves that these isoforms are present in lipid rafts, however, it does not prove the presence of the phospho-forms. In particular, the phosphorylated peptide of interest was not detected. Response in MALDI-TOF is often relatively low for phosphopeptides and this appears to be the case here. To overcome this issue, LC-MS was carried out.

The LC-MS results proved to be more informative than the MALDI-TOF results, by identifying the gamma, eta, theta, epsilon, beta/zeta and alpha/delta isoforms of 14-3-3. However, once again, the phospho-peptide was not detected. Despite this, the mass spectrometry data clarifies the presence of these 14-3-3 isoforms at lipid rafts, concurring with the data that Dr. Brechin produced throughout her Ph.D. This is useful as it confirms that the western blotting data is not due to cross-reaction and is

a true result, validating the antibody specificity. The results of the LC-MS mass spectrometry analysis are detailed in Table 3.2 below.

Table 3.2: LC-MS Results

Mass spectrometry results from raft proteins digested with trypsin and analysed on LC-MS.

Band	Hit Number	Isoform Detected	MOWSE Score
1	2	Epsilon	566
	27	Zeta/Delta	86
2	1	Zeta/Delta	232
	2	Gamma	158
	3	Beta/Alpha	108
	4	Eta	81
	5	Theta	78
	6	Epsilon	58
3	1	Eta	226
	2	Zeta/Delta	212
	5	Theta	104
	6	Beta/Alpha	96
	10	Gamma	47
	37	Epsilon	20

Despite the LC-MS data proving to be more informative and producing much more significant hits with greater MOWSE scores, the phosphorylated peptide was still not detected. The peptide produced from the cleavage with trypsin is large and hydrophobic which may affect detection. To overcome this, the peptides were sub-digested with the enzyme Endoproteinase Glu-C.

When the α and δ isoforms of 14-3-3 are digested with trypsin, they produce the peptide shown in Figure 3.9.



Figure 3.9: Tryptic Digest Sequence of Phospho-14-3-3

Sequence of the peptide produced from digesting phosphorylated 14-3-3 (e.g. α and δ) with trypsin. The amino acids underlined indicate the peptide following trypsin cleavage between the lysine and alanine residues.

Digestion with Endoproteinase Glu-C produces a much shorter peptide, as shown in Figure 3.10.

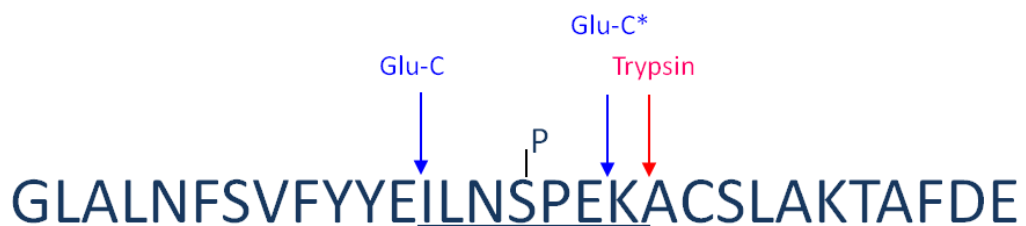


Figure 3.10: Phospho-14-3-3 Peptide Following Endoproteinase Glu-C Digestion

Sequence of the peptide produced following subdigestion of the tryptic peptide with Endoproteinase Glu-C. The amino acids underlined indicate the resulting peptide following cleavage between the glutamine and isoleucine residues. Digestion with Endoproteinase Glu-C alone would also result in cleavage between the glutamine and lysine residue (marked Glu-C*) however due to the prior digestion with trypsin, this cleavage no longer occurs since Glu-C is an end protease. This peptide is much shorter and more likely to be detected by mass spectrometry.

In both figures, the amino acid sequence which is underlined represents the peptide produced following enzyme digestion. Sub-digestion with Endoproteinase Glu-C produces a much shorter peptide, which was anticipated to be detected more easily by mass spectrometry.

Before sub-digesting the raft samples, the effect of digestion with Endoproteinase Glu-C was tested on a control protein. Unfortunately, we had no recent gels with a purified brain 14-3-3 protein band which could be easily excised for enzyme digestion. However, there were some gels from ~20 years ago, which had protein bands of 14-3-3 purified from rat brain. For the purposes of using an appropriate control, one of these bands was excised and digested with both trypsin and Endoproteinase Glu-C, according to the method detailed in section 2.3.7.1. Following enzyme digestion, the peptides were run on LC-MS and the results analysed using database searches on the in-house MASCOT software.

Amazingly, the results from the LC-MS showed that 14-3-3 beta/alpha and 14-3-3 zeta/delta were the two top hits with MOWSE scores of 124 and 101 respectively, and the phosphorylated peptides were also detected for both phosphorylated 14-3-3 isoforms. The results from the LC-MS provided the ms/ms results for the phosphorylated and un-phosphorylated peptide, which provides an indication of the spectra to look for in the raft samples. The ms/ms spectra are shown in Figure 3.11 and Figure 3.12. The difference in mass between the phospho-peptide and the un-phosphorylated peptide is 80 Da.

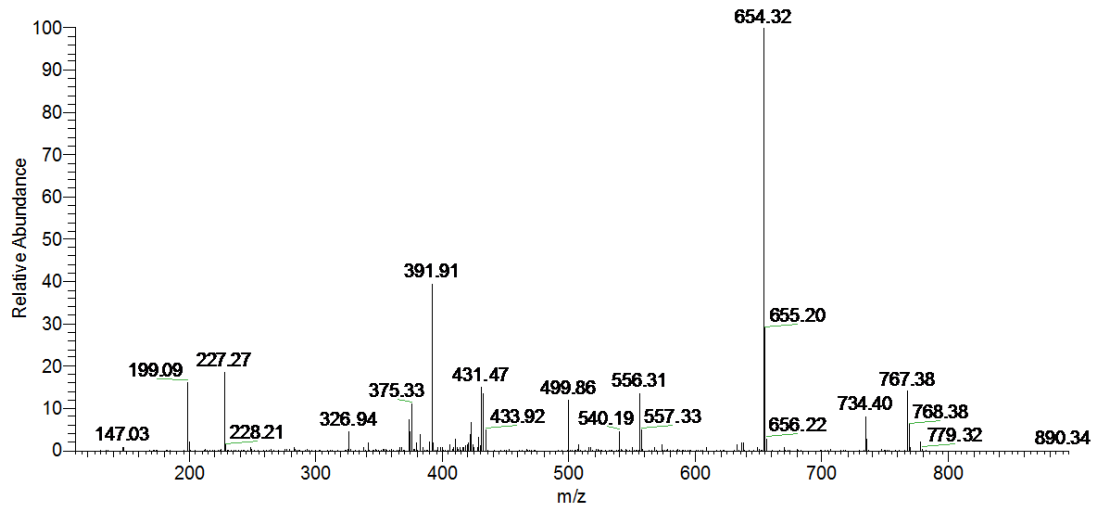


Figure 3.11: MS/MS Control Data from Phosphorylated Peptide
MS/MS fragmentation of the phosphorylated 14-3-3 peptide ILNSPEK.

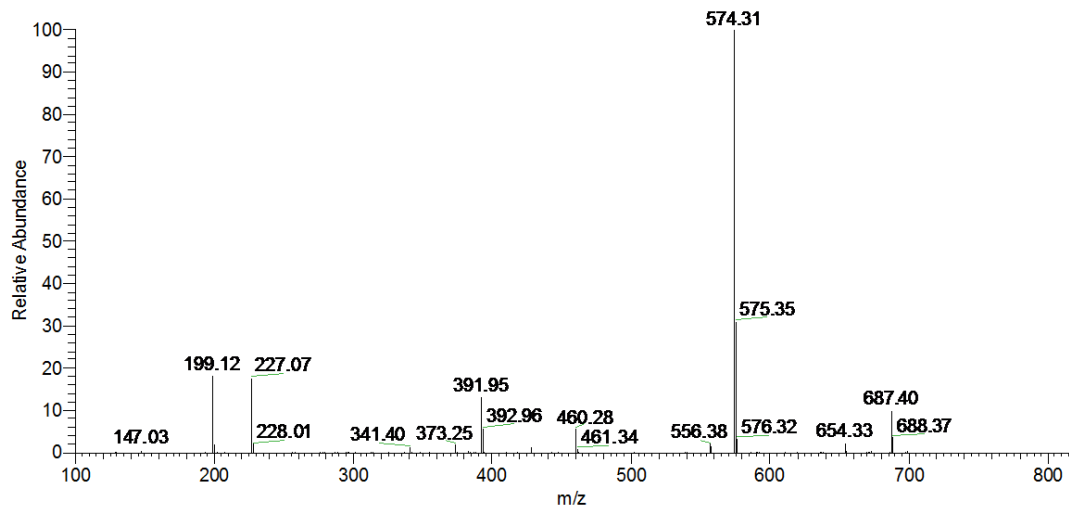


Figure 3.12: MS/MS Control Data from Non-Phosphorylated Peptide
MS/MS fragmentation of the non-phosphorylated 14-3-3 peptide ILNSPEK.

The control sample spectra provided an indication of what to look for in the lipid raft samples which were sub-digested with Endoproteinase Glu-C. In addition to the expected ms/ms data, the control sample also provided an elution time for each isoform, supplying an additional data point to analyse to identify the presence of the phospho-forms of 14-3-3.

To ensure that the phospho-peptide was not lost in any way, both the gel bands which had been digested with trypsin and also the aqueous peptides collected from the trypsin digest were sub-digested with endoproteinase Glu-C. For ease, the aqueous peptides collected from the tryptic digests were combined for the sub-digestion.

The peptides from bands 2 and 3 were analysed by MALDI-TOF to compare the relative amounts of peptides corresponding to the desired masses to determine which band to analyse further by LC-MS. It was clear from the MALDI data (not shown) that band 2 had a significantly higher level of peptides corresponding to the mass of the un-phosphorylated (800 Da) and phosphorylated (880 Da) peptides. Therefore peptides from this band were analysed by LC-MS along with the aqueous peptides from the double digest.

Unfortunately database scans for each of the samples did not identify 14-3-3 and subsequent analysis of the raw data files did not yield any further information. This is disappointing but not entirely unexpected and should not detract from the importance of the identification of phospho-14-3-3 by immunoblotting. Immunoblotting is a much more sensitive technique than mass spectrometry and the fact that detection was only possible through a highly sensitive technique emphasises the hypothesis that the levels of phosphorylated 14-3-3 present at lipid rafts are in much lower abundance than un-phosphorylated 14-3-3. This is not surprising, given that phosphorylation of 14-3-3 on Ser185 negatively regulates a number of protein interactions, including those with FOXO3a, Bax and BAD (Tsuruta et al. 2004; Sunayama et al. 2005; Aitken 2011). It is therefore expected that the levels of phosphorylated 14-3-3 would be lower than un-phosphorylated 14-3-3 at rafts, yet detection of 14-3-3 α and δ does imply that cellular processes may be adversely affected due to the presence of these proteins which may be a contributing factor in neurodegenerative disease pathology.

3.3.6. 14-3-3 Association with Lipid Rafts

Following identification of the phospho-forms of 14-3-3 at lipid rafts, the next important question to address is, do these isoforms have different interaction partners to the un-phosphorylated forms? There are a number of caveats to approaching answering this question. One popular method of identifying interacting proteins is through immuno-precipitation (IP's), however, the process of binding the 14-3-3 proteins to an antibody could inhibit the site of interest. This could lead to either a lack of results due to the competition of the antibody over the interacting protein, or the inability of any proteins to bind to the phosphorylation site, due to the presence of the antibody.

In a bid to overcome such problems and tackle this question, a peptide pull-down method was attempted which involved coupling peptides for the site of interest (SPEKA – un-phosphorylated and pSPEKA – phosphorylated) to magnetic beads through an amine group. A control peptide was also tested and the proteins in lipid rafts which interacted with these peptides were analysed.

Unfortunately, there were no visible protein bands in any of the sample lanes on the gel. The initial thought was that the samples were too dilute and the protein concentration was too low for detection by SDS-PAGE. Therefore, all the samples were concentrated to 50 μ l in a vivaspin concentrator (see section 2.2.4) and re-analysed by SDS-PAGE. Once again, the results were disappointing. There was only one visible band at ~70 kDa in the supernatant samples (data not shown).

The results of this experiment indicate that during cholesterol depletion with M β CD, a number of raft associated proteins become insoluble and are contained in the pellet following centrifugation. This also appears to be the case for the 14-3-3s, indicating that they are binding to a transmembrane protein with such great affinity that they are not released into the supernatant following cholesterol depletion and remain bound to their raft binding partners. This would also account for the lack of targets identified from the pull-down itself. If 14-3-3s are binding with great affinity to transmembrane proteins, the peptides employed for the pull-down experiment

would not have the ability to displace this interaction and therefore pull-down the interacting proteins.

In an attempt to test this theory, and also to identify whether specific isoforms of 14-3-3 associate differently to lipid rafts, a western blot of the pellet and supernatant produced from cholesterol depletion with M β CD was carried out. The supernatant, pellet (resuspended in 120 μ l PBS) and a cytosolic control fraction (loaded at 5 x lower volume) were ran on a 12% SDS-PAGE gel and transferred to nitrocellulose membrane. The blots were treated as described in Chapter 2 and immunoblotted with antibodies specific for all of the five brain isoforms of 14-3-3. The results of these blots are shown in Figure 3.13.

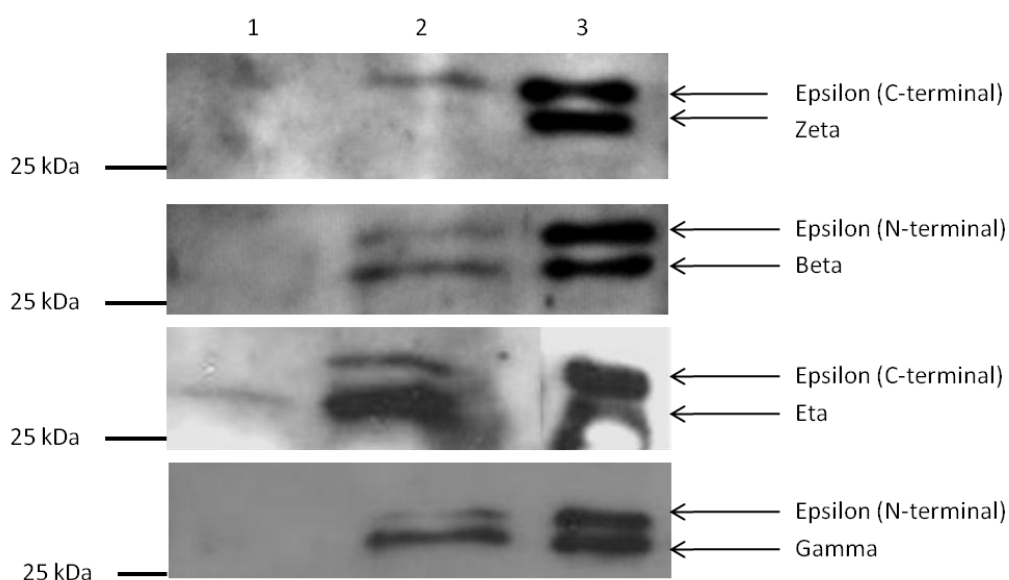


Figure 3.13: 14-3-3 Isoform Association with M β CD Treated Lipid Rafts

Lipid rafts extracted from rat brain were treated with M β CD and immunoblotted with antibodies specific for each of the five main brain isoforms of 14-3-3 following M β CD treatment. Lanes are labelled as follows: Lane 1 – Supernatant; Lane 2 – Pellet; Lane 3 – Cytosolic control (loaded at a 5 x lower volume).

A useful way to confirm that the M β CD treatment was successful would have been to immunoblot for the raft marker proteins flotillin-1 and PrP. These proteins would be detected in the supernatant fraction following their release from disrupted lipid rafts by the cholesterol depletion treatment.

The results shown in Figure 3.13 clearly indicate that the different 14-3-3 isoforms associate differently with lipid rafts. 14-3-3 ζ is undetectable in M β CD treated rafts, as there is no protein detection in either the supernatant or the pellet from the cholesterol treatment. Conversely, 14-3-3 η appears to be highly abundant at raft domains, with strong detection in the pellet sample and a faint, but visible, band present in the supernatant. 14-3-3 β , ϵ and γ clearly do associate with the raft pellet, but it is obvious that in comparison with the cytosolic control, the detectable levels of 14-3-3 proteins at rafts are low. One important observation from these results is that, with the exception of 14-3-3 η , the association of the other 14-3-3 isoforms is with the pellet, supporting the hypothesis that 14-3-3 proteins interact with a raft-bound protein and are not solubilised during cholesterol depletion. These findings indicate that 14-3-3 η is the most prominent isoform present in lipid rafts. This was further tested by a control, where M β CD treatment was substituted with PBS.

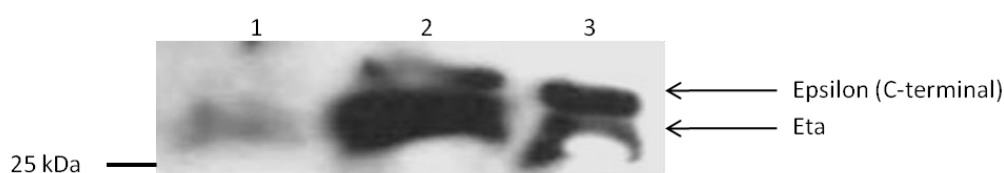


Figure 3.14: 14-3-3 Association with Lipid Rafts

Lipid rafts extracted from rat brain were incubated with PBS as opposed to M β CD and immunoblotted for 14-3-3 η . The lanes are labelled as follows: Lane 1 – Supernatant; Lane 2 – Pellet; Lane 3 – Cytosolic control (loaded at a 5x lower volume).

Unfortunately, the control sample was only immunoblotted with 14-3-3 η and ϵ . What this experiment shows is that the association of 14-3-3 with rafts is not cholesterol dependent. The same pattern of association for these two isoforms is witnessed in rafts both rich in cholesterol and those which are depleted of cholesterol. As the bands from the control blot (Figure 3.14) appear slightly darker than those from the M β CD blots (Figure 3.13) this may suggest that a proportion of 14-3-3 associates directly with cholesterol. However, with the exception of 14-3-3 η , none of the other 14-3-3 isoforms are detected in the supernatant fractions of any of the M β CD blots. If 14-3-3 partly associates with cholesterol, then following

cholesterol depletion, the protein would be released into the supernatant and be detected. In addition, the detection of 14-3-3 η in the supernatant of the control blot suggests that detection in the supernatant of the M β CD blot may not be cholesterol related.

It would be interesting to see if the other isoforms follow this pattern of association in cholesterol rich rafts, particularly the 14-3-3 ζ isoform. However, preliminary results with two different 14-3-3 isoforms indicate that M β CD has little impact on the association of 14-3-3 proteins with rafts. Taken together, the data presented here form a strong argument that association of 14-3-3 proteins with lipid rafts is not cholesterol related and that association is via a membrane-bound protein. It does appear that whatever protein the 14-3-3s are interacting with, the interaction is of high affinity, making identification of the membrane-bound protein difficult.

One possible means of overcoming this issue would be to conduct simultaneous overlay assays, or far western blots, with mass spectrometry analysis. This may help identify raft associated proteins with which 14-3-3s can interact as a starting point to identify these raft proteins.

3.3.7. Purification of 14-3-3 ζ for Sphingosine-Dependent Phosphorylation and Effect on Dimerisation

The sphingolipid sphingosine has been shown to elicit an effect on 14-3-3 ζ phosphorylation. In order to investigate this further, 14-3-3 ζ was cloned into a His-tagged vector (p-Trc-His-A') and the expression conditions were optimised. Once the optimal expression conditions were determined, 14-3-3 ζ was over-expressed and purified by a one step purification procedure using immobilised metal affinity chromatography (IMAC). This one step purification technique produced a highly purified protein for testing the effects of sphingosine. An SDS-PAGE gel of the purified protein from the IMAC column is shown in Figure 3.15.

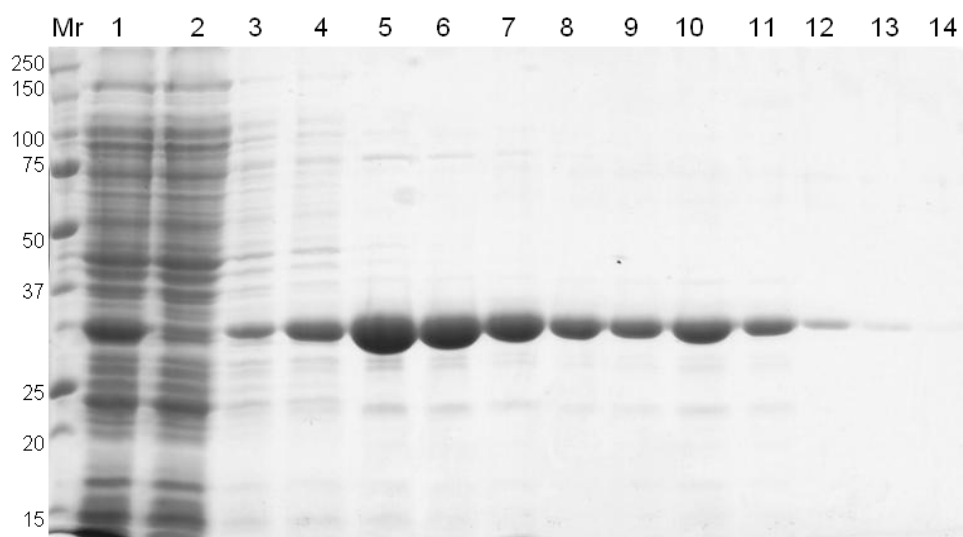


Figure 3.15: SDS-PAGE of 14-3-3 ζ Fractions Collected from IMAC

SDS-PAGE of fractions collected from 14-3-3 ζ IMAC purification. Fractions were analysed on a 12% SDS-PAGE gel. Lanes are labelled as follows: Mr – Molecular Weight Marker; Lane 1 – Lysate; Lane 2 – Flow-Through; Lane 3 – Wash; Lane 4 – Elution 1; Lane 5 – Elution 3; Lane 6 – Elution 5; Lane 7 – Elution 7; Lane 8 – Elution 9; Lane 9 – Elution 11; Lane 10 – Elution 13; Lane 11 – Elution 15; Lane 12 – Elution 17; Lane 13 – Elution 19; Lane 14 – Final Wash.

The fractions collected from the column which were found to contain the protein were pooled together in a vivaspin concentrator with a MWCO of 10 kDa. Once concentrated, the buffer was either exchanged to 1 x PBS or 25 mM HEPES buffer for further experimental procedures. (Full details are given in Chapter 2).

To investigate the effects of sphingosine, cross-linking studies were conducted. The purified 14-3-3 ζ was incubated with the cross-linker dimethyl pimelimidate (DMP) to determine that the protein can adopt a dimer structure. This cross-linker has been shown by previous lab members to be the most optimal for 14-3-3 proteins. The results of this cross-linker can be seen in Figure 3.16.

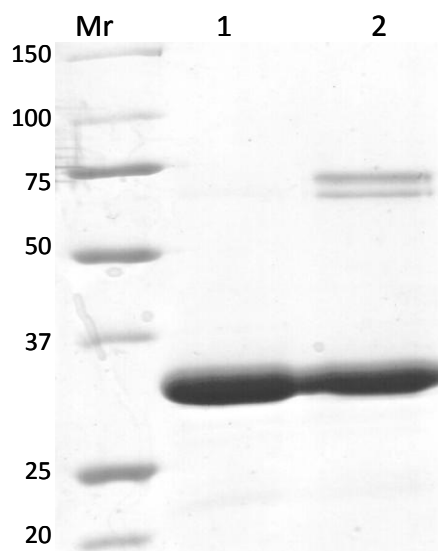


Figure 3.16: SDS-PAGE of 14-3-3 ζ Cross-Linking

14-3-3 ζ was incubated with the cross-linker DMP at room temperature for 16 h. Following incubation, cross-linking samples were boiled in an appropriate volume of 3 x Sample Buffer and separated on 12% SDS-PAGE. Lanes are labelled as follows: Mr – Molecular Weight Marker; Lane 1 – 14-3-3 ζ only control; Lane 2 – 14-3-3 ζ cross-linked with DMP.

It is clear from the gel that the DMP has successfully cross-linked 14-3-3 ζ . The band in the control lane (lane 1) represents the 14-3-3 ζ control and also illustrates the purity of this protein following concentration. The bands in the cross-linked lane (lane 2) represent the monomeric form of 14-3-3 ζ (~30 kDa) and also the dimeric form of 14-3-3 ζ (~60 kDa). The effects of sphingosine are studied in the following sections.

3.3.8. *In Vitro* Kinase Assays to Investigate the Effects of Sphingosine

Sphingosine can influence the phosphorylation of 14-3-3 proteins at Ser58, a residue buried deep within the dimer interface (Megidish et al. 1998; Hamaguchi et al. 2003; Woodcock et al. 2003; Woodcock et al. 2010). It is unclear what conformational effect sphingosine elicits on 14-3-3 proteins to allow this phosphorylation to take place. It has been speculated that interaction with sphingosine alters the conformation of 14-3-3 by opening up the protein at the dimer interface, exposing the phosphorylatable residue. The effect of phosphorylation prevents further 14-3-3 dimerisation, resulting in 14-3-3 remaining in a monomeric state. An alternative method of action may be that the sphingosine molecule acts like a detergent, disrupting the interaction between two 14-3-3 monomers, rendering them unable to dimerise and open to phosphorylation. Either of these scenarios will have a number of implications on 14-3-3 protein function, particularly at lipid rafts, which are rich in sphingolipids which include sphingosine.

To attempt to understand how sphingosine affects the conformation of 14-3-3, and its subsequent phosphorylation, *in vitro* kinase assays were performed. Sphingosine was tested at a final concentration of 50 μ M. This concentration was employed based on the previous research conducted by Woodcock (et al. 2010). The full experimental procedure is detailed in section 2.3.10 of the Materials and Methods and the following assay conditions were tested:

1. 14-3-3 ζ
2. 14-3-3 ζ + PKA
3. 14-3-3 ζ + sphingosine
4. 14-3-3 ζ + sphingosine + PKA

To investigate the effect of sphingosine, two methods were attempted. The first involved cross-linking the kinase samples and analysing these by SDS-PAGE to see if the quaternary structure of 14-3-3 is altered in the presence of sphingosine. The effect of cross-linking is shown in Figure 3.17.

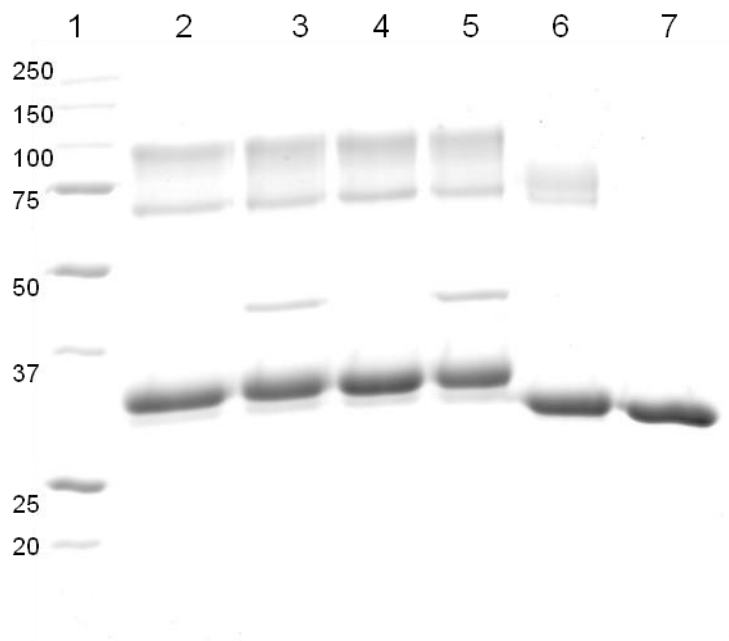


Figure 3.17: SDS-PAGE of Cross-Linked Kinase Assay Samples

Kinase assay samples were treated with 35 mM DMP cross-linker and analysed by 12% SDS-PAGE. Lanes are labelled as follows: Lane 1 – Molecular weight marker; Lane 2 – Kinase assay 1 (14-3-3 ζ only); Lane 3 – Kinase assay 2 (14-3-3 ζ plus PKA); Lane 4 – Kinase assay 3 (14-3-3 ζ plus sphingosine); Lane 5 – Kinase assay 4 (14-3-3 ζ plus sphingosine plus PKA); Lane 6 – Purified 14-3-3 ζ plus cross-linker; Lane 7 – Purified 14-3-3 ζ minus cross-linker. The band in lanes 3 and 5 at ~40 kDa is PKA.

The results of the cross-linking analysis are not promising. All of the samples assayed appear to cross-link to the same degree. This may be due to the protein remaining in a dimeric state until phosphorylated, however the levels of monomeric to dimeric 14-3-3 do not appear to differ in the assay sample containing both PKA and sphingosine.

In addition to cross-linking, the kinase assay samples were analysed by mass spectrometry to look for changes in mass due to phosphorylation. Initial analysis of the individual samples (data not shown) suggested that phosphorylation was occurring in assay 2 (14-3-3 ζ plus PKA) when compared with the control of assay 1 (14-3-3 ζ only). Comparison of assay 4 (14-3-3 ζ plus sphingosine plus PKA) also appeared to show phosphorylation. To clarify this, assays 1+2 and 1+4 were spotted together for mass spectrometry analysis, to see if there were distinct peaks

indicating phosphorylation between the two samples. The spectra for these tests are shown in Figure 3.18 and Figure 3.19.

From the spectra of assay 1 and 2 mixed together (Figure 3.18), there are two clear peaks, representing the unphosphorylated and the phosphorylated protein. This indicates that 14-3-3 is phosphorylated by PKA on a residue other than Ser58, as there is no agent present which can affect the dimeric structure of 14-3-3 to expose this site for phosphorylation. This is useful for analysis of the sphingosine kinase samples. If there is a difference of only ~80 Da, this indicates that there is no phosphorylation occurring in addition to what would be expected by PKA. Interestingly, the spectra of the kinase samples with sphingosine and PKA (Figure 3.19) shows a change in mass from unphosphorylated to phosphorylated protein in the region of ~160 Da; representative of phosphorylation on two residues of 14-3-3. This indicates that in the presence of sphingosine, an additional phosphorylation site on 14-3-3 is exposed. This is consistent with previous studies which have identified phosphorylation of 14-3-3 at Ser58 in the presence of sphingosine (Woodcock et al. 2010). Unfortunately, this does not indicate whether 14-3-3 is monomeric prior to phosphorylation by PKA at Ser58, or whether it is the result of phosphorylation which monomerises 14-3-3.

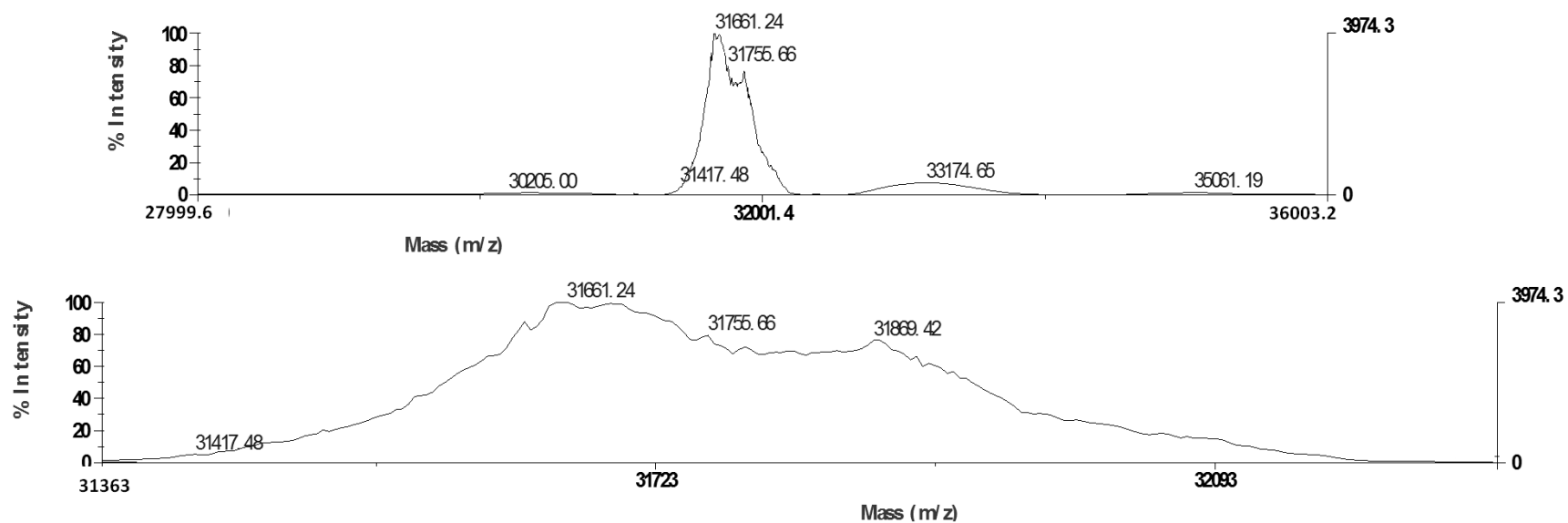


Figure 3.18: Spectra of Kinase Assay Samples 1 and 2

Mass spectrometry analysis of samples from kinase assays 1 and 2 when mixed together. The top spectrum is the observed peaks from a wider mass range. The difference between the two peaks is 94.42 Da, which represents phosphorylation. The lower spectrum is the same as the one above focused in on the peaks of interest.

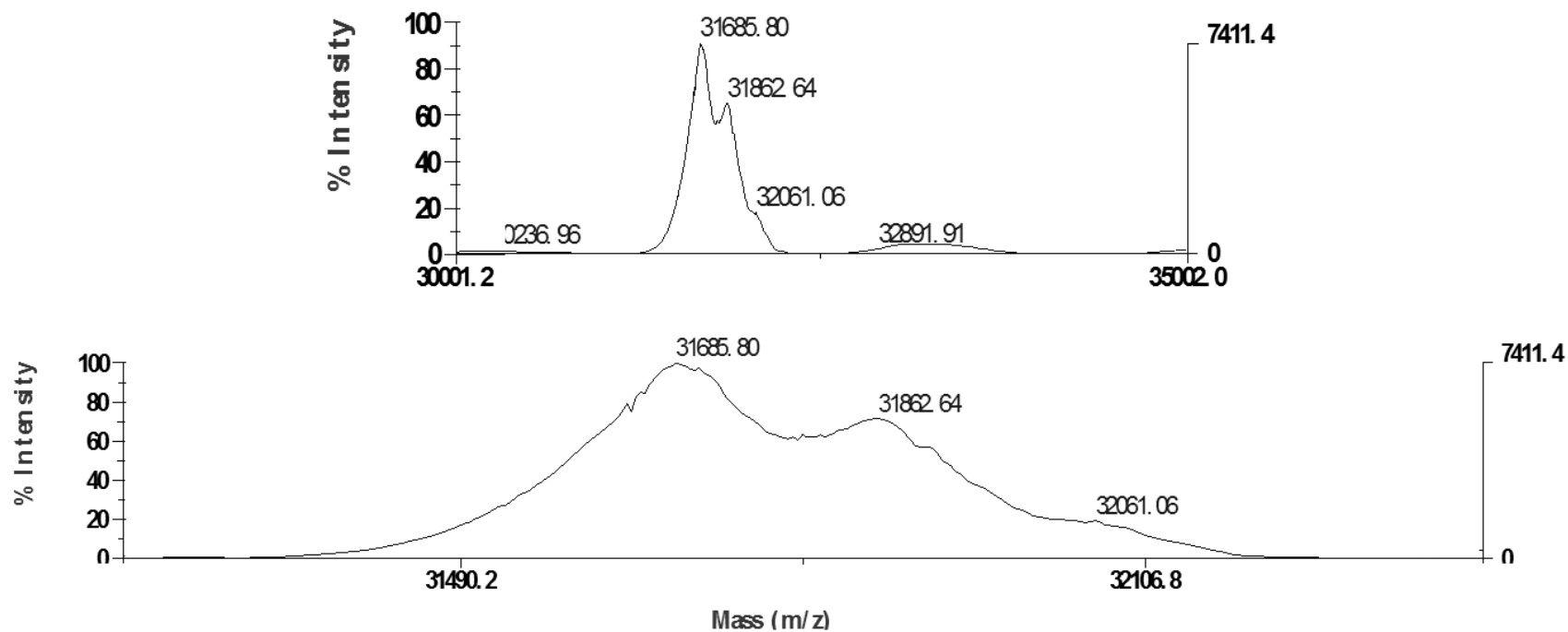


Figure 3.19: Spectra of Kinase Assay Samples 1 and 4

Mass spectrometry analysis of samples from kinase assays 1 and 4 when mixed together. The top spectrum is the observed peaks from a wider mass range. The difference between the two peaks is 176.84 Da, which represents double phosphorylation. The lower spectrum is the same as the one above focussed in on the peaks of interest.

3.3.9. 14-3-3 is Predominantly Monomeric at Lipid Rafts

The presence of sphingosine in lipid rafts raises the question: is the quaternary structure of 14-3-3 altered in lipid rafts? It is already well established that for full functionality, 14-3-3 exists as a dimer. For more information, see Introduction section 1.1.3.1. Monomeric 14-3-3 is highly unstable and is readily degraded (Messaritou et al. 2010) but can form non-specific interactions with unphosphorylated proteins and aggregate (Sluchanko et al. 2011). If 14-3-3 is monomeric in lipid rafts, not only is the stability of the protein itself compromised, but other interacting proteins may also be detracted from their cellular roles.

To investigate the quaternary structure of 14-3-3 proteins in raft domains, rafts isolated from rat brain were cross-linked with DMP and subsequently immunoblotted with the Pan 14-3-3 antibody. The results of the cross-linking are shown in Figure 3.20.

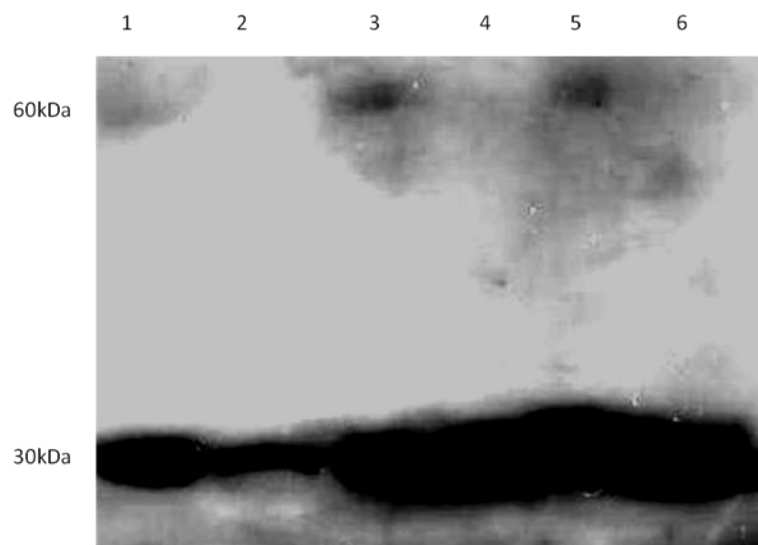


Figure 3.20: Cross-Linking Analysis of 14-3-3 Proteins at Lipid Rafts

Extracted rat brain fractions were treated with the cross-linker DMP prior to western blot analysis. The blot was probed with the Pan 14-3-3 antibody, which recognises all 14-3-3 isoforms. Lanes are labelled as follows: Lane 1 – Raft fraction plus cross-linker; Lane 2 – Raft fraction minus cross-linker; Lane 3 – Cytosolic fraction plus cross-linker; Lane 4 – Cytosolic fraction minus cross-linker; Lane 5 – Cytosolic fraction plus cross-linker; Lane 6 – Cytosolic fraction minus cross-linker. Cytosolic fractions were loaded at a 5 x lower volume. The molecular weights correspond to the size of the monomeric (30 kDa) and the dimeric (60 kDa) forms of 14-3-3.

For comparison, two sets of cytosolic protein fractions isolated from rat brain were also treated with DMP and control (PBS). The Pan 14-3-3 antibody was employed for detection, as it recognises all 14-3-3 isoforms, and as shown in section 3.3.6, different isoforms of 14-3-3 associate differently with lipid rafts.

It can be seen from Figure 3.20 that the 14-3-3 proteins in the cytosolic fractions do cross-link and form dimers; however a large proportion is still monomeric. The result of the cross-linking experiment with purified 14-3-3 ζ (Figure 3.16) does not result in the whole protein sample being cross-linked. The levels of cross-linking witnessed with purified protein are relatively similar to the levels of cross-linking witnessed here in cytosolic brain 14-3-3. In addition, the amount of cytosolic protein analysed here is only a fifth of that in the purified cross-linking and the raft sample analysis.

The immunoblot in Figure 3.20 indicates that 14-3-3 in rafts does cross-link and therefore form dimers. However, the levels of dimeric 14-3-3 in rafts are low, with the band detected very faint and only visible after prolonged exposure. This is evident from the intensity of the monomeric 14-3-3 bands. The monomeric 14-3-3 in the raft sample is almost as intense as those in the cytosolic fractions, yet the dimeric band in the raft sample is barely visible, but prominent in the cytosolic fractions. Coupled with the fact that the cytosolic fractions are loaded at a 5x lower volume than the raft samples, the detected levels of dimeric 14-3-3 in rafts is very low.

This low level of dimeric 14-3-3 in rafts indicates that the raft population of 14-3-3 is predominantly monomeric. This may be as a result of sphingolipids, namely sphingosine, eliciting a structural change of 14-3-3 proteins through disruption of the dimer interface. This suggests that access to Ser58 may be potentiated by monomerisation of the protein. This structural change of 14-3-3 may have a number of implications for protein function and regulation in lipid rafts.

3.3.10. 14-3-3 in Rafts and Akt Phosphorylation

As 14-3-3 proteins appear to be predominantly monomeric at lipid rafts, this opens up the Ser58 phosphorylation site, usually buried within the dimer interface. This therefore invites the question of whether there is an endogenous kinase present in rafts which has the ability to phosphorylate this residue on 14-3-3.

Cell culture studies have found a connection between lipid rafts and the kinase Akt (Zhuang et al. 2002; Adam et al. 2007) and there is also evidence that rafts recruit Akt to the plasma membrane (Lasserre et al. 2008). Recruitment of Akt from the cytosol to the plasma membrane occurs when the pleckstrin homology domain of Akt recognises PIP₃ (phosphatidylinositol-3,4,5-triphosphate). PIP₃ is generated from the phosphorylation of PIP₂ (phosphatidylinositol-4,5-bisphosphate) by PI3K (phosphoinositide-3 kinase). Once in contact with the membrane, phosphorylation by PDK1 and PDK2 (phosphoinositide-dependent kinase 1 and 2) activates Akt, releasing it from the membrane to phosphorylate cytosolic and nuclear targets (Scheid and Woodgett 2003). The study by Lasserre and colleagues suggests that rafts act as 'hot spots' on the membrane for Akt recruitment following PIP₃ accumulation (Lasserre et al. 2008).

In light of this, the decision was taken to immunoblot rat brain fractions for Akt. Cytosolic and raft fractions extracted from whole rat brain by flotation on an OptiPrep density gradient were probed for the presence of the phosphorylated form of Akt; Akt phosphorylated on Ser473, which is the active form of the kinase. Raft fractions were also treated with either M β CD or PBS (control) to test whether cholesterol depletion affects the association of phospho-Akt. The results of the blot are shown in Figure 3.21.



Figure 3.21: Akt Association with Lipid Rafts

Lipid rafts, extracted from whole rat brain by flotation on OptiPrep density gradients, were treated with either M β CD or PBS and immunoblotted for the presence of phospho-Akt. Lanes are labelled as follows: Lane 1 – Supernatant prior to treatment; Lane 2 – Supernatant following M β CD treatment; Lane 3 – Pellet from M β CD treated rafts; Lane 4 – Supernatant prior to treatment; Lane 5 – Supernatant following PBS treatment; Lane 6 – Pellet from PBS treatment; Lane 7 – Cytosolic control. The cytosolic control sample was loaded at a 5 x lower volume. The molecular weight of phospho-Akt is 60 kDa.

The results of this experiment show that phospho-Akt does associate with lipid rafts extracted from rat brain. Importantly, cholesterol depletion does not reduce association; in fact the cholesterol depleted sample produces the most intense band on the blot. The intensity of the bands also indicates that phospho-Akt associates with rafts at a substantial level.

Confirmation of the presence of phospho-Akt in lipid rafts coupled with the finding that 14-3-3 proteins are mainly monomeric in rafts gives rise to the possibility that Akt may phosphorylate 14-3-3 on Ser58.

3.4. Discussion

This chapter focused on the association of 14-3-3 proteins with lipid rafts and the implications this can have for proteins involved in neurodegenerative diseases. Previous research identifying the association of 14-3-3 proteins with lipid rafts provided the basis for this research, which was expanded to investigate association of the two phospho-forms of 14-3-3, α and δ . Extensive investigation successfully identified the 14-3-3 phospho-forms associating with lipid rafts and mass spectrometry analysis indicates that the levels of these isoforms, which constitute approximately 55% of total β and ζ 14-3-3 in brain, are present in rafts at a relatively lower abundance than the unphosphorylated forms.

Following the successful identification of these phospho-forms in lipid rafts, I attempted to establish whether phosphorylation of 14-3-3 has an impact on interactions with other proteins in rafts. Subsequent analysis on the association of 14-3-3s with lipid rafts and the effect of cholesterol depletion identified that 14-3-3 proteins are contained in the insoluble material. This suggests that these protein or proteins interact with 14-3-3 in rafts with high affinity. This is consistent with the finding that low levels of phosphorylated 14-3-3 associate with rafts. Phosphorylation of 14-3-3 on both Ser185 and Thr233 result in the dissociation of protein interactions (Aitken 2011) and it would be expected that phospho-14-3-3 would not be able to interact with the raft-bound protein, promoting association. The low levels of phospho-14-3-3 and the inclusion of unphosphorylated 14-3-3 in the insoluble material in rafts collectively support the theory that 14-3-3 association is through high affinity interactions with protein or proteins which are raft-bound. One possible means of overcoming this issue and identifying potential interacting proteins would be to conduct overlay assays, or far Western blots. Overlay assays of raft samples with 14-3-3 isoforms would identify proteins present in lipid rafts which 14-3-3 can interact with. This would provide a starting point for analysis and is definitely a method which should be considered for future raft investigations.

Another aspect which this chapter addressed was the effect which sphingolipids present in lipid rafts could elicit on 14-3-3 proteins. 14-3-3 has been shown to be

phosphorylated on Ser58 by PKA in the presence of sphingosine; promoting the conversion of 14-3-3 to a monomer (Woodcock et al. 2003). This phosphorylation is a novel regulatory mechanism for 14-3-3 interactions and could explain the lack of observed Ser58 phosphorylation by other kinases of intact 14-3-3 that was purified from mammalian brain (Toker et al. 1992; Dubois et al. 1997; Aitken 2011). Phosphorylation only in the presence of sphingosine suggests that either the dimeric state of 14-3-3 is disrupted, by monomerisation, exposing the residue to be phosphorylated; or sphingosine elicits a conformational change of 14-3-3, which exposes Ser58 for phosphorylation and it is as a result of phosphorylation which results in 14-3-3 monomerisation.

To investigate this further, it was first established that 14-3-3 is phosphorylated in the presence of sphingosine. This was identified by mass spectrometry, where it was evident that in the presence of PKA 14-3-3 is phosphorylated on another residue, and in the presence of PKA and sphingosine, 14-3-3 is doubly phosphorylated; indicating that sphingosine exposes an additional phosphorylation site on 14-3-3. The effect of sphingosine on 14-3-3 was investigated in lipid rafts. As sphingosine is abundant in rafts, if this sphingolipid elicits a structural effect, such as monomerisation of 14-3-3, this should be identifiable through raft analysis. As such, rafts which were isolated from whole rat brain were incubated with the cross-linker DMP and analysed by SDS-PAGE. This procedure identified that in lipid rafts, in comparison to the cytosol, 14-3-3 proteins are predominantly monomeric. Further raft analysis identified that an endogenous kinase in the form of Akt is also present, which may possess the ability to phosphorylate 14-3-3 on Ser58. However, re-examination of the mass spectrometry analysis of 14-3-3 peptides in lipid rafts (section 3.3.5) did not identify this residue as being phosphorylated. It is important to stress that the mass spectrometry conducted was not focussed on the identification of phosphorylation of this residue and that further investigation would be required to positively conclude that 14-3-3 is not phosphorylated at Ser58 in lipid rafts. In light of the results presented here, it appears that sphingosine does elicit a structural effect on 14-3-3 and the results of the raft cross-linking analysis

leads to the suggestion that sphingosine disrupts the dimeric structure of 14-3-3 to produce monomers. It is well established that 14-3-3 proteins exist as dimers for full functionality and that their ability to readily adopt dimers suggests that they are highly unstable in their monomeric form. Studies into monomeric 14-3-3 has also identified that this unstable form of the protein aggregates.

The research presented here can support a role for 14-3-3 and lipid rafts in neurodegenerative diseases. 14-3-3 proteins which are present at lipid rafts can be monomerised in the presence of sphingosine; a major component of rafts. Additionally, neurodegenerative disease proteins are processed at rafts; abnormalities of which can initiate disease. The monomeric forms of 14-3-3 are highly unstable and can form aggregates, as can abnormally processed disease proteins. I therefore hypothesise that the production of monomeric 14-3-3 by sphingosine and abnormal disease protein processing by lipid rafts leads to the formation of the toxic aggregates which are a characteristic of numerous neurodegenerative diseases. This would account for the presence of 14-3-3 proteins in these aggregates and also support one theory that aggregate formation is a neuro-protective mechanism, to sequester abnormal proteins from causing further neuronal damage (Olzmann et al. 2008).

The research presented here provides a basis for further investigation into the roles of 14-3-3 proteins in neurodegenerative disease pathology and the association of 14-3-3 and neurodegenerative disease proteins with lipid rafts. This also raises the intriguing possibility of a unique mode of regulation of 14-3-3 function. Due to the high level of sphingosine in rafts, this induces monomerisation of 14-3-3 which leads to the phosphorylation on Ser58 by Akt.

CHAPTER 4

SPINOCEREBELLAR ATAXIA TYPE 1 AND ATAXIN-1

4.1. Introduction

Spinocerebellar ataxia type 1 (SCA1) is one of seven neurodegenerative conditions termed polyglutamine-repeat diseases, which includes the more commonly known Huntington's (Zoghbi and Orr 2000). All of the diseases follow a similar pathogenesis and are genetically inherited. The gene responsible for SCA1 was first identified in 1993, revealing that the expansion of a translated CAG (glutamine) repeat was responsible for the mutation (Orr et al. 1993). The SCA1 gene, known as ATXN1, encodes a 792-830 residue protein termed ataxin-1, where the variation in length is dependent on the polyglutamine tract (Banfi et al. 1993). In normal alleles, there are between 6 and 44 glutamine repeats in the tract, however, when the number of repeats exceeds 20, the tract stability is maintained through the presence of CAT nucleotides (which encode histidine residues (Chung et al. 1993). In disease alleles, the number of glutamine repeats is greater, between 39 and 82, and the histidine residues are absent (Jodice et al. 1994). This absence of CAT nucleotides suggests that a substitution of CAT to CAG nucleotides may be the initial destabilising event in the disease pathology (Goldfarb et al. 1996).

It is now known that ataxin-1 is involved in many processes, including protein aggregation, phosphorylation and interactions which are important in SCA1. There are various aspects of the protein which are involved in disease pathology, including conformational changes of the protein itself and aggregation into nuclear inclusions. There are also interactions with the protein which play a role in SCA1 (see section 1.3.2 of the Introduction).

Previous studies have identified the phosphorylation sites of ataxin-1 (Emamian et al. 2003; Vierra-Green et al. 2005) and the AXH domain of ataxin-1 has been solved

crystallographically (Chen et al. 2004). In addition, an interaction between ataxin-1 and 14-3-3 has been identified (Chen et al. 2003). The interaction between 14-3-3 and ataxin-1 is a key step in the pathology of SCA1, leading to toxic accumulation and protein aggregation (see section 1.3.3).

The evidence presented in the literature indicates that the protein ataxin-1 plays an important role in development of SCA1 and understanding how to prevent the occurrence of toxic protein interactions is a real possibility for drug targeting. This can be achieved by better understanding the structure of the protein and identifying potential small molecule inhibitors.

In this research, domains of the protein have been identified for structural studies and for potential prevention of deleterious interactions.

4.2. Aims

Identification of Ataxin-1 Domains

As the crystal structure of the AXH domain of ataxin-1 has been solved, this provides a starting point for further structural analysis. As the whole length protein is highly unstable, domains of the protein have been selected to express and purify for further analysis. It is important to identify domains which can be produced in large quantities and which are stable and active for further analysis.

Expression and Purification of Ataxin-1 Domains

The ability to express and purify the domains to be of a sufficient quality to allow for crystal and compound inhibition studies is essential. The main aim here is to identify a bacterial expression system which can be exploited to produce a substantial quantity and quality of proteins for further analysis.

4.3. Results

4.3.1. Identification of Ataxin-1 'C' and 'AC' Domains

The cDNA of ataxin-1 was first identified and characterised in 1994 from two human foetal cDNA libraries and a human adult cerebellar cDNA library (Banfi et al. 1994). This identified ataxin-1 as an 87 kDa protein containing 816 amino acids.

The IMAGE clone (40125676) for the protein is 815 amino acids long, and this is the sequence from which selected domains were derived. To date, Chen and colleagues have crystallised the AXH domain of ataxin-1 (residues 563-694) (Chen et al. 2004). It was not possible to crystallise the whole protein, as the polyglutamine tract makes the protein highly unstable and not suitable for crystallisation. As there is known information for the AXH domain, it makes sense to include this region in domains to be studied, particularly as conditions for the crystallisation of the AXH domain have been discovered.

Constructs were designed to incorporate the AXH domain and the C-terminal region. Two constructs were designed and cloned for analysis by Dr. Beck (Analytical and Environmental Chemistry, Humboldt-Universität zu Berlin, Department of Chemistry, Brook-Taylor-Str. 2, 12489 Berlin, Germany). These were termed as the Ataxin-C domain and the Ataxin-AC domain. The Ataxin-C domain was named as it consisted mainly of the C-terminal region of the protein (residues 704-815). The Ataxin-AC domain was named as it consisted of the AXH domain and the C-terminal region of the protein (residues 561-815).

Both of the constructs were cloned into the bacterial expression vector pTrc-His-A'. This system (Invitrogen, Paisley, UK) has been developed for the efficient expression and purification of recombinant proteins in *E. coli*. High level expression of fusion proteins can be achieved through transcriptional regulation of the *trc* promoter. The pTrc-His-A' expression vector contains an N-terminal hexa-histidine tag to aid protein purification. The His-tag was linked to the ataxin-1 gene by a peptide sequence of 21 residues, 5 of which encode the Enterokinase recognition sequence for cleavage of the fusion tag.

Gly Met Ala Ser Met Thr Gly Gly Gln Gln Met Gly Arg Thr Leu Tyr Asp Asp Asp Asp Lys

Figure 4.1: Peptide Sequence in MCS

Residues in the MCS connecting the hexa-histidine tag to the inserted ataxin-1 gene. Residues underlined encode the Enterokinase cleavage site. Residues highlighted in blue encode the Xpress epitope which allows detection of the recombinant protein using the Anti-Xpress Antibody.

Each of the constructs were cloned into the multiple cloning site (MCS) using the restriction enzymes BamHI and XhoI. A simplified image of the final construct is shown in Figure 4.2.

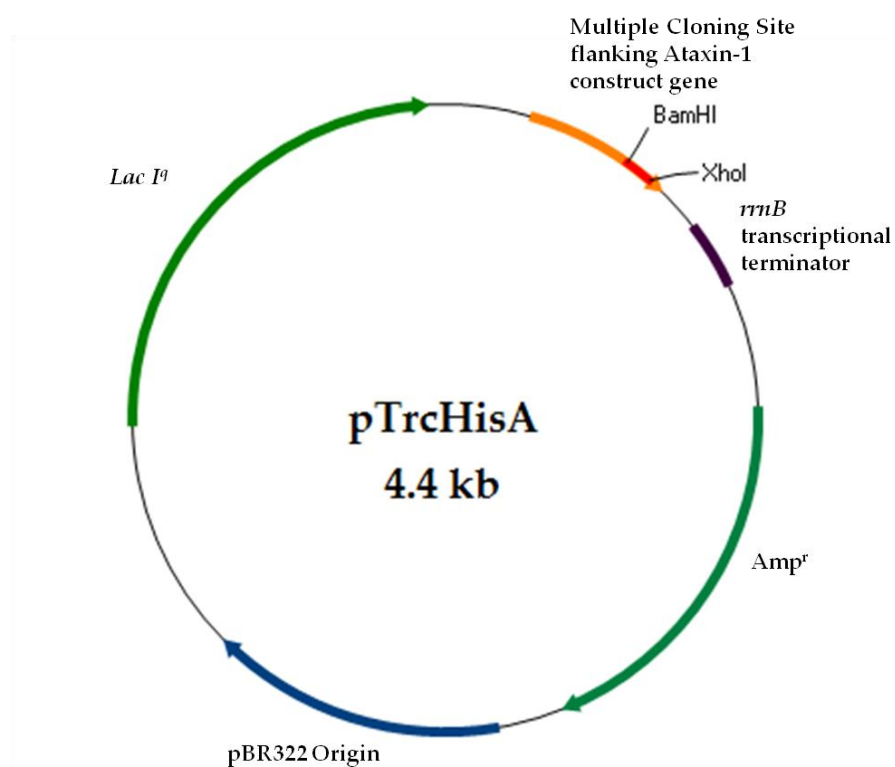


Figure 4.2: Simplified vector map of pTrcHisA'

Vector map of pTrcHisA' depicting the location of the ataxin-1 construct gene. The multiple cloning site contains the *trc* promoter and the hexa-histidine tag. Other regions highlighted are the ampicillin resistance gene (Amp^r), the origin of replication (pBR322 origin) and the *lacI^q* gene which codes for the *lac* repressor protein. The presence of this gene allows efficient transcriptional repression of the cloned insert in *E. coli* whether the strain is *lacI^{q+}* or *lacI^{q-}*.

As stated, the ataxin-1 gene was truncated to remove the polyglutamine tract, which should make the selected domains more stable for analysis. Basic information for each domain in comparison to the full-length protein is given in Table 4.1.

Table 4.1: Ataxin-1 Domains

Information regarding the predicted isoelectric point (pI), molecular weight and number of residues for each selected domain and the full-length protein. These values were calculated by ProtParam (<http://www.expasy.ch/tools/protparam.html>) an online protein parameter predictor.

	Full-Length Ataxin-1	'AC' Domain	'C' Domain
Predicted pI	8.49	7.10	9.52
Predicted Mass	86922.6 Da	27733.6 Da	12286.0 Da
Number of Residues	815	255	112

4.3.2. Expression of Ataxin-1 Domains

Previously, optimum conditions for the expression of the ataxin-1 constructs were determined by Dr. Beck.

The optimum expression of the Ataxin-1 AC domain was obtained under the following conditions;

1. Expression in the *Rosetta 2* strain of *E. coli*
2. Expression in LB media supplemented with ampicillin
3. Temperature remained stable at 37°C until O.D. induction stage was achieved (A_{600} at 0.7-0.8)
4. Addition of isopropyl- β -D-thiogalactopyranoside (IPTG, final concentration 0.5 mM) to induce protein production
5. Culture at 37°C overnight for high yield of protein
6. Cultures were agitated to promote cell growth by shaking at 200 rpm

The optimum expression of the Ataxin-1 C domain was obtained under the following conditions;

1. Expression in the BL21(DE3) strain of *E. coli*
2. Expression in LB media supplemented with ampicillin
3. Temperature was kept stable at 37°C until induction stage was achieved (A_{600} at 0.7-0.8)
4. Addition of IPTG (final concentration 0.5 mM) to induce protein production
5. Overnight culture at 37°C to produce a high yield of protein
6. Agitation of cultures at 200 rpm in a shaker

Protein domains were expressed and collected in 1 L volumes for purification.

4.3.3. Purification of Ataxin-1 Domains

4.3.3.1. First Step: IMAC (Immobilized Metal Affinity Chromatography)

IMAC is a chromatographic technique employed for the purification of recombinant proteins expressed with a histidine-tag. IMAC, as the name suggests, involves immobilized metal ions on chromatographic media through chelating ligands. The metal ions employed in this research were either nickel (Ni^{2+}) or cobalt (Co^{2+}), for which histidine-tagged proteins have a high selective affinity. Metal ions are immobilized on a Sepharose matrix.

The His-tagged protein binds to the matrix whilst other proteins in the lysate pass over the matrix and flow through the column. The column is then washed with 20 mM imidazole to remove any unbound proteins to allow for cleaner protein purification. The His-tagged protein was eluted from the matrix with 200 mM imidazole, which competes for binding to the matrix.

For a first-step purification of the Ataxin-1 AC and C domains, a gravity-flow IMAC column was prepared with the procedure carried out at 4°C. Full details of the protocol are given in Chapter 2 section 2.2.2. Briefly, the lysate was added to the column, which was tumbled for 1 h to allow the matrix and lysate to fully integrate. The flow-through was collected before washing the column with 10 CV of buffer (20 mM imidazole) to remove the unbound proteins. The ataxin-1 domains were eluted with at least 7 CV of elution buffer (200 mM imidazole) and these were collected in 5 ml (1 CV) fractions and analysed by SDS-PAGE.

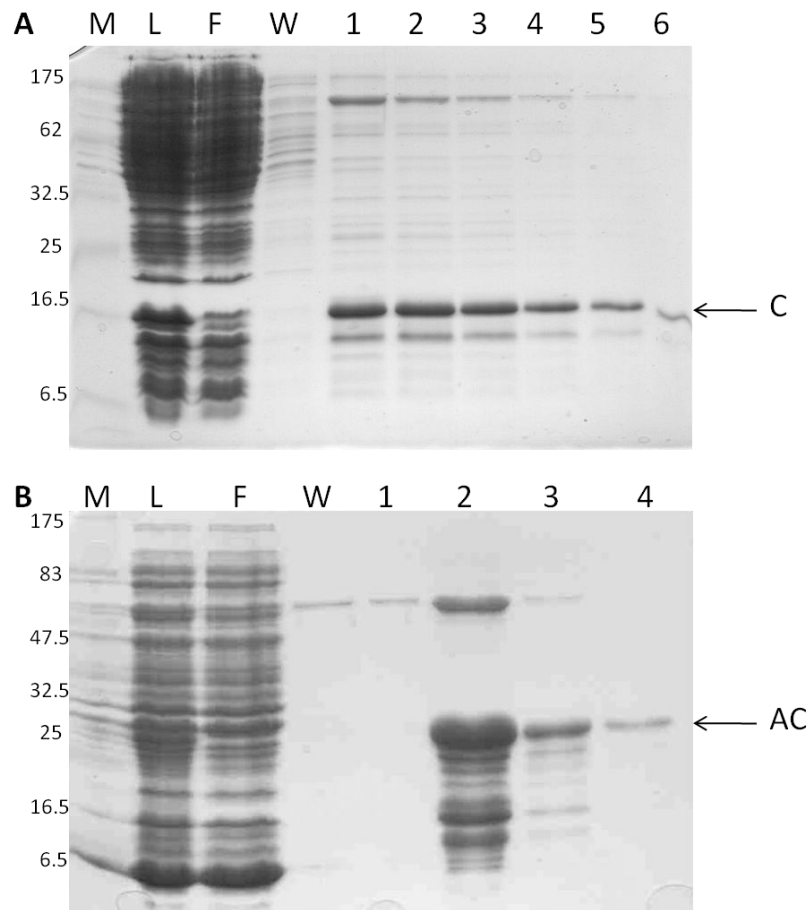


Figure 4.3: SDS-PAGE of Fractions Collected from IMAC Purification

- A. SDS-PAGE of fractions collected from the 'C' domain IMAC purification. Lanes are labelled as follows; M = molecular weight marker; L = lysate which was loaded onto column; F = flow-through from column; W = wash sample; Lanes 1-6 = elution fractions.
- B. SDS-PAGE of fractions collected from the 'AC' domain IMAC purification. Lanes are labelled as follows; M = molecular weight marker; L = lysate loaded onto column; F = flow-through from column; W = wash sample; Lanes 1-4 = elution fractions. Fractions 2, 3 and 4 were pooled for further analysis.

4.3.3.2. Second Step: Cation Exchange Chromatography

Ion-exchange chromatography is a method employed to separate proteins based on their charge. Results can be altered by varying the running pH, salt concentration and more importantly, by changing the ion exchanger. Proteins which have an overall net positive charge adsorb to cation exchangers and proteins with an overall net negative charge adsorb to anion exchangers. The greater the net charge, the greater the strength of the adsorption. The protein of interest can be desorbed from the ion exchanger by either changing the pH to reduce the net charge of the protein or through the addition of an ion competitor to 'block' the ion exchanger charges. A competing ion, NaCl, was used to desorb the ataxin-1 domains from the cation exchanger.

Gradient elution was carried out on a Mono S (methyl sulphonate) ion exchange column. Anion exchange chromatography was also tested on a Mono Q (quaternary ammonium) ion exchange column; however this method yielded very poor results, so Mono S ion exchange was used. Anion exchange with a Mono Q column was possibly unsuccessful due to the high pI of the ataxin-1 constructs. For anion exchange chromatography to be successful, the constructs would have to be in a buffer of very high pH. As the buffer pH employed was pH 6, this ensured optimal conditions for cation exchange, which requires the protein buffer to be lower than the pI of the protein.

The selected ataxin-1 domains were eluted from the cation exchange column with a NaCl gradient on a BioCAD 700E Perfusion Chromatography Workstation. Protein elution was detected by UV sensors at 280 nm. Fractions were collected using an Advantec SF-2120 fraction collector and relevant fractions were separated by SDS-PAGE. Fractions which contained the protein of interest were pooled for further analysis.

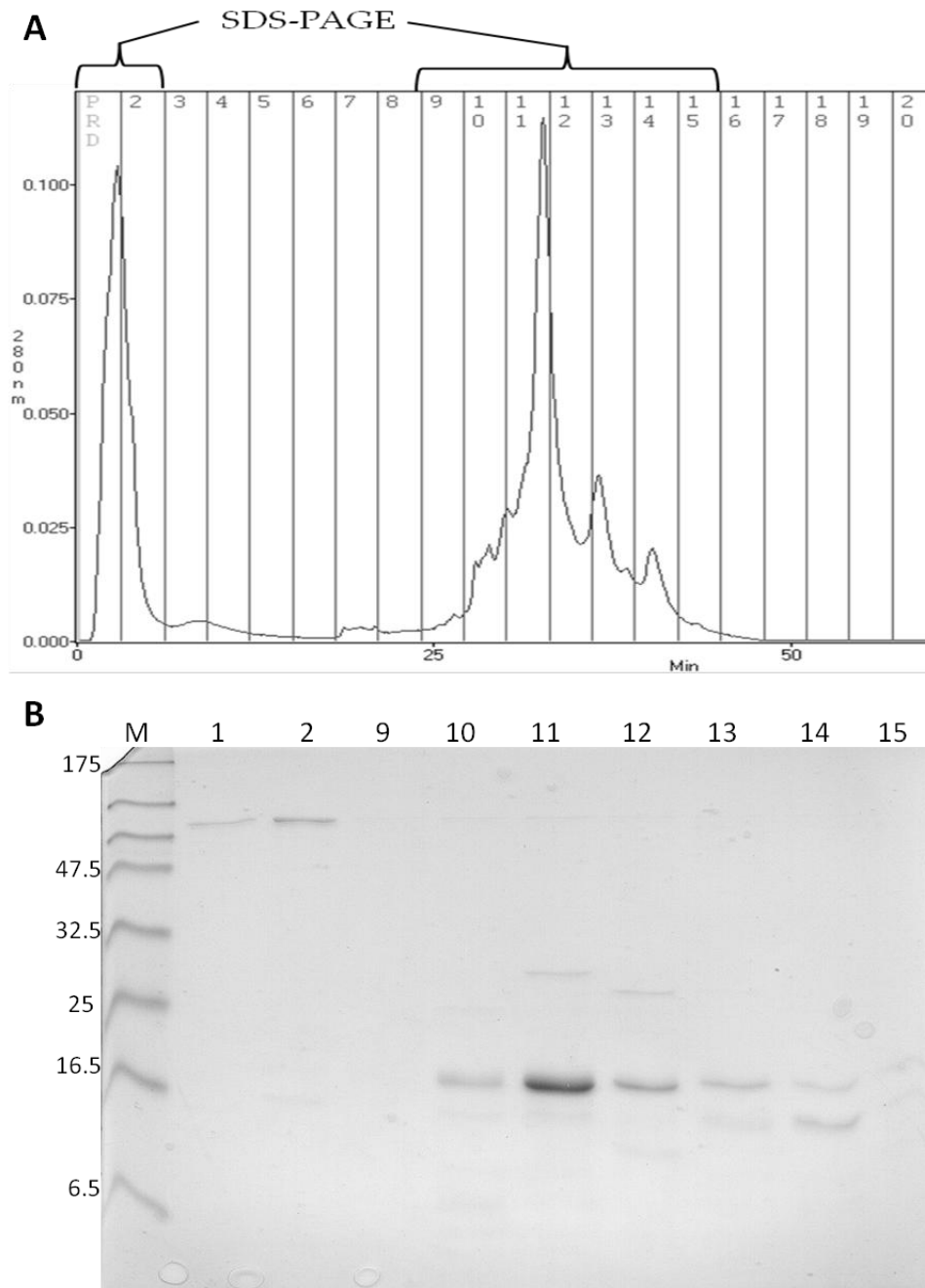


Figure 4.4: Ataxin-C Ion-Exchange

- A. UV trace from Ataxin-C ion-exchange chromatography. Fraction numbers are given at the top of each column along the trace and were 1 ml each. Fractions indicated were further analysed on SDS-PAGE.
- B. SDS-PAGE of selected ion-exchange fractions. Fractions analysed in each well are indicated above the gel image. It is clear from the gel that the protein of interest is present in fractions 11, 12 and 13 in most abundance. These fractions were pooled for further analysis.

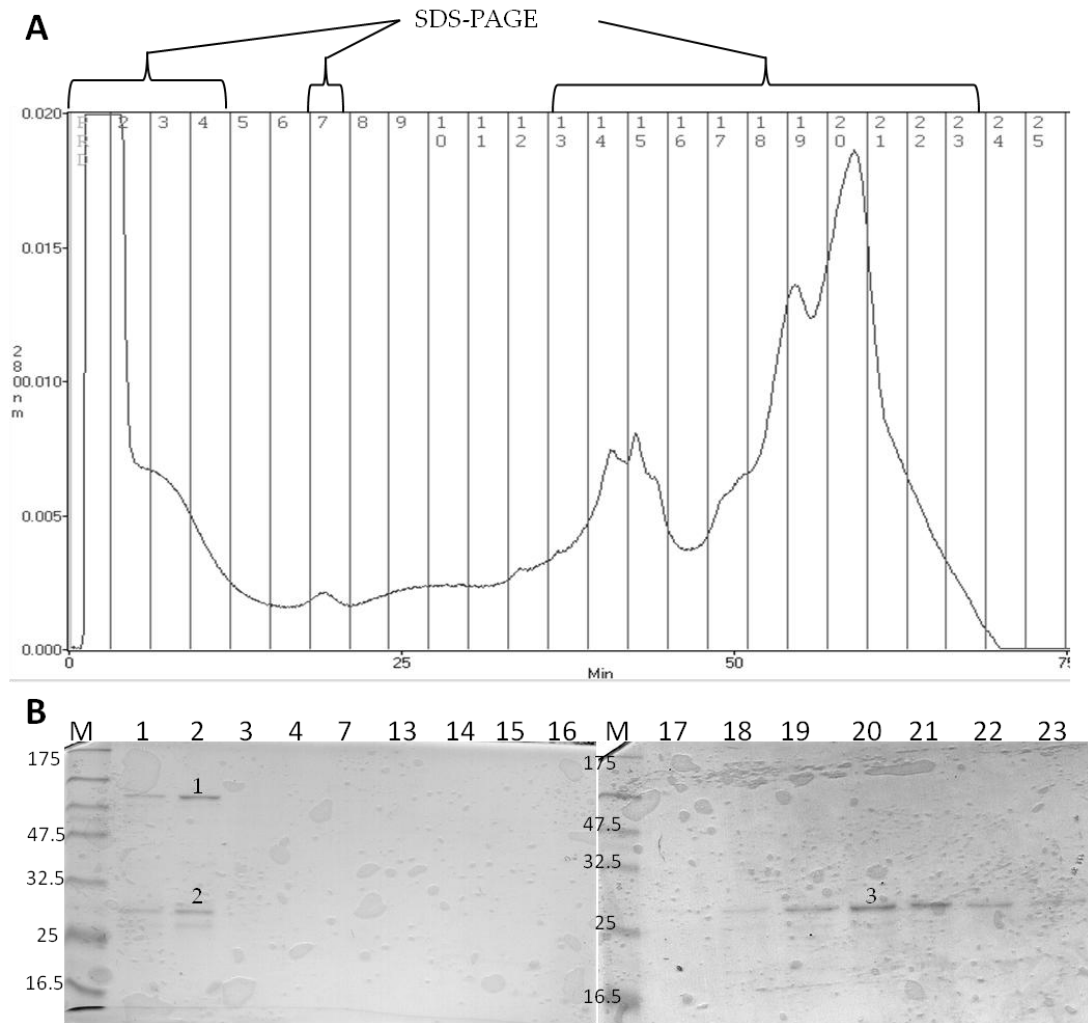


Figure 4.5: Ataxin-AC Ion-Exchange

- A. UV trace from Ataxin-AC ion-exchange chromatography. Fraction numbers are indicated in the top of each column along the trace and were 1 ml each. Indicated fractions were analysed by SDS-PAGE.
- B. SDS-PAGE of selected Ataxin-AC fractions from ion-exchange. Fractions analysed are indicated above the gel lanes. The gel bands numbered (1-3) were excised for mass spectrometry, which is further discussed in section 4.3.4.

4.3.3.3. Third Step: Gel Filtration Chromatography

Gel filtration is employed to separate different oligomeric states of protein samples. This is particularly important for progression to crystallization, as the sample must be pure and homogeneous.

For gel filtration, a Superose 12 10/30 column was used, as detailed in section 2.2.4 of Material and Methods. The column was previously calibrated according to the manufacturer's instructions.

The Ataxin-C domain protein was purified by gel filtration chromatography. A sample of 5.3 mg/ml was diluted 1:5 with distilled water to make a total volume of 100 μ l. The sample was injected into the system and the run was carried out with a simple buffer for equilibration and elution (20 mM Tris, 150 mM NaCl pH 7.4).

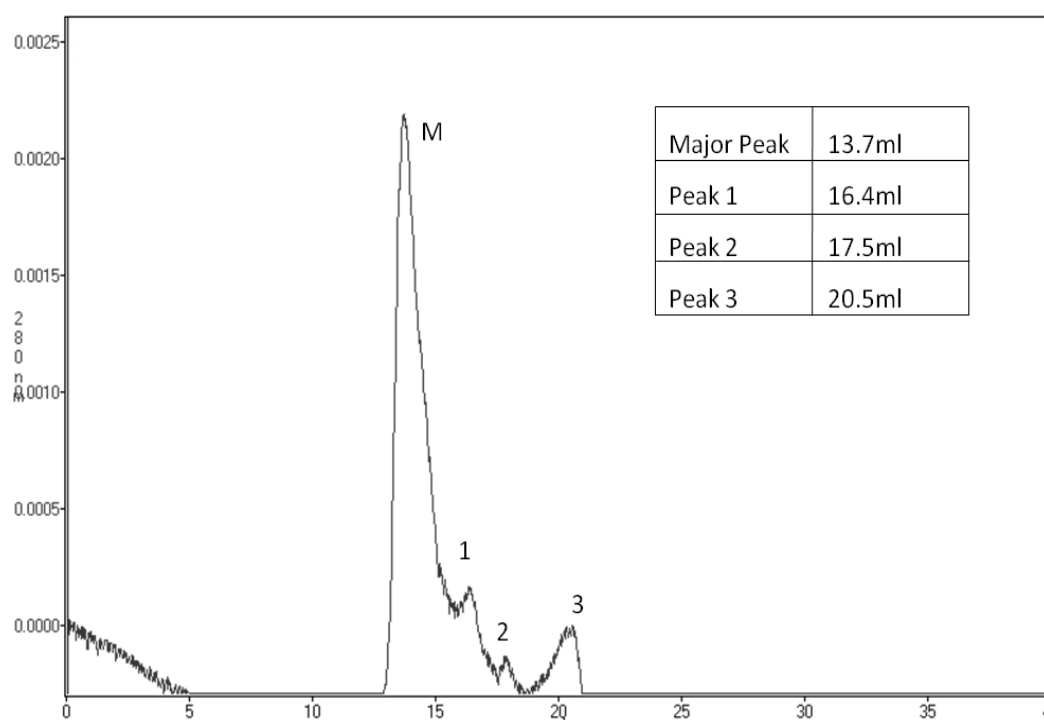


Figure 4.6: Chromatogram of Ataxin-C Gel Filtration

Gel filtration of Ataxin-C protein on the Superose 12 10/30 column. The abscissa indicates the volume of protein elution and the ordinate indicates the absorbance units at 280 nm.

The chromatogram from the gel filtration of the Ataxin-C indicates that the protein elutes at 13.7 ml with a molecular weight of 57 kDa (Figure 4.6). Due to this, I hypothesise that the protein construct may possibly be forming a trimer.

4.3.4. Confirmation of Protein Identity

In order to verify that the protein of interest had been purified, MALDI-TOF was employed. This procedure involved excising bands of interest from SDS-PAGE and subjecting the bands to a tryptic digest (full details in section 2.3.7. of the Materials and Methods). Bands excised from purification of both ataxin-1 constructs were identified as being domains of the ataxin-1 (human) protein. This method is useful in identifying whether a band present on SDS-PAGE is a protein of interest or a contaminating protein. An example of this was during the optimization of Ataxin-C expression conditions. When expression was attempted using the *Rosetta 2* strain of *E. coli*, two contaminating proteins were up-regulated in response to the antibiotic chloramphenicol which is required for selection of this bacterial strain. MALDI-TOF analysis identified that these contaminating proteins were not dimers or trimers of the Ataxin-C construct which was the initial hypothesis. Subsequently, changing the *E. coli* strain eliminated this problem.

This problem of protein contamination can also be seen from the gel shown in Figure 4.5. The numbered bands on the gel were analysed by MALDI-TOF. The results of the top hits for each band are shown in Table 4.2.

Table 4.2: Ataxin-AC MALDI-TOF Results

Each top hit from the bands in Figure 4.5 which were prepared for MALDI-TOF.

Protein Band	MOWSE Score	Protein M.W. (Da)/pI	Species	Protein Name
1	3.31e+6	69116/4.8	ECO57	Chaperone Protein dnaK
2	2743	87051/8.5	HUMAN	Ataxin-1
3	46277	87051/8.5	HUMAN	Ataxin-1

It is clear from the mass spectrometry results that the Ataxin-AC domain is prominent; however, complete purification is an issue. Unfortunately, despite extensive attempts, purification to a sufficiently high level was not obtained. Due to the difficulties in purifying the Ataxin-AC domain, alternative approaches were explored, which are detailed later in this chapter.

4.3.5. Crystallography of Ataxin-C: Initial Trials

As purification of the Ataxin-C domain was more successful than the Ataxin-AC domain, crystallography trials were attempted. Initial screens were carried out using the Hampton Crystal Screen (1+2). The Ataxin-C protein was prepared to 5.3 mg/ml and concentrated in a Vivaspin with PBS. The initial screen was set up in the sitting drop vapour diffusion method (see section 2.3.8.1 in Materials and Methods). From this initial screen, one set of conditions did appear to produce crystals. However, these crystals were not of sufficient size or quality to progress further. Further optimization of the crystallography conditions was attempted based on the original conditions which yielded protein crystals. The conditions which did yield crystals were as follows:

**0.2 M ammonium phosphate monobasic, 0.1 M Tris pH 8.5,
50% v/v (+/-)-2,-methyl-2,4-pentanediol (MPD)**

Employing variations of these conditions, refined screens were set up with Ataxin-C protein which had been prepared to 3.7 mg/ml. Conditions were set up for hanging drop vapour diffusion in a 24 well plate. Details of the conditions tested are shown in Table 4.3.

Table 4.3: Refined Crystallography Conditions for Ataxin-C

Conditions tested based on the initial results from the Hampton Crystallography screen.

	1	2	3	4	5	6
A	0.2 M NH ₄ H ₂ PO ₄ 0.1 M MES pH 5.6 50% MPD	0.2 M NH ₄ H ₂ PO ₄ 0.1 M MES pH 6.5 50% MPD	0.2 M NH ₄ H ₂ PO ₄ 0.1 M PIPES pH 7 50% MPD	0.2 M NH ₄ H ₂ PO ₄ 0.1 M PIPES pH 7.5 50% MPD	0.2 M NH ₄ H ₂ PO ₄ 0.1 M BICINE pH 8 50% MPD	0.2 M NH ₄ H ₂ PO ₄ 0.1 M BICINE pH 8.5 50% MPD
B	0.2 M NH ₄ H ₂ PO ₄ 0.1 M BICINE pH 8.5 30% MPD	0.2 M NH ₄ H ₂ PO ₄ 0.1 M BICINE pH 8.5 40% MPD	0.2 M NH ₄ H ₂ PO ₄ 0.1 M BICINE pH 8.5 45% MPD	0.2 M NH ₄ H ₂ PO ₄ 0.1 M BICINE pH 8.5 50% MPD	0.2 M NH ₄ H ₂ PO ₄ 0.1 M BICINE pH 8.5 55% MPD	0.2 M NH ₄ H ₂ PO ₄ 0.1 M BICINE pH 8.5 60% MPD
C	0.05 M NH ₄ H ₂ PO ₄ 0.1 M BICINE pH 8.5 50% MPD	0.1 M NH ₄ H ₂ PO ₄ 0.1 M BICINE pH 8.5 50% MPD	0.15 M NH ₄ H ₂ PO ₄ 0.1 M BICINE pH 8.5 50% MPD	0.2 M NH ₄ H ₂ PO ₄ 0.1 M BICINE pH 8.5 50% MPD	0.25 M NH ₄ H ₂ PO ₄ 0.1 M BICINE pH 8.5 50% MPD	0.3 M NH ₄ H ₂ PO ₄ 0.1 M BICINE pH 8.5 50% MPD

NH₄H₂PO₄ – Ammonium Phosphate Monobasic.

Unfortunately, despite extensive incubation, no crystal formation occurred despite this refinement of the conditions. One reason may be due to the low protein concentration employed in this technique. Unfortunately purification of the Ataxin-C domain is difficult and during these procedures, it became clear that the protein does not remain stable at 4°C. This poses a number of issues, including protein degradation, which may also have been a problem.

Due to the difficulties experienced with both the 'C' and 'AC' domains of Ataxin-1, alternative avenues of analysis were explored. These are discussed in the next section.

4.3.6. Identification of New Ataxin-1 Domains

As the initial ataxin-1 constructs were not easily purified, an alternative approach was explored. The protein sequence was examined by the online analysis tool PredictProtein (www.predictprotein.org) to predict the secondary structure. By examining the predicted secondary structure of the protein, more stable domains of the protein could be identified. The PredictProtein results showing all of the constructs selected is shown in Figure 4.7.

It is clear from Figure 4.7 that the original constructs started at loop regions of the protein, making them unstable. This could explain the reason why successful purification of these constructs was not achieved. When the initial constructs were designed, this information was unknown and so they were selected based on previous studies where crystallography had been successful (Chen et al. 2004). Constructs were designed to encompass the AXH domain (crystal structure known) and the C-terminal region (structure unknown) of the protein. The AXH domain is included because there is evidence that this region of the protein can be crystallised, suggesting that regions of the protein which are unknown may be driven into crystallisation by the AXH domain. The general design remained the same for selecting new domains. The main difference between the two sets of domains is the specific residues where they begin. A difference of a few residues may be all that is needed to enhance the likelihood of producing more stable constructs, according to the predicted secondary structure.

Three domains of varying sizes were selected, all of which included the 14-3-3 binding site, with one also incorporating the AXH domain. These are highlighted in Figure 4.7. The domains are referred to according to the residues which they encompass; 575-815, 718-815 and 740-815. All of the constructs were cloned into the bacterial expression vector p-Trc-His-A'. Information regarding the expression vector is detailed in section 4.3.1.

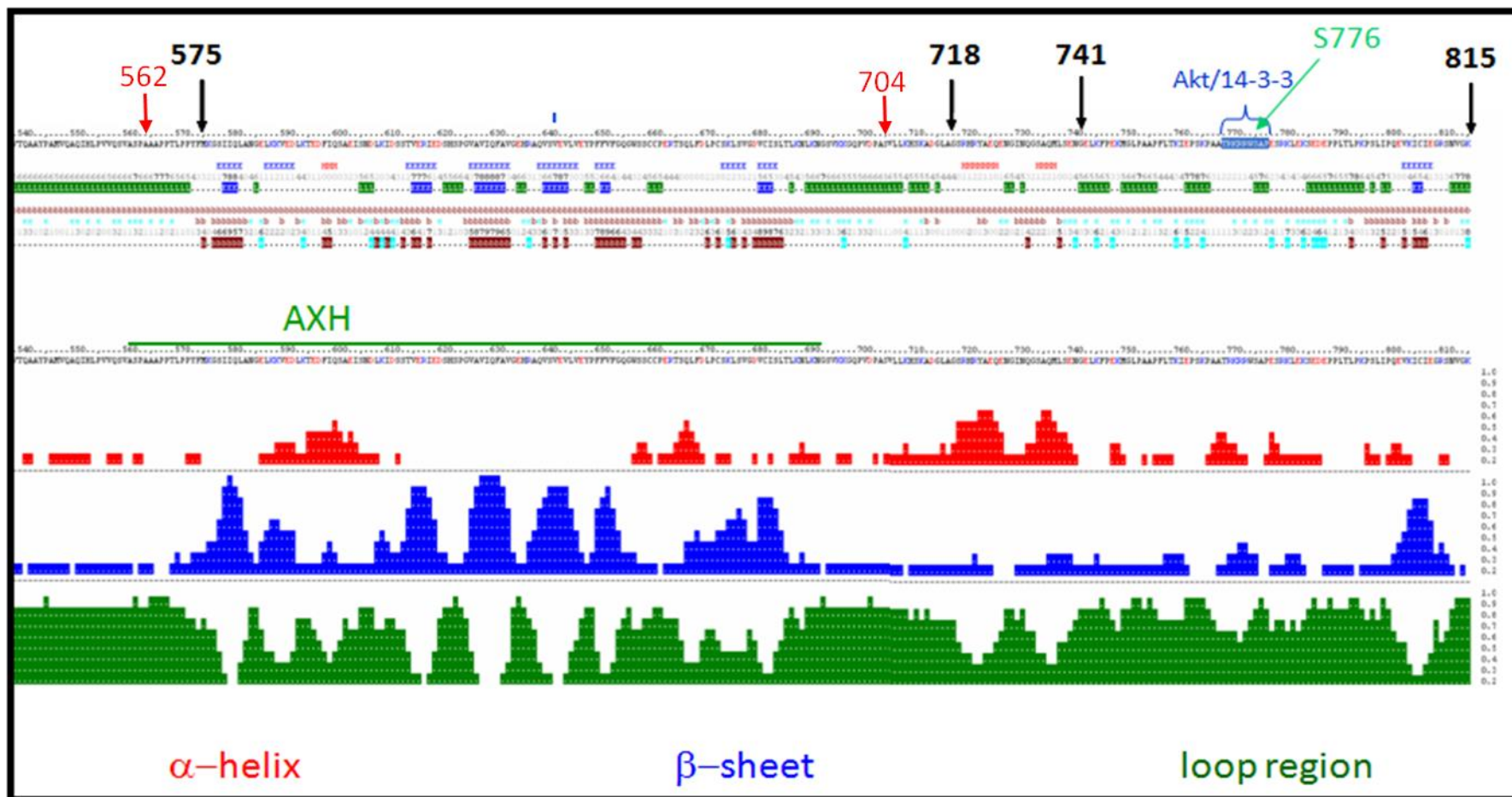


Figure 4.7: Ataxin-1 Sequence and Domains

Red highlighted residues indicate the starting residues of the original domains. Black highlighted residues indicate the starting residue of the second set of domains. In all cases, the C-terminal residue was 815. The Akt and 14-3-3 binding sites are also indicated, as well as the AXH domain.

These constructs were also cloned into the multiple cloning site (MCS) using the restriction enzymes HindIII and XhoI. A simplified image of the final construct is shown in Figure 4.8.

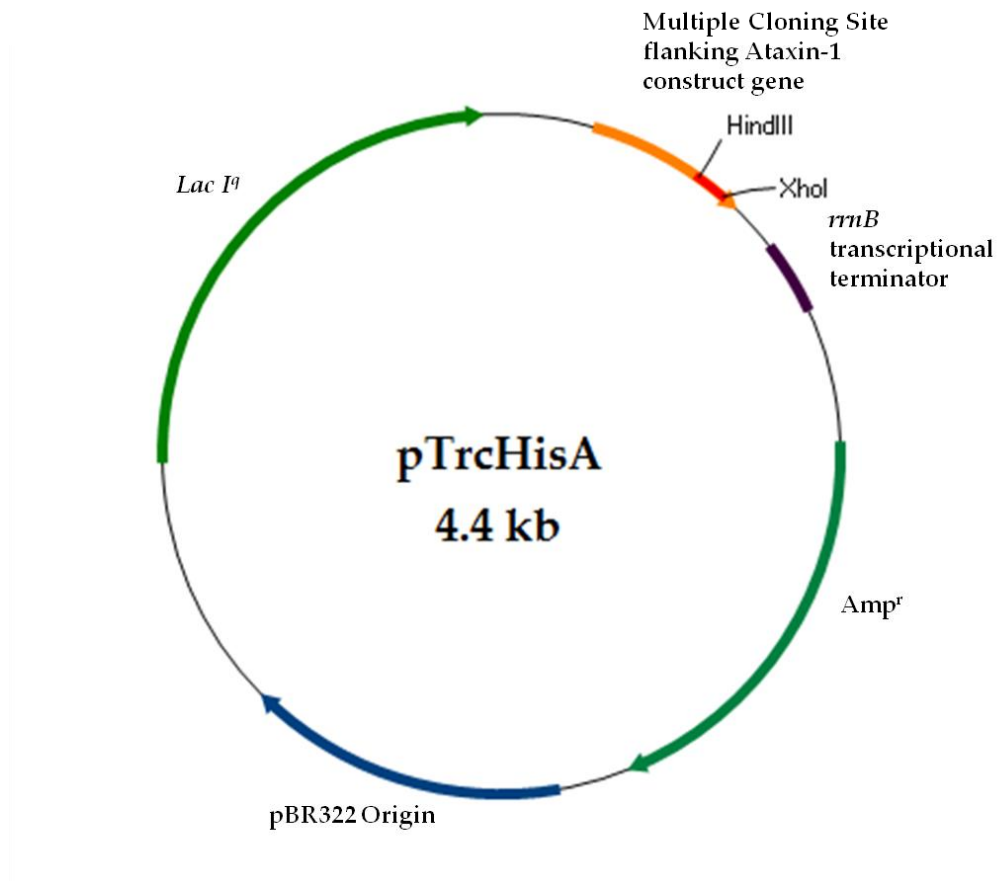


Figure 4.8: Simplified Vector Map for New Domains in pTrcHisA'

Vector map of pTrcHisA' depicting the location of the ataxin-1 construct gene. The multiple cloning site contains the *trc* promoter and the hexa-histidine tag. Other regions highlighted are the ampicillin resistance gene (Amp^r), the origin of replication (pBR322) and the *lacI^q* gene which codes for the *lac* repressor protein.

Again, the domains which were selected were truncated to remove the polyglutamine tract. Basic information regarding each domain in comparison to the full length protein is detailed in Table 4.4.

Table 4.4: New Ataxin-1 Domains

The predicted isoelectric point (pI), molecular weight and number of residues for each new domain and the full-length protein were calculated by ProtParam.

(<http://www.expasy.ch/tools/protparam.html>).

	Full-Length Ataxin-1	575-815	718-815	740-815
Predicted pI	8.49	6.91	9.42	9.67
Predicted Mass	86922.6 Da	26352 Da	10894.4 Da	8349.7 Da
Number of Residues	815	241	98	75

4.3.7. Expression Trials of New Ataxin-1 Domains

Expression trials were carried out in an attempt to identify not only the optimum expression conditions for each of the ataxin-1 domains, but also to determine the greatest soluble protein yield. By optimizing protein expression on a small scale, multiple conditions can be tested simultaneously and provide an indication of the amount of soluble protein which may be produced on a larger scale.

There were several main expression conditions that were varied for the expression trials. These are detailed in Table 4.5.

Trials were carried out systematically for all three domains, varying an individual condition per trial. Controls where protein expression was not induced were carried out alongside each expression trial.

To determine how successful each condition was at expressing each domain, an aliquot from each trial sample, including controls, were separated on a gel. Conditions for cell harvesting and lysis were standardised with all samples and the same volume of material was loaded onto SDS-PAGE gels to correct for variability errors. Full details are provided in chapter 2.

Table 4.5: Expression Trial Conditions for New Ataxin-1 Domains

Details of the conditions tested for the expression of the new ataxin-1 domains. Small scale trials were carried out systematically by varying one of the following conditions per trial alongside appropriate controls.

Expression Condition	Variation
<i>E. coli</i> Cell Strain:	BL21(DE3), Rosetta-gami 2(DE3)pLysS
Culture Media:	LB, Terrific Broth (TB)
IPTG Concentration:	0.2 mM, 0.5 mM, 1 mM final concentration
A₆₀₀ at Induction:	0.2, 0.3, 0.4, 0.5, 0.6 and 0.6-0.8
Incubation Temperature:	Cells were consistently grown to A ₆₀₀ at 37°C. After induction, the temperature was changed to: 16°C, 25°C or 37°C.
Incubation Period:	Following induction, the incubation period varied from 4 h up to 20 h.

Initial trials with LB media and Terrific Broth with varying conditions did not yield any soluble protein for any of the constructs. As the domains are not full-length proteins and are potentially unstable, I hypothesised that there may be an issue with protein expression. In an attempt to overcome this, a new *E. coli* strain, Rosetta-gami 2(DE3)pLysS was employed. This strain of *E. coli* combines features of the Origami™2 and Rosetta™2 strains. In particular, the Origami™ 2 strain aids protein folding, encouraging proteins to adopt a conformation for expression. This is an advantage for the ataxin-1 domains, which are known to have difficulty in folding correctly. The Rosetta-gami 2(DE3)pLysS strain also enhances expression of eukaryotic proteins. Again, this could be advantageous in expressing the ataxin-1 domains, as these are designed from a eukaryotic IMAGE clone. There is one main disadvantage of the Rosetta-gami 2(DE3)pLysS strain over the BL21(DE3) strain, which was the time the cells required to reach A_{600} 0.6. The Rosetta-gami 2(DE3)pLysS cells took approximately double the time required by BL21(DE3) cells to reach induction.

Despite the slow doubling time of the Rosetta-gami 2(DE3)pLysS strain of *E. coli* the potential benefits of the strain seemed positive. Trials were conducted, with varying temperatures and IPTG concentrations, yet ataxin-1 expression of any of the constructs was not visible when samples were analysed by SDS-PAGE. Further investigation into the Rosetta-gami 2(DE3)pLysS strain revealed that this strain of *E. coli* does not allow protein expression with the pTrc-His-A' vector. According to the manufacturer, both the vector and the strain possess functions which suppress the expression of background proteins, in order to aid protein purification. This in turn prevents the expression of the protein of interest. This explained why no expression was seen with these trials, but did not explain the reasoning for the lack of protein expression in other cell lines.

As there was no clear explanation for the lack of protein expression, DNA for all of the constructs was mini-prepped (details in Chapter 2) and sent to the DNA Sequencing Service at the University of Dundee to be sequenced. The purpose of re-sequencing the constructs was to rule out any possibility of any mutations with the

constructs, which could have been having an effect on protein expression. The results of the sequencing clarified that all of the constructs were in the correct sequence and, more importantly, in the correct frame with the His-tag. There were no signs of any possible mutations or other problems with the sequences themselves, which could account for the lack of protein expression. Because of this, I hypothesised that one of the problems could be with the glycerol stocks which the proteins were picked from for expression. The glycerol stocks had been prepared some while previously, and there was a possibility that either they had degraded, or the proteins were too unstable to be expressed from a glycerol stock.

To overcome this potential issue, all of the constructs were transformed into the BL21(DE3) strain of *E. coli* and selected on agarose plates supplemented with ampicillin. One colony from each plate was inoculated with LB media and ampicillin and grown overnight. This pre-culture was used to inoculate larger cultures for expression trials. Trials were carried out at varying concentrations of IPTG (0.2 mM, 0.5 mM and 1 mM) by induction at A_{600} of 0.7. Samples were treated as detailed in section 2.2.1 and separated on an SDS-PAGE gel. Unfortunately, once again, expression of the constructs was unsuccessful.

The next variable to test was the A_{600} at induction. Once again, colonies from the 575-815 ataxin-1 construct transformation into BL21(DE3) cells were used to inoculate 5ml cultures of LB and trials were carried out by inducing protein expression at A_{600} of 0.2, 0.3, 0.4, 0.5 and 0.6. Small culture volumes were used in order to test a range of conditions to identify those which produced the greatest protein expression. Cultures were then transferred to either a 37°C or 16°C incubator. After 4 h, samples of each culture were taken to test for expression and the remaining cultures returned to their respective temperatures for incubation overnight. Following completion of the trial, samples of each condition were taken and separated on 12% SDS-PAGE.

When testing the A_{600} of the culture for induction, absorbance was measured on the spectrophotometer in our lab and also on a spectrophotometer in a neighbouring lab. Interestingly, the reading at A_{600} on our spectrophotometer appeared to be

~1.2% lower than that on our fellow colleagues. To test the accuracy, readings were also obtained from another colleague's spectrophotometer, which also proved our readings to be ~1.2% lower. This suggests that previously, induction of protein expression may have been occurring at a later stage in the growth phase and IPTG may have been added while the cells were in stationary phase and not exponential phase. Subsequently, the induction of protein production may have been too late, hence the lack of protein expression in previous expression trials.

Samples from each O.D. point were separated on the same gel for comparison. The samples from the induction at A_{600} of 0.3, 0.4 and 0.5 showed a small difference at the expected molecular weight area compared to a control sample. There appeared to be a very faint band at ~25 kDa from the culture incubated at 16°C overnight following induction with either 0.2 mM or 0.5 mM IPTG. This is highlighted in Figure 4.9.

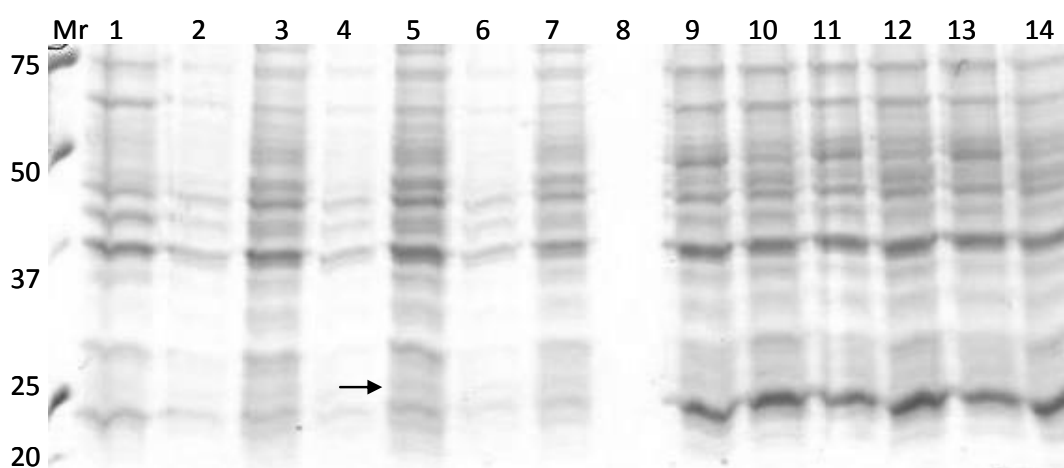


Figure 4.9: SDS-PAGE Following Induction of Ataxin 575-815 at $A_{600}=0.4$

Expression samples were analysed by SDS-PAGE to identify the expression of ataxin 575-815. This gel shows the expression samples of cultures induced with IPTG at $A_{600} = 0.4$. Lanes are identified as follows: 1 = Control sample; 2 = 0.2 mM IPTG, 4 hr incubation; 3 = 0.2 mM IPTG, overnight incubation; 4 = 0.5 mM IPTG, 4 hr incubation; 5 = 0.5 mM IPTG, overnight incubation; 6 = 1 mM IPTG, 4 hr incubation; 7 = 1 mM IPTG, overnight incubation; 8 = blank lane; 9 = 0.2 mM IPTG, 4 hr incubation; 10 = 0.2 mM IPTG, overnight incubation; 11 = 0.5 mM IPTG, 4 hr incubation; 12 = 0.5 mM IPTG, overnight incubation; 13 = 1 mM IPTG, 4 hr incubation; 14 = 1 mM IPTG, overnight incubation. Lanes 1-7 represent samples incubated at 16°C and lanes 9-14 represent samples incubated at 37°C. The very faint band witnessed on the gel is highlighted by the arrow.

To test whether or not this band does represent expression of ataxin-1 (575-815), a larger culture was grown up for a small scale purification test. A large culture was set up and smaller cultures were taken and induced with either 0.2 mM IPTG or 0.5 mM IPTG at A_{600} 0.3, 0.4 and 0.5. Following induction, the cultures were transferred to 16°C to incubate whilst shaking at 200 rpm overnight. An un-induced control was also incubated at the same conditions for comparison. The following morning, two samples of 500 μ l was taken from each small culture. One of the 500 μ l samples from each condition was treated in the usual way; pellet culture and resuspend in Laemmli buffer. The other 500 μ l sample was pelleted and resuspended in lysis buffer (the same used for His-purification). Each sample was then sonicated for 3 x 10 seconds at 10 μ on ice with a 30 second break between each sonication, to prevent the samples from over-heating. Following sonication, samples were centrifuged (13,000 rpm for 5 min) and the supernatant was applied to Co^{2+} charged NTA beads. The bead-supernatant mixture was incubated at 4°C with tumbling for 1 h. The samples were centrifuged gently (2000 rpm for 1 min) and the supernatant removed. The beads were then washed in lysis buffer (20 mM imidazole) by tumbling at 4°C for 30 min. Following the wash, the beads were gently centrifuged again and the supernatant removed. The beads were resuspended in 30 μ l of Laemmli buffer and boiled at 100°C for 5 min. Of this total volume, 15 μ l of each sample was run on a 12% SDS-PAGE gel, stained with Coomassie Blue and destained to visualise the bands.

Unfortunately, following destaining, the only bands visible on the gel were those from the lysate which was run as a control (data not shown). It does not appear that any proteins in the 25 kDa region bound to the Co^{2+} charged beads, suggesting that the ataxin-1 575-815 construct had not actually been expressed.

4.4. Discussion

The research conducted in this chapter focussed on the production of ataxin-1 protein constructs to investigate the role the protein plays in disease pathology. The research began with expression and purification of constructs which had been previously cloned for analysis. These constructs were expressed; however purification did prove to be an issue. This led on to the development of new ataxin-1 constructs, based on the predicted secondary structure of the protein. Following cloning into a His-tagged vector, expression of the constructs was attempted.

Unfortunately, despite numerous attempts, expression of the new ataxin-1 constructs was unsuccessful. There are a number of possible reasons for the lack of protein expression. Firstly, it is known that the ataxin-1 protein is unstable and does not always fold into a stable conformation. This could have resulted in protein expression becoming toxic to the cells. Secondly, the expression system itself could play a part. Due to time and financial constraints, it was not possible to investigate a number of expression systems, which may well have yielded more positive results.

There is always a risk of problems with protein expression when only a construct of the protein is being investigated. Despite attempting to select constructs which appeared to be conformationally more stable and favourable, this has not translated into experimental practice. With hindsight, it now appears that continuing to pursue greater purification of the original constructs may have been a more fruitful avenue of research. However, with more time, expression and subsequent purification of the new ataxin-1 constructs may prove to be successful and efficient for ataxin-1 protein investigations.

CHAPTER 5

IDENTIFICATION OF COMPOUNDS FOR INHIBITION OF 14-3-3 ζ ACTIVITY

5.1. Introduction

Currently there is a great deal of research into treatments for neurodegenerative diseases. As the age of the population increases, the number of patients suffering from neurodegenerative diseases is also on the increase. Therefore, it is essential that successful treatments are developed in order to combat this growing problem.

Many current treatments focus on preventing the loss of, or replacing depleted neurotransmitters; i.e. L-DOPA replaces dopamine in Parkinson's disease and current Alzheimer's treatments prevent the degradation of acetylcholine. Current research into neurodegeneration is still focussed on identifying the pathways which lead to these debilitating diseases, by means of identifying drug targets. There are also studies which are interested in the impact gene therapy and stem cells can have on treating neurodegeneration.

There are a number of studies which have identified the interaction of 14-3-3 with neurodegenerative disease proteins as being a key step in disease pathology. Yet, to date, there are no drugs which specifically target 14-3-3 interactions in a bid to treat these diseases. This research aims to fill that gap, through targeting 14-3-3 interactions as potential treatments in neurodegenerative disease.

The main focus is on the interaction between 14-3-3 ζ and ataxin-1 in Spinocerebellar Ataxia Type 1. This is a model interaction by which 14-3-3 ζ inhibition can be tested. The interaction of these two proteins is well established and is an ideal model to test 14-3-3 ζ inhibitors against.

The aim was to identify inhibitors using an *in vitro* model with 14-3-3 ζ and exoenzyme S (ExoS), an ADP-ribosyltransferase toxin of *Pseudomonas aeruginosa*.

This interaction is phosphorylation independent and can be easily replicated *in vitro* without requiring prior phosphorylation of the test protein. Once inhibitory compounds have been identified from this interaction, they can be tested using the ataxin-1 constructs detailed in Chapter 4.

5.2. Aims

Identification of Compounds which Block 14-3-3 ζ Interactions

The aim of this research is to identify small compound inhibitors which can inhibit the interaction of 14-3-3 ζ with disease proteins. It is not essential to identify compounds which completely inhibit 14-3-3 ζ interaction, due to the number of other interactions which this would affect. More detail on the interactions which 14-3-3 proteins play an important role in, including cell cycle regulation and cell signalling, are detailed in section 1.1.1 of the Introduction. However, reducing the interaction can significantly slow down the progression of aggregation and return the rate of protein degradation back to normal levels.

5.3. Results

5.3.1. Identification of Compounds for 14-3-3 Inhibition

Identifying compounds which block 14-3-3 ζ interactions was a collaborative work with Dr. Wissam Mehio of the Computational Biology Group at the University of Edinburgh. The computational approach docks various compounds in a virtual screening programme and scores them according to their position over suggested points of a protein.

5.3.1.1. EDULISS

EDULISS, Edmunursh Unursh Ligund Seluctuon Sysumsu, is a small molecule database for data mining which is currently maintained by Dr. Kun-Yi Hsin at the University of Edinburgh (Hsin et al. 2010). The EDULISS database was developed originally by Dr. A Hinton (Hinton 2005) and since then, has been expanded to include more suppliers, physicochemical information and is continuously updated. The in-house database contains the 3D atomic coordinates for each of the 5.5 million compounds stored, of which 4 million are unique, along with greater than 1600 calculated molecular descriptors, including structural, molecular, physicochemical, geometric and pharmacophoric properties, to name but a few. The use of a selection of descriptors enables the rapid selection of small related molecular families from the database. This also provides an efficient means of identifying unique compounds, as molecular weight and atom type alone identify only 6% of the compounds in the database as unique (Hsin et al. 2010). Compounds are sourced from 28 different commercial databases and small specialist compound catalogues, ensuring that each compound is currently available for purchase. A chart of the companies and the number of compounds contributed is shown in Figure 5.1.

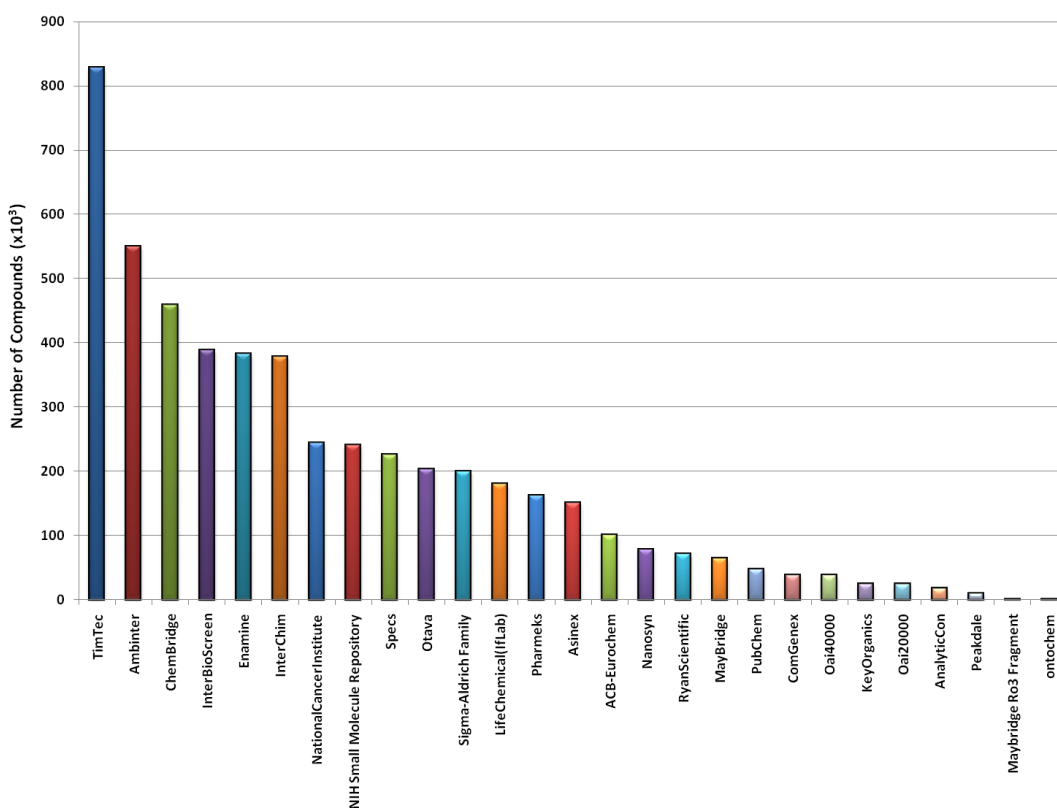


Figure 5.1: Companies Contributing to EDULISS Database

Histogram showing the commercial databases which contribute to EDULISS and the number of compounds each contributes. This information is available on the EDULISS website (<http://eduliss.bch.ed.ac.uk/test/index.jsp>).

Of all the compounds stored in the database, more than 3.9 million fit the Lipinski's rule of five and 3.4 million fit the Oprea lead-like criteria. These pharmacokinetic parameters assess the drug-likeability of chemical compounds with strict criteria which increase the potential likelihood of a compound to be an orally active drug. This provides an alternative means of identifying potential compounds by a descriptor- or rule-based search, which users can select on the EDULISS web interface. Other options include a molecular structure similarity search and an Interatomic Pharmacophore Profile (IPP) search. In addition, users can search the database by compound ID to retrieve information relevant to the compound and also as a means to purchase compounds. In this research, EDULISS was used as a source of compounds for virtual screening through application of the LIDAEUS program (section 5.3.1.3) to detect potential compounds for 14-3-3 ζ inhibition.

5.3.1.2. STP

Dr. Mehio developed a program which can predict the location of potential binding sites (Mehio et al. 2010). This program has been named STP – Surface Triplet Propensities/ Surface Triangle Profiles. STP relies on the propensities of triplet patterns to indicate whether a patch is likely to be a binding site or not.

For identifying compounds which can inhibit the binding pocket of 14-3-3 ζ , the Protein Data Bank (PDB) file 1QJB was used. This file is 14-3-3 ζ and phosphopeptide complex in mode 1 (Rittinger et al. 1999). The PDB file is uploaded to the website (<http://opus.bch.ed.ac.uk/stp/index.php>) to run STP. This identifies hydrogen bond donor and acceptors in the protein. Examples of donors and acceptors are shown in Figure 5.2. The maximum distance between donor and acceptor is 3.8 Å.

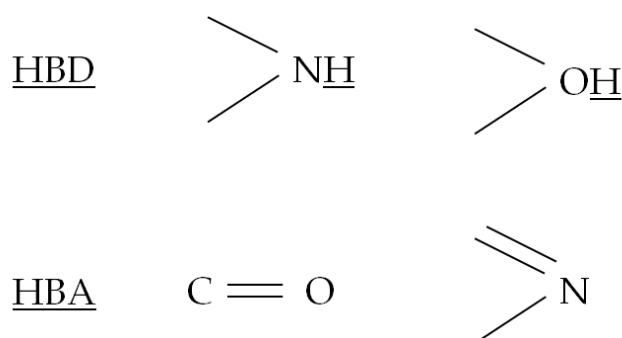


Figure 5.2: Hydrogen Bond Donors and Acceptors

Examples of Hydrogen Bond Donors (HBD) and Hydrogen Bond Acceptors (HBA). In the donors, the underlined hydrogens (H) are donated to the double and triple bonds of the acceptors.

Once HBD's and HBA's have been identified, these are used to predict the location of binding sites through the propensity of triplet patterns. This indicates whether a patch is likely to be a binding site or not. The programme then provides the user with a file and a tutorial in order to visualise the binding sites. The returned PDB file needs to be opened in Pymol to carry out the required steps. The first step is to remove all the hydrogen atoms and then colour the protein by bfactor code. The final step is to show the solvent accessible surface which coats the protein in patches

of colour, with the colour scale going from blue to red, with red coloured patches indicating those most favourable for high affinity binding sites. The STP image generated from the 1QJB PDB file is shown in Figure 5.3.

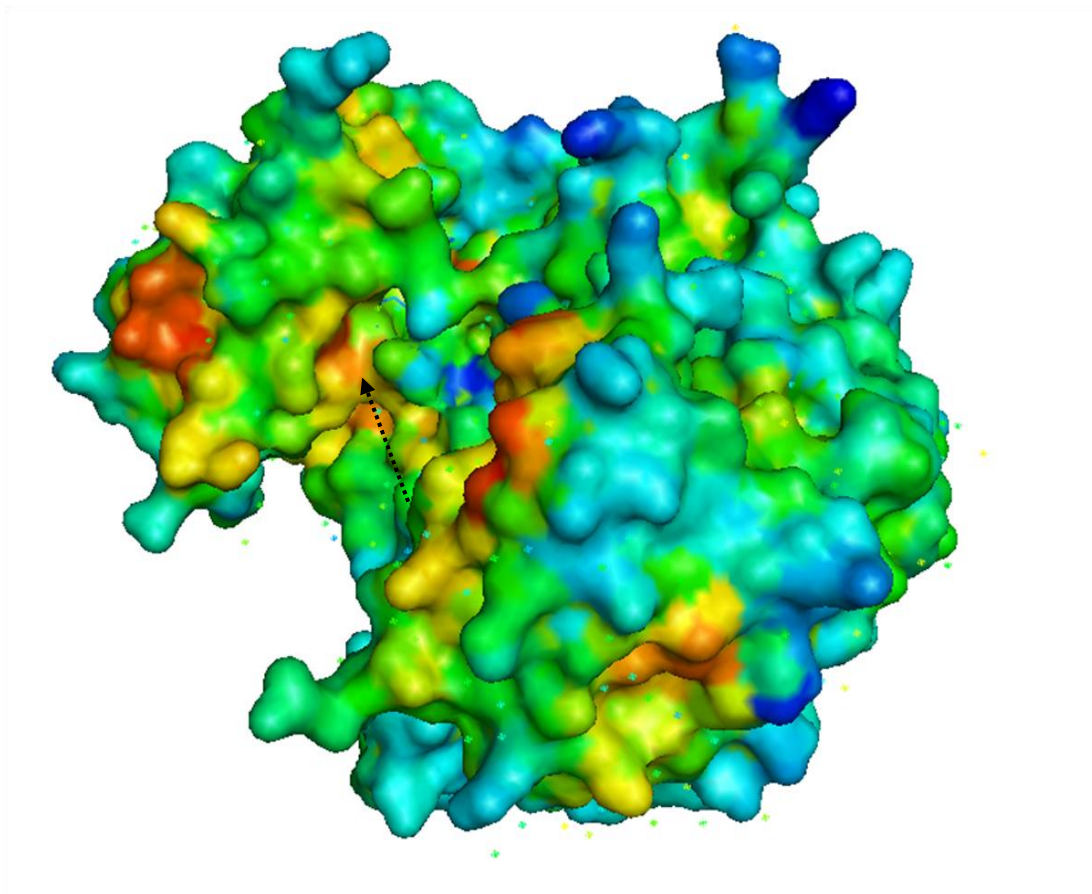


Figure 5.3: STP Image of PDB File 1QJB

STP image showing the most favourable binding sites for the 14-3-3 PDB File 1QJB. The patches coloured red are the most favourable binding sites, whereas the blue areas are the least favourable. The dotted arrow points to the phospho-binding pocket.

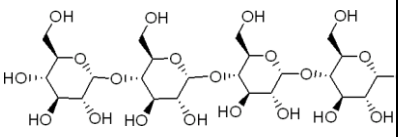
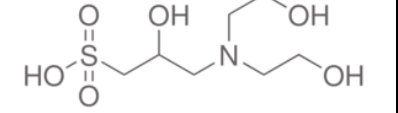
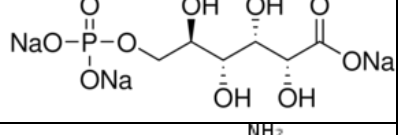
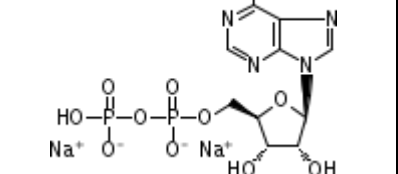
5.3.1.3. LIDAEUS

LIDAEUS, Ligand Discovery at Edinburgh University, is an in-house virtual screening program (Wu et al. 2003; Taylor et al. 2008). To begin, the PDB file of the protein to be screened in complex with its natural ligand is obtained. In this research, this is the PDB file 1QJB. The natural ligand is removed from the file and a map generation program defines the binding pocket of the protein and defines a set of site points. The site points determined are assigned according to their preferred protein interaction; HBA, HBD or hydrophobic. This provides all the information required to run the program.

The potential inhibitors are screened against the 3-D structure of the protein of interest and matched to the site points in as many ways as possible to get a fit. This stage is referred to as 'pose'. Each pose is scored according to a number of factors including Van der Waals and hydrogen bond donor and acceptor bonding energies. At this point, a number of orientations and energy minimization techniques are applied to the ligands to achieve a better score. The final stage of the process is to 'sort' the ligands tested. This maintains a list of the top 1000 best scoring ligands.

The compounds which were selected to test 14-3-3 ζ binding inhibition are shown in Table 5.1. A full list of the compounds identified from this screen is detailed in Table 7.1 in the Appendix.

Table 5.1: Compounds Tested for 14-3-3 ζ Binding Inhibition

Compound Image	Compound Name	Supplier	Solubility
	Maltotetraose (MW 666.58)	Sigma-Aldrich	50 mg/ml in dH ₂ O (0.075 M)
	DIPSO (MW 261.29)	Sigma-Aldrich	0.1 M in dH ₂ O
	6-Phosphogluconic Acid Trisodium Salt (MW 342.08)	Sigma-Aldrich	50 mg/ml in dH ₂ O (0.145 M)
	ADP Adenosine 5'- diphosphate sodium salt hydrate (MW 471.16)	Acros Organics	Soluble in dH ₂ O

5.3.1.4. Compound Selection and the Blood-Brain Barrier

The purpose of identifying potential compounds which can inhibit 14-3-3 interaction is for therapeutic benefits in neurodegenerative diseases. Clearly, this suggests that any potential inhibiting compounds must have the potential to cross the blood-brain barrier (BBB) in order to elicit their therapeutic effects.

The BBB is a continuous layer of endothelial cells which are joined by tight junctions. The BBB was identified by Paul Ehrlich in the late 19th century following intravenous injection of a dye which stained most tissues, however the brain remained unstained. As a consequence, the brain remains inaccessible to a number of drugs, due to lipid solubility which is insufficient to allow penetration of the BBB. However, the integrity of the BBB can be disrupted during inflammation, allowing substances which are normally impermeable to pass. Generally, it is only small, non-polar molecules which have the ability to passively diffuse across the BBB however some neuro-active drugs do so through transporters (Rang 2003).

One treatment which exploits this method is the first-line treatment for Parkinson's disease, levodopa (L-DOPA). Administration of L-DOPA is almost always with a peripheral dopa decarboxylase inhibitor (e.g. carbidopa), to reduce the required dose by 10-fold and the peripheral side-effects. The dopa decarboxylase inhibitor prevents the L-DOPA being metabolised into dopamine by peripheral decarboxylases prior to reaching the brain. The dopa decarboxylase inhibitor cannot pass the BBB, however L-DOPA does gain entry to the brain via the large neutral amino acid transporter. Once L-DOPA passes into the brain, it is quickly converted into dopamine to mediate its therapeutic effects (Golan 2008).

There are a number of peptides which have the ability to increase the permeability of the BBB. These include bradykinin (a potent vasodilator) and enkephalins (small molecule pain killers) and may be useful in improving penetration of the BBB (Rang 2003).

Should any of the compounds tested prove to be effective, progression into clinical trials would require the ability of the compounds to cross the BBB. There are predictive software systems available (Molecular Discovery Ltd) which can determine whether a compound is a potential substrate for the efflux pump, P-glycoprotein, which allows penetration of the BBB. Another factor which also needs to be considered is the presence of the multi-drug-resistance protein (MRP) which actively removes exogenous molecules from within neural endothelial cells.

5.3.2. Purification of Proteins Required for Testing Potential Compounds

In order to be able to test the ability of the identified compounds to inhibit the binding interaction of 14-3-3 ζ , proteins were prepared for analysis. The interaction tested is with 14-3-3 ζ and Exoenzyme S (ExoS), due to the fact this interaction occurs independently of phosphorylation whilst still utilising the phospho-protein binding pocket of 14-3-3 proteins (Masters et al. 1999). By not needing to prior phosphorylate the test protein, a number of potential caveats can be avoided during the initial screening stage.

For the purposes of this screening method, 14-3-3 ζ was used and the purification of this protein is detailed in both section 2.2.2.2 of the Materials and Methods and also section 3.3.7 in Chapter 3. Production of 14-3-3 ζ was from a construct which tags the protein with a histidine-tag. This tag is only 6 residues long and does not interfere with the formation of 14-3-3 ζ (as detailed in section 3.3.7) and should not interfere with any interactions with 14-3-3 ζ . Because of this, the decision was taken to leave the His-tag attached to the protein.

The other protein required for testing compound inhibition was ExoS. A construct of ExoS containing the 14-3-3 binding region had been previously cloned into a GST-tagged vector (see Table 2.3 in Materials and Methods) and the expression conditions were optimised. Full details of the expression and purification conditions are given in sections 2.2.1 and 2.2.2.3 in Chapter 2 respectively. ExoS was over-expressed and purified by a one-step purification procedure employing glutathione-Sepharose beads. The GST-tag has a high affinity for the glutathione-Sepharose beads, meaning the tagged protein of interest binds to the beads and unbound material can be washed off the beads. Once the protein of interest had bound to the beads, reduced glutathione was used to elute the protein from the beads. Following elution, fractions from all stages of the purification procedure were analysed on SDS-PAGE to identify which fractions contained the protein of interest. An SDS-PAGE gel of these fractions is shown in Figure 5.4.

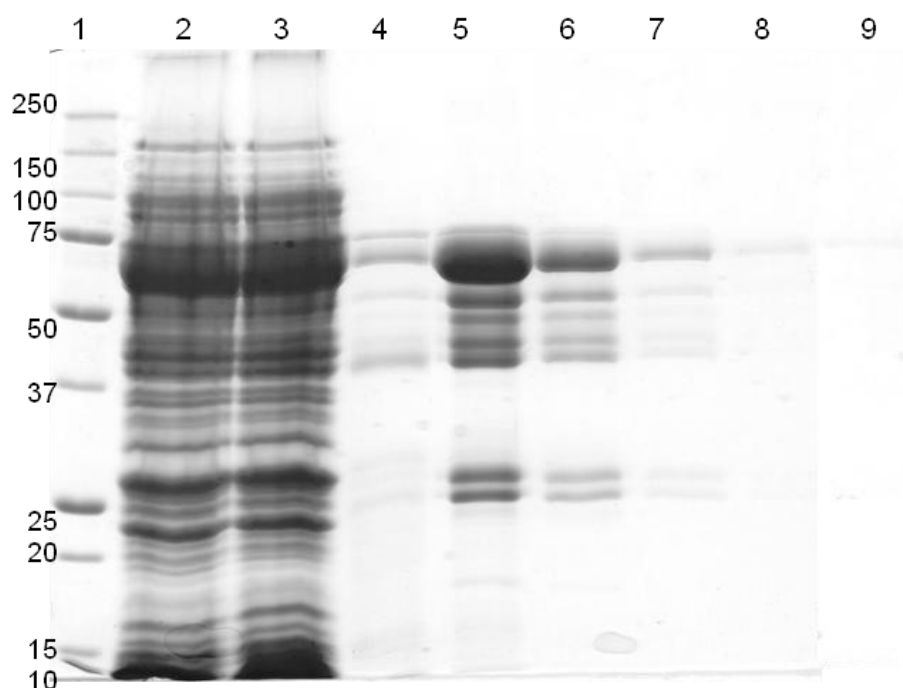


Figure 5.4: SDS-PAGE of Purification Fraction for GST-ExoS

SDS-PAGE of fractions collected from the purification of GST-ExoS. Fractions were analysed on 12% SDS-PAGE. Lanes are labelled as follows: Lane 1 – Molecular weight marker; Lane 2 – Lysate; Lane 3 – Flow-Through; Lane 4 – Wash; Lane 5 – Elution 1; Lane 6 – Elution 2; Lane 7 – Elution 3; Lane 8 – Elution 4; Lane 9 – Final Bead Sample.

The gel image shows that elution fractions 1 and 2 contain the protein of interest. It should be noted that the ladder of bands below the band for the purified protein are not contaminating proteins. During denaturation and reduction conditions, the GST fusion tag degrades and appears as a ladder of bands of lower molecular weight below the full-sized fusion protein on SDS-PAGE. These fractions which were found to contain the protein of interest were pooled together for dialysis to remove the reduced glutathione. To do this, dialysis in a slide-a-lyser was carried out in the presence of PBS (see section 2.2.4).

Following dialysis, to check that the majority of the reduced glutathione had been removed, a test with glutathione-Sepharose beads was carried out. In order to test the ability of the GST-ExoS to rebind to glutathione-Sepharose beads, a small volume of protein (40 μ l) was added to a small amount (15 μ l bead slurry) of beads and incubated at 4°C for a minimum of 1 h whilst tumbling. A sample of the beads

and the supernatant were then analysed by SDS-PAGE to compare how much protein had re-bound to the beads. The results of this test are shown in Figure 5.5.

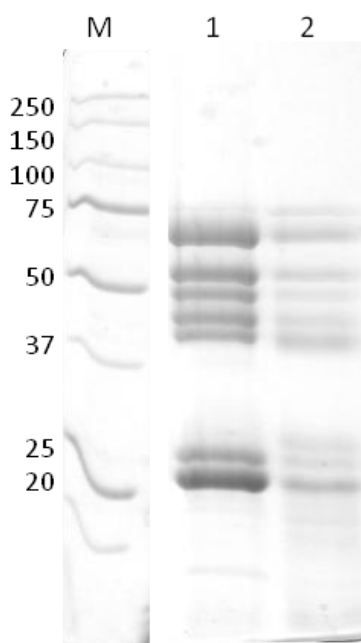


Figure 5.5: SDS-PAGE of Glutathione Test

Protein tested for the ability to re-bind to glutathione-Sepharose was analysed on 12% SDS-PAGE. Lanes are labelled as follows: M – Molecular Weight Marker; Lane 1 – Bead Sample; Lane 2 – Supernatant Sample.

The gel from the glutathione test shows that the majority of the GST-ExoS protein does rebind to the glutathione-Sepharose beads. A small amount does appear not to have bound, possibly due to some reduced glutathione remaining. However, importantly, the majority of the reduced glutathione has been removed and the protein still possesses the ability to bind to glutathione. Despite being unable to completely re-bind all of the protein to the beads, this is still suitable for further procedures. When using the GST-ExoS protein for testing the compounds, the protein will be used in an excess concentration than that required for the procedure, in order to saturate the surface of the chip or well. This means that GST-ExoS which has the ability to bind to glutathione-coated surfaces, or anti-GST antibodies will still have the ability to saturate the surface required to test for 14-3-3 ζ interaction.

5.3.3. Methods for Testing Compound Inhibition

5.3.3.1. SPR

Surface Plasmon Resonance (SPR) is a technique which has been around for over 20 years which has become increasingly popular with current advances in technology. This useful real-time, label-free analysis technique allows the characterisation of biomolecular interactions in terms of binding specificity, kinetics and affinity. The technique supports a range of molecules for analysis including proteins, nucleic acids, lipids and carbohydrates to name but a few.

SPR-based instruments (e.g. BIAcore) measure the refractive index (within ~300 nm) near the surface of a sensor through an optical method. The surface is contained in a sensor chip (BIAcore) which can have a variety of surfaces, depending on the interaction which you plan to investigate. The sensor chips contain a number of micro-fluidic flow cells (typically 2-4) which can hold ~20-60 nl. A continuous flow rate (1-100 μ l/min) delivers the running buffer to the flow cells to be used.

Interactions are tested through immobilizing the 'ligand' to the sensor surface and injecting the 'analyte' to be tested in an aqueous solution over the flow cell. If the analyte binds to the ligand, this accumulation on the surface of the sensor results in an increase in the refractive index. Importantly, there are no moving parts to the optical device, enhancing stability and allowing the change in refractive index to be measured in real time. The refractive index is plotted as resonance units (RU) versus time and displayed as a sensorgram. An SPR angle change of ~0.1% corresponds to 1000 RU. To produce this change, ~1 ng per square mm of protein must bind to the surface of the sensor chip; however the exact relation of RU to ng of bound material varies according to the refractive index of the analyte.

In order to produce an accurate result, a control or reference flow cell is also tested, where either no ligand or a control ligand is immobilized to the surface, which the analyte cannot interact with. The response from this cell provides a background reading which can be subtracted from the sensorgram to produce the actual binding response. If the analyte does not bind to the ligand, the change in refractive indices

of both flow cells will be the same and the actual binding response will be 0 RU. It is only the interaction of the analyte with the ligand which produces a positive response which can be visualised on the sensorgram.

There is one main caveat of SPR which can make this technique very difficult to obtain useful results. When the ligand is injected into the flow cell for immobilization on the sensor surface, there is no way of knowing which way round the analyte has bound to the chip. It may well be that the interaction site of the ligand is inaccessible to the analyte due to its orientation on the sensor surface. In an attempt to overcome this, a number of combinations of 14-3-3 and ExoS with and without GST moieties have been tested. These are detailed in Table 5.2.

Table 5.2: SPR Combinations Tested

Ligand	Analyte	Binding
ExoS	GST-14-3-3 ζ	No
ExoS	14-3-3 ζ	No
GST-14-3-3 ζ	ExoS	No
14-3-3 ζ	ExoS	No
GST-ExoS	14-3-3 ζ	Partial

It is clear from the binding results that these combinations have not yielded great success. This may be due to the orientation of the ligand on the sensor chip however the presence of the GST moiety may also be a factor. A colleague investigated the ability of ExoS and 14-3-3 ζ to interact when one of the proteins was tagged with a GST moiety. She discovered that when 14-3-3 ζ was tagged with GST, there was no interaction with ExoS, however when the GST moiety was tagged to ExoS, the interaction with 14-3-3 ζ could occur. This suggests that the GST tag on 14-3-3 ζ has implications on how the protein can interact and is not a good model for testing compound inhibition.

In light of this information, a model for testing compound inhibition by SPR was designed. A diagram of the proposed model is shown in Figure 5.6.

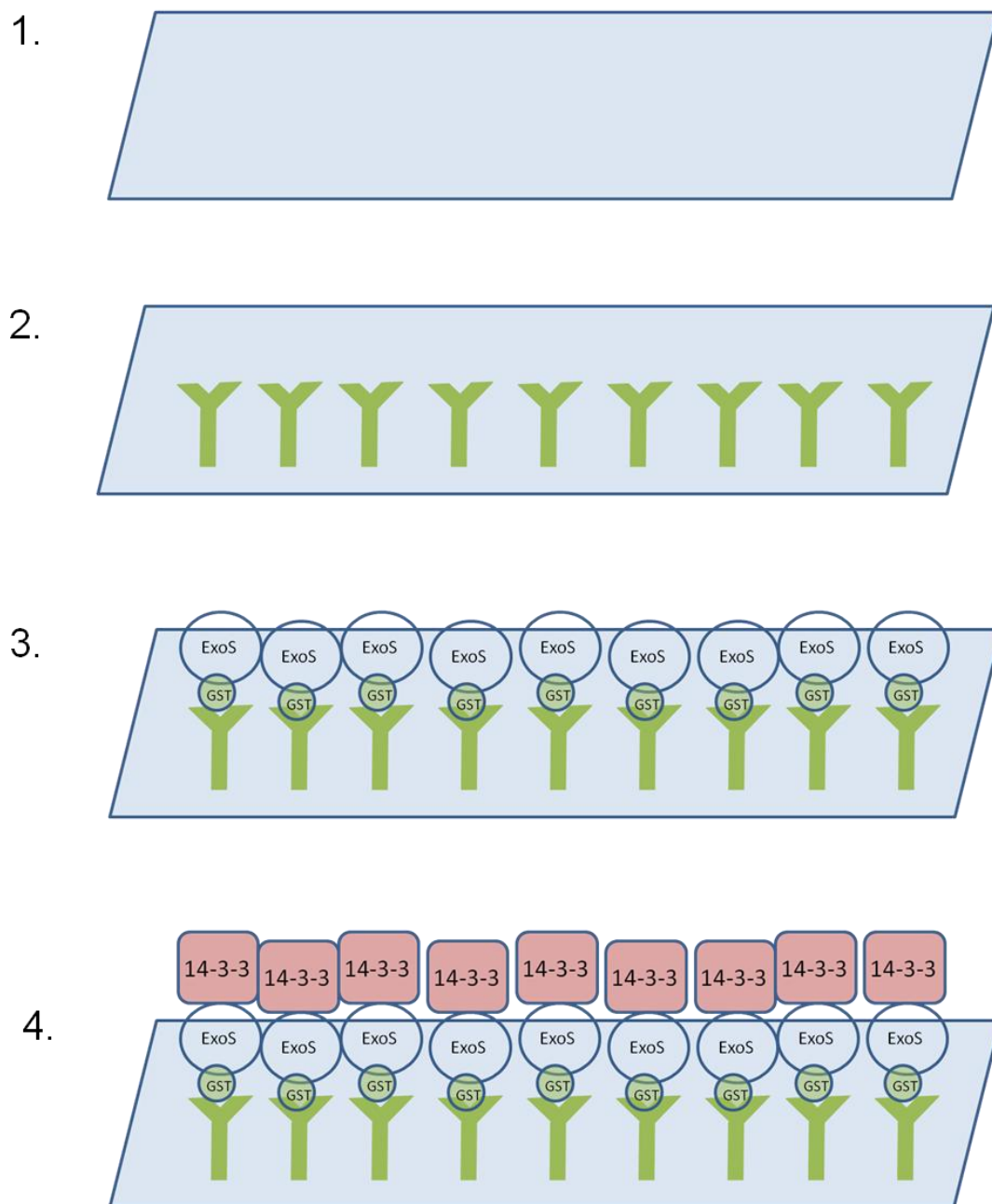


Figure 5.6: Diagram of Proposed SPR Model

Diagram indicating the method of ligand and analyte binding proposed for testing 14-3-3 ζ compound inhibition. Full details of each stage are given in the text.

The stages of the model are detailed as follows:

1. Using a CM5 chip (BIAcore), activate the surface for ligand binding. The chip is activated by a 1:1 solution of EDC: NHS, which reacts with the carboxyl methyl dextran surface of the chip to produce reactive succinamide esters.
2. Following surface activation, inject a GST antibody over the surface of the sensor chip and immobilize through interactions with free amine groups with the chip surface. Following GST antibody immobilization, free GST must be injected over the surface to block any high affinity sites as this can compromise the binding results.
3. Inject the 'ligand' – GST-ExoS over the sensor surface. The GST moiety will interact with the GST antibody and orientate the ExoS in a manner which is accessible to the 'analyte'.
4. Finally, inject the 'analyte' over the sensor surface. The analyte is 14-3-3 ζ which should bind to ExoS, producing a positive response.

For testing compound inhibition, each compound would be incubated with 14-3-3 ζ prior to injecting over the sensor surface to test for 14-3-3 ζ binding to ExoS. If the final binding result is positive, this indicates that the compound being tested has not inhibited the ability of 14-3-3 ζ to bind to ExoS. If the final binding result is negative, this indicates that the compound tested is a successful inhibitor of 14-3-3 binding.

Prior to testing the compounds, the method had to be tested to see if it would be a useful model. Unfortunately, initial tests indicated that the difference in RU following addition of 14-3-3 ζ was only ~16% which is not a viable model. This small change in RU indicates that if an inhibitor was only binding to a fraction of 14-3-3 ζ , it would not be possible to determine this from using SPR. In addition, due to time constraints and the expense of using SPR, alternative methods were explored to obtain more accurate results. An example of the output trace obtained using SPR is shown in Figure 5.7.

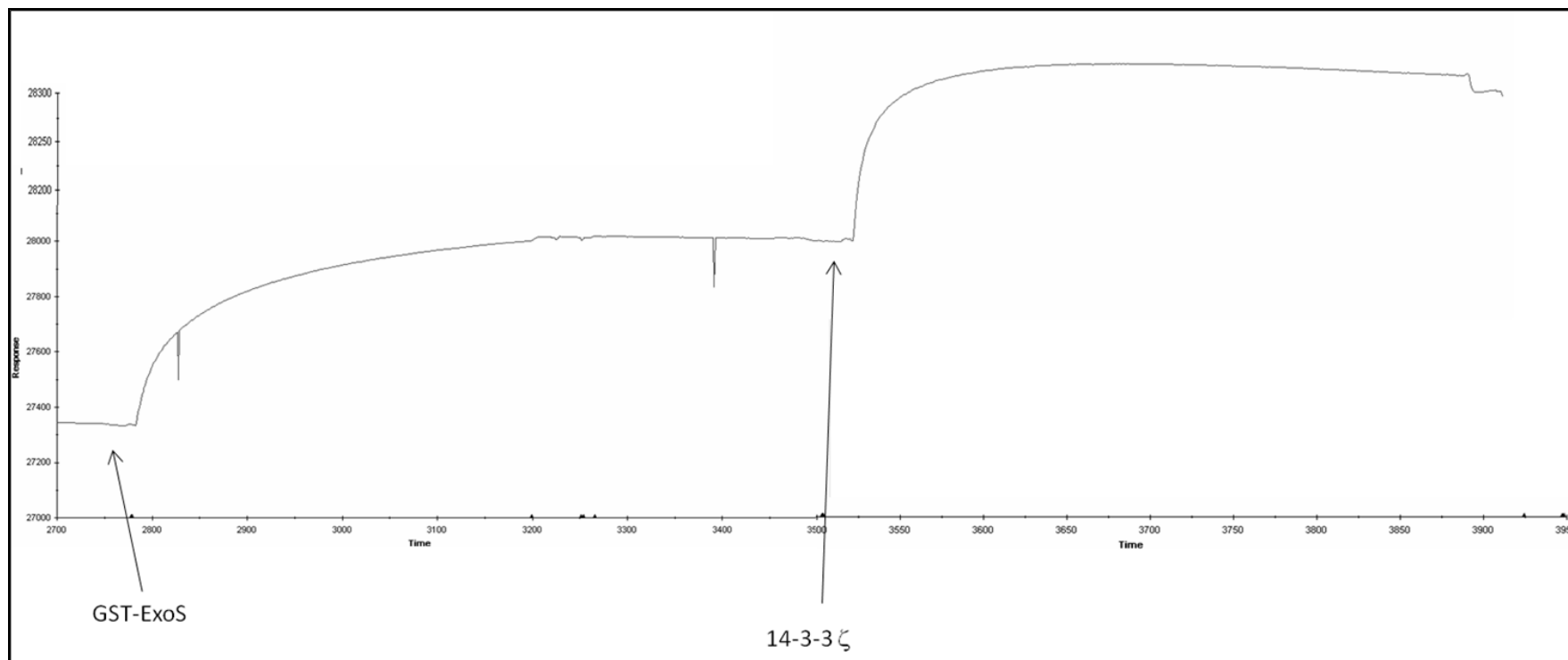


Figure 5.7: Output Trace from SPR Test

Following activation, the flow cell was coated with a GST-antibody. The image shows the point where GST-ExoS was added to the flow-cell and the increase in response units represents protein binding. Once the level of protein binding had stabilised, the 14-3-3 ζ protein was passed over the chip. The increase in response units indicates that the protein does bind to the GST-ExoS which is immobilised on the chip. This image has been magnified to see the response to adding 14-3-3 ζ to the chip; however the overall percentage of response units means that this method is not suitable for detecting small changes such as the presence of an inhibitor.

5.3.3.2. ELISA Assay

Enzyme-linked immunosorbent assays (ELISA) are plate-based assays, mainly employed for detecting and quantifying substances including proteins, peptides and antibodies. This method can also be adapted to test the effectiveness of the 14-3-3 ζ compound inhibitors. This is carried out in 96-well plates that are pre-coated with anti-GST antibody, allowing the GST moiety of GST-ExoS to bind to the surface of the well whilst orientating the ExoS in a manner which allows 14-3-3 ζ to bind. A diagram showing how this works is shown in Figure 5.8.

Each stage of the assay model is detailed below:

1. Begin with a 96-well plate pre-coated with anti-GST antibody.
2. Incubate selected wells with GST-ExoS to immobilise the protein to the wells. The GST-tag also orientates the protein in the wells allowing further protein interactions.
3. Add 14-3-3 protein which has been pre-incubated with test compounds to the selected wells and incubate.
4. Following incubation, wells are washed and successfully inhibiting compounds will prevent the interaction of 14-3-3 with ExoS, however unsuccessful compounds will not prevent 14-3-3 binding to ExoS.
5. The final step is to incubate with 14-3-3 specific antibodies, and subsequent HRP-conjugated secondary antibodies, prior to HRP-conjugate detection. Wells tested with unsuccessful compounds will produce a positive result through HRP detection as the 14-3-3 protein will still have the ability to interact with the ExoS protein. Compounds which successfully inhibit 14-3-3 interaction will produce a negative HRP response, as there will be no 14-3-3 protein present in the well to be detected by the antibodies.

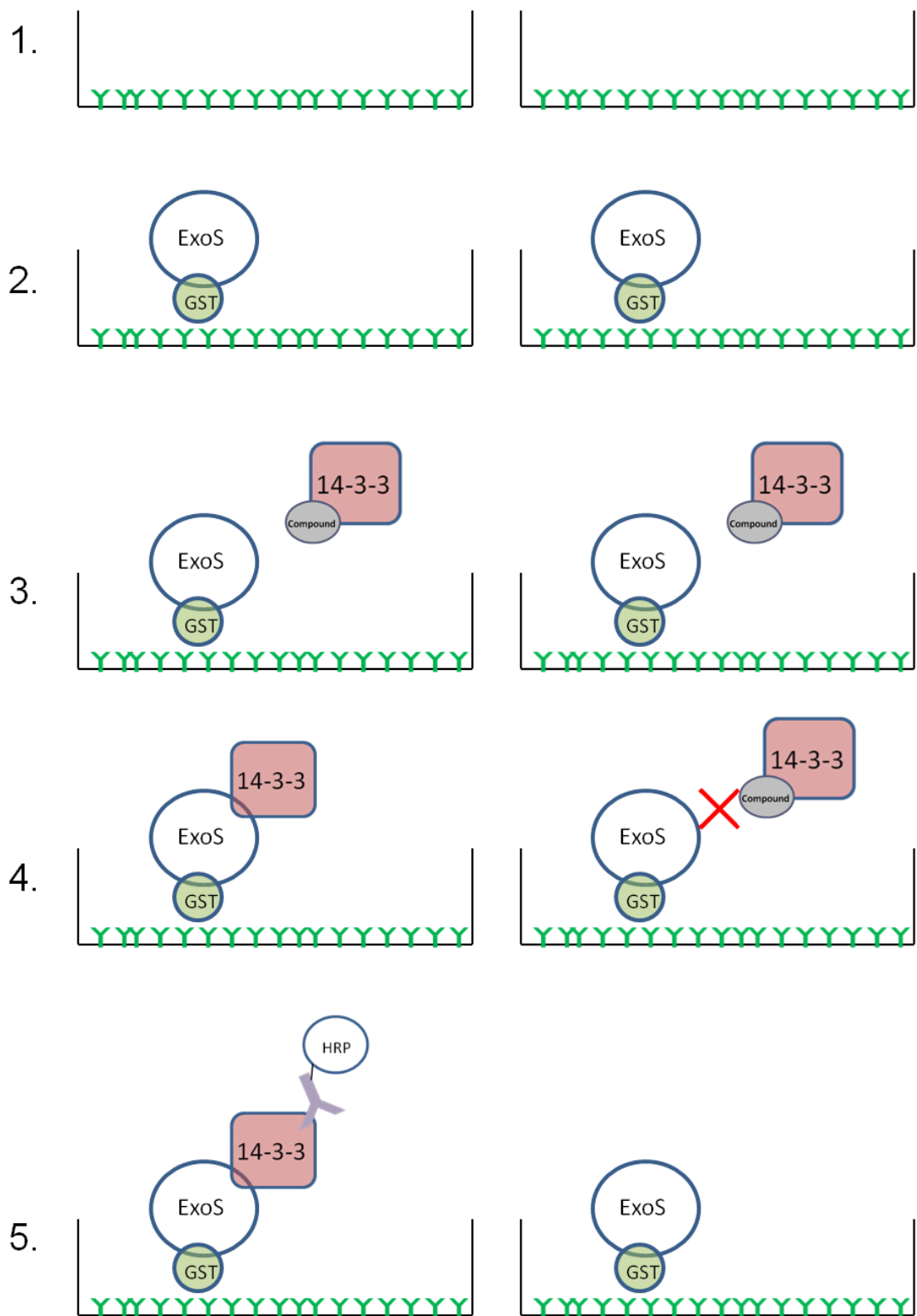


Figure 5.8: ELISA Assay

The steps involved in the ELISA assay are illustrated. Details about each step are provided in the text.

As with SPR, the use of GST-ExoS provides a means of orientating the protein to allow 14-3-3 ζ to interact. The additional benefit of the ELISA assay over SPR is the ability to test a number of compounds at a variety of different concentrations at once. This allows for larger scale screening of compounds and quickly identifying which compounds should be developed further as potential drug leads.

In order to obtain a measurable absorbance in the assay, the HRP substrate 4-chloro-1-naphthol (4-CN) was employed. This is an HRP reagent which is similar to traditional ECL however the reagent produces an insoluble product which creates a blue colour. The optimal absorbance for the resulting product is 495 nm. The spectrophotometer employed for the assay has a 485 nm absorbance filter, which is still within the absorbance range of the substrate and is suitable for reagent detection. A test was carried out with a Western Blot. Following incubation with 4-CN for approximately 45 min a blue band was visible at the expected molecular weight for 14-3-3 which verified its suitability.

The interaction between GST-ExoS and 14-3-3 ζ serves as a control and this interaction was utilised to optimise the assay method. A series of control conditions were tested to optimise the ELISA conditions prior to testing the compounds. The assay was tested following the manufacturer's instructions as a starting point. These initial results were promising, indicating that this method would be successful following further optimisation. One key point to mention is that the suggested buffers for this assay are all PBS-based. However, PBS is not generally a suitable buffer for 14-3-3 proteins. The phosphate group present in the buffer can compete for the phospho-protein binding pocket of 14-3-3. This in turn could reduce the interaction between 14-3-3 ζ and ExoS, leading to a number of false-positive compounds. To test this, control assays were performed with the basis of the buffers used being changed to TBS. In fact, when the buffers were changed to TBS, the absorbance of 4-CN increased by 0.3-0.4 absorbance units. An example of the results obtained by comparison of the different assay buffers is shown in Figure 5.9. This indicates that for compound testing, PBS should be avoided.

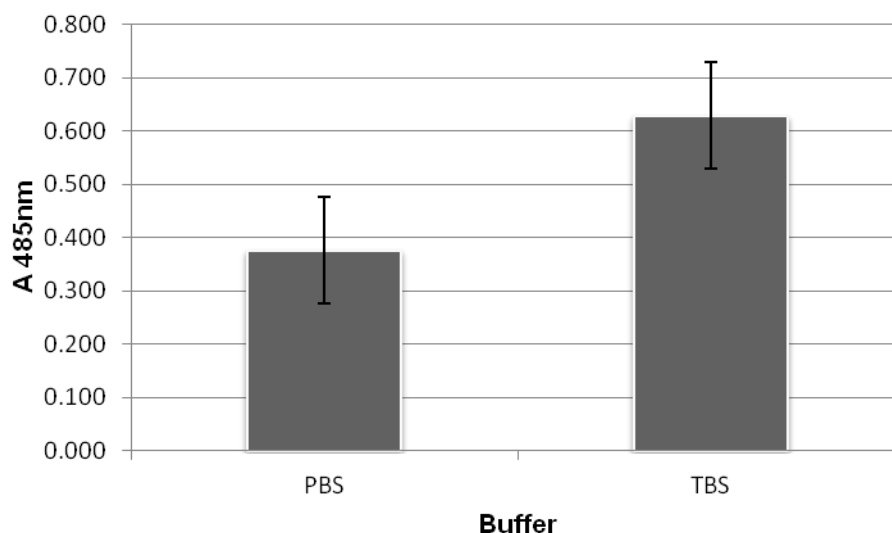


Figure 5.9: Comparison of Assay Buffers

The difference in absorbance detected from identical assay conditions with the only difference being the basis of the buffers used for the assay. It is clear from the chart that the absorbance is greatly increased through the use of TBS-based buffers over PBS-based buffers. This could be due to competition from the phosphate group for the phospho-protein binding pocket of 14-3-3 ζ .

Another factor that was tested was whether an additional blocking step had any effect on the assay. The 96-well plates used are coated in anti-GST antibody and pre-blocked prior to use. However, a series of controls were also tested to determine whether an additional blocking step following addition of GST-ExoS to the wells would affect the outcome of the assay.

The addition of a blocking step decreased the overall response of 14-3-3 ζ binding; suggesting that the blocking step may be preventing non-specific protein binding to the surface of the wells. Non-specific 14-3-3 ζ binding to the wells could lead to a false positive reading and a subsequent false negative result. This step was therefore not omitted from the final assay model. An example of the effect of blocking on the assay is shown in Figure 5.10.

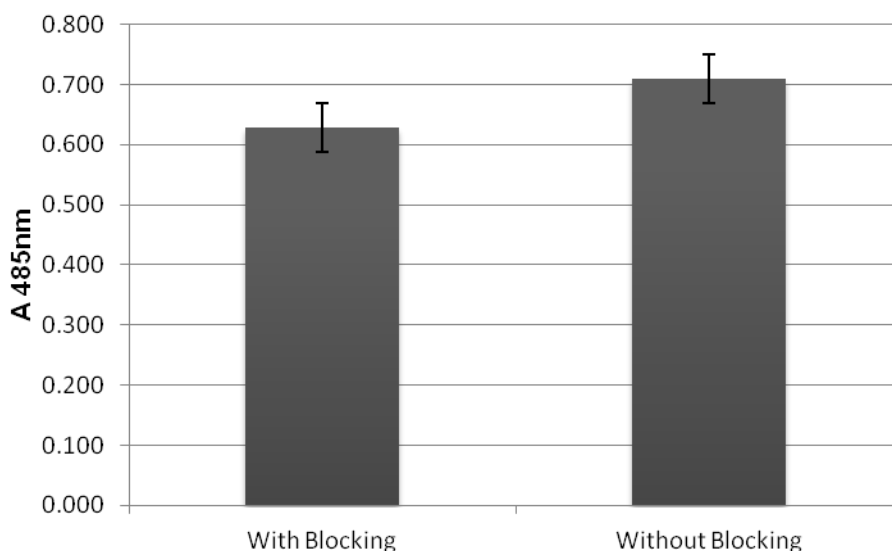


Figure 5.10: Effect of Blocking Conditions on Assay

Identical samples were tested with the only difference being that an additional blocking step following primary protein incubation was introduced to one sample. The chart shows that by introducing a blocking step, the absorbance value detected decreases.

The optimal time to measure absorbance readings was investigated. From testing the 4-CN reagent by Western Blotting, it was clear that the reagent may take some time to produce a visible end product, therefore an assay was set up where the absorbance was measured every 5 min over a 30 min period. To ensure that the highest level of absorbance was not specific to a single condition, a number of different conditions, including appropriate controls, were tested to ensure that the optimal 5 min period correlated across a range of conditions. A chart of the absorbance over time is shown in Figure 5.11 and the different conditions tested are detailed in Table 5.3.

It is very clear from the chart that in all cases, the highest absorbance readings are measured 5 min after addition of the 4-CN reagent. There is no difference between different assay conditions, indicating that for detection in a 96-well plate, the 4-CN reagent is most active within the first 5 min. Conducting this assay has also been very useful in determining background absorbance levels. For the purposes of subtracting background absorbance levels, readings obtained from the 5 min time period have been used. The results from the conditions tested have been normalised

against the reading obtained for the blank well, as this is the condition which has only tested the absorbance of the 4-CN reagent. The normalised absorbance values are charted in Figure 5.12.

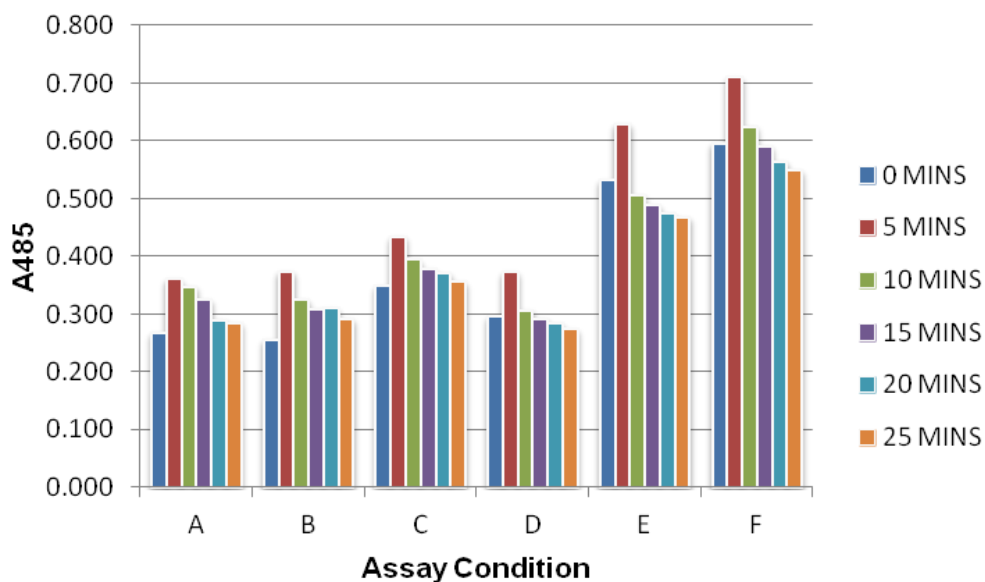


Figure 5.11: Graph of Absorbance Readings over Time

The absorbance of 4-CN signal with time. Readings were taken every 5 min to determine the optimum time after addition of 4-CN to measure absorbance.

Table 5.3: Assay Conditions Tested

A	Blank Well (no protein)
B	No protein plus blocking step
C	Blank well, blocked plus 14-3-3 ζ
D	Blank well plus 14-3-3 ζ
E	GST-ExoS, blocked plus 14-3-3 ζ
F	GST-ExoS plus 14-3-3 ζ

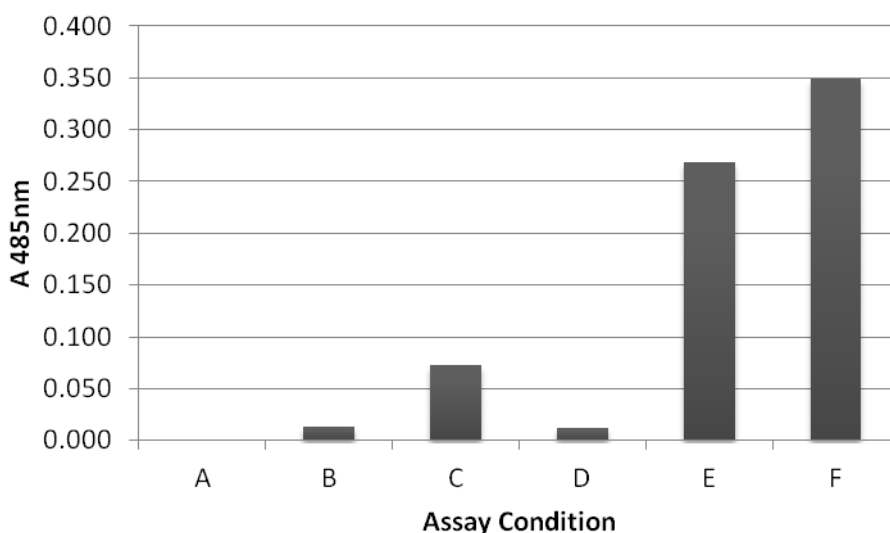


Figure 5.12: Normalised Assay Absorbance Values

The assay conditions, with appropriate controls, were normalised against the value obtained for the completely blank well which is equivalent to the absorbance of the 4-CN reagent. Assay conditions correlate with those detailed in Table 5.3.

It is clear that the control assay wells, i.e. those testing the absorbance of 14-3-3 ζ binding to ExoS, produce the greatest difference in absorbance compared with the control wells to test the absorbance when 14-3-3 ζ and ExoS cannot interact. By identifying the absorbance of the 4-CN reagent alone, it is clear to see that should a compound successfully inhibit the interaction between 14-3-3 ζ and ExoS, the difference in absorbance will be sufficient to give a clear result.

In conclusion, the optimisation of the ELISA assay has proved to be successful with a number of caveats identified and corrected to ensure that compound testing can be conducted efficiently. Full details of the final assay method are given in section 2.3.11 of Materials and Methods. The following section details the outcome of the compounds tested and their ability to prevent interaction between 14-3-3 ζ and ExoS.

5.3.4. Testing Compounds to Block 14-3-3ζ Interaction

Following successful optimisation of the assay conditions for testing the potential inhibiting compounds, the next stage was to test compound effectiveness. The concentrations tested were based on the solubility of the compounds. To test the potential inhibitory effect of the compounds, they were pre-incubated with 14-3-3ζ prior to addition of the solution to the wells containing GST-ExoS immobilised to the surface of the glutathione coated well. Following incubation, the 14-3-3ζ: test compound solution was removed from the wells and the assay completed. Following addition of the 4-CN reagent, the absorbance was compared to the control readings. Once again, a positive result, i.e. a high absorbance, indicated that the compound had been unsuccessful at inhibiting the interaction between 14-3-3ζ and ExoS and a negative result, i.e. a low absorbance, indicated that the compound had successfully inhibited the interaction between 14-3-3ζ and ExoS. In all cases, antibodies used for detection were specific for 14-3-3 protein.

Details of the concentrations and outcomes of the compounds tested are detailed as follows.

5.3.4.1. Maltotetraose

Maltotetraose is soluble in dH₂O up to 50 mg/ml. This is equivalent to a concentration of 75 mM. The ratio of the solution containing the compound to the solution of 14-3-3ζ was 1:1; therefore the highest concentration which could be tested was 37.5 mM. Based on this, a series of concentrations were tested, ranging from 1 mM to 37.5 mM.

To test the different concentrations, assays were set up in triplicate in order to obtain average readings. The compound was pre-incubated with 14-3-3ζ for 20 minutes before adding to the Exo-S coated wells. Following completion of the assay, absorbance readings were measured at 485 nm and normalised against the background reading. A graph of the normalised absorbances is shown in Figure 5.13.

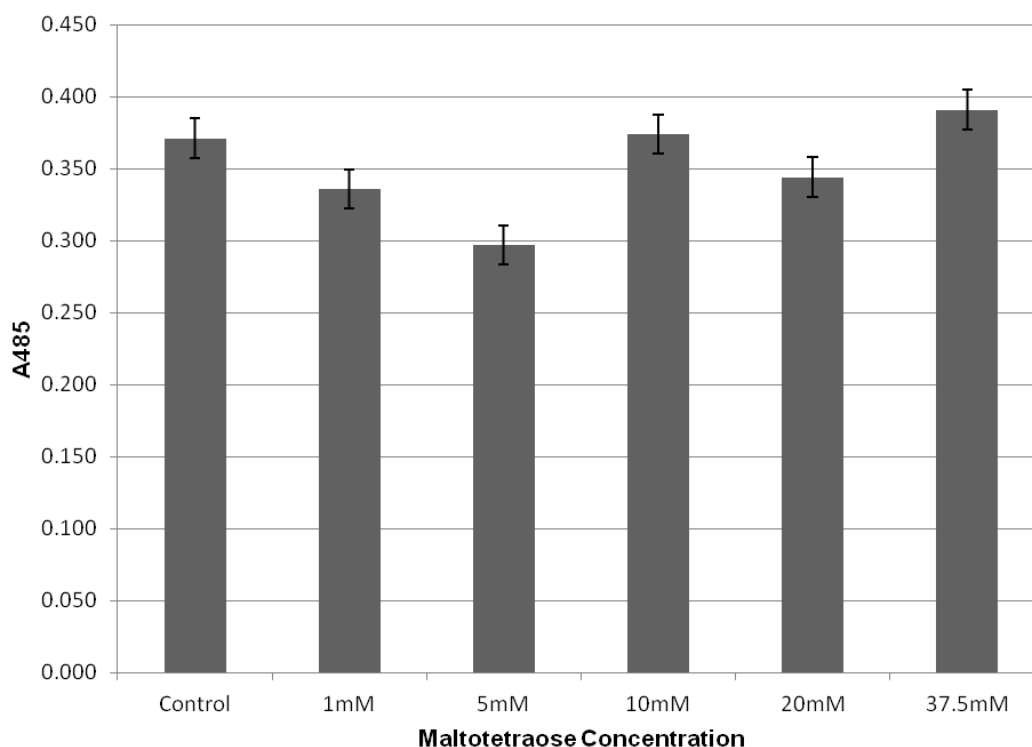


Figure 5.13: Absorbance of Maltotetraose Concentrations Tested

Varying concentrations of maltotetraose were tested for their ability to inhibit 14-3-3 ζ interaction with Exo-S. Conditions were tested in triplicate and the absorbance readings averaged. The background reading was subtracted from each condition to normalise all results against the baseline. The control reading represents the absorbance from an assay where no compound was tested.

Unfortunately, the results of the maltotetraose assay are not promising, as most of the conditions tested produce absorbance readings similar to that of the control. As the control data is representative of an assay where no compound was tested, the results here suggest that maltotetraose does not possess the ability to inhibit the interaction of 14-3-3 ζ . The only indication that maltotetraose, or another similarly structured compound, may have some affinity for the 14-3-3 ζ binding site, is from the reading obtained for the 5 mM concentration tested. This concentration produced the lowest absorbance reading, indicating that the compound may be partially inhibiting the interaction of 14-3-3 ζ . Possibly by looking at other compounds which are of a similar stereochemistry, a more suitable inhibitor could be identified.

5.3.4.2. DIPSO

The solubility of DIPSO is 100 mM in dH₂O. Again, the ratio of 14-3-3 ζ to compound in solution was 1:1; therefore the highest concentration which could be tested for DIPSO was 50 mM. Based on this, a series of concentrations ranging from 1 mM to 50 mM were tested.

Again, conditions were tested in triplicate, in order to obtain average absorbance values. The absorbance values, normalised against the background reading, are shown in Figure 5.14.

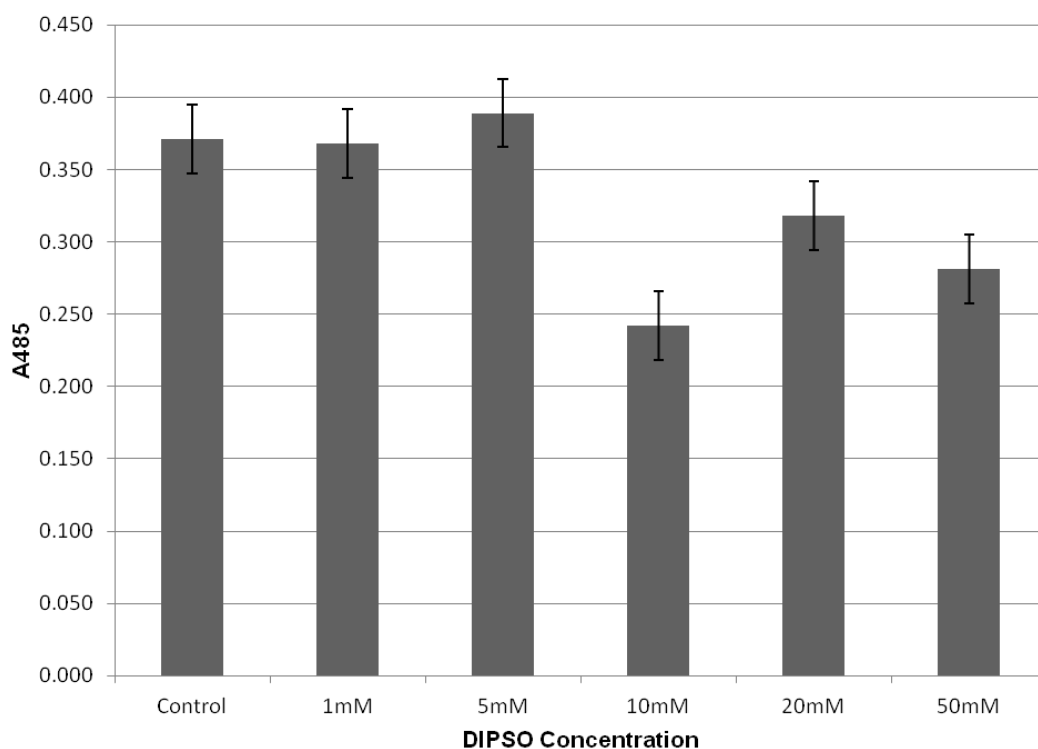


Figure 5.14: Absorbance of DIPSO Concentrations Tested

A range of DIPSO concentrations were tested for their ability to inhibit 14-3-3 ζ interaction with Exo-S. Conditions were tested in triplicate and absorbance readings averaged. Readings were normalised by subtraction of the background absorbance. The control reading represents the absorbance from an assay where no compound was tested.

The results of this assay do seem promising. Despite the lower concentrations tested having no impact on 14-3-3 ζ inhibition, there is a substantial reduction in absorbance with DIPSO concentrations of 10 mM and above. It may be the case that higher concentrations of this compound may confer even greater inhibition of 14-3-3 ζ interaction; however one problem with this is the unrealistic potential of developing a treatment at such a high concentration. Regardless, despite not completely inhibiting the interaction of 14-3-3 ζ , DIPSO does indicate the potential development of a similarly structured compound which may serve as an effective small molecule inhibitor.

In addition, further investigation into this compound may yet yield more promising results. Altering the assay conditions, such as examining a wider range of compound concentrations, increasing the incubation time or altering the temperature of incubation may all influence the effectiveness of the compound. At this stage, DIPSO should not be ruled out as a possible 14-3-3 ζ inhibitor and should be investigated further.

5.3.4.3. 6-Phosphogluconic Acid Trisodium Salt

For testing 6-phosphogluconic acid trisodium salt, a stock solution at a concentration of 10 mM in dH₂O was prepared. As the peptide solution is mixed with an equal volume of the 14-3-3 ζ solution, the maximum concentration tested was 5 mM. Based on this as the highest concentration which could be tested, a range of concentrations from 5 mM down to 0.1 mM were analysed.

Each concentration was tested three times and the results averaged. For each averaged reading, the background absorbance was subtracted. The results of the 6-phosphogluconic acid assay are presented in Figure 5.15.

The results of this assay are rather ambiguous. Whilst all of the concentrations tested result in a reduced absorbance reading in comparison to the control, the reduction in absorbance is minimal.

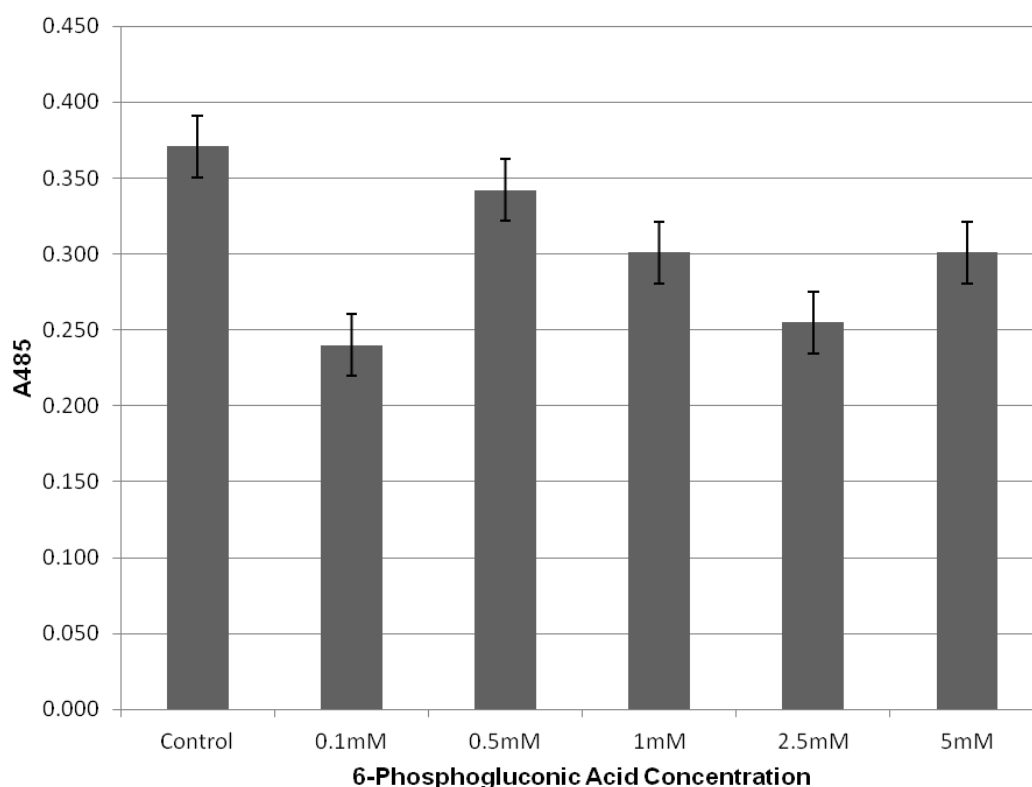


Figure 5.15: Absorbance of 6-Phosphogluconic Acid Concentrations Tested

A range of 6-phosphogluconic acid concentrations were tested for their ability to inhibit 14-3-3 ζ interaction with Exo-S. Conditions were tested in triplicate and absorbance readings averaged. Background absorbance readings were subtracted to normalise the results. The absorbance of the control reading represents an assay where no compound was tested.

The results of this assay are very interesting. Surprisingly, the lowest concentration tested, 0.1 mM, appears to convey the greatest inhibitory potential. There is clear evidence here that 6-phosphogluconic acid has the ability to inhibit 14-3-3 ζ interaction, although only partially. Once again, further investigation may optimise conditions which result in much greater inhibition of 14-3-3 ζ interaction. Alternatively, further investigation into similarly structured compounds may yield a more suitable candidate for therapeutic potential.

5.3.4.4. Adenosine 5'-DiPhosphate Sodium Salt Hydrate

The final compound which was investigated was adenosine 5'-diphosphate sodium salt hydrate (ADP). ADP is readily soluble in dH₂O, presenting minimal limitations with regard to the concentrations which could be tested. Concentrations tested were similar to those for the other compounds. For this reason, the concentrations of ADP investigated ranged from 1 mM to 50 mM. Once again, conditions were tested in triplicate and the readings averaged for analysis. The background absorbance was subtracted from each condition absorbance. The results of the ADP assay are shown in Figure 5.16.

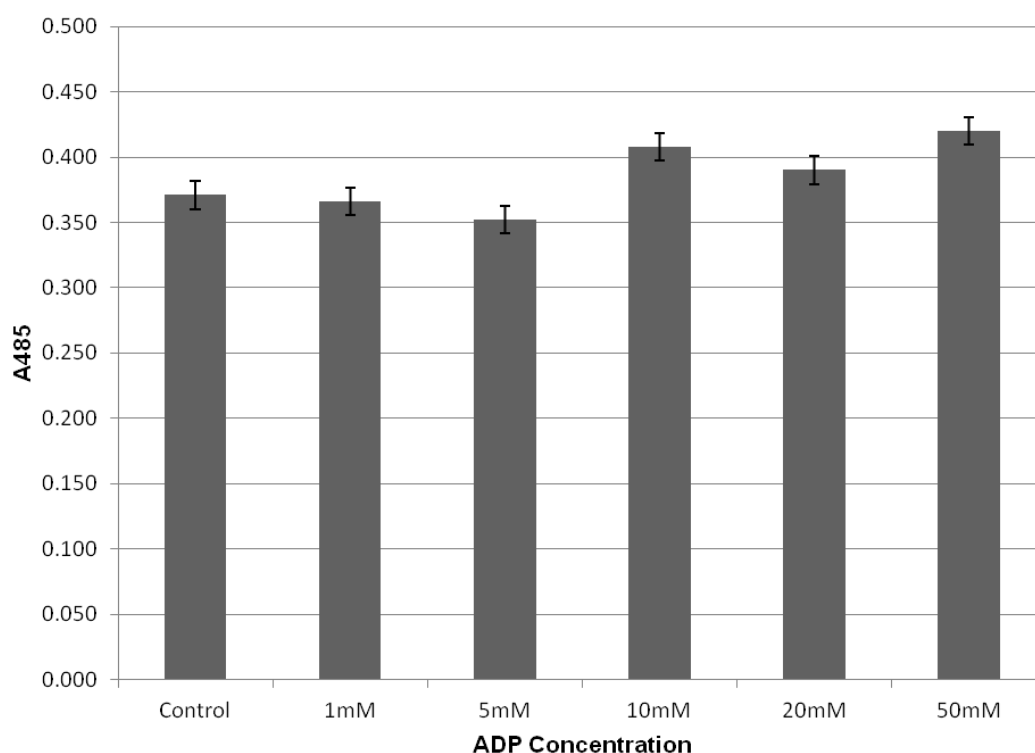


Figure 5.16: Absorbance of Adenosine 5'-Diphosphate Concentrations Tested

Varying concentrations of adenosine 5'-diphosphate sodium salt hydrate were tested against 14-3-3 ζ to inhibit interaction with Exo-S. Each condition was tested in triplicate and the absorbance readings were averaged. Background absorbance readings were subtracted to normalise the results. The absorbance of the control reading represents an assay where no compound was tested.

The results of the ADP assay are very disappointing. All of the conditions tested failed to even partially inhibit the interaction of 14-3-3 ζ with Exo-S. All of the average absorbance readings obtained for this compound are similar to the control data, which represents 14-3-3 ζ and Exo-S where no compound was tested. In fact, some of the absorbance readings for the conditions tested are actually higher than those of the control, clearly indicating that this compound has failed to convey any inhibitory action of 14-3-3 ζ .

5.4. Discussion

This small study into identifying potential inhibitors of 14-3-3 ζ has produced some mixed results. Whilst it is clear that none of the compounds tested to date exhibit complete inhibition of 14-3-3 ζ , there is evidence to suggest that further refinement of test conditions, or investigations into other, structurally similar compounds, may prove to be successful.

The results of the ADP assay show that this compound does not appear to have any inhibitory effect of 14-3-3 ζ and further analysis with this compound should be abandoned. The results of the maltotetraose assay are not promising either. Incubation with maltotetraose at 5 mM does appear to reduce the absorbance of the assay reading, however much greater investigation is required to determine whether this compound would have the therapeutic potential required from the compound being sought.

Conversely, the results from the DIPSO and 6-phosphogluconic acid trisodium salt assays show more potential. These compounds appear to have a partial inhibitory effect of 14-3-3 ζ and further investigation would be useful. One quality desired of a potential inhibitor is to partially inhibit the interaction of 14-3-3 ζ , so as to not adversely affect other cellular processes which the protein is involved in (see section 1.1.3.2 for more information). Failing this, these compounds indicate that structurally, they have the ability to affect the interaction of 14-3-3 ζ and investigations into alternative compounds which are similar in structure may prove to be therapeutically beneficial. Further analysis of the identified compounds listed in Table 7.1 may identify such a lead.

CHAPTER 6

GENERAL DISCUSSION

The main focus of the research conducted in this Ph.D. project was to investigate the protein complexes which are involved in the pathology of neurodegenerative diseases. Currently, the average age of the world population is rising and with it, the increase in occurrence of neurodegenerative disease. At present, the therapeutic treatments required for such diseases do not exist and with more people living longer, the impact this will have on healthcare is frightening. This project focussed on therapeutic targets which influence disease proteins; 14-3-3 proteins. As detailed in section 1.1.4, 14-3-3 proteins are involved in a number of neurodegenerative diseases, therefore making them a prime target for therapeutic potential.

The possibility of 14-3-3 as a therapeutic target was investigated in Chapter 5. Here, the interaction between 14-3-3 and the SCA1 disease protein, ataxin-1, provided the basis for therapeutic intervention. The interaction between 14-3-3 and ataxin-1 has been shown to be a key stage in disease pathology (see section 1.3.3), so the approach taken was to prevent this deleterious interaction from occurring, through the identification of small molecule inhibitors. By employing a number of computer modelling programs through collaboration with the Computational Biology Group based at Edinburgh University, greater than 60 potential compounds were identified. Means of testing these compounds were explored and eventually, the development of an ELISA assay method proved to be the optimal method of choice. The compounds which have been tested to date have produced mixed results, with some exhibiting no inhibitory action at all, whilst others have shown partial inhibition. Only a very small selection of the compounds identified were tested in this research project and further testing of the potential compounds (Table 7.1) may identify a prime therapeutic candidate. Should a therapeutic compound be discovered, the potential benefits would not be restricted to only SCA1 patients. The

interaction of 14-3-3 proteins with other neurodegenerative disease proteins is a key feature of many diseases and by targeting 14-3-3, and not one single specific disease protein, increases the potential number of patients which could benefit from a therapeutic treatment.

As the identification of small molecule inhibitors in this research was primarily based on finding a treatment for SCA1, the disease protein ataxin-1 was also studied. There were a number of research aspects which were planned to be investigated with ataxin-1; however one major problem encountered in this research was the expression of selected protein constructs. A number of constructs of ataxin-1 were created, with a view to attempt protein crystallography and elucidate structural information. All of the constructs cloned also contained the 14-3-3 binding site, to allow testing of any potential inhibiting compounds identified. However, despite creating constructs which would be expected to be conformationally stable, there was great difficulty in expression of the constructs, with a number of different expression conditions being tested, to no avail.

Another aspect of this research also focussed on the plasma membrane domains, lipid rafts. These regions of the plasma membrane are described as processing centres and a number of neurodegenerative disease proteins are processed here. It is at lipid rafts where abnormal processing occurs which leads to the formation of abnormally folded disease proteins, which then go on to aggregate and form toxic neuronal inclusions. Lipid rafts were also an area of interest following previous research conducted in this laboratory; 14-3-3 proteins had been found to associate with lipid rafts. Given the connection between 14-3-3 proteins and lipid rafts with neurodegenerative diseases, this was an obvious area to investigate. One point of particular interest was the presence of phosphorylated 14-3-3 proteins only in brain tissue. This suggests that the presence of phosphorylated 14-3-3 only in brain has a particular neuronal function, which may be implicated in neurodegenerative diseases. The first port of call was identifying whether these phospho-forms also associated with lipid rafts. Following extensive western blot analysis, the phospho-forms were identified as being raft associated and subsequent mass spectrometry

analysis confirmed that the levels of phosphorylated 14-3-3 are significantly lower than unphosphorylated 14-3-3 at rafts compared with the high levels of phosphorylated β and ζ 14-3-3 in brain. Since it has been established that phosphorylation at Ser185 can promote dissociation of interacting proteins, the next step was to investigate how the 14-3-3 proteins are associated with rafts and if phosphorylation has an impact on interacting proteins. This was not an easy question to answer, as 14-3-3 association with rafts revealed that these proteins are contained in the insoluble membrane, indicating that their interaction with a raft-bound protein is of high affinity. This fits with the established literature that only 14-3-3 that is not phosphorylated at Ser185 (nor indeed Ser/Thr233) interacts with its target proteins.

Another raft aspect that was investigated was the impact that the sphingolipid sphingosine has on 14-3-3 proteins. Lipid rafts are comprised of a variety of sphingolipids, which include sphingosine, and studies have revealed that 14-3-3 can be phosphorylated in the presence of sphingosine. The site of phosphorylation is a residue which is found in the dimer interface of 14-3-3 indicating that sphingosine elicits a conformational effect which allows a kinase access to phosphorylate. Mass spectrometry analysis of 14-3-3 kinase assays with sphingosine identified that, in the presence of sphingosine, 14-3-3 is phosphorylated. As sphingosine is found in lipid rafts, the quaternary structure of 14-3-3 at rafts was investigated through cross-linking analysis. This identified levels of monomeric 14-3-3 in rafts much higher than dimeric 14-3-3. This leads to the suggestion that sphingosine in lipid rafts disrupts the dimer conformation of 14-3-3, resulting in a 14-3-3 population at rafts which is mainly monomeric. This subsequently allows phosphorylation on Ser58 by Akt which could inhibit the re-association to dimeric 14-3-3. This would be a unique mode of regulation of 14-3-3 function.

Monomeric 14-3-3 is highly unstable and can aggregate. This may be extremely important with regard to neurodegenerative diseases. As disease proteins abnormally processed at rafts form aggregates; unstable, monomeric 14-3-3 which can also aggregate may contribute to the aggregate formation seen in these diseases.

This would definitely be one way of explaining the presence of 14-3-3 in the aggregates which are a characteristic of many neurodegenerative diseases.

Taken together, the research presented here has not only investigated pathological implications which may contribute to neurodegenerative disease, but also potential therapeutic agents. Further investigation may reveal a possible treatment for the increasing numbers of patients suffering from these debilitating diseases.

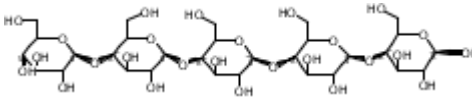
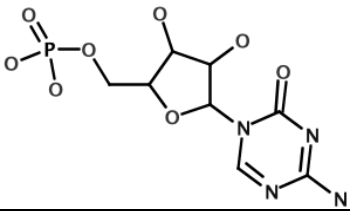
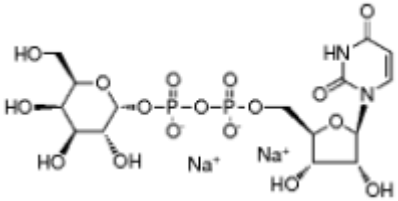
CHAPTER 7

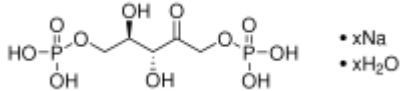
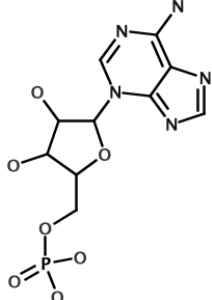
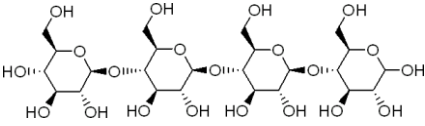
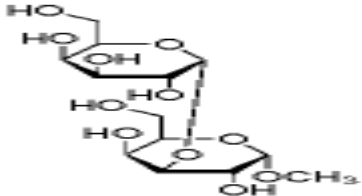
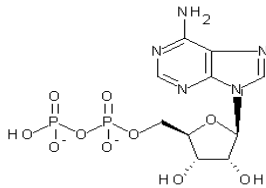
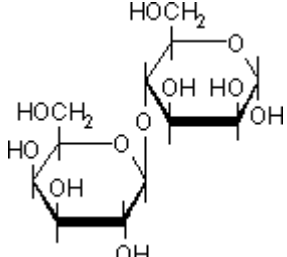
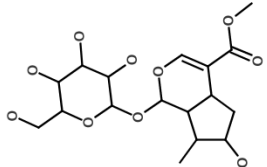
APPENDIX

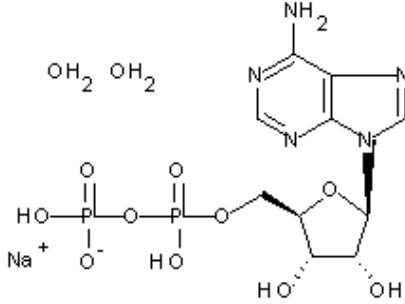
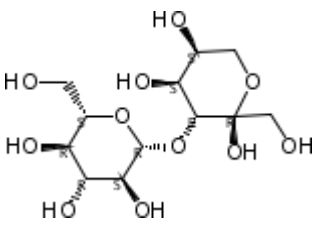
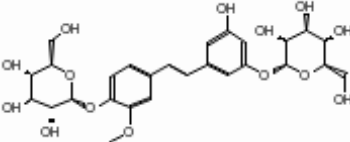
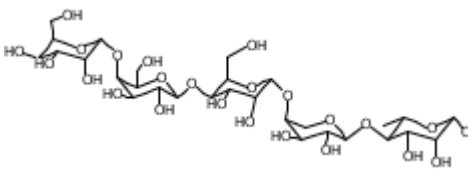
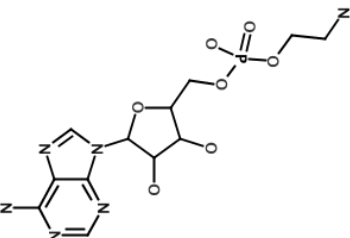
7.1. Compounds Identified for 14-3-3ζ Inhibition

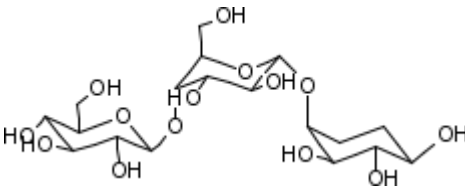
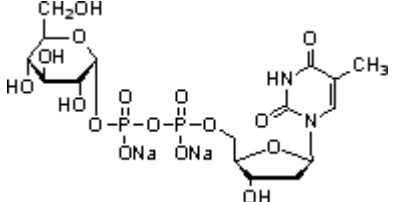
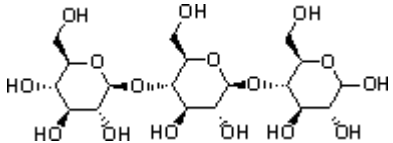
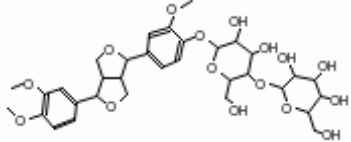
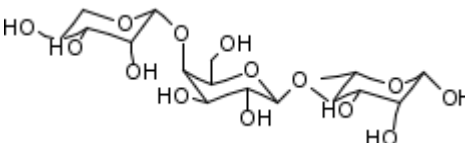
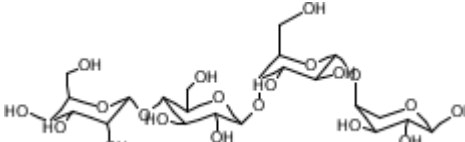
The following table contains the highest scoring, commercially available compounds which were identified from the LIDAEUS search to potentially inhibit the amphipathic binding groove of 14-3-3ζ.

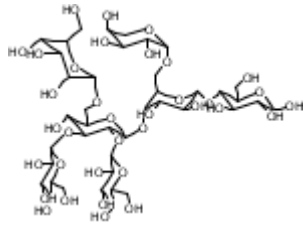
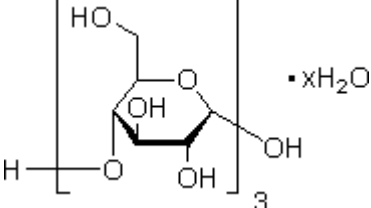
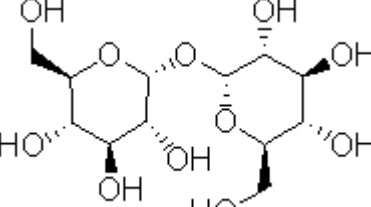
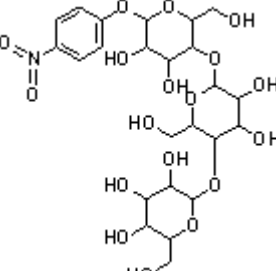
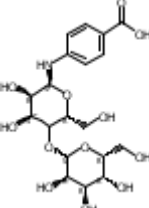
Table 7.1: Full List of Compounds Identified from LIDAEUS

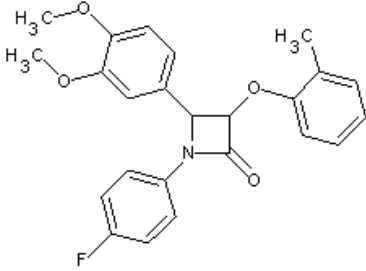
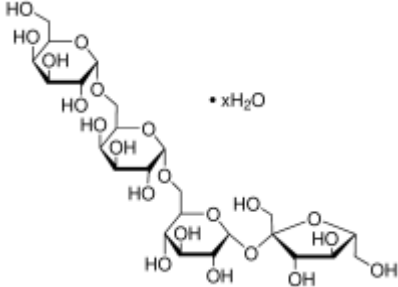
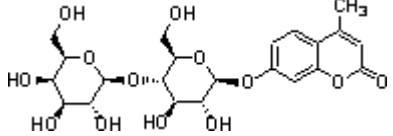
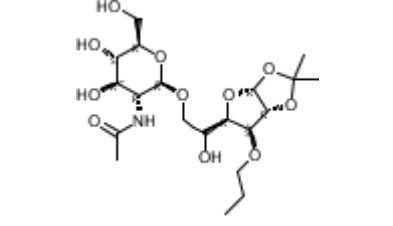
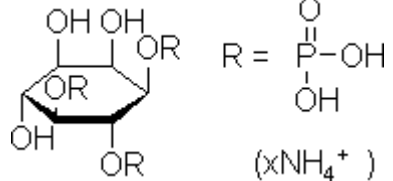
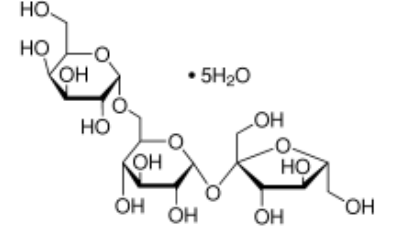
Compound Image	Compound Name	Supplier
	(3R,4R,5S,6R)-5- (((2S,3R,4R,5S,6R)-5- (((2S,3R,4R,5S,6R)-5- (((2S,3R,4R,5S,6R)-3,4- dihydroxy-6-(hydroxymethyl)- 5-(((2S,3R,4S,5S,6R)-3,4,5- trihydroxy-6- (hydroxymethyl)tetrahydro-2H- pyran-2-yl)oxy)tetrahydro-2H- pyran-2-yl)oxy)-3,4-dihydroxy- 6-(hydroxymethyl)tetrahydro- 2H-pyran-2-yl)oxy)-3,4- dihydroxy-6- (hydroxymethyl)tetrahydro-2H- pyran-2-yl)oxy)-6- (hydroxymethyl)tetrahydro-2H- pyran-2,3,4-triol	InterBioScreen
	1,3,5-Triazin-4-one, 4,5- dihydro-2-amino-5-beta-D- arabinofuranosyl-, 5'- monophosphate ester, monolithium salt	National Cancer Institute
	Uridine-5'-diphosphoglucose, disodium salt	Sigma-Aldrich

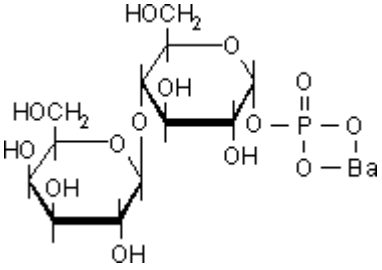
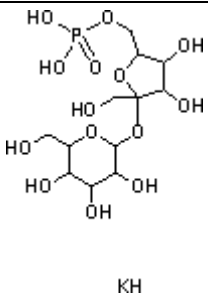
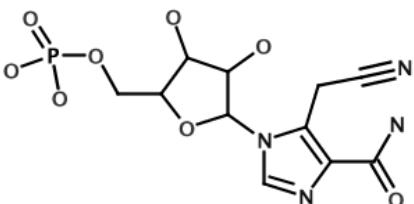
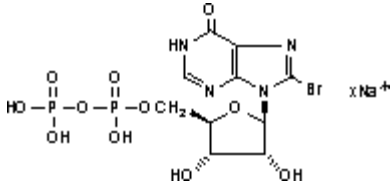
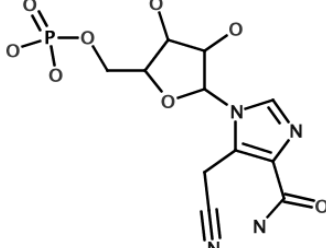
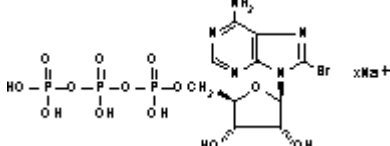
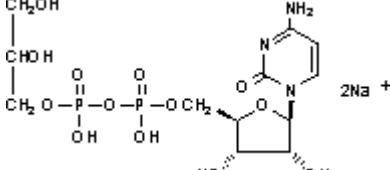
Compound Image	Compound Name	Supplier
	D-Ribulose 1,5-bisphosphate sodium salt hydrate	Sigma-Aldrich
	C ₁₀ H ₁₄ N ₅ O ₇ P ₂ Li	National Cancer Institute
	Cellotetraose	Sigma-Aldrich
	Methyl 3-O-β-D-galactopyranosyl-β-D-galactopyranoside	Sigma-Aldrich
	Adenosine-5'-diphosphate, disodium salt hydrate	TimTec
	4-O-β-Galactopyranosyl-D-mannopyranose	Sigma-Aldrich
	Loganin/Loganoside C ₁₇ H ₂₆ O ₁₀	National Cancer Institute

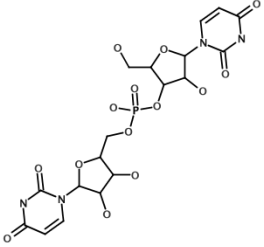
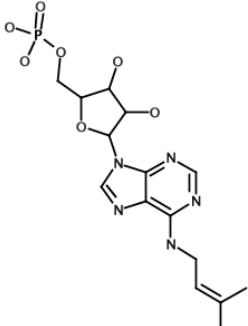
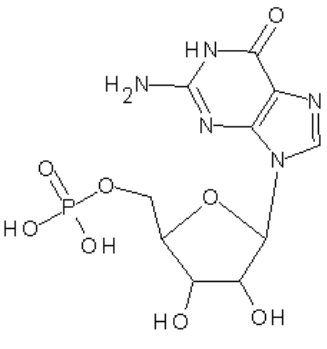
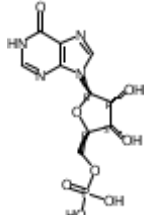
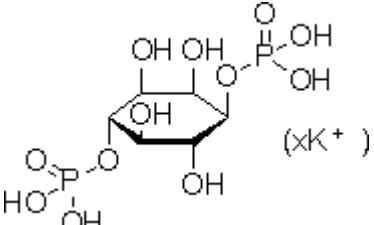
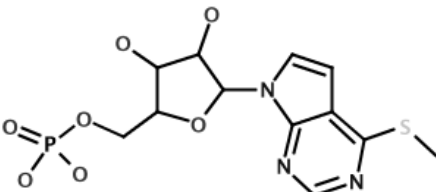
Compound Image	Compound Name	Supplier
	Adenosine 5'-diphosphate, monosodium salt dihydrate	TimTec
	(2S,3S,4R,5R)-2-(hydroxymethyl)-3-(((2S,3R,4S,5S,6R)-3,4,5-trihydroxy-6-(hydroxymethyl)tetrahydro-2H-pyran-2-yl)oxy)tetrahydro-2H-pyran-2,4,5-triol	InterBioScreen
	NP-002944	AnalytiCon
	(2S,3R,4S,5R,6S)-5-(((2S,3R,4R,5S)-5-(((2S,3R,4S,5R,6R)-5-(((2S,3R,4R,5R,6R)-3,4-dihydroxy-6-(hydroxymethyl)-5-(((2R,3R,4R,5R,6R)-3,4,5-trihydroxy-6-(hydroxymethyl)tetrahydro-2H-pyran-2-yl)oxy)tetrahydro-2H-pyran-2-yl)oxy)-3,4-dihydroxy-6-(hydroxymethyl)tetrahydro-2H-pyran-2-yl)oxy)-3,4-dihydroxytetrahydro-2H-pyran-2-yl)oxy)-6-methyltetrahydro-2H-pyran-2,3,4-triol	InterBioScreen
	C12H19N6O7P	National Cancer Institute

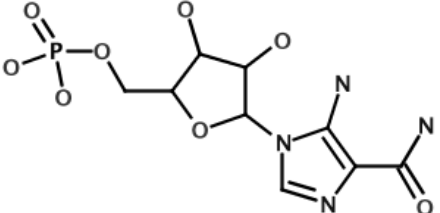
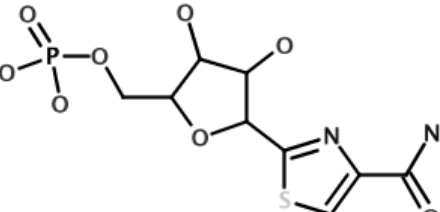
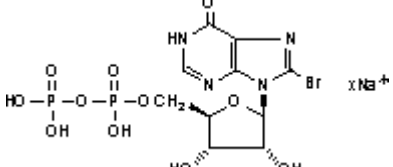
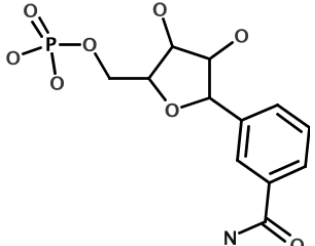
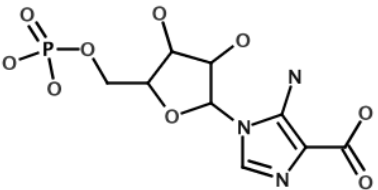
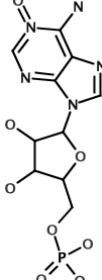
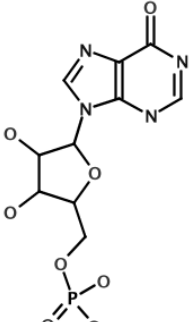
Compound Image	Compound Name	Supplier
	<p>(2S,3R,4S,5S,6R)-2-(((2R,3S,4S,5S,6S)-4,5-dihydroxy-2-(hydroxymethyl)-6-(((1S,2R,3S,4R)-2,3,4-trihydroxycyclohexyl)oxy)tetrahydro-2H-pyran-3-yl)oxy)-6-(hydroxymethyl)tetrahydro-2H-pyran-3,4,5-triol</p>	InterBioScreen
	Thymidine-5'-diphospho- α -D-glucose disodium salt	Sigma-Aldrich
	D-(+)-Cellotriase	Sigma-Aldrich
	NP-007394	AnalytiCon
	<p>2S,3R,4S,5R,6S)-5-(((2S,3R,4R,5R,6R)-3,4-dihydroxy-6-(hydroxymethyl)-5-(((2R,3R,4R,5S)-3,4,5-trihydroxytetrahydro-2H-pyran-2-yl)oxy)tetrahydro-2H-pyran-2-yl)oxy)-6-methyltetrahydro-2H-pyran-2,3,4-triol</p>	InterBioScreen
	<p>(2R,3R,4R,5S)-5-(((2S,3S,4S,5S,6R)-5-(((2S,3R,4R,5S,6R)-3,4-dihydroxy-6-(hydroxymethyl)-5-(((2R,3R,4R,5R,6R)-3,4,5-trihydroxy-6-(hydroxymethyl)tetrahydro-2H-pyran-2-yl)oxy)tetrahydro-2H-pyran-2-yl)oxy)-3,4-dihydroxy-6-(hydroxymethyl)tetrahydro-2H-pyran-2-yl)oxy)tetrahydro-2H-pyran-2,3,4-triol</p>	InterBioScreen

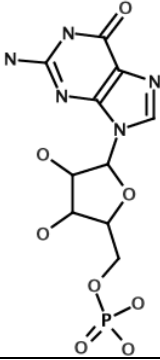
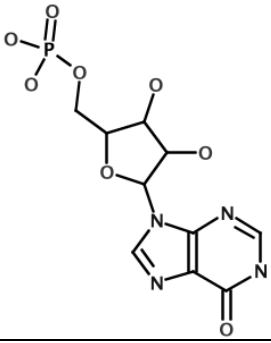
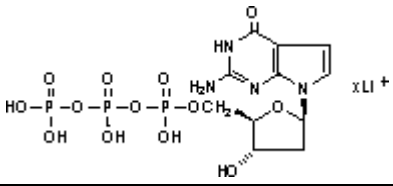
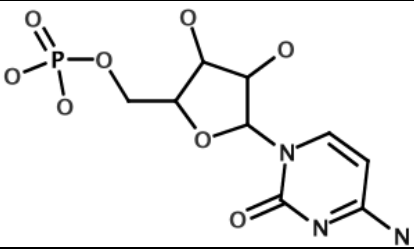
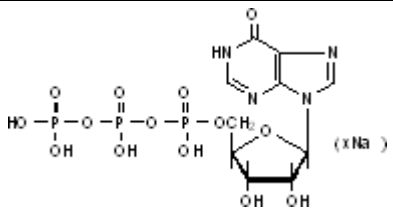
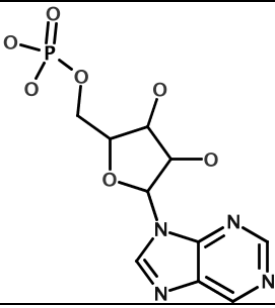
Compound Image	Compound Name	Supplier
	<p>(2R,2'R,3S,3'S,4S,4'S,5R,5'R,6S,6'S)-6,6'-(((2S,3R,4S,5R,6R)-2-(((2R,3S,4S,5S,6R)-4,5-dihydroxy-6-(((2R,3S,4R,5R,6R)-4,5,6-trihydroxy-2-(hydroxymethyl)tetrahydro-2H-pyran-3-yl)oxy)-2-(((2R,3R,4S,5S)-3,4,5-trihydroxytetrahydro-2H-pyran-2-yl)oxy)methyl)tetrahydro-2H-pyran-3-yl)oxy)-5-hydroxy-6-(((2S,3R,4R,5S,6R)-3,4,5-trihydroxy-6-(hydroxymethyl)tetrahydro-2H-pyran-2-yl)oxy)methyl)tetrahydro-2H-pyran-3,4-diyl)bis(oxy))bis(2-(hydroxymethyl)tetrahydro-2H-pyran-3,4,5-triol)</p>	InterBioScreen
	Maltotriose hydrate	Sigma-Aldrich
	D(+)-Trehalose	Sigma-Aldrich
	4-Nitrophenyl β -D-cellobioside	Sigma-Aldrich
	4-(((2S,3R,4S,5R,6R)-3,4-dihydroxy-6-(hydroxymethyl)-5-(((2S,3R,4R,5R,6R)-3,4,5-trihydroxy-6-(hydroxymethyl)tetrahydro-2H-pyran-2-yl)oxy)tetrahydro-2H-pyran-2-yl)amino)benzoic acid	InterBioScreen

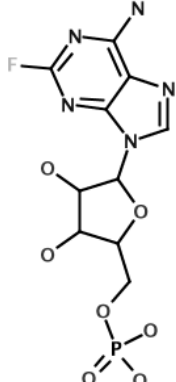
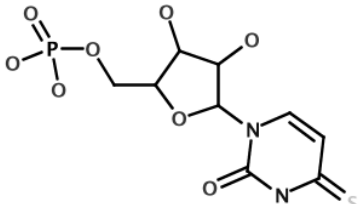
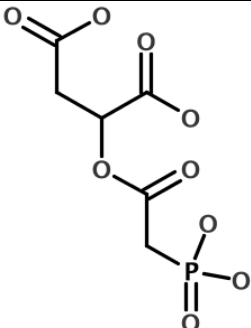
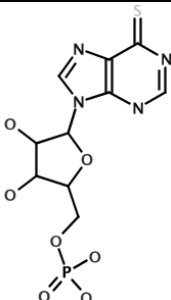
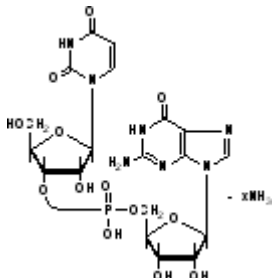
Compound Image	Compound Name	Supplier
	4-(3,4-dimethoxyphenyl)-1-(4-fluorophenyl)-3-(2-methyl	TimTec
	Stachyose hydrate from Stachys tubrifera	Sigma-Aldrich
	4-Methylumbelliferyl β -D-lactopyranoside	Sigma-Aldrich
	N-((2R,3R,4R,5S,6R)-2-(((3aR,5R,6S,6aR)-2,2-dimethyl-6-propoxytetrahydrofuro[2,3-d][1,3]dioxol-5-yl)-2-hydroxyethoxy)-4,5-dihydroxy-6-(hydroxymethyl)tetrahydro-2H-pyran-3-yl)acetamide	InterBioScreen
	D-myo-Inositol 1,5,6-trisphosphate ammonium salt	Sigma-Aldrich
	D-(+)-Raffinose pentahydrate	Sigma-Aldrich

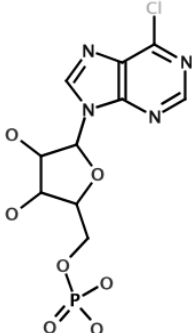
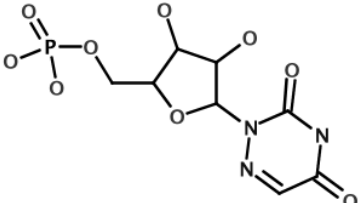
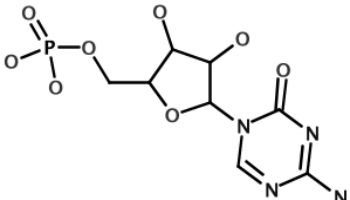
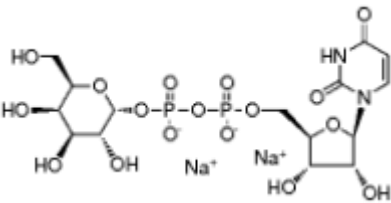
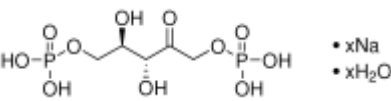
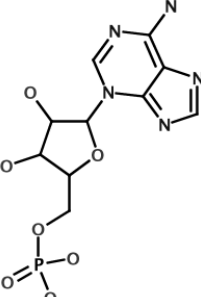
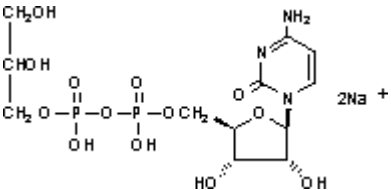
Compound Image	Compound Name	Supplier
	<p>α-Lactose 1-phosphate barium salt</p>	<p>Sigma-Aldrich</p>
 <p style="text-align: center;">KH</p>	<p>Sucrose 6'-monophosphate dipotassium salt</p>	<p>Sigma-Aldrich</p>
	<p>C₁₁H₁₅N₄O₈P</p>	<p>National Cancer Institute</p>
	<p>8-Bromoinosine 5'- diphosphate sodium salt</p>	<p>Sigma-Aldrich</p>
	<p>C₁₁H₁₅N₄O₈P</p>	<p>National Cancer Institute</p>
	<p>8-Bromoadenosine 5'- triphosphate sodium salt</p>	<p>Sigma-Aldrich</p>
	<p>Cytidine 5'- diphosphoglycerol disodium salt</p>	<p>Sigma-Aldrich</p>

Compound Image	Compound Name	Supplier
	<p>Uricase from <i>Candida</i> sp. - recombinant, expressed in <i>Escherichia coli</i>, lyophilized powder, ≥ 2 units/mg solid</p>	<p>Sigma-Aldrich</p>
	<p>C15H22N5O7P</p>	<p>National Cancer Institute</p>
	<p>5-(2-amino-6-oxohydropurin-9-yl)-3,4-dihydroxyoxolan-2</p>	<p>TimTec</p>
	<p>((2R,3S,4R,5R)-3,4-dihydroxy-5-(6-oxo-1H-purin-9(6H)-yl)tetrahydrofuran-2-yl)methyl dihydrogen phosphate</p>	<p>InterBioScreen</p>
	<p>D-myo-Inositol 1,4-bisphosphate potassium salt - from bovine brain, $\geq 98\%$ (TLC)</p>	<p>Sigma-Aldrich</p>
	<p>7H-Pyrrolo[2,3-d]pyrimidine, 4-(methylthio)-7-(5-O-phosphono-.beta.-D-ribofuranosyl)-</p>	<p>National Cancer Institute</p>

Compound Image	Compound Name	Supplier
	5-Amino-4-imidazolecarboxamide ribotide	National Cancer Institute
	4-Thiazolecarboxamide, 2-(5-O-phosphono-.beta.-D-ribofuranosyl)-, monosodium salt	National Cancer Institute
	8-Bromoinosine 5'-diphosphate sodium salt	Sigma-Aldrich
	Benzamide riboside monophosphate	National Cancer Institute
	C ₉ H ₁₄ N ₃ O ₉ P.3Na	National Cancer Institute
	5'-Adenylic acid, 1-oxide; Adenosine 1-oxide 5'-monophosphate	National Cancer Institute
	Disodium inosine 5'-monophosphate	National Cancer Institute

Compound Image	Compound Name	Supplier
	Sodium guanosine 5'-monophosphate	National Cancer Institute
	Polyinosinate:polycytidylate	National Cancer Institute
	7-Deaza-2'-deoxyguanosine 5'-triphosphate lithium salt - 10 mM in H ₂ O	Sigma-Aldrich
	5'-Cytidylic acid, disodium salt	National Cancer Institute
	Inosine 5'-triphosphate trisodium salt	Sigma-Aldrich
	C ₁₀ H ₁₃ N ₄ O ₇ P	National Cancer Institute

Compound Image	Compound Name	Supplier
	C ₁₀ H ₁₃ FN ₅ O ₇ P ₂ .2H ₃ N	National Cancer Institute
	C ₉ H ₁₃ N ₂ O ₈ P ₅ .2Na	National Cancer Institute
	C ₆ H ₉ O ₉ P ₄ .4Na	National Cancer Institute
	C ₁₀ H ₁₃ N ₄ O ₇ P ₅ .Ba	National Cancer Institute
	Uridylyl(3'→5')guanosine ammonium salt	Sigma-Aldrich

Compound Image	Compound Name	Supplier
	(C ₁₀ H ₁₂ ClN ₄ O ₇ P) _x	National Cancer Institute
	6-Azauridine 5'MP disodium salt	National Cancer Institute
	1,3,5-Triazin-4-one, 4,5-dihydro-2-amino- 5-.beta.-D-arabinofuranosyl-, 5'-monophosphate ester, monolithium salt	National Cancer Institute
	Uridine-5'-diphosphoglucose, disodium salt	Sigma-Aldrich
	D-Ribulose 1,5-bisphosphate sodium salt hydrate	Sigma-Aldrich
	C ₁₀ H ₁₄ N ₅ O ₇ P.2Li	National Cancer Institute
	Cytidine 5'-diphosphoglycerol disodium salt	Sigma-Aldrich

Reference List

- Adam, R. M., Mukhopadhyay, N. K., Kim, J., Di Vizio, D., Cinar, B., Boucher, K., Solomon, K. R. and Freeman, M. R. (2007). "Cholesterol Sensitivity of Endogenous and Myristoylated Akt." Cancer Research **67**(13): 6238-6246.
- Agarwal-Mawal, A., Qureshi, H. Y., Cafferty, P. W., Yuan, Z., Han, D., Lin, R. and Paudel, H. K. (2003). "14-3-3 Connects Glycogen Synthase Kinase-3beta to Tau within a Brain Microtubule-associated Tau Phosphorylation Complex." J. Biol. Chem. **278**(15): 12722-12728.
- Aitken, A. (2002). "Functional specificity in 14-3-3 isoform interactions through dimer formation and phosphorylation. Chromosome location of mammalian isoforms and variants." Plant Mol Biol **50**(6): 993-1010.
- Aitken, A. (2006). "14-3-3 proteins: a historic overview." Semin Cancer Biol **16**(3): 162-72.
- Aitken, A. (2011). "Post-translational modification of 14-3-3 isoforms and regulation of cellular function." Semin Cell Dev Biol **22**(7): 673-80.
- Aitken, A., Baxter, H., Dubois, T., Clokie, S., Mackie, S., Mitchell, K., Peden, A. and Zemlickova, E. (2002). "Specificity of 14-3-3 isoform dimer interactions and phosphorylation." Biochem Soc Trans **30**(4): 351-60.
- Aitken, A., Howell, S., Jones, D., Madrazo, J., Martin, H., Patel, Y. and Robinson, K. (1995a). "Post-translationally modified 14-3-3 isoforms and inhibition of protein kinase C." Mol Cell Biochem **149-150**: 41-9.
- Aitken, A., Howell, S., Jones, D., Madrazo, J. and Patel, Y. (1995b). "14-3-3 alpha and delta are the phosphorylated forms of raf-activating 14-3-3 beta and zeta. In vivo stoichiometric phosphorylation in brain at a Ser-Pro-Glu-Lys MOTIF." J Biol Chem **270**(11): 5706-9.
- Aitken, A. and Learmonth, M. (2002). "Protein identification by in-gel digestion and mass spectrometric analysis." Mol Biotechnol **20**(1): 95-7.
- Al-Ramahi, I., Lam, Y. C., Chen, H. K., de Gouyon, B., Zhang, M., Perez, A. M., Branco, J., de Haro, M., Patterson, C., Zoghbi, H. Y. and Botas, J. (2006). "CHIP protects from the neurotoxicity of expanded and wild-type ataxin-1 and promotes their ubiquitination and degradation." J Biol Chem **281**(36): 26714-24.
- Allen, J. A., Halverson-Tamboli, R. A. and Rasenick, M. M. (2007). "Lipid raft microdomains and neurotransmitter signalling." Nat Rev Neurosci **8**(2): 128-140.
- Alperovitch, A., Brown, P., Weber, T., Pocchiari, M., Hofman, A. and Will, R. (1994). "Incidence of Creutzfeldt-Jakob disease in Europe in 1993." Lancet **343**(8902): 918.
- Alzheimer, A. (1907). "Ueber eine eigenartige Erkrankung der Hirnrinde." Allg. Z. Psychiat. Med. **64**: 146-148.

- Alzheimer, A., Stelzmann, R. A., Schnitzlein, H. N. and Murtagh, F. R. (1995). "An English translation of Alzheimer's 1907 paper, "Uber eine eigenartige Erkrankung der Hirnrinde"." Clin Anat **8**(6): 429-31.
- Assossou, O., Besson, F., Rouault, J. P., Persat, F., Brisson, C., Duret, L., Ferrandiz, J., Mayencon, M., Peyron, F. and Picot, S. (2003). "Subcellular localization of 14-3-3 proteins in *Toxoplasma gondii* tachyzoites and evidence for a lipid raft-associated form." FEMS Microbiol Lett **224**(2): 161-8.
- Bachmann, M., Huber, J. L., Athwal, G. S., Wu, K., Ferl, R. J. and Huber, S. C. (1996). "14-3-3 proteins associate with the regulatory phosphorylation site of spinach leaf nitrate reductase in an isoform-specific manner and reduce dephosphorylation of Ser-543 by endogenous protein phosphatases." FEBS Letters **398**(1): 26-30.
- Banfi, S., Chung, M. Y., Kwiatkowski, T. J., Jr., Ranum, L. P., McCall, A. E., Chinault, A. C., Orr, H. T. and Zoghbi, H. Y. (1993). "Mapping and cloning of the critical region for the spinocerebellar ataxia type 1 gene (SCA1) in a yeast artificial chromosome contig spanning 1.2 Mb." Genomics **18**(3): 627-35.
- Banfi, S., Servadio, A., Chung, M. Y., Kwiatkowski, T. J., Jr., McCall, A. E., DuVick, L. A., Shen, Y., Roth, E. J., Orr, H. T. and Zoghbi, H. Y. (1994). "Identification and characterization of the gene causing type 1 spinocerebellar ataxia." Nat Genet **7**(4): 513-20.
- Baron, G. S., Wehrly, K., Dorward, D. W., Chesebro, B. and Caughey, B. (2002). "Conversion of raft associated prion protein to the protease-resistant state requires insertion of PrP-res (PrP(Sc)) into contiguous membranes." Embo J **21**(5): 1031-40.
- Bate, C., Salmona, M., Diomedea, L. and Williams, A. (2004). "Squalenstatin cures prion-infected neurons and protects against prion neurotoxicity." J Biol Chem **279**(15): 14983-90.
- Baxter, H. C., Liu, W. G., Forster, J. L., Aitken, A. and Fraser, J. R. (2002). "Immunolocalisation of 14-3-3 isoforms in normal and scrapie-infected murine brain." Neuroscience **109**(1): 5-14.
- Berg, D., Holzmann, C. and Riess, O. (2003). "14-3-3 proteins in the nervous system." Nat Rev Neurosci **4**(9): 752-62.
- Bickel, P. E., Scherer, P. E., Schnitzer, J. E., Oh, P., Lisanti, M. P. and Lodish, H. F. (1997). "Flotillin and epidermal surface antigen define a new family of caveolae-associated integral membrane proteins." J Biol Chem **272**(21): 13793-802.
- Blonder, J., Hale, M. L., Lucas, D. A., Schaefer, C. F., Yu, L. R., Conrads, T. P., Issaq, H. J., Stiles, B. G. and Veenstra, T. D. (2004). "Proteomic analysis of detergent-resistant membrane rafts." Electrophoresis **25**(9): 1307-18.
- Boston, P. F., Jackson, P. and Thompson, R. J. (1982). "Human 14-3-3 protein: radioimmunoassay, tissue distribution, and cerebrospinal fluid levels in patients with neurological disorders." J Neurochem **38**(5): 1475-82.

- Bowery, N. G. and Enna, S. J. (2000). "gamma-aminobutyric acid(B) receptors: first of the functional metabotropic heterodimers." J Pharmacol Exp Ther **292**(1): 2-7.
- Bowman, A. B., Lam, Y. C., Jafar-Nejad, P., Chen, H. K., Richman, R., Samaco, R. C., Fryer, J. D., Kahle, J. J., Orr, H. T. and Zoghbi, H. Y. (2007). "Duplication of Atxn1l suppresses SCA1 neuropathology by decreasing incorporation of polyglutamine-expanded ataxin-1 into native complexes." Nat Genet **39**(3): 373-9.
- Bradford, M. M. (1976). "A rapid and sensitive method for the quantitation of microgram quantities of protein utilizing the principle of protein-dye binding." Anal Biochem **72**: 248-54.
- Brechin, C. (2006). SNAREs, 14-3-3 proteins and cholesterol dependent membrane domains, University of Edinburgh. **Ph.D. Thesis**.
- Brown, D. A. and London, E. (1998). "Functions of lipid rafts in biological membranes." Annu Rev Cell Dev Biol **14**: 111-36.
- Brown, D. A. and Rose, J. K. (1992). "Sorting of GPI-anchored proteins to glycolipid-enriched membrane subdomains during transport to the apical cell surface." Cell **68**(3): 533-544.
- Brown, P., Gibbs, C. J., Jr., Rodgers-Johnson, P., Asher, D. M., Sulima, M. P., Bacote, A., Goldfarb, L. G. and Gajdusek, D. C. (1994). "Human spongiform encephalopathy: the National Institutes of Health series of 300 cases of experimentally transmitted disease." Ann Neurol **35**(5): 513-29.
- Bruijn, L. I., Becher, M. W., Lee, M. K., Anderson, K. L., Jenkins, N. A., Copeland, N. G., Sisodia, S. S., Rothstein, J. D., Borchelt, D. R., Price, D. L. and Cleveland, D. W. (1997). "ALS-linked SOD1 mutant G85R mediates damage to astrocytes and promotes rapidly progressive disease with SOD1-containing inclusions." Neuron **18**(2): 327-38.
- Celis, J. E., Gesser, B., Rasmussen, H. H., Madsen, P., Leffers, H., Dejgaard, K., Honore, B., Olsen, E., Ratz, G., Lauridsen, J. B. and et al. (1990). "Comprehensive two-dimensional gel protein databases offer a global approach to the analysis of human cells: the transformed amnion cells (AMA) master database and its link to genome DNA sequence data." Electrophoresis **11**(12): 989-1071.
- Cepeda, C., Starling, A. J., Wu, N., Nguyen, O. K., Uzgil, B., Soda, T., Andre, V. M., Ariano, M. A. and Levine, M. S. (2004). "Increased GABAergic function in mouse models of Huntington's disease: reversal by BDNF." J Neurosci Res **78**(6): 855-67.
- Chamberlain, L. H., Burgoyne, R. D. and Gould, G. W. (2001). "SNARE proteins are highly enriched in lipid rafts in PC12 cells: implications for the spatial control of exocytosis." Proc Natl Acad Sci U S A **98**(10): 5619-24.
- Chamberlain, L. H. and Gould, G. W. (2002). "The Vesicle- and Target-SNARE Proteins That Mediate Glut4 Vesicle Fusion Are Localized in Detergent-insoluble Lipid Rafts Present on Distinct Intracellular Membranes." Journal of Biological Chemistry **277**(51): 49750-49754.

- Chan, T. A., Hermeking, H., Lengauer, C., Kinzler, K. W. and Vogelstein, B. (1999). "14-3-3[σ] is required to prevent mitotic catastrophe after DNA damage." Nature **401**(6753): 616-620.
- Chatterjee, S. and Mayor, S. (2001). "The GPI-anchor and protein sorting." Cell Mol Life Sci **58**(14): 1969-87.
- Chaudhri, M., Scarabel, M. and Aitken, A. (2003). "Mammalian and yeast 14-3-3 isoforms form distinct patterns of dimers in vivo." Biochemical and Biophysical Research Communications **300**(3): 679-685.
- Chen, H. K., Fernandez-Funez, P., Acevedo, S. F., Lam, Y. C., Kaytor, M. D., Fernandez, M. H., Aitken, A., Skoulakis, E. M., Orr, H. T., Botas, J. and Zoghbi, H. Y. (2003). "Interaction of Akt-phosphorylated ataxin-1 with 14-3-3 mediates neurodegeneration in spinocerebellar ataxia type 1." Cell **113**(4): 457-68.
- Chen, Y. W., Allen, M. D., Veprintsev, D. B., Lowe, J. and Bycroft, M. (2004). "The structure of the AXH domain of spinocerebellar ataxin-1." J Biol Chem **279**(5): 3758-65.
- Choi, J. Y., Ryu, J. H., Kim, H. S., Park, S. G., Bae, K. H., Kang, S., Myung, P. K., Cho, S., Park, B. C. and Lee do, H. (2007). "Co-chaperone CHIP promotes aggregation of ataxin-1." Mol Cell Neurosci **34**(1): 69-79.
- Chow, C. W. and Davis, R. J. (2000). "Integration of calcium and cyclic AMP signaling pathways by 14-3-3." Mol Cell Biol **20**(2): 702-12.
- Chung, M. Y., Ranum, L. P., Duvick, L. A., Servadio, A., Zoghbi, H. Y. and Orr, H. T. (1993). "Evidence for a mechanism predisposing to intergenerational CAG repeat instability in spinocerebellar ataxia type I." Nat Genet **5**(3): 254-8.
- Cinek, T. and Horejsi, V. (1992). "The nature of large noncovalent complexes containing glycosyl-phosphatidylinositol-anchored membrane glycoproteins and protein tyrosine kinases." J Immunol **149**(7): 2262-70.
- Clokie, S. J., Cheung, K. Y., Mackie, S., Marquez, R., Peden, A. H. and Aitken, A. (2005). "BCR kinase phosphorylates 14-3-3 Tau on residue 233." Febs J **272**(15): 3767-76.
- Clokie, S. J. H. (2005). Protein kinases that phosphorylate 14-3-3 isoforms, University of Edinburgh. **Ph.D. Thesis**.
- Corcoran, L. J., Mitchison, T. J. and Liu, Q. (2004). "A novel action of histone deacetylase inhibitors in a protein aggregates disease model." Curr Biol **14**(6): 488-92.
- Couve, A., Kittler, J. T., Uren, J. M., Calver, A. R., Pangalos, M. N., Walsh, F. S. and Moss, S. J. (2001). "Association of GABA(B) receptors and members of the 14-3-3 family of signaling proteins." Mol Cell Neurosci **17**(2): 317-28.
- Craparo, A., Freund, R. and Gustafson, T. A. (1997). "14-3-3 (epsilon) interacts with the insulin-like growth factor I receptor and insulin receptor substrate I in a phosphoserine-dependent manner." J Biol Chem **272**(17): 11663-9.

- Cummings, C. J., Mancini, M. A., Antalffy, B., DeFranco, D. B., Orr, H. T. and Zoghbi, H. Y. (1998). "Chaperone suppression of aggregation and altered subcellular proteasome localization imply protein misfolding in SCA1." Nat Genet **19**(2): 148-54.
- Cvetanovic, M., Rooney, R. J., Garcia, J. J., Toporovskaya, N., Zoghbi, H. Y. and Opal, P. (2007). "The role of LANP and ataxin 1 in E4F-mediated transcriptional repression." EMBO Rep **8**(7): 671-7.
- Dalal, S. N., Yaffe, M. B. and DeCaprio, J. A. (2004). "14-3-3 Family Members Act Coordinately to Regulate Mitotic Progression." Cell Cycle **3**(5): 670-675.
- Davare, M. A., Saneyoshi, T., Guire, E. S., Nygaard, S. C. and Soderling, T. R. (2004). "Inhibition of calcium/calmodulin-dependent protein kinase kinase by protein 14-3-3." J Biol Chem **279**(50): 52191-9.
- Davidson, J. D., Riley, B., Burright, E. N., Duvick, L. A., Zoghbi, H. Y. and Orr, H. T. (2000). "Identification and characterization of an ataxin-1-interacting protein: A1Up, a ubiquitin-like nuclear protein." Hum Mol Genet **9**(15): 2305-12.
- Davies, A. F., Mirza, G., Sekhon, G., Turnpenny, P., Leroy, F., Speleman, F., Law, C., van Regemorter, N., Vamos, E., Flinter, F. and Ragoussis, J. (1999). "Delineation of two distinct 6p deletion syndromes." Hum Genet **104**(1): 64-72.
- Davy, A., Feuerstein, C. and Robbins, S. M. (2000). "Signaling within a caveolae-like membrane microdomain in human neuroblastoma cells in response to fibroblast growth factor." J Neurochem **74**(2): 676-83.
- de Chiara, C., Menon, R. P., Strom, M., Gibson, T. J. and Pastore, A. (2009). "Phosphorylation of S776 and 14-3-3 Binding Modulate Ataxin-1 Interaction with Splicing Factors." PLoS ONE **4**(12): e8372.
- Dick, F. D., De Palma, G., Ahmadi, A., Scott, N. W., Prescott, G. J., Bennett, J., Semple, S., Dick, S., Counsell, C., Mozzoni, P., Haites, N., Wettinger, S. B., Mutti, A., Otelea, M., Seaton, A., Soderkvist, P. and Felice, A. (2007). "Environmental risk factors for Parkinson's disease and parkinsonism: the Geoparkinson study." Occup Environ Med **64**(10): 666-72.
- Diviani, D., Abuin, L., Cotecchia, S. and Pansier, L. (2004). "Anchoring of both PKA and 14-3-3 inhibits the Rho-GEF activity of the AKAP-Lbc signaling complex." EMBO J **23**(14): 2811-2820.
- Dougherty, M. K. and Morrison, D. K. (2004). "Unlocking the code of 14-3-3." J Cell Sci **117**(Pt 10): 1875-84.
- Draberova, L. and Draber, P. (1993). "Thy-1 glycoprotein and src-like protein-tyrosine kinase p53/p56lyn are associated in large detergent-resistant complexes in rat basophilic leukemia cells." Proc Natl Acad Sci U S A **90**(8): 3611-5.
- Dubois, T., Rommel, C., Howell, S., Steinhussen, U., Soneji, Y., Morrice, N., Moelling, K. and Aitken, A. (1997). "14-3-3 is phosphorylated by casein kinase I on residue 233.

- Phosphorylation at this site in vivo regulates Raf/14-3-3 interaction." J Biol Chem **272**(46): 28882-8.
- Duyckaerts, C., Durr, A., Cancel, G. and Brice, A. (1999). "Nuclear inclusions in spinocerebellar ataxia type 1." Acta Neuropathol **97**(2): 201-7.
- Eddidin, M. (2003). "Lipids on the frontier: a century of cell-membrane bilayers." Nat Rev Mol Cell Biol **4**(5): 414-8.
- Ehehalt, R., Keller, P., Haass, C., Thiele, C. and Simons, K. (2003). "Amyloidogenic processing of the Alzheimer {beta}-amyloid precursor protein depends on lipid rafts." J. Cell Biol. **160**(1): 113-123.
- Emamian, E. S., Kaytor, M. D., Duvick, L. A., Zu, T., Tousey, S. K., Zoghbi, H. Y., Clark, H. B. and Orr, H. T. (2003). "Serine 776 of Ataxin-1 Is Critical for Polyglutamine-Induced Disease in SCA1 Transgenic Mice." Neuron **38**(3): 375-387.
- Fabelo, N., Martin, V., Santpere, G., Marin, R., Torrent, L., Ferrer, I. and Diaz, M. (2011). "Severe alterations in lipid composition of frontal cortex lipid rafts from Parkinson's disease and incidental Parkinson's disease." Mol Med **17**(9-10): 1107-18.
- Fallon, L., Moreau, F., Croft, B. G., Labib, N., Gu, W.-J. and Fon, E. A. (2002). "Parkin and CASK/LIN-2 Associate via a PDZ-mediated Interaction and Are Co-localized in Lipid Rafts and Postsynaptic Densities in Brain." Journal of Biological Chemistry **277**(1): 486-491.
- Fanger, G. R., Widmann, C., Porter, A. C., Sather, S., Johnson, G. L. and Vaillancourt, R. R. (1998). "14-3-3 Proteins Interact with Specific MEK Kinases." Journal of Biological Chemistry **273**(6): 3476-3483.
- Fantl, W. J., Muslin, A. J., Kikuchi, A., Martin, J. A., MacNicol, A. M., Grosst, R. W. and Williams, L. T. (1994). "Activation of Raf-1 by 14-3-3 proteins." Nature **371**(6498): 612-614.
- Feng, Y., Qi, W., Martinez, J. and Nelson, M. A. (2005). "The cyclin-dependent kinase 11 interacts with 14-3-3 proteins." Biochem Biophys Res Commun **331**(4): 1503-9.
- Fernandez-Funez, P., Nino-Rosales, M. L., de Gouyon, B., She, W. C., Luchak, J. M., Martinez, P., Turiegano, E., Benito, J., Capovilla, M., Skinner, P. J., McCall, A., Canal, I., Orr, H. T., Zoghbi, H. Y. and Botas, J. (2000). "Identification of genes that modify ataxin-1-induced neurodegeneration." Nature **408**(6808): 101-6.
- Fiedler, K., Kobayashi, T., Kurzchalia, T. V. and Simons, K. (1993). "Glycosphingolipid-enriched, detergent-insoluble complexes in protein sorting in epithelial cells." Biochemistry **32**(25): 6365-73.
- Field, K. A., Holowka, D. and Baird, B. (1995). "Fc epsilon RI-mediated recruitment of p53/56lyn to detergent-resistant membrane domains accompanies cellular signaling." Proc Natl Acad Sci U S A **92**(20): 9201-5.

- Field, K. A., Holowka, D. and Baird, B. (1997). "Compartmentalized activation of the high affinity immunoglobulin E receptor within membrane domains." J Biol Chem **272**(7): 4276-80.
- Filippov, A. K., Couve, A., Pangalos, M. N., Walsh, F. S., Brown, D. A. and Moss, S. J. (2000). "Heteromeric assembly of GABA(B)R1 and GABA(B)R2 receptor subunits inhibits Ca(2+) current in sympathetic neurons." J Neurosci **20**(8): 2867-74.
- Fischer, A., Baljuls, A., Reinders, J., Nekhoroshkova, E., Sibilski, C., Metz, R., Albert, S., Rajalingam, K., Hekman, M. and Rapp, U. R. (2009). "Regulation of RAF activity by 14-3-3 proteins: RAF kinases associate functionally with both homo- and heterodimeric forms of 14-3-3 proteins." J Biol Chem **284**(5): 3183-94.
- Fortin, D. L., Troyer, M. D., Nakamura, K., Kubo, S.-i., Anthony, M. D. and Edwards, R. H. (2004). "Lipid Rafts Mediate the Synaptic Localization of {alpha}-Synuclein." J Neurosci **24**(30): 6715-6723.
- Foster, L. J., De Hoog, C. L. and Mann, M. (2003). "Unbiased quantitative proteomics of lipid rafts reveals high specificity for signaling factors." Proc Natl Acad Sci U S A **100**(10): 5813-8.
- Freed, E., Symons, M., Macdonald, S. G., McCormick, F. and Ruggieri, R. (1994). "Binding of 14-3-3 proteins to the protein kinase Raf and effects on its activation." Science **265**(5179): 1713-1716.
- Fu, H., Coburn, J. and Collier, R. J. (1993). "The eukaryotic host factor that activates exoenzyme S of *Pseudomonas aeruginosa* is a member of the 14-3-3 protein family." Proceedings of the National Academy of Sciences **90**(6): 2320-2324.
- Fu, H., Xia, K., Pallas, D. C., Cui, C., Conroy, K., Narsimhan, R. P., Mamon, H., Collier, R. J. and Roberts, T. M. (1994). "Interaction of the protein kinase Raf-1 with 14-3-3 proteins." Science **266**(5182): 126-129.
- Fuller, B., Stevens, S. M., Jr., Sehnke, P. C. and Ferl, R. J. (2006). "Proteomic analysis of the 14-3-3 family in *Arabidopsis*." Proteomics **6**(10): 3050-9.
- Furukawa, Y., Ikuta, N., Omata, S., Yamauchi, T., Isobe, T. and Ichimura, T. (1993). "Demonstration of the phosphorylation-dependent interaction of tryptophan hydroxylase with the 14-3-3 protein." Biochem Biophys Res Commun **194**(1): 144-9.
- Galbiati, F., Volonte, D., Goltz, J. S., Steele, Z., Sen, J., Jurcsak, J., Stein, D., Stevens, L. and Lisanti, M. P. (1998). "Identification, sequence and developmental expression of invertebrate flotillins from *Drosophila melanogaster*." Gene **210**(2): 229-37.
- Gamerding, M., Kaya, A. M., Wolfrum, U., Clement, A. M. and Behl, C. (2011). "BAG3 mediates chaperone-based aggresome-targeting and selective autophagy of misfolded proteins." EMBO Rep **12**(2): 149-56.
- Ganguly, S., Weller, J. L., Ho, A., Chemineau, P., Malpoux, B. and Klein, D. C. (2005). "Melatonin synthesis: 14-3-3-dependent activation and inhibition of arylalkylamine

N-acetyltransferase mediated by phosphoserine-205." Proc Natl Acad Sci U S A **102**(4): 1222-7.

- Gardino, A. K., Smerdon, S. J. and Yaffe, M. B. (2006). "Structural determinants of 14-3-3 binding specificities and regulation of subcellular localization of 14-3-3 ligand complexes: a comparison of the X-ray crystal structures of all human 14-3-3 isoforms." Semin Cancer Biol **16**(3): 173-82.
- Garner, A. E., Smith, D. A. and Hooper, N. M. (2008). "Visualization of detergent solubilization of membranes: implications for the isolation of rafts." Biophys J **94**(4): 1326-40.
- Gatchel, J. R., Watase, K., Thaller, C., Carson, J. P., Jafar-Nejad, P., Shaw, C., Zu, T., Orr, H. T. and Zoghbi, H. Y. (2008). "The insulin-like growth factor pathway is altered in spinocerebellar ataxia type 1 and type 7." Proc Natl Acad Sci U S A **105**(4): 1291-6.
- Ge, F., Li, W.-L., Bi, L.-J., Tao, S.-C., Zhang, Z.-P. and Zhang, X.-E. (2010). "Identification of Novel 14-3-3 ζ Interacting Proteins by Quantitative Immunoprecipitation Combined with Knockdown (QUICK)." Journal of Proteome Research **9**(11): 5848-5858.
- Ge, W. W., Volkening, K., Leystra-Lantz, C., Jaffe, H. and Strong, M. J. (2007). "14-3-3 protein binds to the low molecular weight neurofilament (NFL) mRNA 3' UTR." Mol Cell Neurosci **34**(1): 80-7.
- Gil, C., Soler-Jover, A., Blasi, J. and Aguilera, J. (2005). "Synaptic proteins and SNARE complexes are localized in lipid rafts from rat brain synaptosomes." Biochemical and Biophysical Research Communications **329**(1): 117-124.
- Gkantiragas, I., Brugger, B., Stuken, E., Kaloyanova, D., Li, X.-Y., Lohr, K., Lottspeich, F., Wieland, F. T. and Helms, J. B. (2001). "Sphingomyelin-enriched Microdomains at the Golgi Complex." Mol. Biol. Cell **12**(6): 1819-1833.
- Glenner, G. G. and Wong, C. W. (1984). "Alzheimer's disease: Initial report of the purification and characterization of a novel cerebrovascular amyloid protein." Biochemical and Biophysical Research Communications **120**(3): 885-890.
- Goedert, M., Wischik, C. M., Crowther, R. A., Walker, J. E. and Klug, A. (1988). "Cloning and sequencing of the cDNA encoding a core protein of the paired helical filament of Alzheimer disease: identification as the microtubule-associated protein tau." Proceedings of the National Academy of Sciences **85**(11): 4051-4055.
- Golan, D. E., Tashjian, Armen H. Jr., Armstrong, Ehrin, J., Armstrong, April W. (2008). Principles of Pharmacology, Lippincott Williams & Wilkins.
- Goldfarb, L. G., Vasconcelos, O., Platonov, F. A., Lunkes, A., Kipnis, V., Kononova, S., Chabrashvili, T., Vladimirtsev, V. A., Alexeev, V. P. and Gajdusek, D. C. (1996). "Unstable triplet repeat and phenotypic variability of spinocerebellar ataxia type 1." Ann Neurol **39**(4): 500-6.

- Goold, R., Hubank, M., Hunt, A., Holton, J., Menon, R. P., Revesz, T., Pandolfo, M. and Matilla-Duenas, A. (2007). "Down-regulation of the dopamine receptor D2 in mice lacking ataxin 1." Hum Mol Genet **16**(17): 2122-34.
- Haller, P. D. v., Donohoe, S., Goodlett, D. R., Aebersold, R. and Watts, J. D. (2001). "Mass spectrometric characterization of proteins extracted from Jurkat T cell detergent-resistant membrane domains." PROTEOMICS **1**(8): 1010-1021.
- Hamaguchi, A., Suzuki, E., Murayama, K., Fujimura, T., Hikita, T., Iwabuchi, K., Handa, K., Withers, D. A., Masters, S. C., Fu, H. and Hakomori, S. (2003). "Sphingosine-dependent protein kinase-1, directed to 14-3-3, is identified as the kinase domain of protein kinase C delta." J Biol Chem **278**(42): 41557-65.
- Han, D., Ye, G., Liu, T., Chen, C., Yang, X., Wan, B., Pan, Y. and Yu, L. (2010). "Functional identification of a novel 14-3-3 epsilon splicing variant suggests dimerization is not necessary for 14-3-3 epsilon to inhibit UV-induced apoptosis." Biochem Biophys Res Commun **396**(2): 401-6.
- Hanahan, D. (1983). "Studies on transformation of Escherichia coli with plasmids." J Mol Biol **166**(4): 557-80.
- Hancock, J. F. (2006). "Lipid rafts: contentious only from simplistic standpoints." Nat Rev Mol Cell Biol **7**(6): 456-62.
- Harding, A. E. (1982). "The clinical features and classification of the late onset autosomal dominant cerebellar ataxias." Brain **105**(1): 1-28.
- Hardy, J. (1997). "Amyloid, the presenilins and Alzheimer's disease." Trends in Neurosciences **20**(4): 154-159.
- Hardy, J., Duff, K., Hardy, K. G., Perez-Tur, J. and Hutton, M. (1998). "Genetic dissection of Alzheimer's disease and related dementias: amyloid and its relationship to tau." Nat Neurosci **1**(5): 355-8.
- Harrington, M. G., Merrill, C. R., Asher, D. M. and Gajdusek, D. C. (1986). "Abnormal proteins in the cerebrospinal fluid of patients with Creutzfeldt-Jakob disease." N Engl J Med **315**(5): 279-83.
- Harris, T. J. and Siu, C. H. (2002). "Reciprocal raft-receptor interactions and the assembly of adhesion complexes." Bioessays **24**(11): 996-1003.
- Hashiguchi, M., Sobue, K. and Paudel, H. K. (2000). "14-3-3zeta is an effector of tau protein phosphorylation." J Biol Chem **275**(33): 25247-54.
- Hatano, T., Kubo, S., Imai, S., Maeda, M., Ishikawa, K., Mizuno, Y. and Hattori, N. (2007). "Leucine-rich repeat kinase 2 associates with lipid rafts." Hum Mol Genet **16**(6): 678-90.
- Hayashi, H., Igbavboa, U., Hamanaka, H., Kobayashi, M., Fujita, S. C., Wood, W. G. and Yanagisawa, K. (2002). "Cholesterol is increased in the exofacial leaflet of synaptic

- plasma membranes of human apolipoprotein E4 knock-in mice." Neuroreport **13**(4): 383-6.
- Heerklotz, H. (2002). "Triton promotes domain formation in lipid raft mixtures." Biophys J **83**(5): 2693-701.
- Henkin, J. A., Jennings, M. E., Matthews, D. E. and Vigoreaux, J. O. (2004). "Mass processing-an improved technique for protein identification with mass spectrometry data." J Biomol Tech **15**(4): 230-7.
- Henriksson, M. L., Francis, M. S., Peden, A., Aili, M., Stefansson, K., Palmer, R., Aitken, A. and Hallberg, B. (2002). "A nonphosphorylated 14-3-3 binding motif on exoenzyme S that is functional in vivo." Eur J Biochem **269**(20): 4921-9.
- Hermeking, H., Lengauer, C., Polyak, K., He, T. C., Zhang, L., Thiagalingam, S., Kinzler, K. W. and Vogelstein, B. (1997). "14-3-3 sigma is a p53-regulated inhibitor of G2/M progression." Mol Cell **1**(1): 3-11.
- Hinton, A. C. (2005). Database-Mining : EDULISS a descriptor based approach, University of Edinburgh. **Ph.D. Thesis**.
- Hoessli, D. and Rungger-Brandle, E. (1985). "Association of specific cell-surface glycoproteins with a triton X-100-resistant complex of plasma membrane proteins isolated from T-lymphoma cells (P1798)." Exp Cell Res **156**(1): 239-50.
- Honda, R., Ohba, Y. and Yasuda, H. (1997). "14-3-3 zeta Protein Binds to the Carboxyl Half of Mouse Wee1 Kinase." Biochemical and Biophysical Research Communications **230**(2): 262-265.
- Hong, S., Ka, S., Kim, S., Park, Y. and Kang, S. (2003). "p80 coilin, a coiled body-specific protein, interacts with ataxin-1, the SCA1 gene product." Biochimica et Biophysica Acta (BBA) - Molecular Basis of Disease **1638**(1): 35-42.
- Hong, S., Kim, S. J., Ka, S., Choi, I. and Kang, S. (2002). "USP7, a ubiquitin-specific protease, interacts with ataxin-1, the SCA1 gene product." Mol Cell Neurosci **20**(2): 298-306.
- Hsich, G., Kenney, K., Gibbs, C. J., Lee, K. H. and Harrington, M. G. (1996). "The 14-3-3 brain protein in cerebrospinal fluid as a marker for transmissible spongiform encephalopathies." N Engl J Med **335**(13): 924-30.
- Hsin, K.-Y., Morgan, H. P., Shave, S. R., Hinton, A. C., Taylor, P. and Walkinshaw, M. D. (2010). "EDULISS: a small-molecule database with data-mining and pharmacophore searching capabilities." Nucleic Acids Research.
- Huber, S. C., MacKintosh, C. and Kaiser, W. M. (2002). "Metabolic enzymes as targets for 14-3-3 proteins." Plant Mol Biol **50**(6): 1053-63.
- Huntington, G. (1872). "On chorea." Med. Surg. Reporter **26**: 317-321.
- Ichimura, T., Isobe, T., Okuyama, T., Takahashi, N., Araki, K., Kuwano, R. and Takahashi, Y. (1988). "Molecular cloning of cDNA coding for brain-specific 14-3-3 protein, a

protein kinase-dependent activator of tyrosine and tryptophan hydroxylases." Proc Natl Acad Sci U S A **85**(19): 7084-8.

- Ichimura, T., Isobe, T., Okuyama, T., Yamauchi, T. and Fujisawa, H. (1987). "Brain 14-3-3 protein is an activator protein that activates tryptophan 5-monoxygenase and tyrosine 3-monoxygenase in the presence of Ca²⁺, calmodulin-dependent protein kinase II." FEBS Lett **219**(1): 79-82.
- Igbavboa, U., Eckert, G. P., Malo, T. M., Studniski, A. E., Johnson, L. N., Yamamoto, N., Kobayashi, M., Fujita, S. C., Appel, T. R., Muller, W. E., Wood, W. G. and Yanagisawa, K. (2005). "Murine synaptosomal lipid raft protein and lipid composition are altered by expression of human apoE 3 and 4 and by increasing age." J Neurol Sci **229-230**: 225-32.
- Ironside, J. W., Sutherland, K., Bell, J. E., McCardle, L., Barrie, C., Estebeiro, K., Zeidler, M. and Will, R. G. (1996). "A new variant of Creutzfeldt-Jakob disease: neuropathological and clinical features." Cold Spring Harb Symp Quant Biol **61**: 523-30.
- Irwin, S., Vandelft, M., Pinchev, D., Howell, J. L., Graczyk, J., Orr, H. T. and Truant, R. (2005). "RNA association and nucleocytoplasmic shuttling by ataxin-1." J Cell Sci **118**(Pt 1): 233-42.
- Izaki, T., Kamakura, S., Kohjima, M. and Sumimoto, H. (2005). "Phosphorylation-dependent binding of 14-3-3 to Par3beta, a human Par3-related cell polarity protein." Biochemical and Biophysical Research Communications **329**(1): 211-218.
- Jafar-Nejad, P., Ward, C. S., Richman, R., Orr, H. T. and Zoghbi, H. Y. (2011). "Regional rescue of spinocerebellar ataxia type 1 phenotypes by 14-3-3epsilon haploinsufficiency in mice underscores complex pathogenicity in neurodegeneration." Proc Natl Acad Sci U S A **108**(5): 2142-7.
- Jagemann, L. R., Perez-Rivas, L. G., Ruiz, E. J., Ranea, J. A., Sanchez-Jimenez, F., Nebreda, A. R., Alba, E. and Lozano, J. (2008). "The functional interaction of 14-3-3 proteins with the ERK1/2 scaffold KSR1 occurs in an isoform-specific manner." J Biol Chem **283**(25): 17450-62.
- Jick, H., Zornberg, G. L., Jick, S. S., Seshadri, S. and Drachman, D. A. (2000). "Statins and the risk of dementia." Lancet **356**(9242): 1627-31.
- Jin, J., Smith, F. D., Stark, C., Wells, C. D., Fawcett, J. P., Kulkarni, S., Metalnikov, P., O'Donnell, P., Taylor, P., Taylor, L., Zougman, A., Woodgett, J. R., Langeberg, L. K., Scott, J. D. and Pawson, T. (2004). "Proteomic, functional, and domain-based analysis of in vivo 14-3-3 binding proteins involved in cytoskeletal regulation and cellular organization." Curr Biol **14**(16): 1436-50.
- Jodice, C., Malaspina, P., Persichetti, F., Novelletto, A., Spadaro, M., Giunti, P., Morocutti, C., Terrenato, L., Harding, A. E. and Frontali, M. (1994). "Effect of trinucleotide repeat length and parental sex on phenotypic variation in spinocerebellar ataxia I." Am J Hum Genet **54**(6): 959-65.

- Johnson, C., Crowther, S., Stafford, M. J., Campbell, D. G., Toth, R. and MacKintosh, C. (2010). "Bioinformatic and experimental survey of 14-3-3-binding sites." Biochem J **427**(1): 69-78.
- Johnson, R. T. and Gibbs, C. J., Jr. (1998). "Creutzfeldt-Jakob disease and related transmissible spongiform encephalopathies." N Engl J Med **339**(27): 1994-2004.
- Jones, D. H., Ley, S. and Aitken, A. (1995a). "Isoforms of 14-3-3 protein can form homo- and heterodimers in vivo and in vitro: implications for function as adapter proteins." FEBS Lett **368**(1): 55-8.
- Jones, D. H., Martin, H., Madrazo, J., Robinson, K. A., Nielsen, P., Roseboom, P. H., Patel, Y., Howell, S. A. and Aitken, A. (1995b). "Expression and structural analysis of 14-3-3 proteins." J Mol Biol **245**(4): 375-84.
- Jorgensen, N. D., Andresen, J. M., Lagalwar, S., Armstrong, B., Stevens, S., Byam, C. E., Duvick, L. A., Lai, S., Jafar-Nejad, P., Zoghbi, H. Y., Clark, H. B. and Orr, H. T. (2009). "Phosphorylation of ATXN1 at Ser776 in the cerebellum." J Neurochem **110**(2): 675-86.
- Kawamoto, Y., Akiguchi, I., Nakamura, S. and Budka, H. (2004). "14-3-3 proteins in Lewy body-like hyaline inclusions in patients with sporadic amyotrophic lateral sclerosis." Acta Neuropathol **108**(6): 531-7.
- Kawamoto, Y., Akiguchi, I., Nakamura, S., Honjyo, Y., Shibasaki, H. and Budka, H. (2002). "14-3-3 proteins in Lewy bodies in Parkinson disease and diffuse Lewy body disease brains." J Neuropathol Exp Neurol **61**(3): 245-53.
- Kazlauskaitė, J., Sanghera, N., Sylvester, I., Venien-Bryan, C. and Pinheiro, T. J. (2003). "Structural changes of the prion protein in lipid membranes leading to aggregation and fibrillization." Biochemistry **42**(11): 3295-304.
- Kenney, K., Brechtel, C., Takahashi, H., Kurohara, K., Anderson, P. and Gibbs, C. J., Jr. (2000). "An enzyme-linked immunosorbent assay to quantify 14-3-3 proteins in the cerebrospinal fluid of suspected Creutzfeldt-Jakob disease patients." Ann Neurol **48**(3): 395-8.
- Kim, Y., Kim, H., Jang, S. W. and Ko, J. (2011). "The role of 14-3-3beta in transcriptional activation of estrogen receptor alpha and its involvement in proliferation of breast cancer cells." Biochem Biophys Res Commun **414**(1): 199-204.
- King, J. and Laemmli, U. K. (1971). "Polypeptides of the tail fibres of bacteriophage T4." J Mol Biol **62**(3): 465-77.
- Klement, I. A., Skinner, P. J., Kaytor, M. D., Yi, H., Hersch, S. M., Clark, H. B., Zoghbi, H. Y. and Orr, H. T. (1998). "Ataxin-1 Nuclear Localization and Aggregation: Role in Polyglutamine-Induced Disease in SCA1 Transgenic Mice." Cell **95**(1): 41-53.
- Kligys, K., Yao, J., Yu, D. and Jones, J. C. R. (2009). "14-3-3zeta/ tau heterodimers regulate Slingshot activity in migrating keratinocytes." Biochemical and Biophysical Research Communications **383**(4): 450-454.

- Koga, Y. and Ikebe, M. (2008). "A novel regulatory mechanism of myosin light chain phosphorylation via binding of 14-3-3 to myosin phosphatase." Mol Biol Cell **19**(3): 1062-71.
- Kubo, S., Nemani, V. M., Chalkley, R. J., Anthony, M. D., Hattori, N., Mizuno, Y., Edwards, R. H. and Fortin, D. L. (2005). "A combinatorial code for the interaction of alpha-synuclein with membranes." J Biol Chem **280**(36): 31664-72.
- Lai, S., O'Callaghan, B., Zoghbi, H. Y. and Orr, H. T. (2011). "14-3-3 Binding to ataxin-1(ATXN1) regulates its dephosphorylation at Ser-776 and transport to the nucleus." J Biol Chem **286**(40): 34606-16.
- Lam, Y. C., Bowman, A. B., Jafar-Nejad, P., Lim, J., Richman, R., Fryer, J. D., Hyun, E. D., Duvick, L. A., Orr, H. T., Botas, J. and Zoghbi, H. Y. (2006). "ATAXIN-1 interacts with the repressor Capicua in its native complex to cause SCA1 neuropathology." Cell **127**(7): 1335-47.
- Lang, D. M., Lommel, S., Jung, M., Ankerhold, R., Petrausch, B., Laessing, U., Wiechers, M. F., Plattner, H. and Stuermer, C. A. (1998). "Identification of reggie-1 and reggie-2 as plasmamembrane-associated proteins which cocluster with activated GPI-anchored cell adhesion molecules in non-caveolar micropatches in neurons." J Neurobiol **37**(4): 502-23.
- Lasserre, R., Guo, X.-J., Conchonaud, F., Hamon, Y., Hawchar, O., Bernard, A.-M., Soudja, S. M. H., Lenne, P.-F., Rigneault, H., Olive, D., Bismuth, G., Nunes, J. A., Payrastre, B., Marguet, D. and He, H.-T. (2008). "Raft nanodomains contribute to Akt/PKB plasma membrane recruitment and activation." Nat Chem Biol **4**(9): 538-547.
- Layfield, R., Fergusson, J., Aitken, A., Lowe, J., Landon, M. and Mayer, R. J. (1996). "Neurofibrillary tangles of Alzheimer's disease brains contain 14-3-3 proteins." Neurosci Lett **209**(1): 57-60.
- Ledesma, M. D., Da Silva, J. S., Schevchenko, A., Wilm, M. and Dotti, C. G. (2003). "Proteomic characterisation of neuronal sphingolipid-cholesterol microdomains: role in plasminogen activation." Brain Res **987**(1): 107-16.
- Lee, S., Hong, S. and Kang, S. (2008). "The ubiquitin-conjugating enzyme UbcH6 regulates the transcriptional repression activity of the SCA1 gene product ataxin-1." Biochemical and Biophysical Research Communications **372**(4): 735-740.
- Lees, A. J., Hardy, J. and Revesz, T. (2009). "Parkinson's disease." Lancet **373**(9680): 2055-66.
- Li, G., Jiang, H., Chang, M., Xie, H. and Hu, L. (2011a). "HDAC6 alpha-tubulin deacetylase: A potential therapeutic target in neurodegenerative diseases." Journal of the Neurological Sciences **304**(1&2): 1-8.
- Li, X., Wang, Q. J., Pan, N., Lee, S., Zhao, Y., Chait, B. T. and Yue, Z. (2011b). "Phosphorylation-dependent 14-3-3 binding to LRRK2 is impaired by common mutations of familial Parkinson's disease." PLoS One **6**(3): e17153.

- Liang, X., Butterworth, M. B., Peters, K. W., Walker, W. H. and Frizzell, R. A. (2008). "An obligatory heterodimer of 14-3-3beta and 14-3-3epsilon is required for aldosterone regulation of the epithelial sodium channel." J Biol Chem **283**(41): 27418-25.
- Lim, J., Crespo-Barreto, J., Jafar-Nejad, P., Bowman, A. B., Richman, R., Hill, D. E., Orr, H. T. and Zoghbi, H. Y. (2008). "Opposing effects of polyglutamine expansion on native protein complexes contribute to SCA1." Nature **452**(7188): 713-8.
- Lim, J., Hao, T., Shaw, C., Patel, A. J., Szabo, G., Rual, J. F., Fisk, C. J., Li, N., Smolyar, A., Hill, D. E., Barabasi, A. L., Vidal, M. and Zoghbi, H. Y. (2006). "A protein-protein interaction network for human inherited ataxias and disorders of Purkinje cell degeneration." Cell **125**(4): 801-14.
- Lin, X., Antalffy, B., Kang, D., Orr, H. T. and Zoghbi, H. Y. (2000). "Polyglutamine expansion down-regulates specific neuronal genes before pathologic changes in SCA1." Nat Neurosci **3**(2): 157-63.
- Lingwood, D. and Simons, K. (2010). "Lipid Rafts As a Membrane-Organizing Principle." Science **327**(5961): 46-50.
- Liu, D., Bienkowska, J., Petosa, C., Collier, R. J., Fu, H. and Liddington, R. (1995). "Crystal structure of the zeta isoform of the 14-3-3 protein." Nature **376**(6536): 191-4.
- Liu, Y.-C., Elly, C., Yoshida, H., Bonnefoy-Berard, N. and Altman, A. (1996). "Activation-modulated Association of 14-3-3 Proteins with Cbl in T Cells." Journal of Biological Chemistry **271**(24): 14591-14595.
- Liu, Y.-C., Liu, Y., Elly, C., Yoshida, H., Lipkowitz, S. and Altman, A. (1997). "Serine Phosphorylation of Cbl Induced by Phorbol Ester Enhances Its Association with 14-3-3 Proteins in T Cells via a Novel Serine-rich 14-3-3-binding Motif." Journal of Biological Chemistry **272**(15): 9979-9985.
- Low, M. G. (1989). "The glycosyl-phosphatidylinositol anchor of membrane proteins." Biochim Biophys Acta **988**(3): 427-54.
- Ma, Y., Pitson, S., Hercus, T., Murphy, J., Lopez, A. and Woodcock, J. (2005). "Sphingosine activates protein kinase A type II by a novel cAMP-independent mechanism." J Biol Chem **280**(28): 26011-7.
- Mackie, S. and Aitken, A. (2005). "Novel brain 14-3-3 interacting proteins involved in neurodegenerative disease." Febs J **272**(16): 4202-10.
- Madeira, A., Yang, J., Zhang, X., Vikeved, E., Nilsson, A., Andren, P. E. and Svenningsson, P. (2011). "Caveolin-1 interacts with alpha-synuclein and mediates toxic actions of cellular alpha-synuclein overexpression." Neurochem Int **59**(2): 280-9.
- Mahley, R. W. (1988). "Apolipoprotein E: cholesterol transport protein with expanding role in cell biology." Science **240**(4852): 622-30.
- Manke, I. A., Nguyen, A., Lim, D., Stewart, M. Q., Elia, A. E. and Yaffe, M. B. (2005). "MAPKAP kinase-2 is a cell cycle checkpoint kinase that regulates the G2/M

- transition and S phase progression in response to UV irradiation." Mol Cell **17**(1): 37-48.
- Margolis, R. L. (2003). "Dominant spinocerebellar ataxias: a molecular approach to classification, diagnosis, pathogenesis and the future." Expert Review of Molecular Diagnostics **3**(6): 715-732.
- Martens, J. R., Navarro-Polanco, R., Coppock, E. A., Nishiyama, A., Parshley, L., Grobaski, T. D. and Tamkun, M. M. (2000). "Differential Targeting of Shaker-like Potassium Channels to Lipid Rafts." Journal of Biological Chemistry **275**(11): 7443-7446.
- Martin, H., Patel, Y., Jones, D., Howell, S., Robinson, K. and Aitken, A. (1993). "Antibodies against the major brain isoforms of 14-3-3 protein: an antibody specific for the N-acetylated amino-terminus of a protein." FEBS Lett **336**(1): 189.
- Masters, S. C., Pederson, K. J., Zhang, L., Barbieri, J. T. and Fu, H. (1999). "Interaction of 14-3-3 with a Nonphosphorylated Protein Ligand, Exoenzyme S of *Pseudomonas aeruginosa*." Biochemistry **38**(16): 5216-5221.
- Matilla-Duenas, A., Goold, R. and Giunti, P. (2008). "Clinical, genetic, molecular, and pathophysiological insights into spinocerebellar ataxia type 1." Cerebellum **7**(2): 106-14.
- Matilla, A., Koshy, B. T., Cummings, C. J., Isobe, T., Orr, H. T. and Zoghbi, H. Y. (1997). "The cerebellar leucine-rich acidic nuclear protein interacts with ataxin-1." Nature **389**(6654): 974-8.
- Matilla, A., Roberson, E. D., Banfi, S., Morales, J., Armstrong, D. L., Burright, E. N., Orr, H. T., Sweatt, J. D., Zoghbi, H. Y. and Matzuk, M. M. (1998). "Mice Lacking Ataxin-1 Display Learning Deficits and Decreased Hippocampal Paired-Pulse Facilitation." J. Neurosci. **18**(14): 5508-5516.
- Matsumoto, Y., Shindo, Y., Takakusagi, Y., Takakusagi, K., Tsukuda, S., Kusayanagi, T., Sato, H., Kawabe, T., Sugawara, F. and Sakaguchi, K. (2011). "Screening of a library of T7 phage-displayed peptides identifies alphaC helix in 14-3-3 protein as a CBP501-binding site." Bioorg Med Chem **19**(23): 7049-56.
- Megidish, T., Cooper, J., Zhang, L., Fu, H. and Hakomori, S.-i. (1998). "A Novel Sphingosine-dependent Protein Kinase (SDK1) Specifically Phosphorylates Certain Isoforms of 14-3-3 Protein." J. Biol. Chem. **273**(34): 21834-21845.
- Mehio, W., Kemp, G. J. L., Taylor, P. and Walkinshaw, M. D. (2010). "Identification of Protein Binding Surfaces using Surface Triplet Propensities." Bioinformatics.
- Melkonian, K. A., Ostermeyer, A. G., Chen, J. Z., Roth, M. G. and Brown, D. A. (1999). "Role of lipid modifications in targeting proteins to detergent-resistant membrane rafts. Many raft proteins are acylated, while few are prenylated." J Biol Chem **274**(6): 3910-7.

- Messaritou, G., Grammenoudi, S. and Skoulakis, E. M. C. (2010). "Dimerization Is Essential for 14-3-3zeta Stability and Function in Vivo." Journal of Biological Chemistry **285**(3): 1692-1700.
- Mils, V., Baldin, V., Goubin, F., Pinta, I., Papin, C., Waye, M., Eychene, A. and Ducommun, B. (2000). "Specific interaction between 14-3-3 isoforms and the human CDC25B phosphatase." Oncogene **19**(10): 1257-65.
- Miura, Y., Hanada, K. and Jones, T. L. Z. (2001). "G(s) Signaling Is Intact after Disruption of Lipid Rafts." Biochemistry **40**(50): 15418-15423.
- Mizutani, A., Wang, L., Rajan, H., Vig, P. J., Alaynick, W. A., Thaler, J. P. and Tsai, C. C. (2005). "Boat, an AXH domain protein, suppresses the cytotoxicity of mutant ataxin-1." Embo J **24**(18): 3339-51.
- Moore, B. E. a. P., V.J. (1967). Physiological and Biochemical Aspects of Nervous Integration, Prentice-Hall, Englewoods Cliffs.
- Munro, S. (2003). "Lipid rafts: elusive or illusive?" Cell **115**(4): 377-88.
- Muslin, A. J., Tanner, J. W., Allen, P. M. and Shaw, A. S. (1996). "Interaction of 14-3-3 with signaling proteins is mediated by the recognition of phosphoserine." Cell **84**(6): 889-97.
- Muslin, A. J. and Xing, H. (2000). "14-3-3 proteins: regulation of subcellular localization by molecular interference." Cellular Signalling **12**(11-12): 703-709.
- Naslavsky, N., Shmeeda, H., Friedlander, G., Yanai, A., Futerman, A. H., Barenholz, Y. and Taraboulos, A. (1999). "Sphingolipid depletion increases formation of the scrapie prion protein in neuroblastoma cells infected with prions." J Biol Chem **274**(30): 20763-71.
- Naslavsky, N., Stein, R., Yanai, A., Friedlander, G. and Taraboulos, A. (1997). "Characterization of detergent-insoluble complexes containing the cellular prion protein and its scrapie isoform." J Biol Chem **272**(10): 6324-31.
- Nabl, T., Pestonjamas, K. N., Leszyk, J. D., Crowley, J. L., Oh, S. W. and Luna, E. J. (2002). "Proteomic analysis of a detergent-resistant membrane skeleton from neutrophil plasma membranes." J Biol Chem **277**(45): 43399-409.
- Nelson, T. J. and Alkon, D. L. (2007). "Protection against beta-amyloid-induced apoptosis by peptides interacting with beta-amyloid." J Biol Chem **282**(43): 31238-49.
- Nichols, R. J., Dzamko, N., Morrice, N. A., Campbell, D. G., Deak, M., Ordureau, A., Macartney, T., Tong, Y., Shen, J., Prescott, A. R. and Alessi, D. R. (2010). "14-3-3 binding to LRRK2 is disrupted by multiple Parkinson's disease-associated mutations and regulates cytoplasmic localization." Biochem J **430**(3): 393-404.
- Nomura, M., Shimizu, S., Sugiyama, T., Narita, M., Ito, T., Matsuda, H. and Tsujimoto, Y. (2003). "14-3-3 Interacts directly with and negatively regulates pro-apoptotic Bax." J Biol Chem **278**(3): 2058-65.

- Nussbaum, R. L. and Polymeropoulos, M. H. (1997). "Genetics of Parkinson's disease." Hum Mol Genet **6**(10): 1687-91.
- Oesch, B., Westaway, D., Walchli, M., McKinley, M. P., Kent, S. B., Aebersold, R., Barry, R. A., Tempst, P., Teplow, D. B., Hood, L. E. and et al. (1985). "A cellular gene encodes scrapie PrP 27-30 protein." Cell **40**(4): 735-46.
- Okazawa, H., Rich, T., Chang, A., Lin, X., Waragai, M., Kajikawa, M., Enokido, Y., Komuro, A., Kato, S., Shibata, M., Hatanaka, H., Mouradian, M. M., Sudol, M. and Kanazawa, I. (2002). "Interaction between mutant ataxin-1 and PQBP-1 affects transcription and cell death." Neuron **34**(5): 701-13.
- Olzmann, J. A., Li, L. and Chin, L. S. (2008). "Aggresome formation and neurodegenerative diseases: therapeutic implications." Curr Med Chem **15**(1): 47-60.
- Omi, K., Hachiya, N. S., Tanaka, M., Tokunaga, K. and Kaneko, K. (2008). "14-3-3zeta is indispensable for aggregate formation of polyglutamine-expanded huntingtin protein." Neuroscience Letters **431**(1): 45-50.
- Orr, H. T., Chung, M. Y., Banfi, S., Kwiatkowski, T. J., Jr., Servadio, A., Beaudet, A. L., McCall, A. E., Duvick, L. A., Ranum, L. P. and Zoghbi, H. Y. (1993). "Expansion of an unstable trinucleotide CAG repeat in spinocerebellar ataxia type 1." Nat Genet **4**(3): 221-6.
- Osler, W. (1893). "Remarks on the varieties of chronic chorea, and a report upon two families of the hereditary form, with one autopsy." J. Nerv. Ment. Dis. **18**: 97-111.
- Osterhues, A., Liebmann, S., Schmid, M., Buk, D., Huss, R., Graeve, L. and Zeindl-Eberhart, E. (2006). "Stem cells and experimental leukemia can be distinguished by lipid raft protein composition." Stem Cells Dev **15**(5): 677-86.
- Ostrerova, N., Petrucelli, L., Farrer, M., Mehta, N., Choi, P., Hardy, J. and Wolozin, B. (1999). "alpha-Synuclein shares physical and functional homology with 14-3-3 proteins." J Neurosci **19**(14): 5782-91.
- Owen, D. M., Williamson, D., Rentero, C. and Gaus, K. (2009). "Quantitative microscopy: protein dynamics and membrane organisation." Traffic **10**(8): 962-71.
- Pan, K. M., Baldwin, M., Nguyen, J., Gasset, M., Serban, A., Groth, D., Mehlhorn, I., Huang, Z., Fletterick, R. J., Cohen, F. E. and et al. (1993). "Conversion of alpha-helices into beta-sheets features in the formation of the scrapie prion proteins." Proc Natl Acad Sci U S A **90**(23): 10962-6.
- Parkin, E. T., Turner, A. J. and Hooper, N. M. (1999). "Amyloid precursor protein, although partially detergent-insoluble in mouse cerebral cortex, behaves as an atypical lipid raft protein." Biochem J **344 Pt 1**: 23-30.
- Patra, S. K. (2008). "Dissecting lipid raft facilitated cell signaling pathways in cancer." Biochim Biophys Acta **1785**(2): 182-206.

- Perez, R. G., Waymire, J. C., Lin, E., Liu, J. J., Guo, F. and Zigmond, M. J. (2002). "A role for alpha-synuclein in the regulation of dopamine biosynthesis." J Neurosci **22**(8): 3090-9.
- Perutz, M. F., Johnson, T., Suzuki, M. and Finch, J. T. (1994). "Glutamine repeats as polar zippers: their possible role in inherited neurodegenerative diseases." Proc Natl Acad Sci U S A **91**(12): 5355-8.
- Petosa, C., Masters, S. C., Bankston, L. A., Pohl, J., Wang, B., Fu, H. and Liddington, R. C. (1998). "14-3-3zeta binds a phosphorylated Raf peptide and an unphosphorylated peptide via its conserved amphipathic groove." J Biol Chem **273**(26): 16305-10.
- Pike, L. J. (2003). "Lipid rafts: bringing order to chaos." J Lipid Res **44**(4): 655-67.
- Pike, L. J. (2004). "Lipid rafts: heterogeneity on the high seas." Biochem J **378**(Pt 2): 281-92.
- Pike, L. J. (2009). "The challenge of lipid rafts." J Lipid Res **50 Suppl**: S323-8.
- Poston, C. N., Duong, E., Cao, Y. and Bazemore-Walker, C. R. (2011). "Proteomic analysis of lipid raft-enriched membranes isolated from internal organelles." Biochemical and Biophysical Research Communications **415**(2): 355-360.
- Powell, D. W., Rane, M. J., Chen, Q., Singh, S. and McLeish, K. R. (2002). "Identification of 14-3-3zeta as a protein kinase B/Akt substrate." J Biol Chem **277**(24): 21639-42.
- Pozuelo Rubio, M., Geraghty, K. M., Wong, B. H. C., Wood, N. T., Campbell, D. G., Morrice, N. and Mackintosh, C. (2004). "14-3-3-affinity purification of over 200 human phosphoproteins reveals new links to regulation of cellular metabolism, proliferation and trafficking." Biochem. J. **379**(2): 395-408.
- Prusiner, S. B. (1982). "Novel proteinaceous infectious particles cause scrapie." Science **216**(4542): 136-44.
- Prusiner, S. B. (1998). "Prions." Proc Natl Acad Sci U S A **95**(23): 13363-83.
- Rajagopalan, S., Sade, R. S., Townsley, F. M. and Fersht, A. R. (2010). "Mechanistic differences in the transcriptional activation of p53 by 14-3-3 isoforms." Nucleic Acids Research **38**(3): 893-906.
- Rang, H. P., Dale, M.M., Ritter, J.M., Moore, P.K. (2003). Pharmacology, Churchill Livingstone.
- Reuther, G. W., Fu, H., Cripe, L. D., Collier, R. J. and Pendergast, A. M. (1994). "Association of the protein kinases c-Bcr and Bcr-Abl with proteins of the 14-3-3 family." Science **266**(5182): 129-133.
- Riley, B. E., Zoghbi, H. Y. and Orr, H. T. (2005). "SUMOylation of the polyglutamine repeat protein, ataxin-1, is dependent on a functional nuclear localization signal." J Biol Chem **280**(23): 21942-8.

- Rimessi, A., Coletto, L., Pinton, P., Rizzuto, R., Brini, M. and Carafoli, E. (2005). "Inhibitory interaction of the 14-3-3{epsilon} protein with isoform 4 of the plasma membrane Ca(2+)-ATPase pump." J Biol Chem **280**(44): 37195-203.
- Rittinger, K., Budman, J., Xu, J., Volinia, S., Cantley, L. C., Smerdon, S. J., Gamblin, S. J. and Yaffe, M. B. (1999). "Structural Analysis of 14-3-3 Phosphopeptide Complexes Identifies a Dual Role for the Nuclear Export Signal of 14-3-3 in Ligand Binding." Molecular cell **4**(2): 153-166.
- Robbins, S. M., Quintrell, N. A. and Bishop, J. M. (1995). "Myristoylation and differential palmitoylation of the HCK protein-tyrosine kinases govern their attachment to membranes and association with caveolae." Mol Cell Biol **15**(7): 3507-15.
- Rodgers, W., Crise, B. and Rose, J. K. (1994). "Signals determining protein tyrosine kinase and glycosyl-phosphatidylinositol-anchored protein targeting to a glycolipid-enriched membrane fraction." Mol Cell Biol **14**(8): 5384-91.
- Rommel, C., Radziwill, G., Lovric, J., Noeldeke, J., Heinicke, T., Jones, D., Aitken, A. and Moelling, K. (1996). "Activated Ras displaces 14-3-3 protein from the amino terminus of c-Raf-1." Oncogene **12**(3): 609-19.
- Rong, J., Li, S., Sheng, G., Wu, M., Coblitz, B., Li, M., Fu, H. and Li, X. J. (2007). "14-3-3 protein interacts with Huntingtin-associated protein 1 and regulates its trafficking." J Biol Chem **282**(7): 4748-56.
- Rosen, D. R. (1993). "Mutations in Cu/Zn superoxide dismutase gene are associated with familial amyotrophic lateral sclerosis." Nature **364**(6435): 362.
- Rosenquist, M. (2003). "14-3-3 proteins in apoptosis." Braz J Med Biol Res **36**(4): 403-8.
- Rosenquist, M., Sehnke, P., Ferl, R. J., Sommarin, M. and Larsson, C. (2000). "Evolution of the 14-3-3 Protein Family: Does the Large Number of Isoforms in Multicellular Organisms Reflect Functional Specificity?" Journal of Molecular Evolution **51**(5): 446-458.
- Sadik, G., Tanaka, T., Kato, K., Yamamori, H., Nessa, B. N., Morihara, T. and Takeda, M. (2009). "Phosphorylation of tau at Ser214 mediates its interaction with 14-3-3 protein: implications for the mechanism of tau aggregation." Journal of Neurochemistry **108**(1): 33-43.
- Sasaki, H., Fukazawa, T., Yanagihara, T., Hamada, T., Shima, K., Matsumoto, A., Hashimoto, K., Ito, N., Wakisaka, A. and Tashiro, K. (1996). "Clinical features and natural history of spinocerebellar ataxia type 1." Acta Neurol Scand **93**(1): 64-71.
- Sato, S., Chiba, T., Sakata, E., Kato, K., Mizuno, Y., Hattori, N. and Tanaka, K. (2006). "14-3-3beta is a novel regulator of parkin ubiquitin ligase." Embo J **25**(1): 211-21.
- Scheid, M. P. and Woodgett, J. R. (2003). "Unravelling the activation mechanisms of protein kinase B/Akt." FEBS Letters **546**(1): 108-112.

- Schengrund, C.-L. (2010). "Lipid rafts: Keys to neurodegeneration." Brain Research Bulletin **82**: 7-17.
- Schols, L., Linnemann, C. and Globas, C. (2008). "Electrophysiology in spinocerebellar ataxias: spread of disease and characteristic findings." Cerebellum **7**(2): 198-203.
- Schulte, T., Paschke, K. A., Laessing, U., Lottspeich, F. and Stuermer, C. A. (1997). "Reggie-1 and reggie-2, two cell surface proteins expressed by retinal ganglion cells during axon regeneration." Development **124**(2): 577-87.
- Sekimoto, T., Fukumoto, M. and Yoneda, Y. (2004). "14-3-3 suppresses the nuclear localization of threonine 157-phosphorylated p27(Kip1)." Embo J **23**(9): 1934-42.
- Selenko, P., Gregorovic, G., Sprangers, R., Stier, G., Rhani, Z., Kramer, A. and Sattler, M. (2003). "Structural basis for the molecular recognition between human splicing factors U2AF65 and SF1/mBBP." Mol Cell **11**(4): 965-76.
- Serra, H. G., Byam, C. E., Lande, J. D., Tousey, S. K., Zoghbi, H. Y. and Orr, H. T. (2004). "Gene profiling links SCA1 pathophysiology to glutamate signaling in Purkinje cells of transgenic mice." Hum Mol Genet **13**(20): 2535-43.
- Serra, H. G., Duvick, L., Zu, T., Carlson, K., Stevens, S., Jorgensen, N., Lysholm, A., Burright, E., Zoghbi, H. Y., Clark, H. B., Andresen, J. M. and Orr, H. T. (2006). "RORalpha-mediated Purkinje cell development determines disease severity in adult SCA1 mice." Cell **127**(4): 697-708.
- Servadio, A., Koshy, B., Armstrong, D., Antalffy, B., Orr, H. T. and Zoghbi, H. Y. (1995). "Expression analysis of the ataxin-1 protein in tissues from normal and spinocerebellar ataxia type 1 individuals." Nat Genet **10**(1): 94-8.
- Shenoy-Scaria, A. M., Dietzen, D. J., Kwong, J., Link, D. C. and Lublin, D. M. (1994). "Cysteine3 of Src family protein tyrosine kinase determines palmitoylation and localization in caveolae." J Cell Biol **126**(2): 353-63.
- Sichtig, N., Silling, S. and Steger, G. (2007). "Papillomavirus binding factor (PBF)-mediated inhibition of cell growth is regulated by 14-3-3beta." Arch Biochem Biophys **464**(1): 90-9.
- Siddique, T. and Ajroud-Driss, S. (2011). "Familial amyotrophic lateral sclerosis, a historical perspective." Acta Myol **30**(2): 117-20.
- Simons, K. and Ehehalt, R. (2002). "Cholesterol, lipid rafts, and disease." J Clin Invest **110**(5): 597-603.
- Simons, K. and Ikonen, E. (1997). "Functional rafts in cell membranes." Nature **387**(6633): 569-572.
- Simons, K. and Toomre, D. (2000). "Lipid rafts and signal transduction." Nat Rev Mol Cell Biol **1**(1): 31-9.

- Simons, K. and Vaz, W. L. (2004). "Model systems, lipid rafts, and cell membranes." Annu Rev Biophys Biomol Struct **33**: 269-95.
- Simons, M., Keller, P., Dichgans, J. and Schulz, J. B. (2001). "Cholesterol and Alzheimer's disease: Is there a link?" Neurology **57**(6): 1089-1093.
- Singer, S. J. and Nicolson, G. L. (1972). "The Fluid Mosaic Model of the Structure of Cell Membranes." Science **175**(4023): 720-731.
- Skinner, P. J., Koshy, B. T., Cummings, C. J., Klement, I. A., Helin, K., Servadio, A., Zoghbi, H. Y. and Orr, H. T. (1997). "Ataxin-1 with an expanded glutamine tract alters nuclear matrix-associated structures." Nature **389**(6654): 971-4.
- Sluchanko, N. N., Sudnitsyna, M. V., Seit-Nebi, A. S., Antson, A. A. and Gusev, N. B. (2011). "Properties of the Monomeric Form of Human 14-3-3zeta Protein and Its Interaction with Tau and HspB6." Biochemistry **50**(45): 9797-9808.
- Sprenger, R. R., Speijer, D., Back, J. W., De Koster, C. G., Pannekoek, H. and Horrevoets, A. J. (2004). "Comparative proteomics of human endothelial cell caveolae and rafts using two-dimensional gel electrophoresis and mass spectrometry." Electrophoresis **25**(1): 156-72.
- Stahl, N., Borchelt, D. R., Hsiao, K. and Prusiner, S. B. (1987). "Scrapie prion protein contains a phosphatidylinositol glycolipid." Cell **51**(2): 229-240.
- Stien, R. (2005). "Shakespeare on parkinsonism." Mov Disord **20**(6): 768-9.
- Strittmatter, W. J., Saunders, A. M., Schmechel, D., Pericak-Vance, M., Enghild, J., Salvesen, G. S. and Roses, A. D. (1993). "Apolipoprotein E: high-avidity binding to beta-amyloid and increased frequency of type 4 allele in late-onset familial Alzheimer disease." Proc Natl Acad Sci U S A **90**(5): 1977-81.
- Suginta, W., Karoulias, N., Aitken, A. and Ashley, R. H. (2001). "Chloride intracellular channel protein CLIC4 (p64H1) binds directly to brain dynamin I in a complex containing actin, tubulin and 14-3-3 isoforms." Biochem J **359**(Pt 1): 55-64.
- Sunayama, J., Tsuruta, F., Masuyama, N. and Gotoh, Y. (2005). "JNK antagonizes Akt-mediated survival signals by phosphorylating 14-3-3." The Journal of Cell Biology **170**(2): 295-304.
- Tanahashi, H. and Tabira, T. (1999). "Isolation of human delta-catenin and its binding specificity with presenilin 1." Neuroreport **10**(3): 563-8.
- Tanaka, K., Shouguchi-Miyata, J., Miyamoto, N. and Ikeda, J. E. (2004). "Novel nuclear shuttle proteins, HDBP1 and HDBP2, bind to neuronal cell-specific cis-regulatory element in the promoter for the human Huntington's disease gene." J Biol Chem **279**(8): 7275-86.
- Tanner, C. M. (2003). "Is the cause of Parkinson's disease environmental or hereditary? Evidence from twin studies." Adv Neurol **91**: 133-42.

- Taverna, E., Saba, E., Rowe, J., Francolini, M., Clementi, F. and Rosa, P. (2004). "Role of Lipid Microdomains in P/Q-type Calcium Channel (Cav2.1) Clustering and Function in Presynaptic Membranes." Journal of Biological Chemistry **279**(7): 5127-5134.
- Taylor, K. S., Counsell, C. E., Gordon, J. C. and Harris, C. E. (2005). "Screening for undiagnosed parkinsonism among older people in general practice." Age Ageing **34**(5): 501-4.
- Taylor, P., Blackburn, E., Sheng, Y. G., Harding, S., Hsin, K. Y., Kan, D., Shave, S. and Walkinshaw, M. D. (2008). "Ligand discovery and virtual screening using the program LIDAEUS." British Journal of Pharmacology **153**(S1): S55-S67.
- Terry, R. D. and Davies, P. (1980). "Dementia of the Alzheimer type." Annu Rev Neurosci **3**: 77-95.
- Thompson, T. E. and Tillack, T. W. (1985). "Organization of glycosphingolipids in bilayers and plasma membranes of mammalian cells." Annu Rev Biophys Biophys Chem **14**: 361-86.
- Thorson, J. A., Yu, L. W. K., Hsu, A. L., Shih, N.-Y., Graves, P. R., Tanner, J. W., Allen, P. M., Piwnicka-Worms, H. and Shaw, A. S. (1998). "14-3-3 Proteins Are Required for Maintenance of Raf-1 Phosphorylation and Kinase Activity." Molecular and Cellular Biology **18**(9): 5229-5238.
- Todd, A., Cossons, N., Aitken, A., Price, G. B. and Zannis-Hadjopoulos, M. (1998). "Human Cruciform Binding Protein Belongs to the 14-3-3 Family" Biochemistry **37**(40): 14317-14325.
- Toker, A., Sellers, L. A., Amess, B., Patel, Y., Harris, A. and Aitken, A. (1992). "Multiple isoforms of a protein kinase C inhibitor (KCIP-1/14-3-3) from sheep brain. Amino acid sequence of phosphorylated forms." Eur J Biochem **206**(2): 453-61.
- Tong, X., Gui, H., Jin, F., Heck, B. W., Lin, P., Ma, J., Fondell, J. D. and Tsai, C. C. (2011). "Ataxin-1 and Brother of ataxin-1 are components of the Notch signalling pathway." EMBO Rep **12**(5): 428-35.
- Tsai, C. C., Kao, H. Y., Mitzutani, A., Banayo, E., Rajan, H., McKeown, M. and Evans, R. M. (2004). "Ataxin 1, a SCA1 neurodegenerative disorder protein, is functionally linked to the silencing mediator of retinoid and thyroid hormone receptors." Proc Natl Acad Sci U S A **101**(12): 4047-52.
- Tsuda, H., Jafar-Nejad, H., Patel, A. J., Sun, Y., Chen, H. K., Rose, M. F., Venken, K. J., Botas, J., Orr, H. T., Bellen, H. J. and Zoghbi, H. Y. (2005). "The AXH domain of Ataxin-1 mediates neurodegeneration through its interaction with Gfi-1/Senseless proteins." Cell **122**(4): 633-44.
- Tsui-Pierchala, B. A., Encinas, M., Milbrandt, J. and Johnson, E. M., Jr. (2002). "Lipid rafts in neuronal signaling and function." Trends Neurosci **25**(8): 412-7.

- Tsuruta, F., Sunayama, J., Mori, Y., Hattori, S., Shimizu, S., Tsujimoto, Y., Yoshioka, K., Masuyama, N. and Gotoh, Y. (2004). "JNK promotes Bax translocation to mitochondria through phosphorylation of 14-3-3 proteins." EMBO J **23**(8): 1889-1899.
- Twelvetrees, A. E., Yuen, E. Y., Arancibia-Carcamo, I. L., MacAskill, A. F., Rostaing, P., Lumb, M. J., Humbert, S., Triller, A., Saudou, F., Yan, Z. and Kittler, J. T. (2010). "Delivery of GABAARs to synapses is mediated by HAP1-KIF5 and disrupted by mutant huntingtin." Neuron **65**(1): 53-65.
- Tzivion, G., Luo, Z. and Avruch, J. (1998). "A dimeric 14-3-3 protein is an essential cofactor for Raf kinase activity." Nature **394**(6688): 88-92.
- Umahara, T. and Uchihara, T. (2010). "14-3-3 proteins and spinocerebellar ataxia type 1: from molecular interaction to human neuropathology." Cerebellum **9**(2): 183-9.
- Umahara, T., Uchihara, T., Yagishita, S., Nakamura, A., Tsuchiya, K. and Iwamoto, T. (2007). "Intranuclear immunolocalization of 14-3-3 protein isoforms in brains with spinocerebellar ataxia type 1." Neurosci Lett **414**(2): 130-5.
- Van Der Hoeven, P. C., Van Der Wal, J. C., Ruurs, P., Van Dijk, M. C. and Van Blitterswijk, J. (2000). "14-3-3 isotypes facilitate coupling of protein kinase C-zeta to Raf-1: negative regulation by 14-3-3 phosphorylation." Biochem J **345 Pt 2**: 297-306.
- van Heusden, G. P. H., van der Zanden, A. L., Ferl, R. J. and Steensma, H. Y. (1996). "Four Arabidopsis thaliana 14-3-3 protein isoforms can complement the lethal yeast *bmh1 bmh2* double disruption." FEBS Letters **391**(3): 252-256.
- Vessie, P. R. (1932). "Original article on the transmission of Huntington's chorea for 300 years - the Bures family group." J. Nerv. Ment. Dis. **76**(553-573).
- Vey, M., Pilkuhn, S., Wille, H., Nixon, R., DeArmond, S. J., Smart, E. J., Anderson, R. G., Taraboulos, A. and Prusiner, S. B. (1996). "Subcellular colocalization of the cellular and scrapie prion proteins in caveolae-like membranous domains." Proc Natl Acad Sci U S A **93**(25): 14945-9.
- Vierra-Green, C. A., Orr, H. T., Zoghbi, H. Y. and Ferrington, D. A. (2005). "Identification of a novel phosphorylation site in ataxin-1." Biochim Biophys Acta **1744**(1): 11-8.
- Vincenz, C. and Dixit, V. M. (1996). "14-3-3 Proteins Associate with A20 in an Isoform-specific Manner and Function Both as Chaperone and Adapter Molecules." Journal of Biological Chemistry **271**(33): 20029-20034.
- Volkening, K., Leystra-Lantz, C., Yang, W., Jaffee, H. and Strong, M. J. (2009). "Tar DNA binding protein of 43 kDa (TDP-43), 14-3-3 proteins and copper/zinc superoxide dismutase (SOD1) interact to modulate NFL mRNA stability. Implications for altered RNA processing in amyotrophic lateral sclerosis (ALS)." Brain Res **1305**: 168-82.
- Waelter, S., Boeddrich, A., Lurz, R., Scherzinger, E., Lueder, G., Lehrach, H. and Wanker, E. E. (2001). "Accumulation of mutant huntingtin fragments in aggresome-like

- inclusion bodies as a result of insufficient protein degradation." Mol Biol Cell **12**(5): 1393-407.
- Wakui, H., Wright, A. P., Gustafsson, J. and Zilliacus, J. (1997). "Interaction of the ligand-activated glucocorticoid receptor with the 14-3-3 eta protein." J Biol Chem **272**(13): 8153-6.
- Walker, F. O. (2007). "Huntington's disease." Lancet **369**(9557): 218-28.
- Wang, B., Yang, H., Liu, Y. C., Jelinek, T., Zhang, L., Ruoslahti, E. and Fu, H. (1999). "Isolation of high-affinity peptide antagonists of 14-3-3 proteins by phage display." Biochemistry **38**(38): 12499-504.
- Wang, H., Zhang, L., Liddington, R. and Fu, H. (1998). "Mutations in the hydrophobic surface of an amphipathic groove of 14-3-3zeta disrupt its interaction with Raf-1 kinase." J Biol Chem **273**(26): 16297-304.
- Wang, Y., Meriin, A. B., Zaarur, N., Romanova, N. V., Chernoff, Y. O., Costello, C. E. and Sherman, M. Y. (2009). "Abnormal proteins can form aggresome in yeast: aggresome-targeting signals and components of the machinery." Faseb J **23**(2): 451-63.
- Watanabe, M., Dykes-Hoberg, M., Cizewski Culotta, V., Price, D. L., Wong, P. C. and Rothstein, J. D. (2001). "Histological Evidence of Protein Aggregation in Mutant SOD1 Transgenic Mice and in Amyotrophic Lateral Sclerosis Neural Tissues." Neurobiology of Disease **8**(6): 933-941.
- WHO (1998). "Human transmissible spongiform encephalopathies." Wkly Epidemiol Rec **73**(47): 361-372.
- Will, R. G., Ironside, J. W., Zeidler, M., Cousens, S. N., Estibeiro, K., Alperovitch, A., Poser, S., Pocchiari, M., Hofman, A. and Smith, P. G. (1996). "A new variant of Creutzfeldt-Jakob disease in the UK." Lancet **347**(9006): 921-5.
- Wiltfang, J., Otto, M., Baxter, H. C., Bodemer, M., Steinacker, P., Bahn, E., Zerr, I., Kornhuber, J., Kretschmar, H. A., Poser, S., Ruther, E. and Aitken, A. (1999). "Isoform pattern of 14-3-3 proteins in the cerebrospinal fluid of patients with Creutzfeldt-Jakob disease." J Neurochem **73**(6): 2485-90.
- Wischik, C. M., Novak, M., ThÄ,gersen, H. C., Edwards, P. C., Runswick, M. J., Jakes, R., Walker, J. E., Milstein, C., Roth, M. and Klug, A. (1988). "Isolation of a fragment of tau derived from the core of the paired helical filament of Alzheimer disease." Proceedings of the National Academy of Sciences **85**(12): 4506-4510.
- Wolozin, B., Kellman, W., Ruosseau, P., Celesia, G. G. and Siegel, G. (2000). "Decreased prevalence of Alzheimer disease associated with 3-hydroxy-3-methylglutaryl coenzyme A reductase inhibitors." Arch Neurol **57**(10): 1439-43.
- Woodcock, J. M., Ma, Y., Coolen, C., Pham, D., Jones, C., Lopez, A. F. and Pitson, S. M. (2010). "Sphingosine and FTY720 directly bind pro-survival 14-3-3 proteins to regulate their function." Cellular Signalling **22**(9): 1291-1299.

- Woodcock, J. M., Murphy, J., Stomski, F. C., Berndt, M. C. and Lopez, A. F. (2003). "The dimeric versus monomeric status of 14-3-3zeta is controlled by phosphorylation of Ser58 at the dimer interface." J Biol Chem **278**(38): 36323-7.
- Wu, C., Butz, S., Ying, Y.-s. and Anderson, R. G. W. (1997). "Tyrosine Kinase Receptors Concentrated in Caveolae-like Domains from Neuronal Plasma Membrane." Journal of Biological Chemistry **272**(6): 3554-3559.
- Wu, S. Y., McNae, I., Kontopidis, G., McClue, S. J., McInnes, C., Stewart, K. J., Wang, S., Zheleva, D. I., Marriage, H., Lane, D. P., Taylor, P., Fischer, P. M. and Walkinshaw, M. D. (2003). "Discovery of a Novel Family of CDK Inhibitors with the Program LIDAEUS: Structural Basis for Ligand-Induced Disordering of the Activation Loop." Structure (London, England : 1993) **11**(4): 399-410.
- Xiao, B., Smerdon, S. J., Jones, D. H., Dodson, G. G., Soneji, Y., Aitken, A. and Gamblin, S. J. (1995). "Structure of a 14-3-3 protein and implications for coordination of multiple signalling pathways." Nature **376**(6536): 188-91.
- Xu, J., Kao, S. Y., Lee, F. J., Song, W., Jin, L. W. and Yankner, B. A. (2002). "Dopamine-dependent neurotoxicity of alpha-synuclein: a mechanism for selective neurodegeneration in Parkinson disease." Nat Med **8**(6): 600-6.
- Yacoubian, T. A., Slone, S. R., Harrington, A. J., Hamamichi, S., Schieltz, J. M., Caldwell, K. A., Caldwell, G. A. and Standaert, D. G. (2010). "Differential neuroprotective effects of 14-3-3 proteins in models of Parkinson's disease." Cell Death and Dis **1**(1): e2.
- Yaffe, M. B. (2002a). "How do 14-3-3 proteins work?-- Gatekeeper phosphorylation and the molecular anvil hypothesis." FEBS Lett **513**(1): 53-7.
- Yaffe, M. B. (2002b). "How do 14-3-3 proteins work? - Gatekeeper phosphorylation and the molecular anvil hypothesis." FEBS Letters **513**(1): 53-57.
- Yaffe, M. B., Rittinger, K., Volinia, S., Caron, P. R., Aitken, A., Leffers, H., Gamblin, S. J., Smerdon, S. J. and Cantley, L. C. (1997). "The structural basis for 14-3-3:phosphopeptide binding specificity." Cell **91**(7): 961-71.
- Yamauchi, T., Nakata, H. and Fujisawa, H. (1981). "A new activator protein that activates tryptophan 5-monooxygenase and tyrosine 3-monooxygenase in the presence of Ca²⁺-, calmodulin-dependent protein kinase. Purification and characterization." J Biol Chem **256**(11): 5404-9.
- Yoshida, K., Yamaguchi, T., Natsume, T., Kufe, D. and Miki, Y. (2005). "JNK phosphorylation of 14-3-3 proteins regulates nuclear targeting of c-Abl in the apoptotic response to DNA damage." Nat Cell Biol **7**(3): 278-285.
- Yue, S., Serra, H. G., Zoghbi, H. Y. and Orr, H. T. (2001). "The spinocerebellar ataxia type 1 protein, ataxin-1, has RNA-binding activity that is inversely affected by the length of its polyglutamine tract." Hum Mol Genet **10**(1): 25-30.
- Zajchowski, L. D. and Robbins, S. M. (2002). "Lipid rafts and little caves. Compartmentalized signalling in membrane microdomains." Eur J Biochem **269**(3): 737-52.

- Zhai, J., Strom, A. L., Kilty, R., Venkatakrishnan, P., White, J., Everson, W. V., Smart, E. J. and Zhu, H. (2009). "Proteomic characterization of lipid raft proteins in amyotrophic lateral sclerosis mouse spinal cord." Febs J **276**(12): 3308-23.
- Zhang, L., Wang, H., Liu, D., Liddington, R. and Fu, H. (1997). "Raf-1 kinase and exoenzyme S interact with 14-3-3zeta through a common site involving lysine 49." J Biol Chem **272**(21): 13717-24.
- Zhang, T., Zhang, X. and Sun, Z. (2010). "Global network analysis of lipid-raft-related proteins reveals their centrality in the network and their roles in multiple biological processes." J Mol Biol **402**(4): 761-73.
- Zheng, Y. Z. and Foster, L. J. (2009a). "Biochemical and proteomic approaches for the study of membrane microdomains." J Proteomics **72**(1): 12-22.
- Zheng, Y. Z. and Foster, L. J. (2009b). "Contributions of quantitative proteomics to understanding membrane microdomains." J Lipid Res **50**(10): 1976-85.
- Zhu, P., Sang, Y., Xu, H., Zhao, J., Xu, R., Sun, Y., Xu, T., Wang, X., Chen, L., Feng, H., Li, C. and Zhao, S. (2005). "ADAM22 plays an important role in cell adhesion and spreading with the assistance of 14-3-3." Biochemical and Biophysical Research Communications **331**(4): 938-946.
- Zhu, P. c., Sun, Y., Xu, R., Sang, Y., Zhao, J., Liu, G., Cai, L., Li, C. and Zhao, S. (2003). "The interaction between ADAM 22 and 14-3-3zeta: regulation of cell adhesion and spreading." Biochemical and Biophysical Research Communications **301**(4): 991-999.
- Zhuang, L., Lin, J., Lu, M. L., Solomon, K. R. and Freeman, M. R. (2002). "Cholesterol-rich Lipid Rafts Mediate Akt-regulated Survival in Prostate Cancer Cells." Cancer Research **62**(8): 2227-2231.
- Zipp, F., Waiczies, S., Aktas, O., Neuhaus, O., Hemmer, B., Schraven, B., Nitsch, R. and Hartung, H. P. (2007). "Impact of HMG-CoA reductase inhibition on brain pathology." Trends Pharmacol Sci **28**(7): 342-9.
- Zoghbi, H. Y. (1995). "Spinocerebellar ataxia type 1." Clin Neurosci **3**(1): 5-11.
- Zoghbi, H. Y. and Orr, H. T. (2000). "Glutamine repeats and neurodegeneration." Annu Rev Neurosci **23**: 217-47.

Publications

- Brechin C, Houston NP, Clokie S, Fismen L, Peden A, Falconer H, Fu H, and Aitken A (2012), 14-3-3 isoforms and interacting proteins in lipid raft membranes. *FEBS J*, revised version submitted.
- Houston NP, Brechin C, Falconer H, Vigbedor M, Maltas E and Aitken A (2010), 14-3-3 Isoforms in Lipid Rafts: The Role in Neurodegenerative Diseases. *J. Neurochem.* **113** (Suppl. 1), 12.
- Houston N, Brechin C, Falconer H , Vigbedor M , Aitken A (2009), 14-3-3 Protein interactions and drug discovery in Parkinson's disease. *Neurodegenerative Diseases*. Suppl 6: 222.